Investigating the physiological role of glucokinase in the *nucleus tractus solitarius* and the paraventricular nucleus in the regulation of energy homeostasis

A thesis submitted for the degree of Doctor of Philosophy,

Imperial College London

Ivan De Backer

2017

Imperial College London

Section of Investigative Medicine

Division of Diabetes, Endocrinology and Metabolism

Department of Medicine

Abstract

Chronically high circulating glucose levels can lead to metabolic problems such as Type II Diabetes Mellitus (T2DM). Plasma glucose levels are constantly monitored by a process named glucose-sensing. Glucokinase (GK) is a key glucose-sensing enzyme and is expressed in various areas of the brain associated with the control of energy homeostasis. It has been detected in the *nucleus tractus solitarius* (NTS) and the paraventricular nucleus (PVN) but its physiological role in these nuclei in the regulation of energy homeostasis is unclear.

GK's function in the NTS and PVN was determined by both down-regulating and up-regulating its expression in these nuclei using a viral vector encoding glucokinase antisense or sense, respectively. Feeding studies demonstrated that GK knockdown had no effect on food intake. GK knockdown in both the NTS and PVN impaired glucose tolerance and disrupted glucose-stimulated insulin secretion. PVN GK knockdown also reduced glucose-stimulated glucagon-like peptide 1 (GLP-1) release. On the other hand, up-regulating GK expression in the PVN had the opposite effect and improved glucose tolerance by stimulating insulin and GLP-1 release. These effects were reproduced by iPVN injection of K_{ATP} channel modulators during an oral GTT.

Evidence presented in this thesis suggests that NTS and PVN GK play an important role in glucose homeostasis by regulating insulin and GLP-1 (7-36) secretion during the initial insulin response to hyperglycaemia. GK in both the NTS and PVN appears important in restoring euglycaemia following a glucose challenge. In the PVN, this seems to be mediated by the inhibition of K_{ATP} channels. This study sheds light on the previously unexplored function of GK in the NTS and PVN. A role of PVN and NTS GK in modulating insulin and GLP-1 (7-36) release in the regulation of glucose homeostasis has not been suggested before.

Declaration of contributors

The work described in this thesis was performed by the author. All collaboration and assistance is described below.

Recombinant AAV was prepared by Dr James Gardiner. GK-pTR-CGW plasmid was prepared by Dr James Gardiner, Dr Errol Richardson and Dr Sufyan Hussain. *In vitro* testing of rAAV-GKAS and rAAV-GKS was conducted by Dr Errol Richardson.

Stereotactic injections and cannula implantations were conducted with the assistance of Dr David Ma. Aid with feeding studies was given by Dr David Ma and Dr Christopher Holton. Tail vein cannulations and iPVN injections were done by Dr David Ma. Other *in vivo* work, including glucose tolerance tests, insulin tolerance tests and blood sample collection, were done in collaboration with Dr David Ma and Dr Chioma Izzi-Engbeaya. Oral gavage was performed by Mr Phil Rawson. All tissues were collected with Dr David Ma.

Numerous *in vitro* assays were conducted with the help of Dr David Ma, including ELISAs, RIAs, glucokinase activity, RNA extraction and reverse transcription PCR. *In situ* hybridization was performed with the aid of Dr Christopher Holton. The pilot β-cell secretion assay was done by members of Guy Rutter's lab.

Declaration of Copyright

The copyright of this thesis rests with the author and is made available under a Creative Commons Attribution Non-Commercial No Derivatives licence. Researchers are free to copy, distribute or transmit the thesis on the condition that they attribute it, that they do not use it for commercial purposes and that they do not alter, transform or build upon it. For any reuse or redistribution, researchers must the licence terms of this work make clear to others.

Acknowledgements

My sincere thanks go to my supervisor James Gardiner for his leadership and guidance during my Ph.D. I am also grateful to Professor Sir Steve Bloom for welcoming me into his department.

A big thank you goes to David Ma, not only for his invaluable assistance in the lab but also for his continued support and advice throughout my research. I also wish to thank Chris Holton for teaching me the ropes during the first year of my Ph.D., especially with *in vivo* work.

Thank you to everyone in the Department of Medicine who have helped me in any way, particularly with the *in vivo* work. I thoroughly enjoyed my time here and your support was much appreciated.

Finally, I am grateful to my family and friends, particularly Mum, Dad and Lizzie for their love and encouragement.

Abbreviations

2DG 2-Deoxyglucose

3OMG 3-O-methyl-N-acetylglucosamine

5TG 5-thio-D-glucose-6-phosphate

AAV Adeno-associated virus

ACC Acetyl-coenzyme A carboxylase

aCSF Artificial cerebrospinal fluid

ADP Adenosine diphosphate

AgRP Agouti-related peptide

Amp Ampicillin resistance gene

AMPK Adenosine monophosphate-activated protein kinase

α-MSH Alpha melanocyte stimulating hormone

ANOVA Analysis of variance

ARC Arcuate nucleus

AP Area postrema

AS Antisense

ATP Adenosine triphosphate

BBB Blood-brain barrier

BCA Bicinchoninic acid

BCP 1-bromo-3-chloropropane

BDNF Brain-derived neurotrophic factor

BLAST Basic local alignment search tool

Bp Base pairs

BSA Bovine serum albumin

BW Body weight

CART Cocaine-and amphetamine-regulated transcript

cDNA Complementary DNA

CFTR Cystic fibrosis transmembrane regulator

CNS Central nervous system

CpdA Compound A

Cre Cre-recombinase

CRR Counter-regulatory response

CSF Cerebrospinal fluid

CVD Cardiovascular disease

cGMP Cyclic guanosine monophosphate

DAPI 4',6-Diamidino-2-Phenylindole Dihydrochloride

DMEM Dulbeccos modified eagle medium

DMN Dorsal medial nucleus

DMV Dorsal motor nucleus of the vagus

DNA Deoxyribonucleic acid

dNTP Deoxynucleotide triphosphate

DR Diabetic Retinopathy

DREADD Designer receptors exclusively activated by designer drugs

DTT Dithiothreitol

DVC Dorsal vagal complex

EDTA Ethylenediaminetetraacetic acid

ELISA Enzyme-linked immunosorbent assay

FBS Foetal Bovine Serum

FI Food intake

GABA Gamma-aminobutyric acid

GDW Glass distilled water

GE Glucose-excited

GEE General estimating equation

GFP Enhanced green fluorescent protein

GI Glucose-inhibited

GK Glucokinase

GKAS GK antisense

GKRP GK regulatory protein

GKS GK sense

GLP-1 Glucagon-like peptide-1

GLUT Transmembrane glucose transporters

G-6-P Glucose-6-phosphate

GTE Glucose-Tris-EDTA

GTT Glucose tolerance test

HBS HEPES-buffered saline

HEK Human embryonic kidney

HEPG2 Hepatocellular carcinoma

HFD High fat diet

HPLC High pressure liquid chromatography

HRP Horseradish peroxidase

HSV Herpes simplex virus

ICV Intracerebroventricular

IIH Insulin-induced hypoglycaemia

iNTS Intra-NTS

IP Intraperitoneal

iPVN Intra-PVN

ITR Inverted terminal repeats

ITT Insulin tolerance test

JAK Janus kinase

K_{ATP} ATP-sensitive potassium channel

Kb Kilobase

kcal Kilo calorie

kDa Kilodalton

Kir Inward-rectifier potassium ion channel

kJ Kilo joule

Km Michaelis constant

KO Knock out

KRBH Krebs-Ringer Bicarbonate Hepes

LH Lateral hypothalamus

LHA Lateral hypothalamic area

MCH Melanin-concentrating hormone

ME Median eminence

µg Microgram

µg Microlitre

Mg Milligram

Ml Millilitre

mM Milli Molar

mRNA Messenger ribonucleic acid

MSH Melanocyte stimulating hormone

MUP Methyl umbelliferyl phosphate

MW Molecular weight

NADPH Nicotinamide adenine dinucleotide phosphate

NBD Nucleotide binding site

NCBI National Centre for Biotechnology Information

Ng Nanogram

Nl Nanolitre

nM Nano Molar

NO Nitric oxide

NPY Neuropeptide Y

NSB Non-specific binding

NTS Nucleus of the solitary tract

oGTT Oral GTT

OPD O-phenylenediamine dihydrochloride

p Probability

PASK Per-arnt-sim kinase

PBS Phosphate buffered saline

PCR Polymerase chain reaction

pH Power of Hydrogen

PNS Peripheral nervous system

POMC Pro-opiomelanocortin

PVN Paraventricular nucleus

QC Quality control

qPCR Quantitative PCR

rAAV Recombinant adeno-associated virus

rAAV-GFP rAAV enhanced green fluorescent protein

rAAV-GKAS rAAV glucokinase antisense

rAAV-GKS rAAV glucokinase sense

RER Rough endoplasmic reticulum

RIA Radioimmunoassay

RNA Ribonucleic acid

RPM Revolutions per minute

rRNA ribosomal RNA

RT Room temperature

RT-PCR Reverse transcription PCR

SA-HRP HRP-labelled streptoavidin

SAP Shrimp alkaline phosphatase

SC Spin cartridge

SDS Sodium dodecyl sulfate

SEM Standard error of the mean

SGLT Sodium-dependant glucose transporter

SSC Saline sodium citrate

SUR1 Sulfonylurea receptor 1

T2DM Type II Diabetes Mellitus

TAE Tris-acetate EDTA

TE Tris EDTA

TMB Tetramethylbenzidine

tRNA Transfer ribonucleic acid

UV Ultraviolet

VMH Ventromedial hypothalamus

VMN Ventromedial hypothalamic nucleus

V/v Volume per volume

W/v Weight per volume

WHO World Health Organisation

WPRE Woodchuck hepatitis virus post-transcriptional regulatory element

Table of contents

Chapter One – General Introduction 20

1.1 The rising prevalence of obesity 21

1.2 The central nervous system 22

1.2.1 The dorsal vagal complex 22

1.2.2 The hypothalamus 24

1.3 Neuronal regulation of energy homeostasis 26

1.3.1 The role of the dorsal vagal complex in appetite regulation 26

1.3.2 Hypothalamic regulation of feeding behaviour 27

1.3.3 The glucostatic theory of feeding 29

1.4 Glucose sensing 31

1.4.1 Hexokinases 32

1.4.2 Glucokinase 33

1.4.3 K_{ATP} channels 35

1.4.4 Glucose transporters 37

1.4.5 Hexokinase-independent mechanisms of glucose-sensing 39

1.4.6 Glucose-sensing neurons 39

1.4 Approaches for identifying the neuronal mechanisms regulating energy homeostasis 48

1.4.1 Direct administration of pharmacological agents 48

1.4.2 Genetic modification by global mutation 49

1.4.3 Selective modification 50

1.4.4 Viral vectors for genetic transfer 51

1.5 Summary 53

1.6 Hypothesis 53

Chapter Two – Materials and Methods 55

2.1 Methods for producing AAV and plasmids containing GK 56

2.1.1 Production of rAAV 56

2.1.2 Restriction endonuclease digestion 56

2.1.3 Purification of DNA fragments by electroelution 57

2.1.4 Ligation of PCR product into pTR-CGW 59

2.1.5 Transformation of competent bacteria 59

2.1.6 DNA sequencing 60

2.1.7 Large scale preparation of plasmid 61
2.1.8 Caesium chloride gradient purification 62
2.1.9 Plasmid digestion for dot blot and *in situ* hybridisation 64
2.1.10 Determination of total virus titre by dot-blot analysis 65
2.1.11 *In vitro* transfection of GKAS pTR-CGW into cultured cells 68
2.2 *In vivo* methods for investigating the role of NTS and PVN GK in energy homeostasis 69
2.2.1 Animal maintenance 69
2.2.2 Modulation of neuronal GK expression via bilateral stereotactic injection of rAAV in the NTS and PVN of rats 70
2.2.3 Unilateral stereotactic cannulation of the left PVN in rats 72
2.2.4 Intra-PVN administration of pharmacological agents 73
2.2.5 Feeding studies with genetically altered rats 74
2.2.6 Oral glucose tolerance test with genetically altered rats 75
2.2.7 Intraperitoneal glucose tolerance test with genetically altered rats 76
2.2.8 Insulin tolerance test with genetically altered rats 77
2.2.9 Oral gavage of L-arginine with genetically altered rats 78
2.2.10 Collection of tissue samples 79
2.3 *Ex vivo* methods for investigating the role of NTS and PVN GK in energy homeostasis 82
2.3.1 *In situ* hybridisation for glucokinase and WPRE mRNA 82
2.3.2 Glucokinase activity assay in isolated NTS and PVN samples 86
2.3.3 Measurement of glucose in plasma samples using a glucose oxidase assay 89
2.3.4 Measurement of insulin in plasma samples using radioimmunoassay 90
2.3.5 Measurement of insulin in plasma samples using enzyme-linked immunosorbent assay 91
2.3.6 Measurement of glucagon-like peptide 1 in plasma samples using radioimmunoassay 94
2.3.7 Measurement of bioactive glucagon-like peptide 1 in plasma samples using enzyme-linked immunosorbent assay 95
2.3.8 Measurement of glucagon in plasma samples using enzyme-linked immunosorbent assay 97
2.3.9 Measurement of glucose-stimulated insulin secretion from isolated pancreatic islets 99
2.3.10 Extraction of RNA from isolated ileum 101
2.3.11 Generating complementary DNA using reverse transcription 102
2.3.12 Measuring gene expression using quantitative polymerase chain reaction 103
2.3.13 Cresyl violet staining of ink-injected brains 105
2.4 Statistical analysis 106
Chapter 3 – The role of glucokinase in the *nucleus tractus solitarius* 108

3.1 Introduction 109
3.1.1 The NTS and appetite 109
3.1.2 Glucose-sensing neurons in the NTS 110
3.1.3 Glucokinase in the NTS 112
3.2 Hypothesis and Aims 114
3.2.1 Hypothesis 114
3.2.2 Aims 114
3.3 Results 115
3.3.1 The role of NTS GK in the regulation of appetite 115
3.3.2 The role of NTS GK in the regulation of glucose homeostasis 120
3.3.3 Verification of GK knockdown in the NTS 125
3.4 Discussion 127
3.4.1 Decreasing GK expression in the NTS does not influence feeding behaviour 127
3.4.2 NTS GK plays a role in the regulation of glucose homeostasis 128
3.4.3 Methods and measurements of altered GK activity 131
3.4.4 Conclusions 132
Chapter 4 – The role of glucokinase in the paraventricular nucleus 134
4.1 Introduction 135
4.1.1 The PVN and appetite 135
4.1.2 Glucose-sensing neurons in the PVN 137
4.1.3 Glucokinase in the PVN 138
4.2 Hypothesis and Aims 140
4.2.1 Hypothesis 140
4.2.2 Aims 140
4.3 Results 142
4.3.1 The role of PVN GK in the regulation of appetite 142
4.3.2 The role of PVN GK in the regulation of glucose homeostasis 147
4.3.3 Effects of PVN GK knockdown on glucose-stimulated insulin secretion from isolated β-cells 173
4.3.4 The role of PVN GK in ileal GLP-1 (7-36) and PYY gene expression 174
4.3.5 Verifying changes in GK activity in the PVN of genetically altered animals 176
4.3.6 Pharmacological modulation of GK and K_{ATP} channel activity in the PVN 177
4.4 Discussion 188
4.4.1 Knockdown of GK activity in the PVN does not influence feeding behaviour 188

4.4.2 PVN GK plays a role in the regulation of glucose homeostasis 189
4.4.3 Conclusions 196
Chapter Five – General Discussion 198
5.1 Introduction 199
5.2 The role of NTS and PVN GK in the regulation of energy homeostasis 199
5.3 The use of rAAV to alter the genetic expression of neuronal GK 203
5.4 Clinical implications 204
5.5 Limitations of findings 205
5.6 Future studies 207
5.7 Conclusions 210
Chapter Six - References 211
Chapter Seven - Appendix 231
7.1 Solutions 232
7.2 Coronal sections of the rat brain 242
7.2.1 Coronal section of the brainstem showing the *nucleus tractus solitarius* 242
7.2.2 Coronal section of the hypothalamus showing the paraventricular nucleus 243
7.3 Nutritional information for RM1 standard chow diet 244
7.4 DNA sequencing of plasmid for *in situ* hybridization 245
7.5 List of suppliers 245

List of figures and tables

Figure 1.1: Location of the DVC in the rat brainstem……24

Figure 1.2: Location of the various nuclei within the hypothalamus of the rat brain……25

Figure 1.3: Glucokinase activity leads to cellular depolarisation and insulin and neurotransmitter release in pancreatic β-cells and glucose-excited neurons respectively……..41

Figure 1.4: Glucokinase activity leads to neuronal hyperpolarization and inhibits neurotransmitter release in glucose-inhibited neurons……43

Figure 2.1 The pentose phosphate pathway……86

Figure 3.1: GK knockdown had no effect on the rate body weight gain compared to controls animals, both in the absence and presence of glucose solution……113

Figure 3.2: GK knockdown had no effect on food intake compared to controls animals, both in the absence and presence of glucose solution……114

Figure 3.3: GK knockdown had no effect on glucose intake compared to controls animals……115

Figure 3.4: GK knockdown had no effect on total energy intake compared to controls animals….116

Figure 3.5: NTS GK knockdown impaired glucose clearance during an oral GTT……118

Figure 3.6: NTS GK knockdown impaired insulin secretion during an oral GTT……..119

Figure 3.7: NTS GK knockdown did not significantly impair GLP-1 secretion during an oral GTT…120

Figure 3.8: NTS GK knockdown did not affect the response to insulin-induced hypoglycaemia….121

Figure 3.9: rAAV-GKAS injection was accurate and localized to the mNTS……122

Figure 3.10: GK activity in the NTS was reduced by 18% in rAAV-GKAS rats……123

Figure 4.1: GK knockdown had no effect on the rate body weight gain compared to controls animals, both in the absence and presence of glucose solution……140

Figure 4.2: GK knockdown had no effect on food intake compared to controls animals, both in the absence and presence of glucose solution……141

Figure 4.3: GK knockdown had no effect on glucose intake compared to controls animals……142

Figure 4.4: GK knockdown had no effect on total energy intake compared to controls animals, both in the absence and presence of glucose solution……143

Figure 4.5: PVN GK knockdown impaired initial glucose clearance during an oral GTT……146

Figure 4.6: The initial insulin response was impaired by PVN GK knockdown during an oral GTT……147

Figure 4.7: PVN GK knockdown disrupted the initial GLP-1 (7-36) response to glucose during an oral GTT……148

Figure 4.8: PVN GK knockdown did not significantly impair glucagon secretion during an oral GTT……149

Figure 4.9: PVN GK up-regulation enhanced initial glucose clearance during an oral GTT……150

Figure 4.10: PVN GK up-regulation increased the initial insulin response to glucose during an oral GTT……151

Figure 4.11: PVN GK up-regulation enhanced the initial GLP-1 (7-36) response during an oral GTT……152

Figure 4.12: PVN GK knockdown impaired initial glucose clearance during an i.p. GTT……155

Figure 4.13: The initial insulin response to glucose was disrupted by PVN GK knockdown during an i.p. GTT……156

Figure 4.14: GLP-1 (7-36) secretion was unaffected by PVN GK knockdown during an i.p. GTT……157

Figure 4.15: PVN GK knockdown did not affect glucagon secretion during an i.p. GTT……158

Figure 4.16: PVN GK up-regulation enhanced initial glucose clearance during an i.p. GTT……159

Figure 4.17: Up-regulation of PVN GK expression had no effect on insulin secretion during an i.p. GTT……160

Figure 4.18: GLP-1 (7-36) secretion was unaffected by up-regulation of PVN GK during an i.p. GTT……161

Figure 4.19: PVN GK knockdown did not affect the response to insulin-induced hypoglycaemia……..163

Figure 4.20: The response to insulin-induced hypoglycaemia was unaffected by the up-regulation of PVN GK expression……..164

Figure 4.21: PVN GK knockdown did not affect plasma glucose levels following oral gavage of L-arginine……..166

Figure 4.22: PVN GK knockdown did not affect plasma insulin levels following oral gavage of L-arginine……..167

Figure 4.23: PVN GK knockdown did not affect active GLP-1 (7-36) secretion following oral gavage of L-arginine……...168

Figure 4.24: PVN GK knockdown did not affect glucagon secretion following oral gavage of L-arginine……..169

Figure 4.25: Effect of PVN GK knockdown on glucose-stimulated insulin secretion from isolated pancreatic β-cells……170

Figure 4.26: Levels of GCG and PYY mRNA in genetically altered and wild-type rat ileum……..172

Figure 4.27: GK activity in the ARC, VMN and PVN of genetically altered and wild-type rats……174

Figure 4.28: The effect of iPVN injections of various pharmacological agents on plasma glucose levels during an oral GTT……177

Figure 4.29: The effect of iPVN injections of various pharmacological agents on insulin secretion during an oral GTT……..180

Figure 4.30: The effect of iPVN injections of various pharmacological agents on GLP-1 (7-36) secretion during an oral GTT……182

Figure 4.31: Confirmation of cannula placement in rats cannulated into the PVN……184

Figure 7.1: Schematic of a coronal section of the rat brainstem……237

Figure 7.2: Schematic of a coronal section of the rat brain……238

Figure 7.3: Nutritional information for RM1 standard chow diet……239

Figure 7.4: Sequence of GK-pTR-CGW-plasmid……240

Chapter One – General Introduction

1.1 The rising prevalence of obesity

The worldwide prevalence of obesity has doubled in the past thirty years. The World Health Organization (WHO) estimated that in 2014, over 1.9 billion adults were overweight, 600 million of who were obese. Alarmingly, even young children are affected by obesity as 42 million children under the age of five were found to be overweight in 2013 (World Health Organization, 2015a).

Obesity is a result of an imbalance between energy intake and expenditure (Friedman, 2003). Excess energy is stored as triglycerides in adipose tissue that act as a reserve during periods of food shortages. However the apparent lack of a mechanism preventing excess storage when food is abundant leads to uncontrolled weight gain (James, 2008).

Obesity can lead to lethal complications such as cardiovascular disease (CVD), including stroke and myocardial infarction (Morrish et al., 2001). A common result of long-standing obesity is the development of Type II Diabetes Mellitus (T2DM), a progressive chronic condition characterized by hyperglycemia and resistance to the hormone insulin (Michael et al., 2000). The WHO states that, in 2014, over 8% of the world's adult population suffered from T2DM and that it is expected to become the seventh leading cause of death by 2030 (World Health Organization, 2015b). Aside from CVD, other serious problems can arise from obesity-induced T2DM including renal failure and diabetic retinopathy (DR) causing blindness (Stevens et al., 2012).

Pharmacological agents have been relatively unsuccessful in reducing body weight and the necessity for novel therapies is becoming an increasingly pressing concern (Hussain and Bloom, 2011). Identifying the mechanisms regulating energy homeostasis will undoubtedly aid in developing novel targets for the treatment of obesity.

1.2 The central nervous system

Internal organ function is controlled by a complex network of neurons called the nervous system. This system sends, receives and interprets information from all parts of the body. It is generally classified into two parts: the central nervous system (CNS) and the peripheral nervous system (PNS) (Paxinos & Mai, The Human Nervous System, 3rd Edition, Academic Press, 2011).

The PNS essentially sends and receives information from internal organs and external stimuli and relays this information to and from the CNS, which itself processes and integrates the signals received from the periphery (Paxinos & Mai, The Human Nervous System, 3rd Edition, Academic Press, 2011). The CNS mainly consists of the brain and spinal cord. The brain is generally divided into three parts: the hindbrain, midbrain and forebrain. The hindbrain and midbrain together make up the brainstem. Some of the brainstem's numerous responsibilities include the control of autonomic functions such as breathing and heart rate (Paxinos & Mai, The Human Nervous System, 3rd Edition, Academic Press, 2011). A region of the hindbrain called the dorsal vagal complex (DVC) plays an important role in feeding behaviour (Scott et al., 2011). The forebrain, among its many functions, receives and processes sensory information, thinking, and producing and understanding language (Paxinos & Mai, The Human Nervous System, 3rd Edition, Academic Press, 2011). Within the forebrain lies the hypothalamus, a crucial region responsible for numerous homeostatic processes (Lam et al., 2009).

1.2.1 The dorsal vagal complex

The DVC is a relatively small region of the brain located in the caudal brainstem, adjacent to the fourth ventricle (Blevins et al., 2003). It is comprised of several nuclei: the nucleus of the solitary tract (also known as *nucleus tractus solitarius*, NTS), area postrema (AP) and dorsal motor nucleus of the vagus (DMV) (Fig. 1.1) (Abraham et al., 2014, De Backer et al., 2016).

The DVC is a key element in the integration of energy-related cues. It is involved in the regulation of energy homeostasis, more specifically of appetite and glycaemia (Grill and Hayes, 2009, Shapiro and Miselis, 1985, Rinaman, 2010).

The DVC processes energy status information in several ways. It directly senses alterations in levels of metabolites and hormones released by peripheral organs. Its ability to sense these changes is largely due to the AP, a circumventricular organ with highly fenestrated capillaries which allows nutrients and signalling peptides to pass through the blood-brain barrier (BBB) (Schneeberger et al., 2014, Stein and Loewy, 2010, Baraboi et al., 2010). The DVC also monitors GI tract function by integrating sensory information, such as nutrient content, transmitted from the GI tract through afferent vagal neurons (Grill and Hayes, 2009, Travagli et al., 2006). Inversely, it provides feedback through parasympathetic projections from the DVC back to peripheral organs (Shapiro and Miselis, 1985, Rinaman, 2010). Finally, DVC neurons project to the hypothalamus and merge information from sensory afferents with central pathways regulating energy homeostasis (Schneeberger et al., 2014).

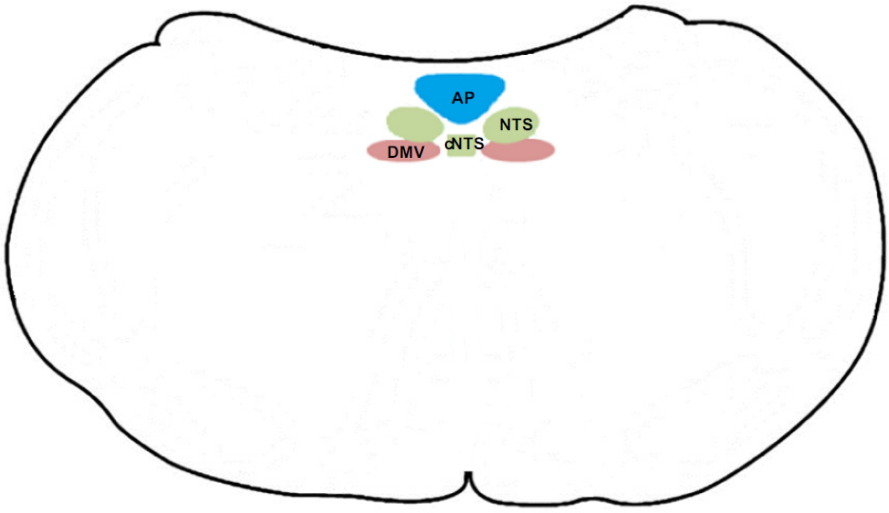


Figure 1.1: Location of the DVC in the rat brainstem. Coronal section diagram of the brainstem at coordinates: Bregma -14.04mm, interaural -5.04mm. AP: area postrema, DMV: dorsal motor nucleus of the vagus, NTS: *nucleus tractus solitarius*, cNTS: central *nucleus tractus solitarius*. Modified from De Backer et al, 2016.

1.2.2 The hypothalamus

The hypothalamus is located at the base of the brain and borders the third ventricle. It is composed of several nuclei, each of which has discrete populations of neurons (De Backer et al., 2016). The ventromedial hypothalamus (VMH) encompasses two major nuclei, the arcuate (ARC) and the ventromedial nucleus (VMN). The paraventricular nucleus (PVN) is divided into the parvocellular and the magnocellular regions. The lateral hypothalamus (LH) and the dorsal medial nucleus (DMN) are located above the VMH (Fig. 1.2) (De Backer et al., 2016).

The hypothalamus plays an important role in a number of processes including the control of body temperature, blood pressure, heart rate and circadian rhythms (Lam et al., 2009, Morrison, 2016, Schroder et al., 2014, Maranon et al., 2015, Wood and Loudon, 2014). Its major function, however, is arguably the regulation of energy homeostasis, as it is involved in both feeding behaviour and

glucose homeostasis (Hussain et al., 2015, Zheng et al., 2013, Katsurada et al., 2014). The medial ARC, which is adjacent to the median eminence, possesses capillaries which form fenestrations during times of low glucose availability to ensure the movement of glucose from the bloodstream into the ARC in order to maintain a steady nutrient supply during hypoglycaemia (Morita and Miyata, 2013). These fenestrations also permit the entry of various other macronutrients and appetite-regulating hormones into the hypothalamus and thus enable information regarding nutritional status to be conveyed to the hypothalamus (Peruzzo et al., 2000).

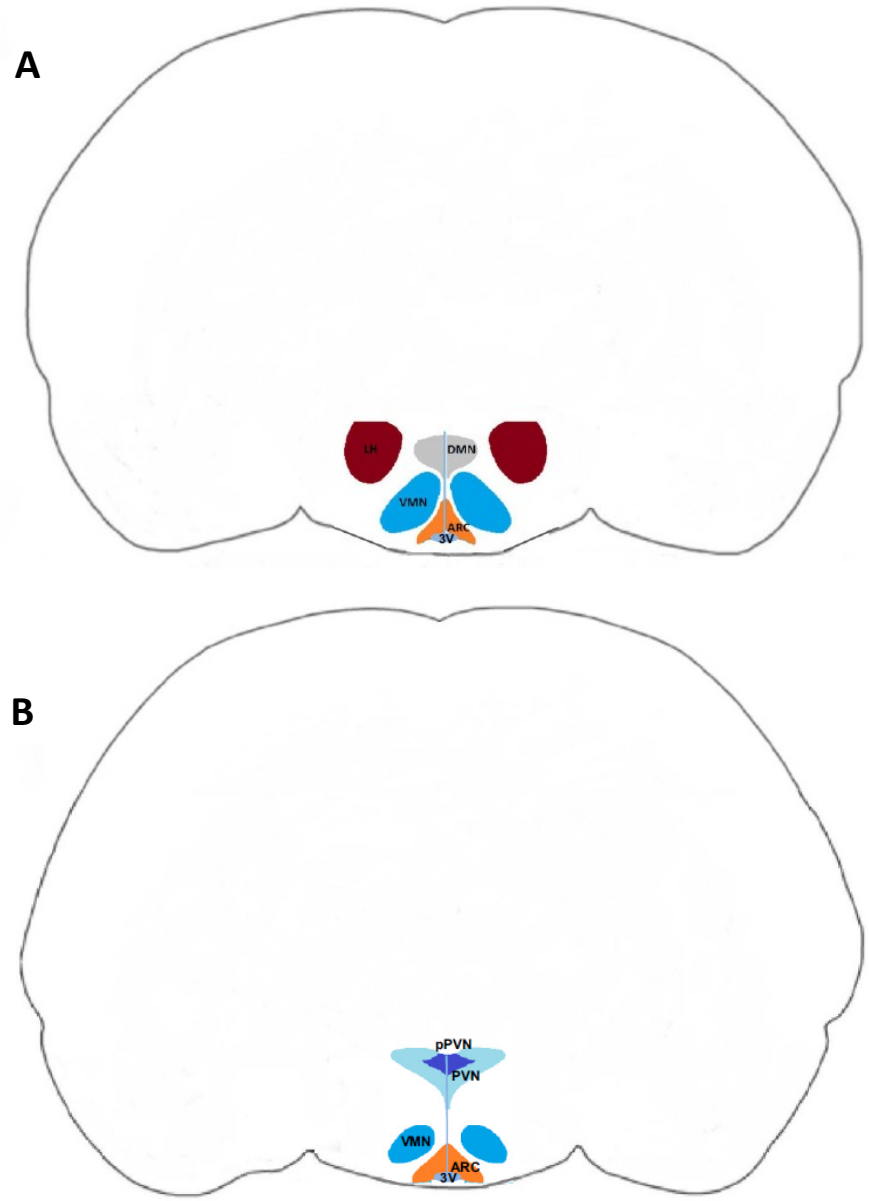


Figure 1.2: Location of the various nuclei within the hypothalamus of the rat brain. (A) Coronal section diagram of the hypothalamus at coordinates: Bregma -2.64mm, interaural 6.36mm. **(B)** Coronal section diagram of the hypothalamus at coordinates: Bregma -1.92mm, interaural 7.08mm. 3V: third ventricle, ARC: arcuate nucleus, DMN: dorsomedial nucleus, LH: Lateral hypothalamus, PVN: paraventricular nucleus, pPVN: parvocellular division of the PVN, VMN: ventromedial nucleus. Modified from De Backer *et al.*, 2016.

1.3 Neuronal regulation of energy homeostasis

Energy homeostasis controls the balance between energy intake, expenditure and body adiposity. Every cell in an organism requires an adequate source of nutrients to function properly and the continuous supply of nutrients to cells is managed by homeostatic processes.

A complex interaction of signals originating from the gut including the liver, pancreas and gastrointestinal (GI) tract regulates energy homeostasis (Buhmann et al., 2014). These signals are transmitted from the gut to the brain through various pathways, including the blood and afferent sensory vagal neurons (Buhmann et al., 2014). Information is integrated by neuronal mechanisms within the brain, particularly within the various nuclei of the hypothalamus and DVC (Grill and Hayes, 2009, Shapiro and Miselis, 1985, Rinaman, 2010, Thorens, 2011, Oh et al., 2014).

1.3.1 The role of the dorsal vagal complex in appetite regulation

The DVC is a crucial a relay centre for the transmission of signals from the gut to the forebrain. Many studies have implicated the DVC in the regulation of feeding behaviour (Emond et al., 2001, Blevins et al., 2004, Blevins et al., 2009, Hayes et al., 2010). For instance, lesions in the AP resulted in an

increase in food intake in rodents (Adachi et al., 1995). The DVC has widely been shown to play a role in the determination of meal size, and has even been suggested to be involved in the onset of nausea in humans (Grill and Hayes, 2009, Borison and Wang, 1953, Monroe et al., 2014).

Important anorexigenic peptides are expressed in the DVC. Leptin acts in the DVC to reduce appetite, as was demonstrated by ICV administration of leptin into the fourth ventricle (Scott et al., 2011, Zhao et al., 2012). Peptides such as cholecystokinin 8 (CCK8) and glucagon-like peptide 1 (GLP-1) are believed to mediate the appetite-suppressing effects of leptin and are hence crucially involved in the gut-DVC-hypothalamic pathway (Emond et al., 2001, Blevins et al., 2004, Blouet et al., 2009, Sutton et al., 2004, Williams et al., 2006). The effects of leptin may interact with those of GLP-1 in an additive manner to suppress food intake (Zhao et al., 2012). Insulin receptors are also expressed in each DVC nucleus and acute infusion of insulin directly into the DVC was sufficient to reduce food intake in rodents (Filippi et al., 2014).

The NTS is a key DVC nucleus as it is critically involved in the regulation of energy homeostasis. It is the direct recipient of afferent vagal signals from the gut and controls the subsequent relay of this information to the AP and DMV as well as to the hypothalamus (Schneeberger et al., 2014, Grill and Hayes, 2009, Travagli et al., 2006). The role of the NTS in the regulation of energy homeostasis will be discussed in detail in Chapter 3.

1.3.2 Hypothalamic regulation of feeding behaviour

The ventromedial hypothalamus (VMH) is considered a crucial centre for the regulation of energy homeostasis. Early studies revealed that lesions of the VMH produced profound hyperphagia and provided the initial evidence implicating the hypothalamus in the control of food intake

(Hetherington, 1983). The VMH appears to control food intake via the vagus nerve as the VMH ablation phenotype was considerably blunted by vagotomy (Cox and Powley, 1981). The ARC is thought to be the main VMH nucleus involved in controlling feeding behaviour as it contains both appetite-stimulating and –suppressing neurons. Anorexigenic neurons expressing pro-opiomelanocortin (POMC) and cocaine- and amphetamine-regulated transcript (CART) are activated by leptin and synapse with extra-arcuate downstream neurons to reduce feeding (Cone et al., 2001, Tong et al., 2008). Indeed, chronic ICV administration of CART led to a substantial reduction in food intake and weight gain in both lean and obese rats, although animals receiving these injections initially exhibited disturbances in locomotor activity (Larsen et al., 2000). Genetic ablation of ARC POMC neurons increased food intake and resulted in obesity (Zhan et al., 2013). The orexigenic neurons of the ARC co-express neuropeptide Y (NPY) and agouti-related peptide (AgRP) (Gropp et al., 2005, Tong et al., 2008, Kageyama et al., 2012, Minor et al., 2009, Sainsbury and Zhang, 2010). They are activated by the hunger-stimulating peptide ghrelin and are inhibited by leptin (Cone et al., 2001, Wang et al., 2014). The appetite-inducing effects of these peptides have been demonstrated as ICV injections of NPY leads to increased feeding and genetic knockdown of NPY in the ARC led to a reduction in food intake and weight gain (Stanley et al., 1986, Stanley et al., 1989, Gardiner et al., 2005). Similarly while optogenetic stimulation of just 800 AgRP neurons caused hyperphagia, post-embryonic ablation of AgRP neurons in mice produced a lean, hypophagic phenotype (Aponte et al., 2011, Bewick et al., 2005). In the VMN, brain-derived neurotrophic factor (BDNF) is an important regulator of appetite. Peripheral administration of BDNF significantly decreases food intake and ameliorates hyperglycaemia in various models of leptin resistance (Nakagawa et al., 2003, Tsuchida et al., 2001), while ICV infusion prevented excessive weight gain in obese mice with deficient melanocortin signalling (Xu et al., 2003).

The lateral hypothalamus (LH) also plays a critical role in appetite regulation as lesions in this region induced a considerable decrease in feeding (Anand and Brobeck, 1951). It contains two distinct

orexigenic neuronal populations expressing either orexin or melanin concentrating hormone (MCH) (de Lecea et al., 1998, Broberger et al., 1998). Ablating MCH neurons in mice decreased their preference for sucrose over non-caloric sweeteners (Domingos et al., 2013). Anorexigenic NPY projections from the ARC inhibit both orexin and MCH neurones and reduce food intake (Mercer et al., 2011).

The dorsomedial nucleus (DMN) of the hypothalamus is also believed to induce hunger, as was demonstrated decades ago when lesions to this nucleus produced hypophagia (Bellinger and Bernardis, 2002). This is largely attributed to NPY, as overexpression of this neuropeptide in the DMN caused hyperphagia (Zheng et al., 2013). In addition, DMN NPY expression significantly increases in rodent models of obesity (Guan et al., 1998, Bi et al., 2001). Neurons within the DMN communicate with the nearby ARC in relation to energy balance and DMN neurons have been hypothesized to modulate ARC feeding signals (Dhillo et al., 2002).

While the above hypothalamic areas are important contributors to the hypothalamic regulation of energy homeostasis, another nucleus plays a crucial role in this process. The paraventricular nucleus (PVN) expresses several peptides which are involved in the regulation of appetite. Pharmacological and genetic manipulation of these peptides has led to alterations in feeding behaviour and body weight in a number of studies, presenting the PVN as an attractive novel target for the investigation of neuronal mechanisms regulating energy homeostasis (Blevins et al., 2004, Crawley et al., 1993, Kyrkouli et al., 2006, Larsen et al., 2003, Sawchenko and Swanson, 1985, Smith et al., 2008). The role of the PVN in the regulation of energy homeostasis will be discussed in detail in Chapter 4.

1.3.3 The glucostatic theory of feeding

The glucostatic theory, first proposed by Carlson in 1916 (Carlson, 1916), became a prominent hypothesis regarding appetite regulation after it was re-considered and published by Jean Mayer approximately sixty years ago (Mayer, 1955). While he recognised that peripheral signals such as insulin must be integrated by a specific regulatory network, he believed that the main signalling molecule should be a metabolite that can affect hunger and satiety. His theory states that glucose levels determine feeding behaviour, arguing that low glucose levels in certain brain regions stimulate food intake while high concentrations induce satiety (Mayer, 1953).

Much evidence supporting the glucostatic hypothesis has been generated. First, an increase in feeding following glucoprivation has been demonstrated in numerous studies (Miselis and Epstein, 1975, Biggers et al., 1989, Dunn-Meynell et al., 2009). Accordingly, acute and chronic glucose infusion decreases food intake in rodents (Kurata et al., 1986, Davis et al., 1981). Furthermore, intravenous glucose and insulin injections have been shown to alter neuronal activity during electrophysiological studies performed as many as 50 years ago (Anand et al., 1964). Intracerebroventricular (ICV) injection of glucose reduced food intake in rats (Panksepp and Rossi, 1981, Kurata et al., 1986). Conversely injections of 2-deoxyglucose (2-DG), a non-metabolizable glucose analogue, resulted in an increase in food intake (Tsujii and Bray, 1990). More recently, hypoglycaemic and euglycaemic clamps have shown an influence of glucose levels on appetite, particularly for high-calorie foods (Page et al., 2011). The effects on food intake is specific to glucose, as ICV of glucose epimers such as D-mannose and D-galactose do not have any effect on food intake (Kurata et al., 1986).

Several studies failed to demonstrate a correlation between glycaemia and food intake, leading some to question the validity of the glucostatic theory. For instance a study demonstrated that glucose-rich foods, such as bread and rice, induced a weaker glucose response than apples while also generating a lower satiety effect in physically active humans (Bornet et al., 2007). Similarly, a

study in humans found no relationship between the glucose intake and satiety or glycaemic response as carbohydrate consumption prior to a meal had no effect on subsequent feeding behaviour compared to water consumption (Stewart et al., 1997). Furthermore, a study examining the short-term effects of insulin on feeding showed no association between independent manipulation of glucose and insulin concentration and alterations of appetite (Chapman et al., 1998).

1.4 Glucose sensing

Glucose is the primary nutrient used by the central nervous system (CNS) (Amiel, 1995). In non-diabetic humans pre-prandial glucose levels are typically 4.0-5.9mM and 2 hour post-prandial levels rise up to 8.0mM. Similar levels are observed in rodents (Wynne et al., 2005).

As it is required to maintain proper cellular function, glucose levels in the bloodstream and in cells are constantly monitored by a process named glucose sensing (Levin, 2006). Maintaining stable plasma glucose levels is essential as both hypo and hyperglycaemia can have adverse effects on an organism. For instance, hypoglycaemia impairs cognitive function and may affect a number of processes including those required for attention, speed of response and judgement (Ogunnowo-Bada et al., 2014). On the other hand, chronic hyperglycaemia can damage blood vessels and nerves and may lead to cardiovascular problems or renal failure (Morrish et al., 2001).

Variations in glycaemia are mainly detected by the pancreas, liver and brain, which act as the body's main glucose-sensing centres (Matschinsky et al., 2006, Thorens, 2011). During periods of hypoglycaemia, a phenomenon known as the counter-regulatory response (CRR) is initiated in order to restore plasma glucose levels to normal. During such times, the secretion of the pancreatic

hormone glucagon is up-regulated while that of insulin is lessened. This is mediated by the glucose-sensing centres of both the pancreas and the brain (Evans et al., 2004, Ogunnowo-Bada et al., 2014, Gerich et al., 1973, McCrimmon and Sherwin, 2010). The release of adrenaline is also increased (Verberne et al., 2014, Fanelli et al., 1992). Upon sensing a fall in glycaemia as well as a rise in plasma glucagon and adrenaline, the liver increases glucose production through glycogenolysis and gluconeogenesis (Oosterveer and Schoonjans, 2014, Szepietowska et al., 2013, Rojas and Schwartz, 2014). In addition to increased hepatic glucose production, the combination of these responses contributes to the restoration of euglycaemia by reducing glucose uptake by peripheral tissues such as muscle and adipocytes (Wang et al., 2016, Khoo et al., 2014). Conversely, rises in plasma glucose concentrations cause an increase in insulin release and decreases the secretion of glucagon from the pancreas. They also promote glucose uptake in muscle, fat, and liver, thus relieving hyperglycaemia (LeRoith, 2002). Variations in plasma glucose levels may also be counteracted by altering feeding behaviour. For instance, hyperglycaemia caused by intravenous injection of glucose decreases feeding in several mammal species (Woods et al., 1984, Burggraf et al., 1997). Conversely, insulin-induced hypoglycaemia (IIH) rapidly increases food intake (Biggers et al., 1989, Dunn-Meynell et al., 2009).

1.4.1 Hexokinases

Hexokinases are a family of enzyme which catalyse the first step of glucose metabolism by converting intracellular glucose to G-6-P. This triggers the glycolysis (breakdown of glucose to pyruvate), glycogenesis (generation of glycogen from glucose) and pentose phosphate pathways. Most hexokinases are strongly inhibited by G-6-P through a negative feedback loop (Wilson, 1995, Mayer et al., 1966).

Four kinds of hexokinases exist in mammalian cells, named hexokinase I, II, III and IV. Hexokinases I, II and III are referred to as "low-K_m" isozymes as they have a high affinity for glucose even at low concentrations (below 1mM). They are found in all mammalian tissues (Wilson, 2003, Katzen and Schimke, 1965). Hexokinase I is the main hexokinase found in the brain and is responsible for catalysing glucose phosphorylation in most cells (Wilson, 2003). Hexokinase II is the main isoform and is found in insulin-sensitive organs such as adipose, skeletal muscle and heart tissue (Roberts and Miyamoto, 2015, Tsai and Wilson, 1996). Hexokinases I and II are also expressed on the mitochondrial membrane (Wilson, 2003, Katzen and Schimke, 1965, Tsai and Wilson, 1996). Their location enables the immediate shuttling of ADP into the mitochondria following glucose phosphorylation, which aids in ATP production (Roberts and Miyamoto, 2015). Little is known about the regulatory characteristics of hexokinase III, which is substrate-inhibited by glucose at physiological concentrations (Wilson, 2003).

The main role of hexokinases I-III is glucose metabolism and ATP production. Hexokinase IV is believed to be involved in a different cellular process, glucose-sensing.

1.4.2 Glucokinase

Hexokinase IV, otherwise known as GK, is a critical component of the glucose-sensing machinery (Levin et al., 2004). Like other hexokinases, GK phosphorylates glucose to form G-6-P (Noguchi et al., 2013, Remedi et al., 2005). However, it possesses a various properties which distinguish it from the other three hexokinase isoform.

GK has a low affinity for glucose compared to other hexokinases (*K*m ~10mmol/l vs. <1mmol/l for hexokinase I-III) (Matschinsky et al., 2006). GK's higher *K*m for glucose means that it is not saturated

at physiological glucose concentrations (Efeyan et al., 2015, Printz et al., 1993). Also unlike other hexokinases, is not inhibited by the product of the reaction it catalyzes (Matschinsky et al., 2006). The rate of glucose phosphorylation by GK is therefore proportional to cellular glucose concentrations, which are in turn dependent upon plasma glucose levels.

There are two major functional isoforms of GK, neuroendocrine and hepatic GK (Thorens et al., 1988, Iynedjian et al., 1989). They are encoded by the same gene but have different splicing patterns as they possess separate promoters. Thus, these variants of the GK enzyme have the same kinetic properties but different functions (Iynedjian, 2009, Roncero et al., 2000). Neuroendocrine GK, a 465 amino acid peptide, is expressed in both β-cells and the CNS and plays a central role in glucose-sensing. It is 15 amino acids longer than the hepatic isoform (Roncero et al., 2000, Magnuson and Shelton, 1989). Neuronal GK mRNA has a comparable splicing pattern to the pancreatic isoform and is hence thought to have a similar role to the pancreatic isoform (Roncero et al., 2000, Salgado et al., 2014). Post-transcriptional processing of neuroendocrine GK produces an additional, minor form of GK in β-cells which has a lower affinity for glucose and is not thought to participate in glucose sensing (Magnuson and Shelton, 1989). In the liver, GK has a central role in promoting the uptake of glucose and its subsequent conversion to glycogen for energy storage (Thorens et al., 1988, Remedi et al., 2005, Noguchi et al., 2013, Efeyan et al., 2015, Massa et al., 2011). Mutations in the GK gene lead to abnormalities in glucose homeostasis in rodents and humans, while abnormalities in GK function in the pancreas and liver have been implicated in diabetes mellitus (Osbak et al., 2009, Baker et al., 2014).

The expression of GK mRNA and protein has been demonstrated in multiple neuronal populations in the CNS in rats, mice and humans (Lynch et al., 2000, Dunn-Meynell et al., 2002, Adachi et al., 1995, Maekawa et al., 2000, Blouet and Schwartz, 2012, Roncero et al., 2000, Roncero et al., 2004, Halmos et al., 2015, Li et al., 2003). GK is expressed in numerous hypothalamic nuclei including the arcuate

nucleus (ARC), ventromedial nucleus (VMN), paraventricular nucleus (PVN), and lateral hypothalamus (LH) (Lynch et al., 2000, Li et al., 2003). GK mRNA has also been detected in the dorsomedial nucleus (DMN), although very little is known about its function there. The activity of neuronal GK is regulated by glucokinase regulatory protein (GKRP) in some parts of the CNS including the hypothalamus; however the importance of this regulatory process in energy homeostasis is unclear (Alvarez et al., 2002). Outside of the hypothalamus GK has been identified in the medial amygdalar nucleus (MAN) (Lynch et al., 2000) and in the DVC of the brainstem in the NTS, AP and DMV (Dunn-Meynell et al., 2002, Li et al., 2003); all of which play an important part in regulating homeostatic processes. In MAN, GK-expressing neurons have been shown to project to the VMN and influence the CRR to hypoglycaemia (Zhou et al., 2010).

Hexokinases I, II and III are present in glucokinase-expressing cells, presumably to maintain a steady supply of G-6-P regardless of ambient glucose concentrations. It is possible that glucose sensing involving GK is a compartmentalised reaction within cells as not to interfere with normal ATP production. In support of compartmentalisation, glucose transporters and K_{ATP} channels are located proximal to each other on the cell membrane (Arkhammar et al., 1987).

1.4.3 K_{ATP} channels

K_{ATP} channels have been implicated in the glucose-sensing mechanism of neurons. These channels are widely expressed in numerous cell types including cardiac, skeletal muscle and smooth muscle tissue (Seino and Miki, 2003) and play a crucial role in triggering cellular depolarisation by regulating the movement of K^+ ions across the cell membrane.

K_{ATP} is an octameric protein made up of two subunits. One subunit is an inward rectifying K^+ channel, Kir6.1 or Kir6.2, which makes up the pore. The other component is sulfonylurea receptor (SUR), the regulatory subunit (Seino and Miki, 2003, Inagaki et al., 1996). The composition of K_{ATP} channels varies according to the location of their expression, giving K_{ATP} channels in each cell type different electrophysiological properties (Seino and Miki, 2003). For instance K_{ATP} channels in β-cells and hypothalamic neurons consist of K_{ir}6.2 and SUR1 (Inagaki et al., 1996, Miki et al., 2001), while the cardiac type is composed of Kir6.2 and SUR2A (Inagaki et al., 1996). The gating activity of K_{ATP} channels depends on ambient ATP and ADP concentrations. Increases in ATP, combined with the concomitant lowering of ADP, close the channel, and vice versa (Seino and Miki, 2003). ATP is believed to mediate K_{ATP} channel inhibition by acting primarily at K_{ir}6.2, as genetic manipulation of the Kir6.2 subunit significantly altered ATP's ability to cause channel inhibition (Tucker et al., 1998). ADP, on the other hand, activates K_{ATP} channels during periods of high Mg^{2+} concentrations by binding to the SUR subunit (Gribble et al., 1997).

K_{ATP} channel inhibition in β-cells prevents K^+ ions efflux and leads to insulin secretion, and mutations in this channel cause hyperinsulinaemic hypoglycaemia (Arkhammar et al., 1987, Thomas et al., 1995). These channels are therefore highly involved in the pancreas' insulin response to glucose. Kir6.2 and SUR1 are widely expressed in the CNS, including in the hypothalamus and DVC (Dallaporta et al., 2000, Evans et al., 2004, Ashford et al., 1990, Karschin et al., 1997, Li et al., 2010). Due to the similar structure of pancreatic and neuronal K_{ATP} channels, the neuronal type is also believed to be involved in glucose-sensing. Global Kir6.2 knockout markedly impaired the hypothalamic neuronal response to glucose (Park et al., 2011). Additionally, pharmacological modulation of K_{ATP} channels using sulfonylureas induced changes in the responsiveness of glucose-sensing neurons to glucose (Parton et al., 2007, McCrimmon et al., 2005). The importance of K_{ATP} channels in the mechanism of glucose-sensing neurons has been

demonstrated in ARC POMC and NPY neurons as well as in the DVC (Parton et al., 2007, Ibrahim et al., 2003, Hussain et al., 2015, van den Top et al., 2007, Dallaporta et al., 2000).

K_{ATP} channels in pancreatic β-cells and glucose-sensitive neurons are thought to couple GK activity with cellular depolarisation (Remedi et al., 2005, Hussain et al., 2015). Co-localisation of GK and K_{ATP} channels has been demonstrated in several studies (Lynch et al., 2000, van den Top et al., 2007).

1.4.4 Glucose transporters

Glucose transporters regulate the influx of glucose. They are expressed glucose-sensitive cells including pancreatic β-cells and the CNS. There are two types of glucose transporters, sodium glucose transporters (SGLTs) and facilitative transporters (GLUTs).

SGLTs use the electrochemical sodium gradient to transport glucose against concentration gradients. They are mostly expressed in the intestines and kidneys; however some neurons also express this type of transporter (Bano, 2013, O'Malley et al., 2006). The SGLT1 activator α-methylglucopyranosid stimulated neurons *in vitro*, while intracerebroventricular (ICV) injection of the SGLT1 antagonist phloridzin stimulated feeding in rats (Tsujii and Bray, 1990). SGLTs are believed to work independently of GK and K_{ATP} channels and may thus form part of an alternative neuronal glucose-sensing mechanism.

GLUTs enable the movement of glucose into a cell in a manner that is not energy-dependent and provide glucose transport under basal conditions. Fourteen isoforms of GLUT have been identified, many of which are expressed in the human brain.

GLUT1 is expressed in astrocytes and endothelial cells and plays an integral role in transporting glucose across the BBB (Simpson et al., 2001, Mueckler and Thorens, 2013). GLUT4 is found in skeletal muscle, heart, and adipose tissues and may mediate insulin-stimulated glucose uptake (Bano, 2013). GLUT6, 8 and 10 are also expressed in the brain but their specific roles in glucose homeostasis, if any, remain unclear.

GLUT3 is considered to be the main neuronal transporter of glucose uptake (Leino et al., 1997). Its high affinity for glucose (around 3mM) renders it suitable for glucose transport in the brain in a low glucose environment (Uldry et al., 2002).

GLUT2 is located in tissues exposed to large glucose fluxes, such as the intestines, liver, and kidneys (Bano, 2013). It is the main glucose transporter in pancreatic β-cells and may hence form part of the glucose-sensing mechanism of the CNS (Navarro et al., 1996, Schuit et al., 2001, Uldry et al., 2002). GLUT2 has a low affinity for glucose (17-20mM), although the GLUT2-mediated glucose uptake into β-cells is higher than the rate of glucose phosphorylation by pancreatic GK (Mueckler and Thorens, 2013). Unlike GLUT3, which is widely distributed, GLUT2 expression in the CNS is low but co-localises with GK in glucose-sensing neurons of the hypothalamus and DVC (Navarro et al., 1996, Kang et al., 2004, Roncero et al., 2004, Li et al., 2003, Maekawa et al., 2000). The importance of GLUT2 in glucose-sensing has been demonstrated in several studies. GLUT2 knockout mice have an impaired regulation of NPY expression in response to fasting and re-feeding that is not due to impaired β-cell function (Bady et al., 2006). Furthermore, ICV injection of 2-DG does not promote feeding in GLUT2 knockout mice. Selective knockdown of GLUT2 in the ARC inhibits glucose sensing and insulin secretion (Leloup et al., 1998).

1.4.5 Hexokinase-independent mechanisms of glucose-sensing

Glucose-sensing is not exclusively driven by GK. The cellular energy-sensor adenosine monophosphate-activated protein kinase (AMPK) may also act as a glucose-sensor. Knockdown of AMPK in the VMN abolished the glucagon response of rats to hypoglycaemia, and pharmacological activation of AMPK in the VMN improved it (McCrimmon, 2008, McCrimmon et al., 2006). Through a mechanism involving nitric oxide (NO) and cyclic guanosine monophosphate (cGMP), it may enable the depolarisation of ventromedial hypothalamic neurons in response to a decrease in ambient glucose concentrations (Murphy et al., 2009), with hyperglycaemia having the opposite effect (Canabal et al., 2007). Per-arnt-sim kinase (PASK) may also be involved in neuronal glucose-sensing. Its expression changes based on variations in glucose levels and it may form part of the glucose-sensing mechanism of AMPK (Hurtado-Carneiro et al., 2013, Hurtado-Carneiro et al., 2014). Glucose-sensing may also be mediated by SGLT 1-3 (O'Malley et al., 2006). The mechanism by which signals from different metabolites are integrated to generate a net neuronal output effecting homeostasis and the complex interplay between neuronal sensors such as SGLTs, AMPK and PASK still needs further investigation.

1.4.6 Glucose-sensing neurons

Glucose-sensing also occurs within the CNS in order to allow the brain to regulate peripheral metabolic functions involved in energy and glucose homeostasis. Neurons which are sensitive to glucose are referred to as glucose-sensing neurons as they detect changes in extracellular glucose concentrations and alter their activity accordingly. Two types of glucose-sensing neurons exist. In response to an increase in glucose levels, glucose-excited (GE) neurons increase the frequency of

their action potentials while glucose-inhibited (GI) neurons decrease their firing rate (Spanswick et al., 2000, Song et al., 2014).

The neuroendocrine isoform of GK is involved in the glucose-sensing machinery of both GE and GI neurons (Dunn-Meynell et al., 2002, Kang et al., 2006, Jetton et al., 1994, Alvarez et al., 1996). For instance, in a low glucose environment pharmacological activation of GK increased neuronal activity of GE neurons and decreased that of GI neurons, as demonstrated by changes in Ca^{2+} oscillations (Kang et al., 2006, Routh, 2002, Kang et al., 2004).

GE neurons detect changes in glucose concentrations via a similar mechanism to pancreatic β-cells (Hussain et al., 2015, Levin et al., 2004). Phosphorylation of glucose by GK results in the closure of K_{ATP} channels and leads to neuronal depolarisation, causing Ca^{2+} entry and the release of a neurotransmitter (Fig. 1.3). In addition to GLUT2 transporters, glucose may enter GE neurons via sodium-dependent glucose transporters (SGLT) and drive glucose-sensing in a K_{ATP} channel-independent manner. As opposed to GLUT2 transporters, SGLTs enable glucose entry against the concentration gradient. The SGLT1 activator α-methylglucopyranosid activates GE neurons in primary cultures of rat hypothalamic neurones independent of K_{ATP} channel sensitivity and may thus be part of an alternative mechanism for GE neuron glucose-sensing (O'Malley et al., 2006).

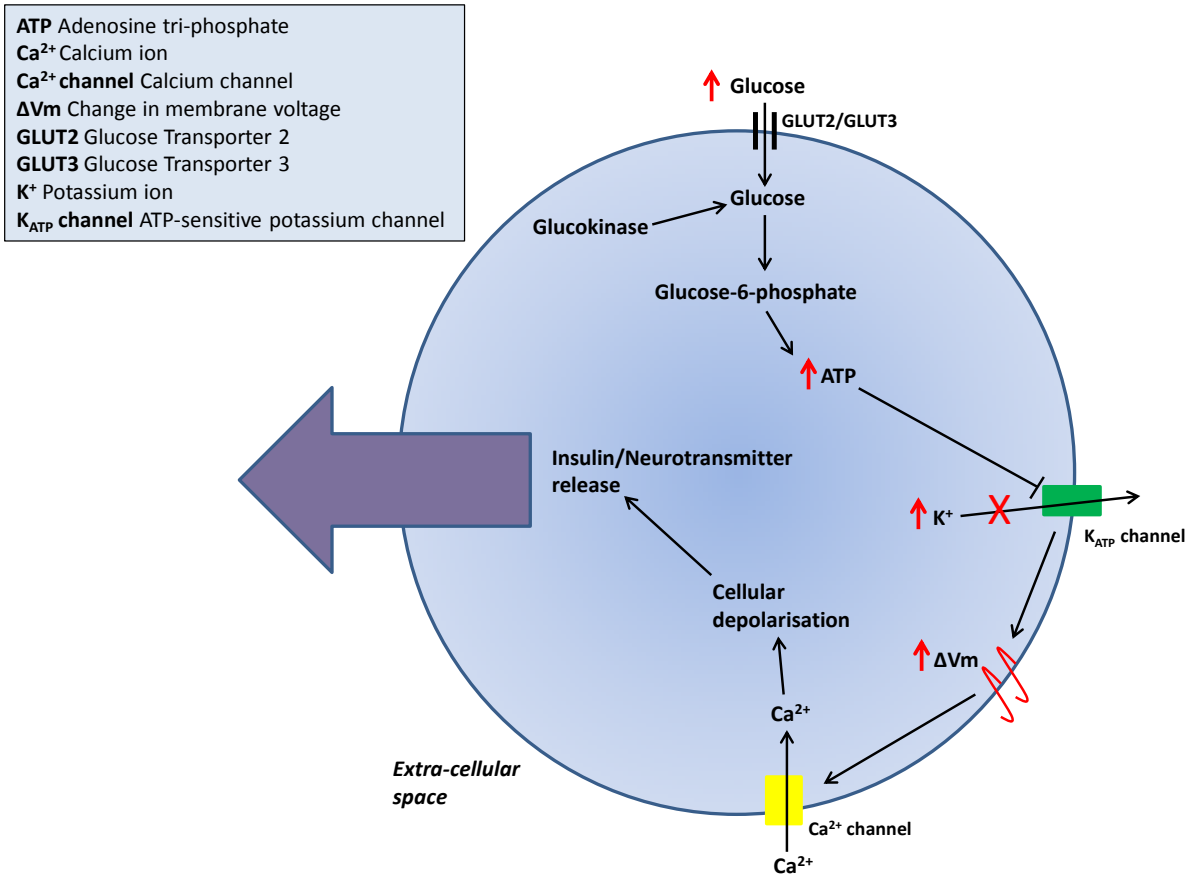


Figure 1.3: Glucokinase activity leads to cellular depolarisation and insulin and neurotransmitter release in pancreatic β-cells and glucose-excited neurons respectively. As extra-cellular glucose concentrations increase, glucose is taken up into the islet cell predominantly by GLUT2 and into the neuron predominantly via GLUT3 glucose transporters. Once in the cytosolic space, glucose is phosphorylated by glucokinase to form glucose-6-phosphate. Although this reaction consumes adenosine tri-phosphate (ATP), the levels of ATP ultimately rise due to further glycolysis of glucose. The coupling of glucose entry with glycolysis and ATP production allows the increase in ATP concentration to inhibit ATP-sensitive potassium (K_{ATP}) channels. This prevents the efflux of K^+ ions. As a result K^+ ions accumulate within the neuron and the membrane potential of the cell rises. The difference in membrane voltage triggers the influx of Ca^{2+} ions through voltage-gated Ca^{2+} channels. Ca^{2+} entry causes cellular depolarisation, which in turn leads to an action potential. This proposed mechanism allows glucokinase to function as a glucose-sensor by coupling glucose availability with β-cell and neuronal activity and insulin and neurotransmitter release, respectively (De Backer et al., 2016).

The glucose-sensing mechanism of GI neurons is less understood than that of GE neurons and may occur via several different molecular mechanisms (Thorens, 2012). While it is believed that GI neuronal glucose-sensing depends on glucose transporters and GK, the involvement of K_{ATP} channels is unlikely (Kurita et al., 2015, Murphy et al., 2009, Burdakov et al., 2005, Song and Routh, 2005, Fioramonti et al., 2004, Canabal et al., 2007). Inhibiting GK activity altered the kinetics of intracellular Ca^{2+} concentration oscillations in GI neurons, indicating that GK is involved in glucose-sensing in GI neurons. Their activity is reduced in the presence of glucose due to hyperpolarization of the cell. The extent of GK involvement is unclear although hyperpolarization has been proposed to occur via stimulation of Na^{+}/K^{+} ATPase pumps caused by a glucokinase-induced rise of ATP levels within neurons, leading to inhibition of neuronal activity (Fig. 1.4) (Kurita et al., 2015). An alternative, glucokinase-independent mechanism has also been postulated. GI neurons may become hyperpolarized following glucose-induced activation of post-synaptic cystic fibrosis transmembrane regulator (CFTR) Cl^{-} channels via the activation of adenosine monophosphate-activated protein kinase (AMPK) and nitric oxide signalling (Burdakov et al., 2005, Song and Routh, 2005, Murphy et al., 2009). CFTR channels regulate chloride ion flow and may control membrane potential in GI neurons (Sheppard and Robinson, 1997).

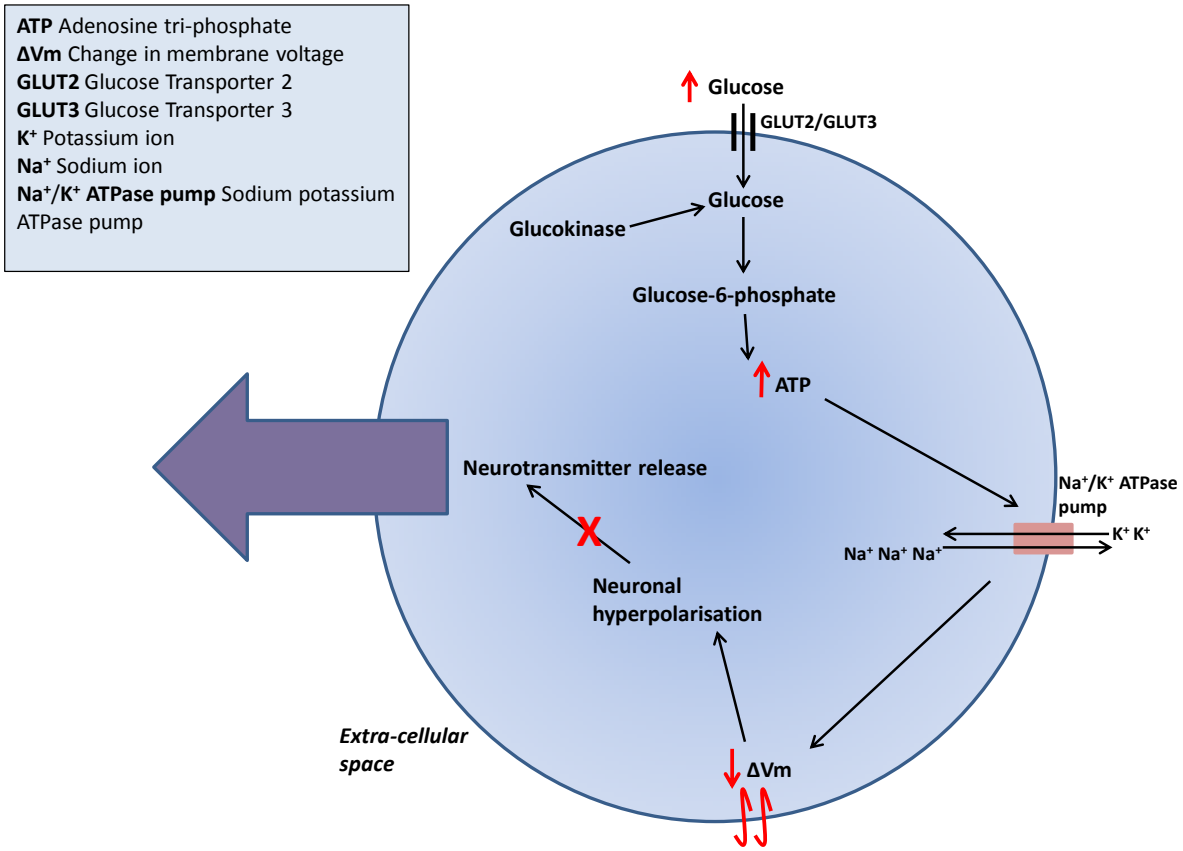


Figure 1.4: Glucokinase activity leads to neuronal hyperpolarization and inhibits neurotransmitter release in glucose-inhibited neurons. As extra-cellular glucose concentrations increase, glucose is taken up into the islet cell predominantly by GLUT2 (Thorens, 2014) and into the neuron predominantly via GLUT3 glucose transporters (Uldry et al, 2002). Once in the cytosolic space, glucose is phosphorylated by glucokinase to form glucose-6-phosphate (Matschinsky et al, 2006). Although this reaction consumes adenosine tri-phosphate (ATP), the levels of ATP ultimately rise due to further glycolysis of glucose. The coupling of glucose entry with glycolysis and ATP production allows the increase in ATP concentration to stimulate sodium potassium ATPase (Na+/K+ ATPase) pumps. For one ATP molecule, each pump pumps three Na+ ions out of the cell and enables the entry of two K+ ions. This causes a decrease in membrane voltage and results in hyperpolarization of the cell (Kurita et al, 2015), ultimately leading to a decrease in neuronal firing (De Backer et al., 2016).

1.4.6.1 Glucose-sensing neurons of the dorsal vagal complex

All three nuclei of the DVC are sensitive to glucose, indicating an important role in glucose-sensing (Adachi and Kobashi, 1985, Blouet and Schwartz, 2012, Adachi et al., 1995, Funahashi and Adachi, 1993). Neurons of the DVC are both activated and inhibited by rising glucose concentrations, indicating that both GE and GI neurons are present (Balfour et al., 2006). Indeed, electrophysiological recordings of brainstem slices demonstrated that glucose stimulated some AP neurons and inhibited others (Funahashi and Adachi, 1993, Riediger et al., 2002).

The DVC is considered an important centre for glucose homeostasis. The NTS and DMV have been implicated in various homeostatic responses. For instance, detection of variations in glucose levels by the CNS activates vagal projections to the pancreas via the DMV and NTS (Loewy and Haxhiu, 1993). Parasympathetic preganglionic fibres innervating the pancreas emanate from the DMV and stimulation of this pathway increases insulin, glucagon and somatostatin release (Streefland et al., 1998, Rinaman and Miselis, 1987, Berthoud and Powley, 1990, Berthoud and Powley, 1987, Berthoud, 2006, Love et al., 2007).

Various glucose-sensing components are expressed in the DVC. Some neurons express K_{ATP} channels while the presence of GLUT2 has also been shown, particularly in the NTS and AP (Maekawa et al., 2000, Lamy et al., 2014, Balfour et al., 2006, Blake and Smith, 2012). GK is also found in all three DVC nuclei and these three components are co-expressed in certain neurons, suggesting a glucose-sensing role of these neurons (Navarro et al., 1996, Maekawa et al., 2000, Lamy et al., 2014, Balfour et al., 2006).

The AP has been proposed as an important glucose-sensing site of the DVC, in part because it is a circumventricular organ enabling more glucose to enter the CNS than other brain regions (Schneeberger et al., 2014, Stein and Loewy, 2010, Baraboi et al., 2010). Tanycytes in the AP closely

resemble those in the median eminence, suggesting that ambient glucose concentrations in the AP may more accurately reflect those of plasma glucose than other brain regions (Langlet et al., 2013). Peripheral injections of gold thioglucose, which is toxic to glucose-sensitive neurons, produced lesions in the AP of golden hamsters and caused gliosis in the DVC of mice (Brown and Floody, 1987, Powley and Prechtl, 1986). Lesions of the AP suppressed the feeding response induced by monosodium glutamate, an excitotoxin targeting glucose-responsive neurons that does not cross the BBB (Ritter and Stone, 1987).

The NTS integrates afferent sensory signals and relays them to the hypothalamus, as well as to the efferent preganglionic neurones of the DMV (Travagli et al., 2006, Craig, 1996, Burcelin and Thorens, 2001). While it is known to play a crucial role in the relay of energy-related signals between the hypothalamus and the viscera, its involvement in this process and the mechanism by which this occurs remain relatively unclear. My thesis therefore focuses on the role of the NTS in the regulation of energy homeostasis, which will be discussed in Chapter 3.

1.4.6.2 Hypothalamic glucose-sensing neurons

The hypothalamus has long been described as an important centre for the regulation of glucose-sensing (Thorens, 2012, Burdakov et al., 2005, Dunn-Meynell et al., 2009, Lam et al., 2009, McCrimmon, 2008, Mountjoy and Rutter, 2007, Routh, 2002). Glucokinase is expressed in several hypothalamic nuclei, including the ARC and VMN. Extracellular VMH glucose concentrations vary between 0.5 and 2.5mM and can rise as high as 4.5mM during bouts of hyperglycaemia, whereas concentrations remain around 0.5mM in other regions of the CNS (de Vries et al., 2003, Wang et al., 2004). The neuroendocrine form of GK is most sensitive to glucose concentrations ranging from 0.5 to 2.5mM, identifying the VMH as ideal for glucose sensing (Kang et al., 2006).

The VMH is a major hypothalamic glucose-sensing region. For instance, intra-carotid infusion of glucose led to activation of VMH neurons, indicating that changing plasma glucose levels alter neuronal activity in the VMH (Guillod-Maximin et al., 2004). ICV injection of glucose reduced food intake in rats while injection of 2-DG increased it (Tsujii and Bray, 1990) . Injection of 2-DG into the VMH also raised blood glucose concentrations (Borg et al., 1995). These results suggest that varying glucose concentrations within the VMH are detected by glucose-sensing neurons, which alter energy intake accordingly to maintain homeostasis.

Pharmacological activation of K_{ATP} channels in the VMH enhanced the CRR to hypoglycaemia in rats (McCrimmon et al., 2005). K_{ATP} channels thus appear to play a role in glucose-sensing neurons and may help to adapt VMH neuronal activity to changing glucose concentrations. The role of K_{ATP} channels in the CRR is supported by Evans *et al*, who reported that iVMH injection of K_{ATP} channel blockers reduced the glucagon and adrenaline responses to brain glucopenia (Evans et al., 2004).

Glucose-sensing properties have been demonstrated in both the ARC and the VMN (Yang et al., 2004, Hussain et al., 2015). Electrophysiological recordings in rats revealed that 14-19% of VMN neurons are GE while 3-14% are GI (Song et al., 2001, Dunn-Meynell et al., 2002). In the medial portion of the ARC, 14% of neurons are GI and 3% are GE; in the lateral portion of the ARC, 13% of neurons are GE and 1% are GI (Wang et al., 2004).

Following the detection of acute drops in blood glucose, VMN glucose-sensing neurons may respond by sending signals to the pancreas and adrenal glands to stimulate glucagon secretion and adrenaline, respectively, in order to raise circulating glucose concentrations (Levin et al., 2008). The glucose-sensing enzyme GK has been linked to the mediation of this response. Increasing GK activity *in vivo* decreases the release of several peripheral hormones including adrenaline, noradrenaline

and glucagon. In contrast, reducing the expression or activity of VMN GK elicits the opposite response by stimulating adrenalin release and increasing glucose availability (Levin et al., 2008).

Whole cell patch clamp recordings performed on mouse brain slices showed that most POMC neurons of the ARC have GE properties (Ibrahim et al., 2003). For instance, selective knockout of K_{ATP} channels in these neurons prevents glucose-induced depolarisation (Parton et al., 2007). In contrast, most GI responses occur in NPY neurons (Muroya et al., 1999). These studies suggest that POMC neurons are GE while NPY neurons are GI in type. Upon detecting increases in circulating glucose levels, ARC POMC neurons activate the melanocortin system to induce satiety (Cone et al., 2001). NPY neurons have been linked to a taste-independent mechanism promoting the consumption of glucose-rich foods (Hussain et al., 2015), likely activated to restore euglycaemia when glucose levels are low.

A glucose-sensing role of certain LH neurons was demonstrated when neuronal activity was altered by varying glucose concentrations. The firing rate of LH glucose-sensitive neurons (forming about 30% of LH cells) increased following a reduction in glucose concentration. Raising glucose levels had the opposite effect, suggesting that LH glucose-responsive cells are GI in type (Silver and Erecinska, 1998). The glucose-sensing centre of the LH is traditionally divided into two sections, the lateral hypothalamic area (LHA) and the perifornical area. Both LH areas possess glucose-sensing properties, as increases in peripheral glucose concentrations induced c-fos immunoreactivity (Stanley et al., 2013), and contain orexin-expressing neurons which are activated by hypoglycaemia (Moriguchi et al., 1999, Cai et al., 2001, Briski and Sylvester, 2001).

1.4 Approaches for identifying the neuronal mechanisms regulating energy homeostasis

Numerous approaches enable the investigation of physiological processes regulating energy homeostasis *in vivo*. Neuronal mechanisms can be examined using pharmacological agents delivered directly into neurons of interest through a permanent indwelling cannula. Genes of interest can be genetically modified to observe the effect on a system. This can be done either through global or selective modification, depending on whether it needs to be modified in an entire organism or in a particular tissue. Viral vectors can also be utilised to induce genetic changes in targeted areas.

1.4.1 Direct administration of pharmacological agents

The role of specific neuronal peptides in the regulation of energy homeostasis has been investigated by direct administration of pharmacological compounds in brain regions associated with this process. This is performed via insertion of a permanent indwelling cannula in the area of interest. For example, intracerebroventricular (ICV) injections into the third ventricle are often performed to examine the role of the hypothalamus in energy homeostasis. This approach has revealed much about the neuronal control of appetite, including the role of ghrelin, leptin, glucagon-like peptide 1 (GLP-1) and oxytocin, and glucose homeostasis (Sakurazawa et al., 2013, Arletti et al., 1990, Nowak and Bojanowska, 2008, da Silva et al., 2015, Miselis and Epstein, 1975). Intra-nuclear injections are also used to investigate the role of particular peptides in specific nuclei in this process (Hussain et al., 2015, Evans et al., 2004, Stanley et al., 2013). The physiological role of neuronal GK in glucose-sensing was also investigated using these methods, particularly in the hypothalamus (Hussain et al., 2015, Osundiji et al., 2010).

1.4.2 Genetic modification by global mutation

The role of specific genes can be studied in the long term by selectively alter the expression of genes and comparing the resulting phenotype with appropriate controls. Global mutation has been used extensively in mice to examine the involvement of many genes in the regulation of energy homeostasis (Grupe et al., 1995, Imai et al., 2007, Wynick and Bacon, 2002). For instance a global knockout of leptin causes substantial weight gain and hyperphagia, demonstrating its importance in satiety signalling (D'Souza A et al., 2014).

Although global mutations are commonly used, they possess several limitations which restrict their value. The existence of compensatory mechanisms to rectify the loss or gain of function of a protein has been established (Barbaric et al., 2007). Transgenic mice also experience health complications, as global gene modification can affect its function in other organs. For example knocking out AgRP or NPY does not affect food intake or body weight compared to wild types, however post-embryonic ablation of AgRP or NPY neurons results in a lean phenotype and hypophagia (Qian et al., 2002, Bewick et al., 2005, Erickson et al., 1996, Luquet et al., 2005, Mercer et al., 2011).

Global mutations have been used to study the function of glucokinase. Homozygous ablation of the glucokinase gene results in death within one week (Yang et al., 2007, Remedi et al., 2005). In addition, hexokinases do not appear to compensate for the loss of GK, highlighting its physiological importance as a glucose-sensor and to development. Heterozygous glucokinase knockout mice, although they express a milder phenotype, still exhibit impaired glucose homeostasis and insulin-resistance (Baker et al., 2014). The limitations of global transgenic models demonstrate a need for

targeted genetic modifications, which would avoid complications by leaving the gene expression outside of the area of interest intact.

1.4.3 Selective modification

Gene expression can be altered in specific tissues using site specific recombinase technology, a technique which relies on the flanking of a gene of interest by Lox-P sequences. This site is cleaved by Cre-recombinase (Cre), an enzyme which removes or inverts DNA situated between Lox-P sequences (Hoess and Abremski, 1985), when a mouse expressing Cre is crossed with a mouse that has lox-P sites intersecting the gene of interest (Orban et al., 1992). A site-specific promoter ensures that the modification of the gene of interest takes place specifically in cells expressing the promoter, leaving the gene in other tissues intact.

Cre-Lox recombination has been used extensively to study the neuronal control of energy homeostasis. For instance, it revealed that hypothalamic non-POMC non-AgRP neurons are greatly involved in mediating NPY-induced hyperphagia by disrupting of GABAergic release from these neurons (Kim et al., 2015). It was also shown using this technology that leptin acts directly on GLP-1-expressing neurons of the hindbrain to regulate feeding as mice lacking the GLP-1 receptor in these neurons were hyperphagic (Scott et al., 2011).

Despite the numerous advantages of Cre-Lox recombination studies using this technology can only be performed in transgenic mice, which can be costly and time-consuming to generate. In addition, developmental compensation may occur and the required promoters are not universally expressed and may not be present in the area of interest.

1.4.4 Viral vectors for genetic transfer

Genetic transfer can be performed in specific sites within the CNS through stereotactic injection of DNA. Other methods exist to deliver DNA within host cells, such as the use of liposomes or electroporation; however they yield variable and short-lasting results (Lam and Dean, 2010, Gardlik et al., 2005). Similarly, injection of naked DNA does not efficiently transfect the targeted tissue. The most effective way to yield selective genetic modification *in vivo* is to package the DNA into a viral vector. These vectors utilise the properties of viruses to insert their genome into the host cell nucleus and utilise the host's machinery to replicate their genetic information.

A number of different viruses have been tested to perform genetic transfer. These include adenovirus, herpes simplex virus (HSV), retrovirus, lentivirus, and adeno-associated virus (AAV) (Kantor et al., 2014). Adenovirus can pack large sequences of DNA and has a fast rate of transgene expression, which can occur as quickly as one or two days post-delivery (Lentz et al., 2012). However despite numerous genetic modifications to reduce its immunogenicity, this viral vector causes strong immune responses and is therefore not appropriate for *in vivo* transfection (Muruve, 2004). Although several genetic modifications have been performed to improve its use and despite its ability to carry large transgenes, HSV is not utilised as a vector for gene transfer as it is pathogenic and cytotoxic in neurons (Krisky et al., 1998). Retroviral vectors are able to integrate into the host's chromosomes to increase their effectiveness, however with the exception of the lentivirus; they are unable to transfect non-dividing cells (Roe et al., 1993, Bukrinsky et al., 1993), which decreases their value as viral vectors in the research of CNS-regulated energy homeostasis. Lentivirus, on the other hand, is a viable vector for gene delivery in numerous tissues, including the CNS (Consiglio et al., 2001, Kantor et al., 2014). However, it poses a potential safety risk during production as it is evolved from the human immunodeficiency virus, and a replication-competent virus can potentially be

generated (Consiglio et al., 2001). This vector has also been suggested to spread further than the targeted brain area, thus limiting its value when examining neuronal pathways (Blomer et al., 1997).

AAV is considered one of the safest and most viable vectors for genetic modification (Lentz et al., 2012). It integrates stably into the host cell gene, has no known associated pathologies and causes a very mild immune response as it cannot replicate without a helper virus (Atchison et al., 1965, Kantor et al., 2014). In addition, it has a small genome which can be easily manipulated to include a transgene for gene delivery, although this means that only small transgenes can be packaged into the vector (Xie et al., 2002). The long-lasting effects of AAV are a strong advantage, as effects have been reported to last for over 6 months in mouse brain and 10 years in the human brain (Klein et al., 1999, Leone et al., 2012). It is made of single stranded DNA which needs to be converted into double stranded DNA after its insertion into the host genome, a process which can take up to 3 weeks *in vivo* (Sonntag et al., 2010). Upon delivery to the nucleus, AAV uses its genomic inverted terminal repeats (ITRs) to self-prime the synthesis, using host-cell machinery, of its complementary DNA strand (Daya and Berns, 2008). Multiple serotypes of AAV exist, each having distinct tissue selectivity and transduction efficiency based on the composition of the capsid protein. Twelve human serotypes and over 100 primate serotypes have been identified, each having tropism for particular cell types (Howard et al., 2008). AAV2 is the most widely used serotype (Kantor et al., 2014). It has a tropism for neurons and is hence often used in studies involving gene delivery to the CNS (Gardiner et al., 2005). Much of the viral genetic material is removed, such as Rep and Cap coding sequences, and instead expressed on a helper plasmid. This creates a larger insertion cassette for the transgene. Among the remaining viral DNA are ITRs located at both ends, which are essential for transfection. AAV2 attaches to the cell using the cellular receptor heparan sulfate proteoglycan and enters it by interacting with several membrane-bound receptors including $\alpha_V\beta_5$ integrins, fibroblast growth factor receptor 1, hepatocyte growth factor receptor, $\alpha_v\beta_1$ integrin, and laminin receptor (Summerford and Samulski, 1998, Summerford et al., 1999, Qing et al., 1999, Kashiwakura et al.,

2005, Asokan et al., 2006, Akache et al., 2006). It may be internalized through clathrin-coated vesicles, a process which appears to be partially dependent on dynamin activity (Duan et al., 1999). Intracellular trafficking to the nucleus is thought to be mediated by the activation of the Rac1 protein as well as endosomal cysteine proteases and cathepsin B and L (Sanlioglu et al., 2000, Akache et al., 2007). The exact mechanism by which AAV enters the nucleus is currently unclear. Transfection of rAAV containing GK antisense (GKAS) and sense (GKS) has previously been successful *in vivo* in our laboratory (Hussain et al., 2015). Once synthesized by the host neuron, the GKAS strand binds to GK mRNA and causes its degradation via RNase H, thus inhibiting translation of the protein (Ezquer et al., 2005). GKS induces the generation of GK mRNA and thus promotes GK activity.

1.5 Summary

The CNS integrates metabolic and hormonal signals from the gut to regulate energy intake. The hypothalamus and the brainstem are critically involved in this process. The role played by some nuclei contained within these brain regions is well documented while that of others remains unclear. Evidence supports the involvement of the NTS and PVN in the regulation of energy homeostasis. Both regions express the enzyme GK; however its function within these metabolic centres has not been investigated. This project examines the physiological role of GK in the NTS and the PVN in the regulation of glucose homeostasis and feeding behaviour. The findings presented in this thesis may provide a gateway for novel treatments of obesity and T2DM.

1.6 Hypothesis

GK in both the NTS and PVN is hypothesized to play an important role in energy homeostasis. It is likely to play an important role in generating the satiety response to food. Additionally, it may contribute to the regulation of glucose homeostasis by mediating glucose clearance from the blood following a meal, perhaps via the release of insulin.

Chapter Two – Materials and Methods

2.1 Methods for producing AAV and plasmids containing GK

2.1.1 Production of rAAV

The recombinant AAV (rAAV) was generated by Dr James V Gardiner and Dr Sufyan S Hussain (Division for Diabetes, Endocrinology and Metabolism) as well as by Dr Errol Richardson (Division of Women's Health, King's College London). Full length glucokinase (GK) complementary deoxyribonucleic acid (cDNA) was isolated and amplified by polymerase chain reaction (PCR) from the plasmid pCMV4.GKB1 encoding full length GK cDNA (gift from Prof. Magnuson, Nashville).
To construct GK sense (GKS) and antisense (GKAS), GK DNA was cloned in the forward and reverse orientation, respectively, into the plasmid pTR-CGW (gift from Dr. Verhaggen, Amsterdam). A two-plasmid system with a helper plasmid pDG was utilized to produce recombinant AAV particles (Grimm et al., 1999), which were then recovered and purified using an iodixanol gradient to make rAAV-GKS and rAAV-GKAS.

2.1.2 Restriction endonuclease digestion

The fragment of interest was isolated via restriction endonuclease digestion. The previous PCR products from isolated GK cDNA were cut using the restriction endonucleases BamH1 and BsaI.

Materials

GK-pTR-CGW plasmid (AAV-CMV-eGFP-WPRE-Amp)

Restriction endonuclease: BamHI (New England Biolabs, Hitchin, UK)

10x Restriction buffer (New England Biolabs)

10x Bovine serum albumin (BSA) (New England Biolabs)

Shrimp alkali phosphatase (SAP) 4U/µl (GE Healthcare, Pollards Wood, UK)

Phenol/chloroform pH8 (VWR, Lutterworth, UK)

2M Sodium acetate pH5.2 (Appendix I)

100% ethanol (VWR)

Methods

In separate microcentrifuge tubes, GK-pTR-CGW was diluted in glass-distilled water (GDW). Restriction buffer as well as bovine serum albumin (BSA) was added to give a final concentration of 1x. BamHI and BsaI (30U each) were then added to give the volume of enzyme added as less than 10% of the final volume. The reaction was incubated at 37°C for at least 1 hour. 8U SAP, which prevents self-ligation of the plasmid by removing 5" phosphate groups, was added to one reaction 30 minutes prior to the end of the incubation. The nucleic acids were extracted with an equal volume of phenol/chloroform and the phases separated by centrifugation for 3 minutes at 13,000xg. The deoxyribonucleic acid (DNA) was ethanol precipitated using absolute ethanol and sodium acetate (pH 5.2). It was incubated at -20°C for at least one hour, following which the DNA was recovered by centrifugation at 13,000xg for 7 minutes.

2.1.3 Purification of DNA fragments by electroelution

The DNA fragment was purified and any contaminating fragments were removed following the PCR reaction. This was performed as the maximal efficiency of restriction digests is not attained with plasmids as small amounts of closed plasmid DNA could produce a high background during transformations. The DNA was therefore size fractionated by electrophoresis on an agarose gel and the bands of interest electroeluted.

Materials

Agarose, type II-A medium EEO (VWR)

50x TAE (Appendix I)

Ethidium Bromide (10mg/ml) (VWR)

Dialysis tubing (VWR)

Gel loading buffer (Appendix I)

1Kb plus DNA marker (Thermo Fisher Scientific, Paisley, UK)

DNA fragments

Methods

A 1% (w/v) agarose gel was prepared. 3g agarose and 6ml 50X TAE were added to 300ml GDW. The mixture was boiled and allowed to cool. 13µl ethidium bromide was then added to the mixture before being poured into a cassette.

The DNA product from restriction digestion was dissolved in 20µl GDW. 6µl loading buffer was added, after which 1µl of DNA marker was added to 9µl GDW and 3µl loading buffer. The samples were loaded onto the agarose gel and electrophoresed at 10V/cm.

The DNA was visualised by illumination with ultraviolet (UV) light at 300nm. Using a scalpel, the band of interest was cut out from the gel and placed into dialysis tubing which had one end sealed with a clip. 400µl of 0.5x TAE was added to the gel slice. The DNA was eluted from the gel by electrophoresis at 20V/cm for 20 minutes. The TAE was then removed from the tubing, after which the DNA was recovered via phenol/chloroform extraction and ethanol precipitation.

The quantity of DNA was then measured using a spectrophotometer. 10µl DNA was diluted 1:100 in a quartz cuvette and absorbance was read at 260nm and 280nm using a UV 1101 spectrophotometer (WPA). As proteins and phenol absorb more strongly at 280nm than DNA, reading the absorbance at 280nm reveals the level of purity of the sample. The concentration of the DNA was calculated using the following formula:

Concentration (µg/ml) = (A_{260} x dilution factor) x 50

2.1.4 Ligation of PCR product into pTR-CGW

Materials

T4 DNA ligase, 6U/µl (New England Biolabs)

10x Ligase buffer (New England Biolabs)

Digested plasmid: insert (27ng/µl) and cut plasmid (46ng/µl)

Methods

The digested GK was incorporated into the pTR-CGW plasmid using DNA ligation. 20ng of digested plasmid DNA were dissolved in GDW, after which a fourfold molar excess of PCR product was added. Ligase buffer (1x final concentration) and 6U T4 DNA ligase were added to give a final volume of 10µl. The reaction was incubated at 16°C overnight.

2.1.5 Transformation of competent bacteria

The plasmid containing GK was introduced into bacterial cells by adding calcium chloride to the environment. The divalent cations open temporary pores in the bacterial plasma membrane and reduce electrostatic repulsion between the bacterial cell membrane and the plasmid, thus enabling the movement of the plasmid into the cells. The efficiency of the transformation was enhanced by introducing a sudden increase in temperature. PTR-GCW contains an ampillicin resistance gene, and subsequent incubation allows the expression of the resistance genes. The cells were then exposed to the antibiotic to discard cells which have not taken up the plasmid.

Materials

LB culture medium (Appendix I)

LB (amp) plates (Appendix I)

E. coli BL21 bacteria (Thermo Fisher Scientific) in frozen aliquots of 0.1M $CaCl_2$ and 15% glycerol

Methods

5ng of ligation products were added to an aliquot of thawed bacteria, mixed gently and incubated on ice for 10 minutes. The mixture was then incubated for 45 seconds at 42°C, then immediately placed on ice again and allowed to cool. Following the addition of 450µl LB, the mixture was shaken vigorously at 250 rotations per minute (RPM) at 37°C for 1 hour. 150µl of the transformed bacteria were then added to previously warmed agar plates supplemented with 100µg/ml ampicillin. The bacteria were spread over the surface of the agar. The plate was then inverted and incubated at 37°C overnight. The colonies that had undergone transformation were collected and sequenced.

2.1.6 DNA sequencing

Sequencing of GKS-pTR-CGW plasmid was conducted by the Imperial College Genomics Core Laboratory.

Materials

GKS-pTR-CGW

20µM GK forward primer 5'-ACGTACCGGTATTCACATCTGGTACCTGGG -3' (Oswel DNA Service)

20µM GK reverse primer 5'-AGCTCGTACGTATTAGGACAAGGCTGGTGG-3' (Oswel DNA Service)

Methods

200ng of plasmid DNA was diluted and mixed with 3.2pmole of the reverse primer used in the initial generation of the plasmid. Cycle sequencing of the samples was performed using BigDye v3.1 (Thermo Fisher Scientific, Paisley, UK). The results of the DNA sequencing were analysed for homology to known rat GK gene sequences using the Basic Local Alignment Search Tool (BLAST) on the National Centre for Biotechnology Information (NCBI) website.

2.1.7 Large scale preparation of plasmid

A large supply of high quality plasmid was obtained by performing a large scale preparation of a plasmid, or maxi prep.

Materials

LB (amp) (Appendix I)

GTE (Appendix I)

Lysozyme (Sigma-Aldrich, Gillingham, UK)

0.2M sodium hydroxide/1% (w/v) SDS (Appendix I)

5M potassium acetate (KAc) (VWR)

Propan-2-ol (VWR)

100x TE buffer (Appendix I)

DNase free RNase A 10mg/ml in GDW (GE Healthcare)

Phenol/Chloroform (VWR)

Eppendorf 5417R Centrifuge (Eppendorf, Stevenage, UK)

Methods

A small quantity of bacteria containing pTR-CGW was inoculated into 500ml LB (amp) and incubated overnight at 37°C with shaking (250 RPM). The samples were split into two and the bacteria recovered by centrifugation for 8 minutes at 3000xg at 4°C, after which the pellets were re-suspended in 12.5ml GTE containing lysozyme (2mg/ml). The samples were subsequently incubated for 5 minutes at room temperature (RT). Twenty five millilitres of NaOH/SDS were added to the samples. They were then mixed by inversion and incubated on ice for 5 minutes until they became clear. 18.75ml 5M KAc were added and the samples were again mixed by inversion and incubated on ice for 5 minutes. The samples were then centrifuged at 9000xg for 10 minutes at 4°C in an Eppendorf 5417R Centrifuge (Eppendorf) to remove bacterial debris and the supernatant was transferred to a clean tube containing 0.6 volumes of isopropanol and incubated on ice for 15 minutes. The samples were again centrifuged at 9000xg for 15 minutes at 4°C to recover the bacterial DNA, following which the pellets were dissolved in 5ml GDW and combined together. 100µl 100x TE and 0.1mg/ml RNase A were added and the samples were incubated at 37°C for 60 minutes. The reaction was extracted with an equal volume of phenol/chloroform and phase separation was performed by centrifugation for 20 minutes at 10000xg and 4°C. The DNA was recovered by first adding 0.1 volumes 2M sodium acetate (pH 5.2) and one volume isopropanol and then incubating the samples at -20°C for at least one hour. The DNA was then purified by caesium chloride gradient as detailed in the section below.

2.1.8 Caesium chloride gradient purification

Large scale plasmid purification was carried out using a caesium chloride gradient (Sambrook J., 1989). This purification method is based on ethidium bromide's ability to decrease the density of nucleic acids by binding to them. It intercalates into DNA, which causes unwinding of the helix. In closed circular DNA such as plasmids where supercoiling is increased, the binding of ethidium

bromide is limited. This gives the plasmid a higher buoyant density than linear or nicked plasmids. The difference in buoyant density enables the separation of the plasmid on a caesium chloride density gradient.

Materials

TES: 50mM Tris-HCL (pH 8.0), 50mM NaCl, 5 mM EDTA in GDW (Appendix I)

Caesium chloride (Boehringer Ingelheim, Bracknell, UK)

10mg/ml ethidium bromide (VWR)

Caesium chloride-saturated propan-2-ol (Appendix I)

Sorvall 100SE centrifuge (Thermo Fisher Scientific)

Methods

DNA obtained from large scale plasmid purification was recovered by centrifugation for 20 minutes at 24,000xg at 4°C. The DNA was then dissolved in 8.20ml TES, after which 8.4 grams of caesium chloride were dissolved in the DNA solution. 200µl of ethidium bromide were then added and the solution was mixed by shaking. The sample was divided into two polyallomer tubes (Ultracrimp, Du Pont), balanced, and overlaid with paraffin oil. The tubes were sealed and centrifuged for 16 hours at 20°C and 60,000 RPM in a T-8100 rotor in a Sorvall 100SE centrifuge (Thermo Fisher Scientific). DNA bands were visualised by UV illumination following centrifugation. Using a 20-gauge needle and a 2ml syringe, the band containing the closed pTR-CGW DNA was removed. Ethidium bromide was then removed from the plasmid by repeated extraction with an equal volume of caesium chloride saturated isopropanol until both phases became colourless. Two volumes of GDW and six volumes of absolute ethanol at RT were added to induce precipitation of the DNA, which was then recovered by centrifugation at for 20 minutes 24,000xg and 20°C. After the supernatant was discarded, the DNA pellet was dissolved in 0.4ml GDW, ethanol precipitated with 0.1 volume of sodium acetate and 2.5 volumes of absolute ethanol at -20°C for 60 minutes and recovered by centrifugation for 7 minutes

at 13,000xg. The DNA was then air dried for 10 minutes before being dissolved in 1ml GDW. GK-pTR-CGW was quantified by spectrophotometric measurement at a wavelength of 260nm, for which 10µl of DNA was diluted 1:00 and placed into a quartz cuvette. Protein contamination was confirmed by a low absorbance at 280nm as phenol absorbs more strongly at 280nm than DNA. The concentration of DNA was determined using the following formula:

Concentration (µg/ml) = (A_{260} x dilution factor) x 50

2.1.9 Plasmid digestion for dot blot and *in situ* hybridisation

GK-pTR-CGW plasmid was cut by restriction endonucleases to produce a linear cDNA fragment that could be used for dot blot analysis and *in situ* hybridisation.

Materials

GK-pTR-CGW (1.6mg/ml) and pTR-CGW (4.5mg/ml)

Restriction endonuclease: BamHI (New England Biolabs)

10x Restriction buffer (New England Biolabs)

10x Bovine serum albumin (BSA) (New England Biolabs)

Phenol/chloroform pH8 (VWR)

2M Sodium acetate pH5.2 (appendix I)

Absolute ethanol (VWR)

Methods

Samples were subjected to endonuclease digestion as described in 2.1.2 (without SAP). The antisense probe was produced by cutting GK-pTR-CGW using BamHI. PTR-CGW containing WPRE

antisense was prepared by Dr Errol Richardson by digesting the plasmid with BamHI. Products were diluted to a final concentration of 200ng/µl using GDW.

2.1.10 Determination of total virus titre by dot-blot analysis

As the concentration of rAAV indicates the level of transgene expression to be expected, the total particle number was determined by dot-blot analysis. This technique follows a similar principle to that of northern and southern blotting. It measures the amount of ribonucleic acid (RNA) or DNA present in a sample using a radio-labelled probe. In dot-blot analysis, the sample being analysed is placed directly onto a membrane rather than being separated by size and transferred to a membrane. The accuracy of DNA analysis by dot-blot is greater than that of other techniques such as RT-PCR as the probe, which uses the original genome sequence, has a higher specificity.

Materials

RAAV-GFP, rAAV-GKS and rAAV-GKAS viral preparations

Solution A: 10mM Tris-HCl (pH 8.0), 1mM MgCl2 and 8U/ml DNase I in GDW (Appendix I)

Solution B: 10mM Tris-HCl (pH 8.0), 100mM NaCl, 10mM EDTA, 0.5% SDS and 1mg/ml proteinase K in GDW (Appendix I)

Phenol: chloroform: iso-amyl alcohol (pH 8.0) 25:24:1 (VWR)

5M Glycogen (5mg/ml) (Thermo Fisher Scientific)

100% Ethanol (VWR)

75% Ethanol

2M Sodium acetate (pH 5.2) (Appendix I)

Denaturing solution: 2M NaCl in 0.5M NaOH (Appendix I)

Neutralising solution (pH 7.5): 2M NaCl, 0.5M Tris-HCl (Appendix I)

PTR-CGW plasmid (4.5mg/ml)

Hybridisation buffer for Northern blot analysis (Appendix I)

Woodchuck post-transcriptional regulatory element (WPRE) cDNA fragment

5x ABC Buffer containing deoxynucleotides, random oligonucleotides and mercaptoethanol (Appendix I)

BSA, fraction V (10mg/ml) (Sigma-Aldrich)

(α-32P)-dCTP: 10Ci/ml, 3Ci/mol (Perkin Elmer, Wokingham, UK)

DNA polymerase I, Klenow fragment (9U/µl) (GE Healthcare)

Sephadex G50 (Appendix I)

1x TE (pH 7.5) (Appendix I)

Amasino wash buffer: 1mM Na phosphate buffer (pH 7.2), 1mM EDTA and 2% SDS in GDW (Appendix I)

Universal wash buffer: 0.2% SDS and 0.02x SSPE in GDW (Appendix I)

Nylon filter paper (Hybond N+, GE healthcare)

Eppendorf 5417R Centrifuge (Eppendorf)

Methods

Forty five microlitres of solution A were added to 5µl rAAV virus stock and incubated for 30 minutes at 37°C. Two hundred microlitres of solution B were then added and the sample was incubated at 55°C for one hour. An equal volume of phenol/chloroform was added to extract the DNA and the phases were separated by centrifuging the sample at 13,000xg for 3 minutes. The top phase containing the DNA was ethanol precipitated by adding 0.1 volumes sodium acetate, 40µg glycogen and 2.5 volumes ice cold 99.7-100% ethanol and incubating the mixture at -20°C for one hour. The solution was then centrifuged for seven minutes at 8,000xg and 4°C in an Eppendorf 5417R Centrifuge (Eppendorf) and the supernatant discarded, after which the pellet was washed in 450µl 75% ice cold ethanol. It was then centrifuged as before and the supernatant was removed and air-

dried. The pellet was re-suspended in 10µl GDW and 1µl applied to a nylon membrane. A standard curve (0.1 to 50ng) made from the original plasmid pTR-CGW was also applied. The membrane was washed for five minutes in denaturing solution then twice for five minutes in neutralising solution. It was then baked at 80°C for two hours. 10ml hybridization buffer without probe was added to a heat sealed polythene bag for pre-hybridization. The membrane was placed into the bag, which was then incubated at 60°C for four hours.

A cDNA fragment of WPRE was used as a probe for rAAV transgenes. 20ng of DNA in 13µl GDW were boiled for five minutes. The solution was then made up to a total volume of 25µl using 1x ABC buffer, 2mg/ml BSA, 10µCi dCTP and 1U Klenow. The reaction was incubated at 37°C for at least one hour. A mini Sephadex G50 column was used to assess the integration of radio-labelled nucleotide into the DNA probe. To prepare the column, a glass Pasteur pipette was plugged with glass wool and Sephadex G50 added. The volume of the labelling reaction was made up to 200µl 1x TE before being loaded onto the column. The column was then eluted with 1x TE and 200µl fractions collected. The fractions were counted and the percentage incorporation calculated, following which the hottest two fractions were pooled and half was boiled and added to 10ml hybridisation buffer. The pre-hybridisation buffer was emptied from the polythene bag and fresh buffer containing probe was added, after which the bag was re-sealed. Hybridisation was carried out overnight at 60°C.

Following hybridization any non-specifically bound probe was removed by washing the membrane. This consisted of three separate washes in amasino wash buffer at 60°C for twenty minutes, followed by three additional twenty minute washes in universal wash buffer at 60°C. The filter was then exposed to a storage phosphorimager screen (GE Healthcare) for 48 hours after being sealed in a clean plastic bag. Radio-labelled areas were visualised and quantified by image densitometry using ImageQuant software (GE Healthcare). Quantification was performed by comparing viral DNA to known amounts of pTR-CGW in the standard curve.

2.1.11 *In vitro* transfection of GKAS pTR-CGW into cultured cells

Before in vivo experiments could be performed with rAAV-GKAS, the ability of the plasmid to reduce GK activity was measured *in vitro* in a hepatocellular carcinoma (HEPG2) cell line by Dr Errol Richardson (Division of Women's Health, King's College London). This type of cell is known to express high levels of GK, thus allowing the determination of the effects of GKAS plasmid on GK expression.

Materials

Human hepatocellular carcinoma (HEPG2) (ATCC)

Dulbeccos modified eagle medium (DMEM) (Thermo Fisher Scientific)

Foetal Bovine Serum, heat inactivated (FBS) (Thermo Fisher Scientific)

2.5% Trypsin in hanks balanced salt solution (Thermo Fisher Scientific)

Versene (appendix I)

2x HEPES-buffered saline (HBS) (appendix I)

2M calcium chloride (appendix I)

40µg/ml plasmid DNA in 0.1x TE

DMEM (Thermo Fisher Scientific)

Methods

HEPG2 cells were cultured in DMEM containing 4.5mg/ml glucose and 1mM sodium pyruvate supplemented with 10% (v/v) FBS at 37°C in 5% carbon dioxide. Fresh medium was added to replace the old one every three days. When the cells reached 70-80% confluence, they were sub-cultured using 0.25% trypsin in versene. This was done by aspirating the medium before incubating the cells with fresh trypsin/versene for 5 minutes at 37°C to detach them from the flask. 10ml of fresh medium were subsequently added to inactivate the trypsin. The cells were recovered by

centrifugation at 100xg for 5 minutes, after which they were re-suspended in fresh medium and transferred to a new flask at a 1:10 dilution.

The transfection of cells was performed at approximately 60% confluence. They were sub-cultured and plated in 90mm Petri dishes (density: $1x10^4$cells/cm^2). The following day, the medium was changed. Large quantities of exogenous DNA were transfected using calcium phosphate co-precipitation. A co-precipitate was formed by mixing 300µl 10xHBS with 28µg plasmid DNA in 2.5ml GDW and slowly adding 180µl 2M calcium chloride. The solution was gently mixed while aerating it with a pipette aid. It was then incubated for 5 minutes at RT to allow precipitation to occur. The precipitate was added to the cells before incubating them for 18 hours at 37°C in 5% carbon dioxide, following which the medium containing the precipitate was replaced with fresh media. The cells were then incubated for 48 hours, after which they were lysed in GK extraction buffer. A GK activity assay was performed as described below.

2.2 *In vivo* methods for investigating the role of NTS and PVN GK in energy homeostasis

2.2.1 Animal maintenance

Male Wistar rats (specific pathogen free, Charles River UK Ltd) were individually housed and maintained under a controlled environment (temperature 21-23°C, 12 hour light-dark cycle, lights on at 07:00) with *ad libitum* access to standard chow (RM1 diet, Special Diet Services UK Ltd), except where stated, and water. All animal procedures were approved under the British Home Office Animals (Scientific Procedures) Act 1986 (Project Licence no. 70/7229). Prior to all experiments, animals were acclimatised to the Imperial College animal holding rooms for 7 days. For each study,

animals were pseudo-randomised to treatment and control groups of approximately equal mean and standard error of mean bodyweight.

2.2.2 Modulation of neuronal GK expression via bilateral stereotactic injection of rAAV in the NTS and PVN of rats

Endogenous GK expression was altered through the use of rAAV encoding either GKAS to knockdown GK expression or GKS to increase it. In separate studies, rAAV-GKAS (titre: $3.42x10^{12}$ genome particles/ml) or rAAV-GKS (titre: $2.96x10^{12}$ genome particles/ml) was bilaterally injected either into the NTS or PVN of male Wistar rats by means of a stereotactic frame. RAAV encoding green fluorescent protein (GFP), which is often used as a marker of successful gene transfer and has been shown to be effective in mammalian cells (Zhang et al., 1996), was used as a control in all studies (titre: $5.04x10^{12}$ genome particles/ml).

Materials

Stereotactic frame (Kopf Instruments, Tujunga, CA, USA)

Isoflurane (Abbott Laboratories Ltd, Maidenhead, UK)

Betadine (10% w/v povidine-iodine solution) (Seton Scholl Healthcare Ltd, London, UK)

RAAV-GFP (titre: $5.04x10^{12}$ genome particles/ml)

RAAV-GKS (titre: $2.96x10^{12}$ genome particles/ml)

RAAV-GKAS (titre: $3.42x10^{12}$ genome particles/ml)

Amoxicillin powder for injection (500mg) (CP Pharmaceuticals, Wrexham, UK)

Flucloxacillin powder for injection (500mg) (CP Pharmaceuticals, Wrexham, UK)

0.9% NaCl (Braun Medical Ltd., Sheffield, UK)

Buprenorphine hydrochloride (Temgesic) (0.3mg/ml) (Schering-Plough Ltd., Welwyn Garden City)

Internal cannula custom cut to length (Plastics One, Sevenoaks, UK)

Guide cannula custom cut to length (Plastics One)

Electric Micro Motor Drill (Foredom, Bethel, CT, USA)

Programmable Syringe Pump (World Precision Instruments, Hitchin, UK)

Method

The working area was disinfected using 70% ethanol and surgical tools sterilised by incubation at 200°C for two hours. Male Wistar rats (approximately 250g) were anesthetised under 2L/minute oxygen and 4% isoflurane. Upon the loss of the pedal reflex they were mounted onto a stereotactic frame (Kopf Instruments). The surgical area was shaved and cleaned with betadine. A rostro-caudal incision approximately 1cm in length was made in the skin over the vertex of the skull using a disposable scalpel, following which bregma was exposed by removing the periosteum from the underlying bone. According to coordinates calculated previously using the 'The rat brain in stereotactic coordinates' (Franklin and Paxinos, 2007), bilateral burr holes were drilled using an electric micro motor drill (Foredom) mounted onto the stereotactic frame. The coordinates used for the injections in the NTS were 13.8mm posterior to bregma, ±0.7mm lateral to bregma and 7.8mm below the skull surface and 1.8mm, ±0.5mm and 8mm for the PVN, respectively. The injection (rAAV-GFP, rAAV-GKS or rAAV-GKAS) was delivered at a rate of 12µl/hour over five minutes using a stainless steel injector and a programmable syringe pump (World Precision Instruments). Following the injection, the cannula and injector were kept in position for five minutes to limit back-diffusion before being slowly withdrawn. 1µl of AAV was injected per side in each rat (n=12 per group). The scalp incision was then sutured using a 4.0 polypropylene suture (Ethicon).

After surgery, rats were placed in a warming chamber to aid recovery. Prophylactic flucloxacillin (50mg/kg) and amoxicillin (50mg/kg) as well 2.5ml 0.9% NaCl were administered intraperitoneally to prevent injections and for rehydration, respectively. Analgesia was provided by subcutaneous injection of 0.12mg/kg buprenorphine hydrochloride at anaesthetic induction.

2.2.3 Unilateral stereotactic cannulation of the left PVN in rats

Stereotactic cannulation enables the injection of drugs directly into the nucleus of interest in freely moving, conscious animals. It was utilized so that the effects of a compound on energy homeostasis could be measured immediately after the injection.

Materials

Stereotactic frame (Kopf Instruments)

Isoflurane (Abbott Laboratories Ltd)

Betadine (10% w/v povidine-iodine solution) (Seton Scholl Healthcare Ltd)

Amoxicillin powder for injection (500mg) (CP Pharmaceuticals)

Flucloxacillin powder for injection (500mg) (CP Pharmaceuticals)

0.9% NaCl (Braun Medical Ltd)

Buprenorphine hydrochloride (Temgesic) (0.3mg/ml) (Schering-Plough Ltd)

Guide cannula custom cut to length (Plastics One)

Acrylic dental cement and powder (Kemdent, Swindon, UK)

Miniature 1.6 x 3 stainless steel screws (Montrose Fasteners, High Wycombe, UK)

Dummy cannula custom cut to length (Plastics One)

Electric Micro Motor Drill (Foredom)

Methods

Animals were prepared and placed onto a stereotactic frame (Kopf Instruments) as described previously. Anaesthetic, analgesia and antibiotics were administered as previously detailed. A unilateral burr hole was drilled using an electric micro motor drill (Foredom) according to

coordinates listed previously; 1.8mm posterior to bregma and -0.5mm lateral to bregma. A stainless steel guide cannula held by an arm mounted onto the stereotactic frame was inserted 7mm below the skull surface to allow 1mm projection to reach the target of interest during iPVN injections. Three stainless steel screws were then gently inserted into the skull using a hand drill to act as anchors. Dental acrylic was used to hold the cannula securely in place with support from the mounting screws. This was left to dry and the scalp incision was sutured over the pedestal if necessary with a 4.0 polypropylene suture (Ethicon). A dummy cap was screwed onto the cannula to prevent infection.

At the end of the study, 1µl India ink was injected through the cannula, the brains were dissected and cresyl violet staining was performed on brain slices to assess the accuracy of the PVN cannulation.

2.2.4 Intra-PVN administration of pharmacological agents

The effects of direct administration of various pharmacological agents into the PVN on glucose homeostasis were examined. This was performed in a cross-over study on iPVN-cannulated animals prior to an oral glucose tolerance test (oGTT), the procedure of which is described in section 2.2.6. The concentration of each compound was based on results from previous studies and the literature.

<u>Materials</u>

CpdA (Calbiochem, Nottingham, UK)

Diazoxide (Sigma-Aldrich)

Glibenclamide (Sigma-Aldrich)

D-glucose (Sigma-Aldrich)

Internal cannula custom cut to 7mm with 1mm projection (Plastics One)

Guide cannula custom cut to 7mm (Plastics One)

Programmable Syringe Pump (World Precision Instruments)

Methods

The glucokinase activator compound A (CpdA) (Calbiochem), K_{ATP} channel blocker glibenclamide (Sigma-Aldrich, Gillingham, UK) and K_{ATP} channel activator diazoxide (Sigma-Aldrich) were administered directly into the PVN at concentrations 0.5nmol, 2nmol and 1nmol, respectively. D-Glucose (Sigma-Aldrich) was also injected into the PVN - at a concentration of 1.5mg/ml - to test the ability of this nucleus' glucose-sensing machinery to respond to a local, central rise in glucose concentration. For each compound, a single injection of 1µl was administered. The internal injector used was cut 1mm longer than the implanted cannula to ensure microinjection into the left PVN. The injection was administered at a speed of 120µl/hour using a programmable syringe pump (World Precision Instruments). Before being withdrawn, the injector was left in position for thirty seconds after the end of the injection in order to reduce back-diffusion into the cannula.

2.2.5 Feeding studies with genetically altered rats

Changes in chow intake and body weight of the animals that received a bilateral injection of rAAV-GKAS or rAAV-GFP into the NTS or PVN were monitored three times per week for 33 days. The animals had *ad libitum* access to standard diet and water during the feeding study.

Chronic glucose feeding studies were also conducted, in which animals were provided with *ad libitum* 10% (w/v) glucose solution alongside the water bottles. The animals were acclimatised to the glucose solution prior to the start of the study for a period of 72-96 hours. Appropriate concentrations of glucose solution were calculated previously. Body weight (BW), glucose and chow intake were measured three times per week for 33 days.

For both acute and chronic glucose feeding studies, total caloric intake was measured. It was calculated using 16.035kJ/g for RM1 diet (appendix II) and 16.0kJ/g for glucose.

2.2.6 Oral glucose tolerance test with genetically altered rats

An oral glucose tolerance test (GTT) was performed on rats that had received a bilateral injection of rAAV-GFP, rAAV-GKS or rAAV-GKAS in either the NTS or PVN. Previous work has demonstrated that rats will voluntarily consume glucose presented to them during a GTT, thus eliminating the need for i.p. delivery which may increase the release of stress hormones and hence influence plasma glucose levels. As with the feeding studies, each animal was acclimatised to drinking glucose solution by being given *ad libitum* access to 10% glucose solution in addition to water for 72-96 hours prior to start of the study.

Materials

Restraining tube (Vet Tech Solutions Ltd, Congleton, UK)

21 gauge needles (Tyco Healthcare Ltd, Hampshire, UK)

24 gauge/19mm Cannulae (Millpledge Veterinary, Retford, UK)

Zinc Oxide surgical adhesive tape (Millpledge Veterinary)

Heparin sodium 1000IU/ml (Wockhardt)

Microvette CB300 LH (Sarstedt, Leicester, UK)

20% glucose solution (Clintech, Guildford, UK)

Contour glucose test strips (Bayer, Newbury, UK)

Glucometer (Bayer)

Methods

Animals were fasted overnight prior to the study. In the morning they were placed in a warming cabinet at 39°C for two minutes to expose the tail vein, after which they were placed within a restraining tube and a 24 gauge/19mm cannula was inserted into the tail vein. The cannula was fixed onto the tail using adhesive tape. A small dose of heparin diluted 1:10 in 0.9% NaCl was then injected into the cannula to prevent clotting.

A basal blood sample (approximately 250µl) was collected. A 21 gauge needle was inserted into the cannula and a collection tube was clipped onto it to allow the efflux of blood from the cannula into the tube. A 2.5g/kg dose of glucose (20% dextrose diluted in GDW) was then administered orally to each animal. Following glucose consumption, additional blood samples were taken at 15, 30, 60 and 120 minutes post-glucose. A glucose reading was also recorded at each time point using a Contour glucose test strip (Bayer) and a glucometer (Bayer). Heparin was administered after each sample to prevent clotting.

Following the study, the animals were returned to their cage and given *ad libitum* access to standard diet and water. Plasma was separated from blood cells by centrifugation at 13,000xg for 5 minutes at 4˚C and was stored at -80°C.

2.2.7 Intraperitoneal glucose tolerance test with genetically altered rats

An i.p. glucose tolerance test (GTT) was performed on rats that had received a bilateral injection of rAAV-GFP, rAAV-GKS or rAAV-GKAS in the PVN. This test was performed to verify whether i.p. delivery alters the release of stress hormones and influences plasma glucose levels.

Materials

Restraining tube (Vet Tech Solutions Ltd)

21 gauge needles (Tyco Healthcare Ltd)

24 gauge/19mm Cannulae (Millpledge Veterinary)

Zinc Oxide surgical adhesive tape (Millpledge Veterinary)

Heparin sodium 1000IU/ml (Wockhardt)

Microvette CB300 LH (Sarstedt)

20% glucose solution (Clintech)

Contour glucose test strips (Bayer)

Glucometer (Bayer)

Methods

The study was conducted following the protocol described in 2.2.5, with the following exception. Instead of an oral dose of glucose, each animal received an intraperitoneal injection of 1.2g/kg D-glucose.

2.2.8 Insulin tolerance test with genetically altered rats

An insulin tolerance test was performed on rats that had received a bilateral injection of rAAV-GFP, rAAV-GKS or rAAV-GKAS in the PVN. The dose of insulin administered was determined from literature as well as from previous studies.

Materials

Humulin S, soluble insulin 100 IU/ml (Eli Lilly & Co. Ltd, Basingstoke, UK)

Restraining tube (Vet Tech Solutions Ltd)

21 gauge needles (Tyco Healthcare Ltd)

24 gauge/19mm Cannulae (Millpledge Veterinary)

Zinc Oxide surgical adhesive tape (Millpledge Veterinary)

Heparin sodium 1000IU/ml (Wockhardt)

Microvette CB300 LH (Sarstedt)

20% glucose solution (Clintech)

Contour glucose test strips (Bayer)

Glucometer (Bayer)

Methods

The study was conducted following the protocol described in 2.2.5, with the following exception. Instead of an oral dose of glucose, 2IU/kg insulin was administered intraperitoneally to each animal.

2.2.9 Oral gavage of L-arginine with genetically altered rats

An oral gavage of the amino acid L-arginine was performed on rats that had received a bilateral injection of rAAV-GFP, rAAV-GKS or rAAV-GKAS in the PVN. L-arginine was chosen as the literature demonstrates oral consumption of this amino acid causes gut hormone release. The dose of L-arginine administered was determined from literature as well as from previous studies. The gavage was performed by Mr Phil Rawson.

Materials

Restraining tube (Vet Tech Solutions Ltd)

21 gauge needles (Tyco Healthcare Ltd)

24 gauge/19mm Cannulae (Millpledge Veterinary)

Zinc Oxide surgical adhesive tape (Millpledge Veterinary)

Heparin sodium 1000IU/ml (Wockhardt)

Microvette CB300 LH (Sarstedt)

L-arginine monohydrochloride (Sigma-Aldrich)

Contour glucose test strips (Bayer)

Glucometer (Bayer)

Methods

The study was conducted following the protocol described in 2.2.5, with the following exception. Instead of an oral dose of glucose, each animal was given a 16mmol/kg dose of L-arginine monohydrochloride dissolved in GDW via oral gavage.

2.2.10 Collection of tissue samples

Unless otherwise stated in the methods, animals from all studies were euthanized by carbon dioxide asphyxiation and death was confirmed via cervical dislocation. Various tissues were collected from or cannulated genetically altered rats following the termination of a study. These included the brain, pancreas and ileum.

2.2.10.1 Brain

The brains from both cannulated and genetically altered animals were removed following a study.

Materials

Isopentane (VWR)

Dry ice (BOC, Guildford, UK)

1.25% India ink (VWR)

4% (v/v) formaldehyde in 0.01M phosphate buffered solution (Appendix I)

40% sucrose solution (Appendix I)

Dissection tools

Methods

Following cervical dislocation, the brains were removed and snap-frozen by immersion in dry ice-cooled isopentane. Tissues were stored at -80°C and used for *in situ* hybridisation and a glucokinase activity assay.

For cresyl violet staining, a 1µl iPVN injection of India ink was performed after euthanisation. Brains were then rapidly removed and fixed in 4% formaldehyde solution for 24 hours. The tissue was then dehydrated in 40% sucrose solution for 3 days and snap-frozen by immersion in ice cold isopentane on dry ice.

2.2.10.2 Pancreas

The pancreas of genetically altered animals was dissected as well as the brain. Two methods were used during dissection. The first consisted of incubating the dissected pancreas in paraformaldehyde four double immunohistochemical staining, while the second involved injecting a collagenase-based solution into the pancreatic duct for islet isolation. This work was conducted by Marie-Sophie Nguyen Tu from Guy Rutter's laboratory.

Materials

Ice box

Paraformaldehyde (Sigma-Aldrich)

Phosphate buffered saline (PBS) solution (Appendix I)

Krebs Ringer Bicarbonate buffer (Appendix I)

Collagenase

DNase I

Dissection tools

Nikon SMZ645 stereo dissecting microscope (Nikon, Kingston Upon Thames, UK)

Sigma 1-14 Microfuge (Sigma-Aldrich)

Methods

For double immunohistochemical staining, the pancreas was collected, weighed and placed in PBS on ice. Following a PBS wash, each pancreas was incubated in 8ml 4% paraformaldehyde in PBS. The staining was performed immediately on the dissected pancreata to examine β- and α-cell mass.
For the islet isolation, 3 ml of 1 mg/ml filtered collagenase in Krebs Ringer Bicarbonate buffer (Appendix I) were injected into the pancreatic duct with a 30-gauge needle. The inflated pancreas was excised, weighed and cut into small pieces of 1-2mm per piece which were then transferred into 20ml plastic tubes containing KRB buffer. The samples were incubated in a water bath at 37°C for eleven minutes, following which the pancreata were disturbed by adding 10ml of ice cold KRB buffer and shaking the tubes vigorously for one minute. The tubes were topped up with KRB buffer containing DNase I (~0.02µg/ml) and centrifuged at 300xg for ten seconds in a Sigma 1-14 Microfuge (Sigma-Aldrich). The supernatant was discarded and more KRB buffer containing DNase I was added to each sample and the pellet re-suspended. The tubes were centrifuged again as described above, the supernatant discarded and the pellet re-suspended in KRB + DNase I buffer. The islets were handpicked using a Nikon SMZ645 stereo dissecting microscope (Nikon). The suspension was poured into a sterile glass Petri dish, the islets were handpicked using a sterile fire polished siliconized glass Pasteur pipette and transferred to another sterile Petri dish placed on ice and containing KRB buffer. The isolated islets were immediately used in an insulin secretion assay to determine their level of responsiveness to glucose.

2.2.10.3 Ileum

The ileum of genetically altered animals was dissected along with the brain and pancreas. The ileum was used to examine the difference in expression of GLP-1 (7-36) in rAAV-GFP and rAAV-GKAS or rAAV-GKS and animals using reverse transcription polymerase chain reaction (RT-PCR).

Materials

Liquid nitrogen

Dissection tools

Methods:

The ileum was collected after confirmation of death. It was snap-frozen in liquid nitrogen and stored at -80°C until use.

2.3 *Ex vivo* methods for investigating the role of NTS and PVN GK in energy homeostasis

2.3.1 *In situ* hybridisation for glucokinase and WPRE mRNA

The knockdown of GK was verified by locating endogenous GK in the area of interest and using Woodchuck hepatitis virus Post-transcriptional regulatory Element (WPRE) as a marker of successful trans-gene expression. *In situ* hybridization is a widely used method for detecting and locating mRNA

while maintaining the structural integrity of the tissue. It is based on the hybridisation of a complimentary probe to the mRNA of interest.

Single stranded mRNA is often used as a probe as it significantly improves the sensitivity of examination of gene expression by *in situ* hybridisation (Cox et al., 1984). Probes have been labelled using digoxigenin, biotin or fluorescent markers. Nucleotides can also be bound to different radioactive isotopes, and radio-labelling the probe with ^{35}S is a highly sensitive method when performing *in situ* hybridisation on brain sections (Wilcox, 1993).

Materials

Cryostat (Bright Instruments, Luton, UK)

200ng/µl of linearised GK template (from section 2.1.9)

100mM DTT (VWR)

RNase inhibitor RNase Out (40U/µl) (Thermo Fisher Scientific)

10x nucleotide mix (10mM of each ATP, UTP, GTP) (New England Biolabs)

T3 and T7 RNA polymerase (20U/µl) (Thermo Fisher Scientific)

5x RNA polymerase buffer (Promega, Southampton, UK)

[35S]-CTPαS (46.2TBq/mmol, 2.6GBq/ml) (Perkin Elmer)

DNase 1 (2U/µl) (Thermo Fisher Scientific)

10x DNase buffer (New England Biolabs)

5M Ammonium acetate (Appendix I)

Absolute ethanol stored at -20°C (VWR)

4% (v/v) formaldehyde in 0.01M phosphate buffered solution (Appendix I)

0.25% (v/v) acetic anhydride in 0.1M TEA pH8.0 (Appendix I)

20% (w/v) Sodium dodecyl sulphate (SDS) (Appendix I)

50, 70, 95 and 100% ethanol in GDW (VWR)

Chloroform (VWR)

De-ionised formamide (VWR) (Appendix I)

5M sodium chloride (VWR)

1M Tris-HCl, pH 8.0 (VWR)

0.5M EDTA (VWR)

1M DTT (VWR)

10mg/ml Baker's yeast tRNA (VWR)

100x Denhart's solution (Appendix I)

50% (w/v) dextran sulphate (mw >500,000) in GDW at 60°C (Sigma-Aldrich)

1x RNase A (10g/ml) (Appendix I)

1M Dithiothreitol (DTT)

Biomax film (Kodak, Hemel Hempstead, UK)

Developing solution (Jet X-Ray, London, UK)

Fixing solution (Jet X-Ray)

Wallac Jet 1450 Microbeta Liquid Scintillation Counter (LabX, Midland, Canada)

Methods

Twelve micrometre brain sections were cut on a cryostat at -22°C (Bright Instruments). They were immediately mounted onto poly-D-lysine coated slides and stored at -80°C until hybridisation.

Radioactively labelled RNA was generated in a transcription reaction. 9.5µl GDW (warmed to 37°C) was pipetted into a 1.5ml eppendorf and two hundred nanograms of template were added. Following this DTT, RNase inhibitor, NTPs, 0.5µl CTPαS, and RNA polymerase were added in this order. T3 polymerase was used in the eppendorfs containing GK and WPRE antisense and T7 polymerase for those containing GK and WPRE sense. The reaction was incubated for at least 2 hours at 37°C, after which 1µl 10x DNase buffer and 3µl DNase 1 was added as well as 6µl GDW. After 15 minutes of incubation at 37°C, ammonium acetate (final concentration 2.5M) and 2.5 volumes of ice cold absolute ethanol were added to induce RNA precipitation. The mixture was

incubated at -20°C for at least 1 hour before centrifuging for 8 minutes at 8,000xg to recover the RNA. The pellet was dissolved in 200µl GDW, following which 1µl of the mixture was placed in triplicate in a Wallac Jet 1450 Microbeta Liquid Scintillation Counter (LabX) in order to measure the level of the radioactively labelled probe. A radioactive count above 200,000/µl was considered to represent a successfully transcribed probe.

After being thawed at RT, slides were fixed in 4% formaldehyde in 0.1M PBS for 20 minutes on ice. They were washed twice in 0.01M PBS for 5 minutes then briefly in autoclaved GDW. 0.25% acetic anhydride was prepared using 0.1M TEA, and the slides were acetylated in this solution for 10 minutes before being washed twice in 0.01M PBS for 2 minutes. They were then dehydrated for 2 minutes each in ascending concentrations of ethanol (50, 70, 95 and 100%, diluted with GDW) then delipidated in chloroform for 5 minutes. Finally, slides were slightly rehydrated in descending concentrations of ethanol (100 and 95%) for 2 minutes and air dried.

3ml of hybridization buffer was produced by combining in a sterilin 375mM NaCl, 31% (v/v) formamide, 0.5mg/ml tRNA, 1.25X Denhart's solution, 12.5mM Tris, 10mM DTT and 1.25mM EDTA, with 1ml of 50% dextran sulphate added last. Appropriate volumes of the sense and antisense probes for GK and WPRE were added in order to give 1 million counts per 70µl. Seventy microlitres of hybridisation buffer were applied onto coverslips and were stuck onto the slides, avoiding air bubbles. The slides were incubated at 60°C overnight.

Slides were washed in 4 X SSC for 5 minutes to remove the coverslips, after which this was repeated four additional times. They were then incubated in a solution containing 20mg/ml RNase A, 0.5M NaCl, 10mM Tris and 1mM EDTA for 30 minutes at 37°C. To remove incompletely bound probe, a series of washing steps were subsequently performed in 2 X SSC, 1 X SSC, 0.5 X SSC and 0.1 X SSC, the latter at 60°C. Slides were cooled in 0.1 X SSC then dehydrated in ascending concentrations of ethanol as previously described before being allowed to air dry completely. They were then placed into a photoplate cassette and exposed to X-ray film paper for 2-7 days. To develop, the film was bathed in developing solution until the slides appeared, rinsed briefly in water and fixed using fixing

solution for at least 3 minutes. This was performed under red lighting as the paper is light-sensitive. Slides could then be visualised on a light box or using a high resolution scanner.

2.3.2 Glucokinase activity assay in isolated NTS and PVN samples

A GK activity assay was performed to assess the change in GK activity produced by the stereotactic injection of rAAV-GKAS or rAAV-GKS.

Under normal conditions, in a reaction known as the pentose phosphate pathway, GK catalyses the phosphorylation of glucose to glucose-6-phosphate (G-6-P) by converting ATP to ADP. G-6-P is then converted to 6-Phospho-D-Gluconolactone by Glucose-6-Phosphate Dehydrogenase, and NADP is turned into NADPH (Fig. 2.1). This pathway occurs in parallel to glycolysis.

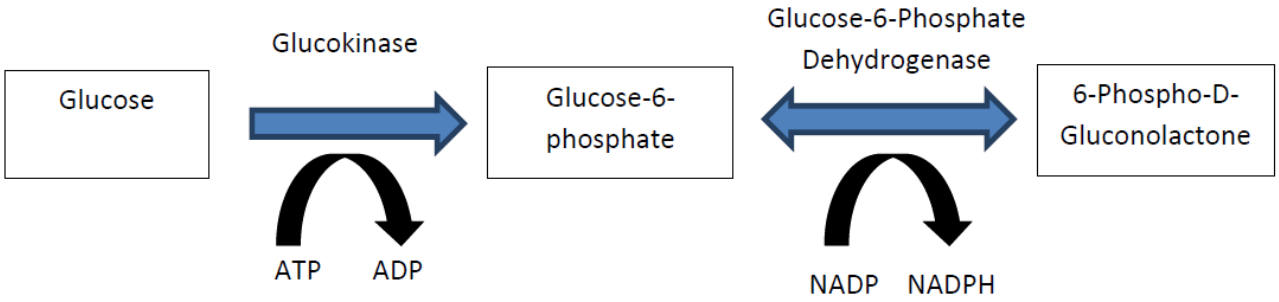


Figure 2.1 The pentose phosphate pathway. Glucose is converted to G-6-P by glucokinase, a reaction which utilizes ATP and produces ADP. G-6-P is then metabolised into 6-Phospho-D-Gluconolactone, during which NADPH is formed from NADP.

The GK activity assay measures the level of glucose phosphorylation by GK by quantifying the amount of NADPH produced in the reaction using spectrophotometry. It was modified from a previously reported G-6-P dehydrogenase assay to measure GK activity in small tissue samples (Goward et al., 1986) and functions even with small amounts of tissue.

To ensure that the phosphorylation of glucose leading to the production of NADPH is due to GK activity, hexokinases other than GK which may be present in the sample are inhibited using 5-thio-D-glucose-6-phosphate and 3-O-methyl-N-acetylglucosamine (3OMG). The glucose analogue 5-thio-D-glucose is an antagonist for hexokinases except for GK (Wilson and Chung 1989). Similarly, 3-O-methyl-N-acetylglucosamine inhibits glucose phosphorylation by N-acetylglucosamine kinase but not GK (Miwa et al., 1994).

Materials

GK extraction buffer (Appendix I)

Micropunch needles (custom made 1mm diameter)

Cryostat (Bright Instruments)

Poly-D-lysine glass slides (VWR)

Glucokinase from Bacillus stearothermophilus (0.25µg/ml) (Sigma-Aldrich)

Glycine buffer (50mM) (VWR)

5-Thio-D-glucose-6-phosphate (45µM) (Sigma-Aldrich)

$MgCl_2$ (7.5mM) (VWR)

ATP (10mM) (VWR)

NADP (0.75mM) (VWR)

Glucose (100mM) (VWR)

3-O-methyl-N-acetylglucosamine (0.5mM) (Enzo Life Science, Exeter, UK)

G-6-PD (type IX, from Baker's yeast) (1.25 units) (VWR)

ELx808 Microplate Reader (Biotek Instruments Ltd, Swindon, UK)

Eppendorf 5417R Centrifuge (Eppendorf)

Methods

Three hundred micrometre thick coronal sections of brain tissue were cut using a cryostat at -7°C and transferred to glass slides kept on dry ice. A rat brain atlas (Paxinos & Watson, 1998) was used to locate the section of interest (NTS, PVN), which was isolated using a micropunch needle and placed in a 1.5ml eppendorf.

200µl extraction buffer, which lyses the cell to facilitate the removal of proteins such as GK, was added to the punched sample before homogenisation using a handheld homogeniser. The eppendorfs were centrifuged at 14,000 RPM at 4°C for 3 minutes in an Eppendorf 5417R Centrifuge (Eppendorf). Reaction mix was prepared in a 30ml sterilin by adding the following reagents (final concentration): 50mM glycine buffer, 7.5mM $MgCl_2$, 10mM ATP, 0.75mM NADP, 100mM glucose, 45µM 5-Thio-D-glucose-6-phosphate, 0.5mM 3-O-methyl-N-acetylglucosamine and 1.25 units of G6P dehydrogenase. 450µl reaction mix was pipetted into cuvettes. Fifty microlitres of the supernatant were then added and the cuvettes were incubated at 37°C for one hour. Fifty microlitres of various concentrations of GK (0.5, 0.25, 0.1, 0.05, 0.025, 0.01, 0.005, 0.0025, 0.001µg/ml) were also added to cuvettes containing 450µl reaction mix to generate a standard curve.

The absorbance of each sample was read at 340nm using a microplate-reading spectrophotometer (Biotek Instruments Ltd) and the concentration of NADPH was determined using the following equation:

Absorbance at 340nm (A) = Molar absorptivity of NADPH (ε) x Concentration (c) x length (l)

$C\ molL^{-1} = A / (6.2x10^3\ Lmol^{-1}cm^{-1} \times 1\ cm)$

GK concentration was calculated by extrapolating values with the standard curve. Samples were normalised to protein content using a Pierce bicinchoninic acid (BCA) assay. Twenty five microlitres of sample leftover from the GK activity assay were added in triplicate to a 96 well plate. 25µl of BioRad Reagent A were added to each well, followed by 200µl of BioRad Reagent B. The plate was then incubated at RT for 15 minutes. Absorbance at 620nm was read using a spectrophotometric

microplate reader. It was compared with known protein concentrations on a standard curve constructed using BSA. Samples were thus measured in units of GK activity per mg protein.

2.3.3 Measurement of glucose in plasma samples using a glucose oxidase assay

A glucose oxidase assay (Randox, Crumlin, UK) was used to determine the level of glucose present in plasma samples of genetically altered animals during various studies (described previously). Glucose oxidase assays are a cheap, quick and accurate method of quantifying glucose levels in a sample. They rely on the actions of glucose oxidase, an enzyme highly specific for glucose which does not react with other blood saccharides, making it a suitable method of plasma glucose detection.

In the assay, glucose oxidase oxidises glucose to produce gluconic acid and hydrogen peroxide. The enzyme horseradish peroxidase then catalyses the breakdown of hydrogen peroxide to oxygen and water. The oxygen reacts with phenol and 4-aminophenazone to form a red/violet quinoneimine dye. The intensity of the signal is measured by reading its absorbance at 505nm. The level of absorbance is directly proportional to the amount of hydrogen peroxide produced and hence to the glucose concentration in the sample.

<u>Materials</u>

Gluc-PapR1 reagent (Randox, Crumlin, UK)

0.01M Phosphate buffered saline (Appendix I)

ELx808 Microplate Reader (Biotek Instruments Ltd)

<u>Methods</u>

All buffers were supplied ready to use. Plasma samples of genetically altered animals collected following a GTT and ITT were thawed on ice until defrosted. On a 96 well plate, 200µl phosphate buffer were mixed with 3µl of each sample. 200µl Gluc-PapR1 reagent (Randox) was then added to each well. The mixture was incubated for 25 minutes at RT and the absorbance was read using a microplate-reading spectrophotometer (Biotek Instruments Ltd) at 505nm. Glucose concentration was determined by extrapolating values with a standard curve constructed using methods provided by Randox. Absorbance values of the blank readings were subtracted from the absorbance readings of all samples and standards, and the standard curve was plotted.

2.3.4 Measurement of insulin in plasma samples using radioimmunoassay

The levels of insulin in blood samples of animals injected with rAAV-GKAS or rAAV-GFP into the NTS collected during an oral GTT and ITT were measured by radioimmunoassay (RIA). This method measures the concentration of insulin present in a sample by competing two forms of the hormone, one radioactivity-labelled and one unlabelled, for a specific binding site of an antibody. Unlike that of the unlabelled insulin, the concentration of antibody and labelled insulin are fixed. The higher the concentration of unlabelled insulin, the less radioactively labelled peptide will be bound to the antibody. The bound and free peptide is separated by addition of a secondary antibody which acts as a precipitating agent by binding to the primary antibody. The activity in the bound and free components is measured in a gamma scintillation counter and the data used to construct a standard curve.

The lowest level of rat insulin that can be detected by this assay is 0.081ng/ml + 2SD when using 100µL sample size, as reported by the manufacturer. The coefficient is reported to be between 8.5-

9.4%, as determined from five duplicate determinations of five rat serum samples in five separate assays.

Materials

^{125}I-labelled insulin (Millipore, Watford, UK)

Guinea pig anti-rat insulin antibody (Millipore)

Goat anti-guinea pig antibody (Millipore)

Rat insulin standards (Millipore)

Assay buffer (Millipore) (Appendix I)

Methods

Plasma insulin levels were measured using reagents and methods as described in the manufacturer's protocol. Three millilitre RIA tubes were labelled in RIA racks each holding 128 tubes. In addition to samples, the following were added to the RIA rack: duplicated tubes of NSB (non-specific binding; without antibody), half label concentration, 2 x label concentration, zeroes (no sample), standard curve dilutions, zeroes and duplicated excess antibody tubes. All unknown samples were assayed in singlet. The standard curve (10-0.156ng/ml) was constructed using rat insulin. The reaction was incubated at 4°C for 24 hours. Free and antibody-bound label were separated by goat anti-guinea pig antibody and centrifugation at 3,000xg for 20 minutes at 4°C. The free and bound fractions were counted for one minute in a gamma scintillation counter and sample concentrations were calculated using a data reduction programme (NE1600, NE Technology, UK).

2.3.5 Measurement of insulin in plasma samples using enzyme-linked immunosorbent assay

The levels of insulin in blood samples of animals injected with rAAV-GFP and rAAV-GKAS or rAAV-GKS into the PVN collected during various studies were measured using enzyme-linked immunosorbent assay (ELISA). As well as being quick and cost-effective, this assay requires small amounts of sample.

Briefly, the microplate wells are coated with guinea-pig anti-insulin antibody, which the rat insulin in the sample binds to. Following the removal of unbound material during a washing step, horseradish peroxidase (HRP)-conjugated anti-insulin antibody binds to the rat insulin that is bound to the guinea-pig anti-insulin antibody. Another washing step ensures the removal of excess HRP-conjugate. The bound HRP conjugate in the microplate well is detected through the addition of a substrate, tetramethylbenzidine (TMB), following which the absorbance is measured. The standard curve produced by plotting absorbance versus the corresponding concentration of rat insulin standard is used to determine the insulin concentration via interpolation. The enzymatic activity of the immunocomplex bound to insulin is directly proportional to the amount of insulin in the sample.

This assay has a high sensitivity for rat insulin as it can detect as little as 0.05 ng/ml using 5 µL sample. The intra-assay and inter-assay coefficient of variation is reported to be below 10.0%.

Materials

Antibody-coated Microplate (Crystal Chem Inc, Downers Grove, IL, USA)

Rat insulin standard, lyophilized (Crystal Chem Inc)

Anti-insulin enzyme conjugate stock solution (Crystal Chem Inc)

Enzyme conjugate diluent (Crystal Chem Inc)

Enzyme substrate (TMB) solution (Crystal Chem Inc)

Enzyme reaction Stop Solution (Crystal Chem Inc)

Sample Diluent (Crystal Chem Inc)

Wash buffer stock concentrate (Crystal Chem Inc)

Frame for affixing the microplate well module (Crystal Chem Inc)

Plastic Microplate cover (Crystal Chem Inc)

Wellwash Versa Microplate Washer (Thermo Fisher Scientific)

ELx808 Microplate Reader (Biotek Instruments Ltd)

Wellwash Versa Microplate Washer (Thermo Fisher Scientific)

ELx808 Microplate Reader (Biotek Instruments Ltd)

Methods

Insulin standards were prepared and diluted from stock at the following concentrations: 6.4, 3.2, 1.6, 0.8, 0.4, 0.2, 0.1, 0ng/ml. 95µl of sample diluent were added to each well, followed by 5µl of either sample or standards. The microplate was covered and incubated for 2 hours at 4°C. The microplate was washed five times with wash buffer diluted 1:20 using an automated plate washer (Thermo Fisher Scientific), after which 100µl of pre-prepared anti-insulin enzyme conjugate were dispensed in each well. The microplate was again covered and incubated at RT for 30 minutes. Another washing step was performed, where the microplate was washed seven times. 100µl of enzyme substrate solution was then added to each well and incubated for 40 minutes at RT. Exposure to light was avoided until the enzyme reaction Stop Solution was added as the substrate is light-sensitive. The absorbance was read at 450nm and 630nm using a spectrophotometric microplate reader (Biotek Instruments Ltd). To calculate the insulin concentration present in the sample, the value of A_{630} was subtracted from that of A_{450}. The insulin standard curve was constructed by plotting the mean absorbance value for each standard versus the corresponding standard rat insulin concentration. The insulin concentration was interpolated using the standard curve and mean absorbance values for each sample.

2.3.6 Measurement of glucagon-like peptide 1 in plasma samples using radioimmunoassay

A previously established in-house glucagon-like peptide 1 (GLP-1) RIA kit was used to detect GLP-1 in blood samples of animals injected with rAAV-GKAS or rAAV-GFP into the NTS collected during an oral GTT and ITT (Kreymann et al., 1987). GLP-1 RIA follows the same principle as insulin RIA, with the exception that separation of bound and free GLP-1 occurs by addition of dextran-coated charcoal which binds free antigen in the charcoal pellet.

The GLP-1 antibody was produced in rabbits against GLP-1 coupled to bovine serum albumin (BSA). Although this antibody does not cross-react with GLP-11-37 and GLP-17-37 or any other gut hormones, it exhibits 100% cross-reactivity with the amidated forms of GLP-1. ^{125}I-GLP-1 was generated by Professor Mohammad Ghatei via the Iodogen method (Wood et al., 1981), following which it was purified using high pressure liquid chromatography (HPLC).

This assay was produced in-house and the sensitivity and precision coefficient of variation have not been properly determined.

It should be noted that the measurement of GLP-1 was limited by the delay between collecting the blood and freezing the plasma samples. GLP-1 is rapidly degraded by the enzyme dipeptidyl peptidase-4 and has a half-life of approximately two minutes. It is therefore possible that, although samples were kept on ice during the study, some of the hormone present in the samples may have been broken down by DPP-4 before they were stored at -80C. The reported levels of GLP-1 in all treatment groups may therefore not accurately reflect the circulating levels of the hormone in each animal.

<u>Materials</u>

Assay buffer (Appendix I) containing 1% TWEEN 0.2% BSA

GLP-1 standard (Produced in-house)

^{125}I-labelled GLP-1 (Produced by Prof M. Ghatei)

Anti-rat GLP-1 antibody (Produced in-house)

Methods

The RIA assay was set up in the same manner as previously described (2.3.4) and the same protocol was followed, with the following exceptions. The reaction was incubated at 4°C for 4 days before separation of the free from antibody-bound label by adding 250µl of dextran-coated charcoal (Merck) and centrifuging at 3,000xg for 20 minutes at 4°C. The supernatant (containing the bound-GLP-1) was separated by aspiration and collected in fresh tubes. The free and bound fractions were counted for four minutes in a gamma scintillation counter. Peptide concentrations in each sample were calculated using a non-linear plot.

2.3.7 Measurement of bioactive glucagon-like peptide 1 in plasma samples using enzyme-linked immunosorbent assay

After stereotactic injection of animals in the PVN with rAAV-GFP and rAAV-GKAS or rAAV-GKS, blood samples were taken from each animal during various studies. The concentration of plasma bioactive GLP-1 (7-36) was determined using enzyme-linked immunosorbent assay (ELISA). This assay enables the quantification of bioactive GLP-1 (7-36) specifically as it does not detect other forms of the peptide, making it a reliable method of measurement of biologically important GLP-1 levels. It utilizes a monoclonal antibody coated to the wells of a microwell plate to capture GLP-1 (7-36) from the sample. After a wash to remove any unbound material, an anti-GLP-1 alkaline phosphatase detection conjugate binds to the immobilized GLP-1. Unbound conjugate is then washed off, after

which the bound detection conjugate is quantified using methyl umbelliferyl phosphate (MUP), which forms the fluorescent product umbelliferone in the presence of alkaline phosphatase. The intensity of the fluorescent signal generated is directly proportional to the concentration of GLP-1 (7-36) present in the samples.

The lowest level of GLP-1 (7-36) that can be detected by this assay is 2pM using 100µl plasma. The inter-assay and intra-assay precision are reported to be 8% ± 4.8 and 7.4% ± 1.1, respectively.

As was mentioned in 2.3.6, the accurate measurement of GLP-1 was hindered by the delay before storage of samples at -80C in which some of the hormone may have been degraded by DPP-4. The levels of GLP-1 described may hence not accurately represent the circulating GLP-1 concentration of each animal.

Materials

GLP-1 (Active) ELISA Plate coated with anti-GLP-1 Monoclonal Antibody (Millipore)

Adhesive Plate Sealer (Millipore)

10X Wash Buffer Concentrate (Millipore)

GLP-1 (7-36) amide ELISA Standards (Millipore)

ELISA GLP-1 (Active) Quality Controls 1 and 2 (Millipore)

GLP-1 (Active) Assay Buffer (Millipore)

GLP-1 (Active) Detection Conjugate (Millipore)

Methyl umbelliferyl phosphate (MUP) Substrate (Millipore)

Substrate Diluent (Millipore)

Stop Solution (Millipore)

Wellwash Versa Microplate Washer (Thermo Fisher Scientific)

ELx808 Microplate Reader (Biotek Instruments Ltd)

Methods

300μl Wash Buffer (diluted 1:10 with GDW) was added to each well of the antibody-coated 96 well plate and it was incubated at room temperature for 5 minutes. The buffer was decanted and 200μl of Assay Buffer were added to non-specific binding (NSB) wells. 100μl of Assay Buffer were added to the remaining wells. 100μl of standards, quality control (QC) and sample were then added and the microplate was gently shaken to mix the contents of the wells. The plate was then covered with a plate sealer and incubated for 24 hours at 4°C. Following incubation the liquid was decanted and the plate washed five times with 300μl diluted Wash Buffer per well using an automated plate washer (Thermo Fisher Scientific). 200μl of Detection Conjugate were then added to each well and the plate was incubated for two hours at RT. The plate was again washed three times with 300 μL diluted Wash Buffer per well as described above. Exposure to light was avoided from this point onwards. 200μl Substrate diluted 1:200 in Substrate Diluent was added to each well, after which the plate was incubated for thirty minutes at RT. Finally, 50μl of Stop Solution was added to each well and the plate was incubated for 5 minutes at RT. Absorbance was then measured at 355nm and 460nm using a spectrophotometric microplate reader (Biotek Instruments Ltd).

2.3.8 Measurement of glucagon in plasma samples using enzyme-linked immunosorbent assay

The levels of insulin in blood samples of animals injected with rAAV-GKAS, rAAV-GKS or rAAV-GFP into the PVN collected during various studies were measured using enzyme-linked immunosorbent assay (ELISA). This assay offers the valuable advantage of being specific to pancreatic glucagon and requires small amounts of sample.

In brief, the microplate supplied in the kit is pre-coated with anti-glucagon antibody. When the samples and labelled antigen are added, glucagon binds to the antibody on the plate. Following an incubation period and several washing steps, HRP-labelled streptoavidin (SA-HRP) is added. This forms an HRP-labelled streptoavidin-biotinylated pancreatic glucagon-antibody complex on the surface of the wells. An enzymatic substrate of HRP is subsequently added, after which the reaction is terminated by substantially lowering the environmental pH.

This assay can detect glucagon at concentrations as little as 1.1pg/ml, with a dynamic range of 7.8 - 500pg/ml. The inter-assay and intra-assay coefficients of variation are not reported by the manufacturer.

Materials

Antibody-coated Microplate (96 wells) (Crystal Chem Inc)

Standard (10ng/vial) (Crystal Chem Inc)

Labelled antigen (Crystal Chem Inc)

HRP-labelled streptoavidin Solution (Crystal Chem Inc)

Substrate Buffer (Crystal Chem Inc)

O-phenylenediamine dihydrochloride (OPD) tablet (Crystal Chem Inc)

Stop Solution (Crystal Chem Inc)

Buffer Solution A (Crystal Chem Inc)

Buffer Solution B (Crystal Chem Inc)

Washing Solution (20X Concentrated) (Crystal Chem Inc)

Adhesive foil (Crystal Chem Inc)

Wellwash Versa Microplate Washer (Thermo Fisher Scientific)

ELx808 Microplate Reader (Biotek Instruments Ltd)

Methods

Plasma glucagon levels were measured using reagents and methods as described in the manufacturer's protocol. Glucagon standards were prepared at the following concentrations: 0, 41, 123, 370, 1,111, 3,333 and 10,000pg/ml. 50µl of sample or standard were added to each well, followed by 50µl of labelled antigen solution. The microplate was then covered with adhesive foil and incubated for 48 hours at 4°C. The wells were washed three times with 350µl of Wash Buffer diluted 1:20 using an automated plate washer (Thermo Fisher Scientific). 100µl of SA-HRP solution were then added to each well, following which the plate was covered with adhesive foil and incubated at RT for 1 hour on a gentle shake. The wells were again washed three times with 350µl of diluted Wash Buffer using an automated plate washer. One OPD tablet was dissolved in 12ml substrate buffer, after which 100µl of working substrate solution were added to each well. The plate was again covered with adhesive foil and incubated at RT for 20 minutes. The reaction was subsequently terminated by adding 100µl of Stop Solution, after which the absorbance was measured within 30 minutes at A_{490} and A_{630} using a spectrophotometric microplate reader (Biotek Instruments Ltd). To calculate the glucagon concentration of each sample, the value of A_{630} was subtracted from that of A_{450}. The glucagon standard curve was constructed by plotting the mean absorbance value for each standard versus the corresponding standard rat glucagon concentration. The glucagon concentration was interpolated using the standard curve and mean absorbance values for each sample.

2.3.9 Measurement of glucose-stimulated insulin secretion from isolated pancreatic islets

Glucose-stimulated insulin secretion from isolated islets of rAAV-GKAS and rAAV-GFP rats was determined during a pilot study in which the islets were exposed to glucose. This experiment was performed by Guy Rutter's laboratory.

Materials

Krebs-Ringer Bicarbonate Hepes (KRBH) solution (Appendix I)

1M glucose solution

1M KCl solution

10x Bovine serum albumin (BSA) (New England Biolabs)

Acidified ethanol (Appendix I)

Sigma 1-14 Microfuge (Sigma-Aldrich)

Methods

Ten islets were used for each condition and the assay was run in triplicate. The islets were twice washed with KRBH buffer containing 0.1% BSA (pH 7.4) then incubated at 37°C on a gentle shake for one hour in 500µl KRBH-BSA buffer containing 3mM glucose. After incubation, matching size islets from different conditions were selected were placed in different wells of a 12 well plate. They were then incubated at 37°C on a gentle shake for 30 minutes in 500µl KRBH-BSA buffer (pH 7.4) pre-warmed to 37°C and containing either 3mM glucose, 17mM glucose or 20mM KCl. Following this, both the islets and buffer were pipetted into 1.5ml eppendorfs and placed on ice. Once the buffer and islets from each well were collected, the samples were centrifuged for three minutes at 350xg in a Sigma 1-14 Microfuge (Sigma-Aldrich). Approximately 250l of the supernatant of each sample was transferred to fresh eppendorfs. The islets were then lysed by adding 1ml of acidified ethanol (Appendix I) and sonicating for ten seconds. The insulin levels present in the supernatant and lysed cells was then measured. Insulin secretion from the islets was reported as a percentage of total islet insulin content.

2.3.10 Extraction of RNA from isolated ileum

The total RNA from previously dissected ileum was extracted to enable the analysis of gene expression in these tissues.

Materials

Liquid nitrogen

Mortar & Pestle

Qiazol Lysis Reagent (VWR)

PureLink DNase Set (Thermo Fisher Scientific)

1-bromo-3-chloropropane (Sigma-Aldrich)

Absolute ethanol (VWR)

Spin Cartridges (Thermo Fisher Scientific)

Collection tubes (Thermo Fisher Scientific)

Recovery tubes (Thermo Fisher Scientific)

Wash Buffer I (Thermo Fisher Scientific)

Wash Buffer II (Thermo Fisher Scientific)

Nuclease-Free water (Thermo Fisher Scientific)

Eppendorf 5417R Centrifuge (Eppendorf)

Methods

The ileum of genetically altered animals was collected. The tissue was placed in a mortar, snap-frozen in liquid nitrogen and ground to a fine powder using a pestle. The powder for each sample was placed in separate, autoclaved 2ml eppendorfs. 1ml of Qiazol lysis reagent was added to each eppendorf, which was then incubated at 4°C for twenty minutes. 100µl of 1-bromo-3-chloropropane (BCP) (Sigma-Aldrich) was then added; the eppendorfs were shaken vigorously until the mixture

turned milky and the samples were incubated at 4°C for twenty minutes. They were then centrifuged for at 13,000 RPM for fifteen minutes at 4°C in an Eppendorf 5417R Centrifuge (Eppendorf), following which the clear supernatant was transferred into fresh autoclaved 2ml eppendorfs and the rest was discarded. Another 100µl of BCP was added to each eppendorfs, which were then shaken vigorously until the mixture turned milky. The eppendorfs were centrifuged again as described previously and the supernatant was again transferred to fresh autoclaved 2ml eppendorfs while the rest was discarded. The samples were then diluted 1:1 with 70% ethanol to yield a final ethanol concentration of 35%. The mixture was filtered through a spin cartridge (SC) (Thermo Fisher Scientific) via centrifugation at 14,000 RPM for 15 seconds at RT. The flow-through was discarded and the SCs placed in fresh collection tubes (Thermo Fisher Scientific). The filters were washed by adding 400µl of Wash Buffer I (Thermo Fisher Scientific) and centrifuging at 14,000 RPM for 15 seconds at RT. This step was repeated once, after which 80µl of DNase mixture containing 3U/µl PureLink DNase (Thermo Fisher Scientific) suspended in DNase buffer (Thermo Fisher Scientific) and water were added to each SC. The samples were left to incubate at RT for 20 minutes, following which the filters were twice washed with 400µl Wash Buffer I as previously described. The washing process was then repeated with Wash Buffer II. Finally, the SCs were placed in recovery tubes and the RNA was eluted from the filters by adding 60µl of nuclease-free water and centrifuging at 14,000 RPM for one minute at RT. The total RNA collected was stored at -20°C.

2.3.11 Generating complementary DNA using reverse transcription

The total RNA collected previously from tissue was utilized to generate single stranded cDNA through reverse transcription.

Materials

96 Well PCR Plate, semi skirted with straight edges (StarLab, Milton Keynes, UK)

25x dNTP mix (100mM) (Thermo Fisher Scientific)

10x RT Random Primers (Thermo Fisher Scientific)

10x RT Buffer (Thermo Fisher Scientific)

Multiscribe Reverse Transcriptase (50U/µl) (Thermo Fisher Scientific)

Nuclease-Free Water (Thermo Fisher Scientific)

Adhesive foil (Thermo Fisher Scientific)

Rotina 420 microplate centrifuge (Hettich Zentrifugen, Salford, UK)

Veriti 96 Well Thermal Cycler (Thermo Fisher Scientific)

Methods

10µl of each total RNA sample were pipetted into the wells of a 96 well PCR plate (StarLab) placed in ice. A 'reaction buffer' was then prepared and a volume of 10µl was added to each well. The reaction mix contains, for each sample, 2µl of 10X RT Buffer (Thermo Fisher Scientific), 0.8µl 25x dNTP mix (100mM) (Thermo Fisher Scientific), 2µl of 10x RT Random Primers (Thermo Fisher Scientific), 1µl of Multiscribe Reverse Transcriptase (50U/µl) (Thermo Fisher Scientific) and 4.2µl of nuclease-free water (Thermo Fisher Scientific). The plate was covered with adhesive PCR plate foil (ThermoFisher Scientific) and centrifuged briefly in a Rotina 420 microplate centrifuge (Hettich Zentrifugen) to ensure all reagents were properly mixed at the bottom of the wells. It was then placed in a Veriti 96 Well Thermal Cycler (Thermo Fisher Scientific) and run in the following cycle: 25°C for ten minutes, followed by 37°C for sixty minutes then 85°C for five minutes. The 96 well plate containing the cDNA produced was stored at -20°C.

2.3.12 Measuring gene expression using quantitative polymerase chain reaction

Following the generation of cDNA from total RNA, the expression level of various genes of interest was then measured by detecting and quantifying their mRNA using quantitative polymerase chain reaction (qPCR). This method measures the quantity of a target sequence, such as cDNA, which can be monitored in real time on screen using a fluorophore-containing DNA probe such as TaqMan. TaqMan probes bind between the DNA bases and release a fluorescent substance when they are encountered by DNA polymerase during the elongation step. A primer for detection of eukaryotic 18s ribosomal RNA (rRNA), which is the structural RNA for the small component (40S) of eukaryotic cytoplasmic ribosomes, was used as the endogenous control.

Materials

96 Well PCR Plate, semi skirted with straight edges (StarLab)

MicroAMP Optical 384-well reaction plate with barcode (Thermo Fisher Scientific)

Eukaryotic 18S rRNA Endogenous Control (FAM™/MGB probe, non-primer limited) (Thermo Fisher Scientific)

Rn00562293_m1 Gcg (Thermo Fisher Scientific)

Rn01460420_g1 PYY (Thermo Fisher Scientific)

TaqMan Gene Expression Mastermix (Thermo Fisher Scientific)

Nuclease-Free Water (Thermo Fisher Scientific)

MicroAMP Optical Adhesive Film (Thermo Fisher Scientific)

Rotina 420 microplate centrifuge (Hettich Zentrifugen)

7900 HT Fast Real-Time PCR System (Thermo Fisher Scientific)

Methods

A portion of each sample was diluted 1:10 by adding 2µl of each to 18µl of nuclease-free water in a 96 well PCR plate. This diluted sample was used as the endogenous control. 1µl of each diluted sample was transferred in triplicate to a 384-well PCR plate (Thermo Fisher Scientific). The same

volume of undiluted sample was also added in triplicate to a separate section of the 384 well PCR plate. 10µl of TaqMan Gene Expression Mastermix (Thermo Fisher Scientific) and 8µl of nuclease-free water were then added to all wells. Finally, 1µl of primer encoding for either the endogenous control or gene of interest was added to the wells containing diluted and undiluted sample, respectively. The plate was covered with a MicroAMP Optical Adhesive Film (Thermo Fisher Scientific) and centrifuged briefly in a Rotina 420 microplate centrifuge (Hettich Zentrifugen) to ensure all reagents were properly mixed at the bottom of the wells. The plate was placed in a 7900 HT Fast Real-Time PCR System (Thermo Fisher Scientific) and the Product obtained was stored at -20°C.

2.3.13 Cresyl violet staining of ink-injected brains

The accuracy of the iPVN cannulation described earlier was assessed using cresyl violet staining of the ink-injected rat brains. Cresyl violet is an organic compound often used for staining in histology for light microscopy sections (Urrutia and Ortiz, 2016). The brain slices are de-hydrated in ethanol in order to differentiate the stain, causing myelin and other components to lose colour whereas perikarya retain the colour. Cresyl violet stains the neuronal Nissl bodies, large granular bodies containing the rough endoplasmic reticulum (RER) and free ribosomes (Urrutia and Ortiz, 2016).

<u>Materials</u>

Ethanol (VWR)

1% Cresyl Violet Stain (Appendix I)

Xylene (VWR)

DPX (Thermo Fisher Scientific)

Poly-D-lysine glass slides (VWR)

Methods

Rat brains were placed into a sled microtome, were sliced thirty micrometres thick and mounted onto glass slides. The slides were delipidated in xylene, immersed in descending concentrations of ethanol and stained in 1% cresyl violet for twenty minutes. They were briefly rinsed in GDW then dehydrated in ascending concentrations of ethanol, after which they were again bathed in xylene. Finally, the slides were mounted with DPX and coverslips the following morning and were viewed under a Nikon Eclipse 50i light microscope (Nikon). Images were taken using a Visicam 10.0 camera (VWR) mounted on the microscope. Animals with ink more than 0.2mm outside the PVN were removed from subsequent analysis.

2.4 Statistical analysis

The Generalised Estimating Equation (GEE) was used to compare cumulative data from feeding studies (BW gain, glucose intake, chow intake and total energy intake). Based on generalised linear models, it is often used for analysis of longitudinal data. It accounts for small variation in two groups that are time-dependently different.

Data from GTTs, ITTs, oral gavage and GK activity assays were analysed using an unpaired t-test, which was used to measure differences in glucose and various hormones between genetically altered and WT animals. This test was chosen as it permits the measurement of two groups following a normal distribution. It was chosen instead of paired t-test as the latter compares the study subjects at two different times. It should be noted that other statistical tests could have been used instead which may have offered a more comprehensive analysis of the cumulative nature of

the observations made during GTTs and ITTs. Although unpaired t-test are a powerful tool for comparing two sample populations, they do not account for any previous observations. As the measurements were on a time course and were inter-related, using GEE may have been a more suitable statistical test as it would have enabled the analysis of the data cumulatively.

Results were expressed as the means ± standard error of the mean (SEM). Data analysis was performed using GraphPad Prism 6 software (GraphPad Software; San Diego, USA) except for GEE, which was performed using Stata 9 software (Stata, Stata Corp LP, London, UK). Significance was set at $P<0.05$ for all analyses.

Chapter 3 – The role of glucokinase in the *nucleus tractus solitarius*

3.1 Introduction

The NTS is a wishbone shaped nucleus flanking the posterior part of the fourth ventricle. Along with the area postrema (AP) and the dorsal motor nucleus of the vagus (DMV), it forms part of the dorsal vagal complex (DVC) within the caudal brainstem (Abraham et al., 2014). The NTS is regarded as a major sensory relay nucleus for numerous organs and tissues including the lungs, heart and blood vessels. Much of the literature investigates its role in cardiorespiratory control. The NTS also plays a crucial role in relaying both sympathetic and parasympathetic signals between the gut and the forebrain. NTS neurons receive input from several peripheral tissues including the gastrointestinal (GI) tract, pancreas and liver (Grill and Hayes, 2009, Shapiro and Miselis, 1985, Rinaman, 2010), suggesting that the NTS may be involved in the regulation of energy homeostasis.

3.1.1 The NTS and appetite

The NTS forms a crucial element of a neuronal satiety signalling pathway operating via a forebrain-hindbrain neurocircuit (Emond et al., 2001). It evaluates energy status by processing descending melanocortinergic and leptin input from the mediobasal hypothalamus (MBH), principally the ARC and PVN, as well as vagal signals originating from the gut to determine food intake (Blevins et al., 2009, Sutton et al., 2005).

POMC neurons in the NTS play a crucial role in its control of appetite. POMC neuronal activation induced by designer receptors exclusively activated by designer drugs (DREADD) produced an immediate inhibition of feeding behaviour (Zhan et al., 2013). Leptin receptors (LepRs) are also expressed in the NTS and iNTS delivery of leptin reduced both body weight gain and food intake

(Hayes et al., 2010). Conversely, genetic knockdown of leptin receptors using adeno-associated virus short hairpin RNA interference (AAV-shRNAi) had the opposite effect (Hayes et al., 2010).

Hypothalamic leptin is critically involved in the generation of satiety and its effects appear to be partially mediated by the NTS. After meal ingestion, leptin binds to leptin receptors (LepRs) in the arcuate nucleus (ARC). LepR activation is believed to stimulate proopiomelanocortin (POMC) neurons while inhibiting neurons expressing the orexigenic peptides neuropeptide Y (NPY) and Agouti-related peptide (AgRP). This causes the release of alpha melanocyte stimulating hormone (αMSH) from the ARC, which binds to melanocortin 4 receptors (MC4Rs) in the parvocellular paraventricular nucleus (PVN) (Konner et al., 2009). MC4R activation has been shown to trigger oxytocin signalling in the PVN (Jovanovic and Yeo, 2010) and may in turn increase the sensitivity of the NTS to satiety signals such as cholecystokinin-8 (CCK-8) and glucagon-like peptide 1 (GLP-1) (Blevins et al., 2003, Blevins et al., 2004, Sutton et al., 2005). The signal is then propagated to the gut via the vagus nerve to induce satiety.

The role of oxytocin in the above mechanism has been clearly demonstrated as injection of oxytocin receptor antagonists into the fourth ventricle stimulated food intake and blocked the anorexigenic effect of CCK-8 (Blevins et al., 2004). GLP-1 also appears to be involved in the mediation of leptin's effects as both intraperitoneal and fourth ventricle intracerebroventricular (ICV) injection of exendin (9-39), a GLP-1 receptor antagonist, completely abolished the suppressing effect of both peripheral and fourth ventricle ICV leptin on food intake and body weight gain (Nowak and Bojanowska, 2008).

3.1.2 Glucose-sensing neurons in the NTS

Glucose-sensitive neurons have been demonstrated in the NTS (Adachi et al., 1995, Young, 2012). The glucose analogs 2-deoxyglucose and 5-thioglucose were utilised by numerous groups as they induce hypoglycaemia-like conditions. These analogs have a modified structure preventing their phosphorylation and deprive cells of glucose as an energy source by inhibiting one or more enzymes in the glycolytic pathway (Ritter and Taylor, 1990). They provoke physiological responses that mimic those evoked by low glucose availability, including feeding and elevation of endogenous glucose production via gluconeogenesis or glycogenolysis, and lead to hyperglycemia (Ritter and Taylor, 1990). Both 2-deoxyglucose and 5-thioglucose increased food intake following administration in the 4th ventricle, suggesting that the DVC plays a role in glucose-sensing (Miselis and Epstein, 1975, Slusser and Ritter, 1980). Feeding in response to 2-deoxyglucose was lost upon lesioning of the NTS, thus revealing possible glucose-sensing properties of this nucleus (Ritter and Taylor, 1990). Microinjections of 5-thioglucose into the NTS increased both food intake and plasma glucose levels (Ritter et al., 2000). More recently whole cell and on-cell patch-clamp recordings have demonstrated both increased and decreased neuronal excitability in the NTS in response to an elevation in environmental glucose, indicating the presence of both GE and GI neurons. Most GI neurons were identified in the lateral NTS while GE neurons were largely expressed in the medial NTS (Boychuk et al., 2015).

ATP-sensitive inward rectifying potassium (K_{ATP}) channels are well established glucose-sensing components forming part of the downstream signalling cascade following GK activation in glucose-excited (GE) neurons and pancreatic β-cells (Evans et al., 2004, McCrimmon et al., 2005, Miki et al., 2001). Evidence supports the presence of these channels in the NTS (Dallaporta et al., 2000, Qiao et al., 2011, Boychuk et al., 2015). For instance, Boychuk *et al.* showed that glucose-induced responses to variations in glucose levels were blocked by the K_{ATP} channel blocker tolbutamide (Boychuk et al., 2015). Glucose transporter 2 (GLUT2) plays a crucial role in pancreatic glucose-sensing (Thorens, 2014) and is expressed within the NTS (Lamy et al., 2014, Boychuk et al., 2015). There it has been

linked with the detection of hypoglycaemia and the initiation of the counter-regulatory response (CRR) (Lamy et al., 2014). GLUT2-expressing neurons are believed to form a distinct population of GABAergic neurons activated by low glucose levels (GI neurons). These hypoglycaemia-activated neurons stimulate glucagon secretion via the vagus nerve by increasing AMPK activity and inhibiting K_{ATP} channels (Lamy et al., 2014). Hence, the NTS can detect hypoglycaemia and induce glucagon secretion to trigger the CRR, indicating a role in glucose homeostasis.

A brain-liver axis has been postulated in which the NTS may contribute to the regulation of glucose homeostasis (Lam and Dean, 2010). The oxidation of long chain fatty acids was blocked by infusing a pharmacological inhibitor of an enzyme involved in this process into the third ventricle. The infusion caused selective activation of NTS neurons and decreased liver gluconeogenesis. The NTS hence may form part of a forebrain-hindbrain-liver pathway and appears to be involved in reducing hepatic glucose production. The brain-liver axis seems to be dependent on K_{ATP} channels and linked by the vagus nerve as central activation of K_{ATP} channels and descending fibres within the hepatic branch of the vagus nerve was necessary for the effect to occur (Pocai et al., 2005).

3.1.3 Glucokinase in the NTS

Various factors involved in the regulation of energy homeostasis have been discovered in the NTS, including brain-derived neurotrophic factor (BDNF), glucagon-like peptide 2 (GLP-2) receptors, prokineticin and adenosine monophosphate-activated protein kinase (AMPK) (Montero et al., 2012, Guan, 2014, Delaere et al., 2013, Lam et al., 2011). GK-like immunoreactivity was also identified in the NTS (Maekawa et al., 2000) and its expression was detected by reverse transcription polymerase chain reaction (RT-PCR) (Dunn-Meynell et al., 2002). *In situ* hybridization studies did not detect its

presence within this nucleus however, perhaps because *in situ* hybridization may not be sensitive enough to detect the low levels of GK present in the NTS (Lynch et al., 2000).

Although the NTS appears to play an important role in energy homeostasis, the function of GK in this nucleus has not been deeply examined and remains unclear. As the NTS is involved the regulation of satiety, the expression of GK may indicate a potential role in this process. Likewise, it may contribute to the control of plasma glucose levels as GK is an important glucose-sensor. The NTS therefore represents an area of interest and GK a promising target for the treatment of metabolic disorders.

3.2 Hypothesis and Aims

3.2.1 Hypothesis

GK in the NTS plays an important role in the regulation of energy homeostasis. Reducing GK's expression within the NTS will lead to an increase in food and glucose intake. It will also disrupt glucose homeostasis as plasma glucose clearance will be impaired while secretion of insulin and bioactive GLP-1 will be reduced.

3.2.2 Aims

The role of glucokinase in the NTS in the regulation of energy homeostasis will be investigated. Its effects on the regulation of appetite and glucose homeostasis will be examined.

1. GK expression will be knocked down via stereotactic injection of rAAV-GKAS. The accuracy of the injection will be confirmed using *in situ* hybridization and a GK activity assay.
2. GK-deficient and control rats' chow and glucose solution intake, as well as total energy intake and body weight gain, will be measured.
3. An oral glucose tolerance test and insulin tolerance test will be performed following tail vein cannulation in which blood samples will be collected at various time points. Plasma glucose, insulin and GLP-1 levels will be analysed.

3.3 Results

3.3.1 The role of NTS GK in the regulation of appetite

To determine whether NTS GK plays a role in feeding behaviour, a feeding study was conducted where GK-deficient (rAAV-GKAS) and control (rAAV-GFP) rats were offered either offered standard chow diet alone or both standard chow diet and glucose 10% w/v solution.

NTS GK knockdown had no significant effect on the rate of body weight gain when the animals were offered chow alone or when glucose solution was also presented (Fig. 3.1). Likewise, there was no difference in food intake regardless of the availability of glucose (Fig. 3.2). Additionally, GK knockdown did not induce a preference for glucose solution as there was no difference in glucose intake between the two groups (Fig 3.3). Total energy intake was found to be statistically different in GK-deficient animals compared to controls, although the difference between groups was very slight (GFP: 17.40±0.48MJ, n=9; GKAS: 18.40±0.35MJ, n=10; $p<0.05$) (Fig. 3.4).

Data collected from the feeding study suggests that NTS GK does not play a role in the regulation of appetite.

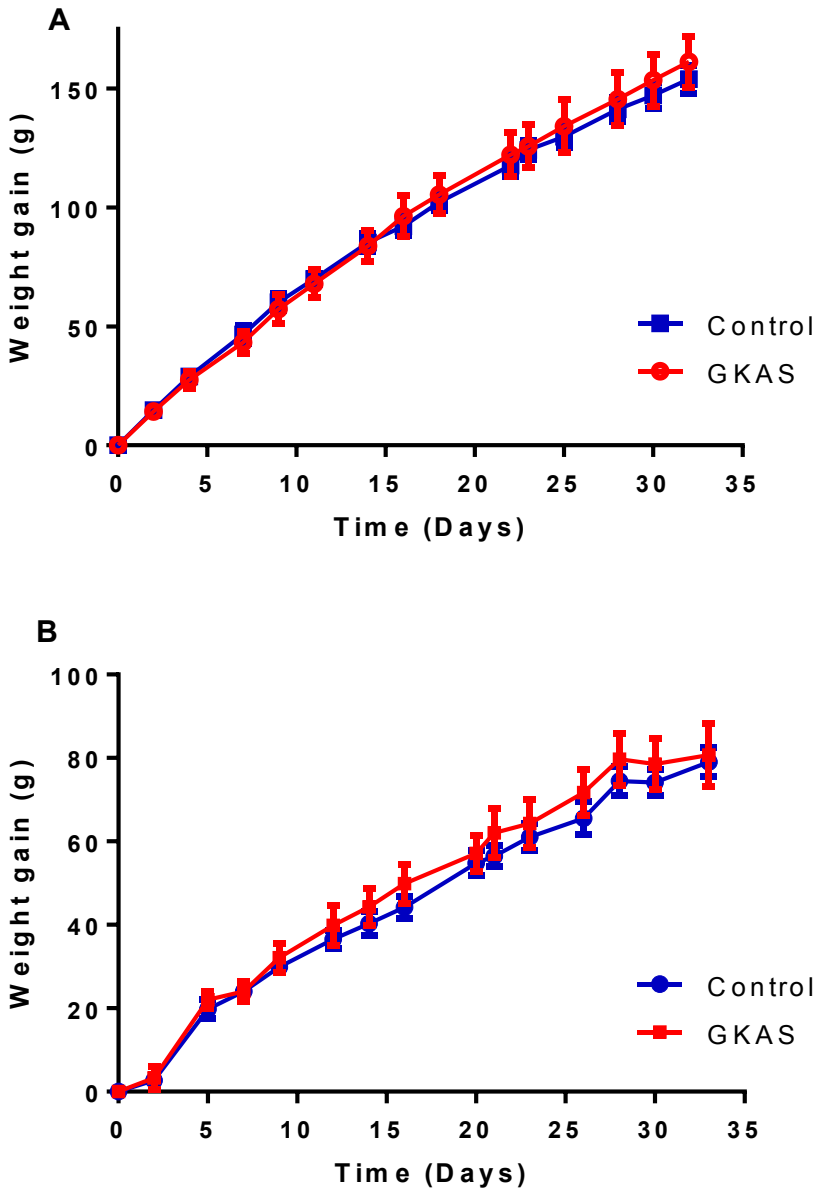


Figure 3.1: GK knockdown had no effect on the rate body weight gain compared to controls animals, both in the absence and presence of glucose solution. Feeding study comparing male Wistar rats injected with either rAAV-GKAS (blue, n=7) or rAAV-GFP (filled, n=9) into the NTS. The rate of body weight gain of the animals with *ad libitum* access to **(A)** food only or **(B)** both food and 10%w/v glucose solution was monitored. All values are expressed as mean ± SEM. Data were analysed using Generalized Estimating Equation.

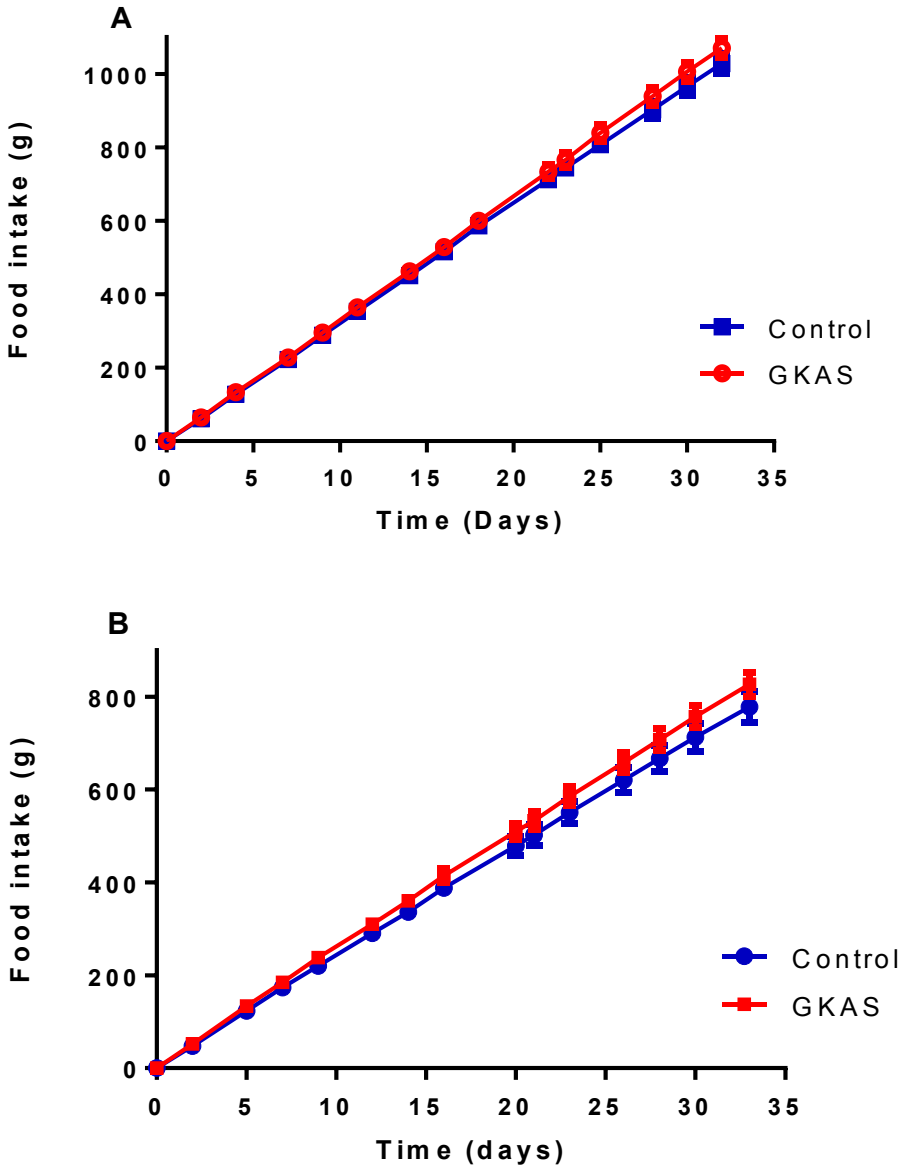


Figure 3.2: GK knockdown had no effect on food intake compared to controls animals, both in the absence and presence of glucose solution. Feeding study comparing male Wistar rats injected with either rAAV-GKAS (blue, n=7) or rAAV-GFP (filled, n=9) into the NTS. Food intake of the animals with *ad libitum* access to **(A)** food only or **(B)** both food and 10%w/v glucose solution was monitored. All values are expressed as mean ± SEM. Data were analysed using Generalized Estimating Equation.

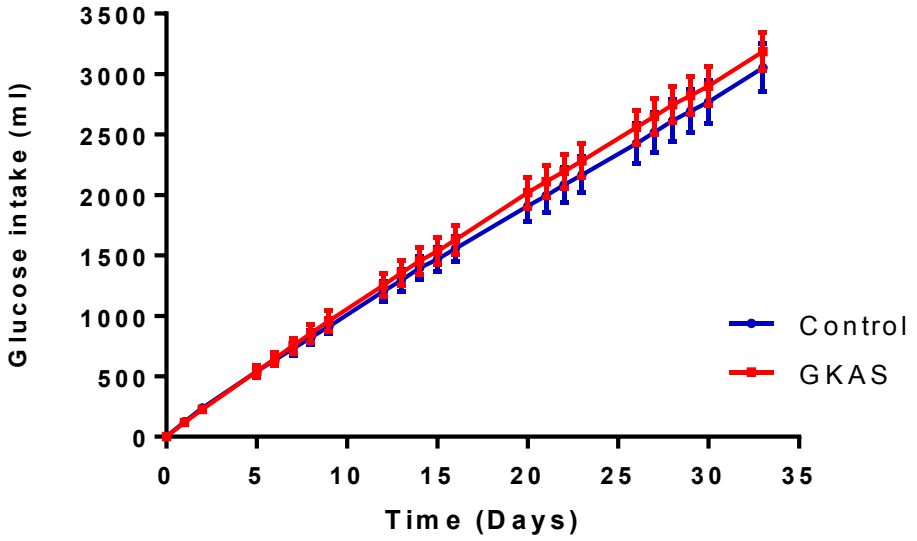


Figure 3.3: GK knockdown had no effect on glucose intake compared to controls animals. Feeding study comparing male Wistar rats injected with either rAAV-GKAS (blue, n=7) or rAAV-GFP (filled, n=9) into the NTS. Glucose intake of the animals with *ad libitum* access to both food and 10%w/v glucose solution was monitored. All values are expressed as mean ± SEM. Data were analysed using Generalized Estimating Equation.

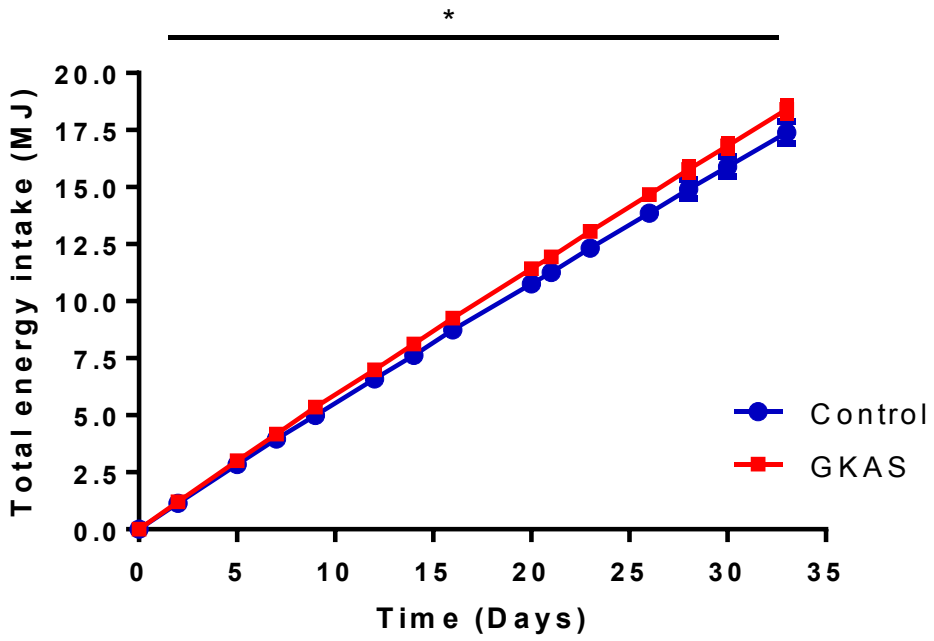


Figure 3.4: GK knockdown increased total energy intake compared to controls animals. Feeding study comparing male Wistar rats injected with either rAAV-GKAS (blue, n=7) or rAAV-GFP (filled, n=9) into the NTS. Total energy intake (glucose solution + food) of the animals with *ad libitum* access to both food and 10%w/v glucose solution was monitored. All values are expressed as mean ± SEM. Data were analysed using Generalized Estimating Equation: *p<0.05 versus corresponding control values.

3.3.2 The role of NTS GK in the regulation of glucose homeostasis

Both an oral glucose tolerance test (GTT) and an insulin tolerance test (ITT) were conducted to determine the effect of NTS GK knockdown on glucose homeostasis. For the oral GTT, the animals were given an oral dose of glucose (2.5g/kg) after being fasted overnight and blood samples were collected at various time points through a cannula inserted in the tail vein. For the ITT, rats were fasted 4 hours prior to the study, at the start of which they were administered a 2IU/kg dose of insulin intraperitoneally (i.p.). Blood was collected following to the above mentioned procedure.

The oral GTT suggested that NTS GK knockdown disrupted the process of glucose homeostasis as the rAAV-GKAS rats had significantly higher glucose levels than control animals after 30 minutes (GFP: 6.41±0.18mmol/L, n=10; GKAS: 7.56±0.40mmol/L, n=9; $p<0.01$) (Fig. 3.5A). The significant difference in plasma glucose levels between the two groups is demonstrated in the AUC graph (Fig.3.5B, $p<0.01$). Correspondingly, insulin levels were significantly lower after 15 minutes in rAAV-GKAS rats compared to control animals (GFP: 2.67±0.27mmol/L, n=10; GKAS: 1.87±0.25mmol/L, n=9; $p<0.05$) (Fig. 3.6A), and overall concentrations of the hormone during the two hour study are shown to be less in rAAV-GKAS animals in the AUC graph (Fig.3.6B, $p<0.05$). GLP-1 secretion following NTS GK knockdown appeared to decrease in RAAV-GKAS rats after 30 minutes compared to rAAV-GFP animals (GFP: 7.23±0.22mmol/L, n=10; GKAS: 6.74±0.30mmol/L, n=9; $p<0.05$) (Fig. 3.7A). Unlike glucose and insulin, however, AUC analysis did not reveal a significant difference in plasma GLP-1 concentration between the two groups during the GTT (Fig. 3.7B). During an ITT, no difference in plasma glucose levels was observed between the two groups (Fig. 3.8).

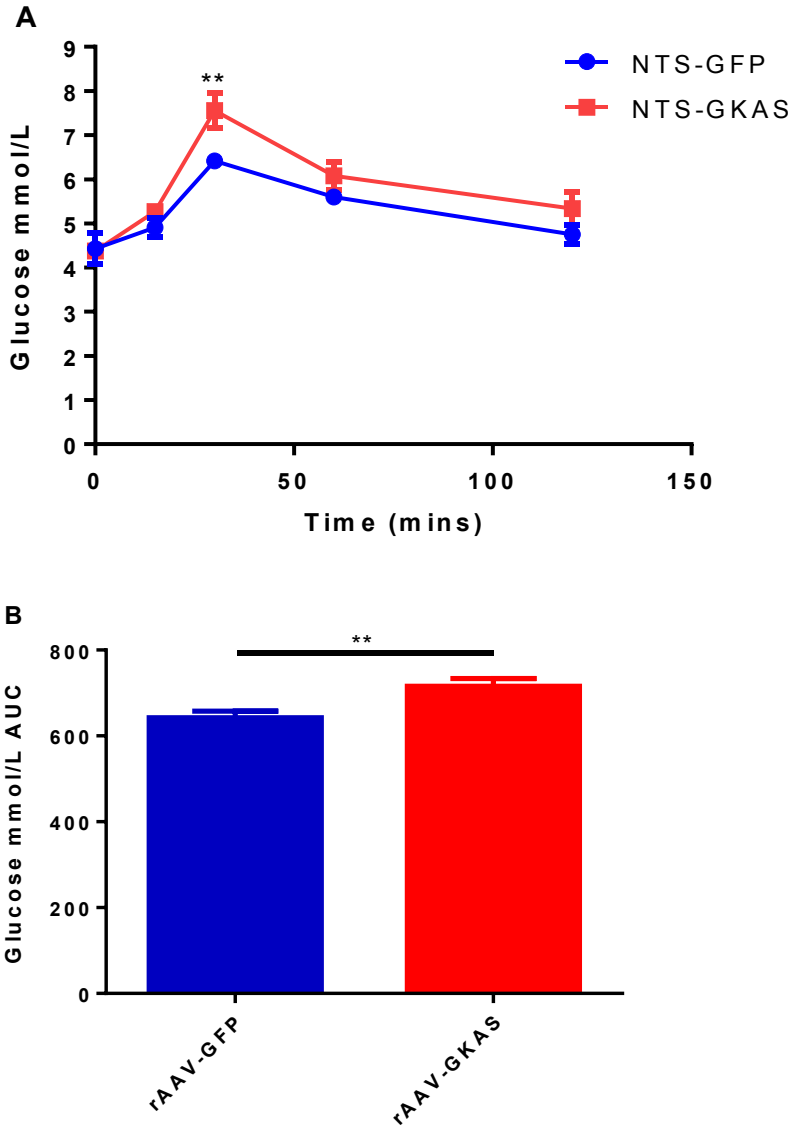


Figure 3.5: NTS GK knockdown impaired glucose clearance during an oral GTT. Glucose tolerance test comparing plasma glucose concentration of male Wistar rats stereotactically injected with rAAV-GFP (n=10) or rAAV-GKAS (n=9) in the NTS. **(A)** Glucose concentration was measured using a glucose oxidase assay and **(B)** the area under the curve was determined. Blood samples were collected via a tail vein cannula at t=0, 15, 30, 60 and 120 minutes post-ingestion of a 2.5g/kg oral glucose dose. Data is expressed as mean ± SEM and was analysed using an unpaired T-test at each time point: **p<0.01.

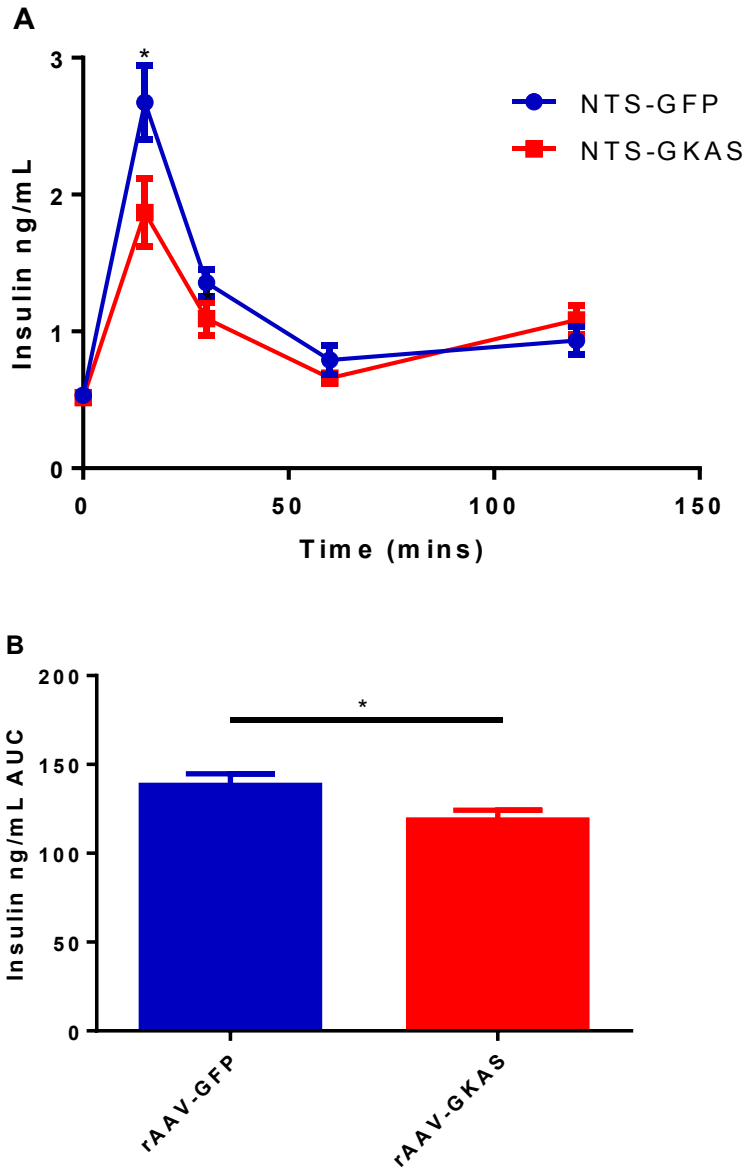


Figure 3.6: NTS GK knockdown impaired insulin secretion during an oral GTT. Glucose tolerance test comparing the plasma insulin concentration of male Wistar rats stereotactically injected with rAAV-GFP (n=10) or rAAV-GKAS (n=9) in the NTS. **(A)** Insulin concentration was measured using RIA and **(B)** the area under the curve was determined. Blood samples were collected via a tail vein cannula at t=0, 15, 30, 60 and 120 minutes post-ingestion of a 2.5g/kg oral glucose dose. Data is expressed as mean ± SEM and was analysed using an unpaired T-test at each time point: *p<0.05.

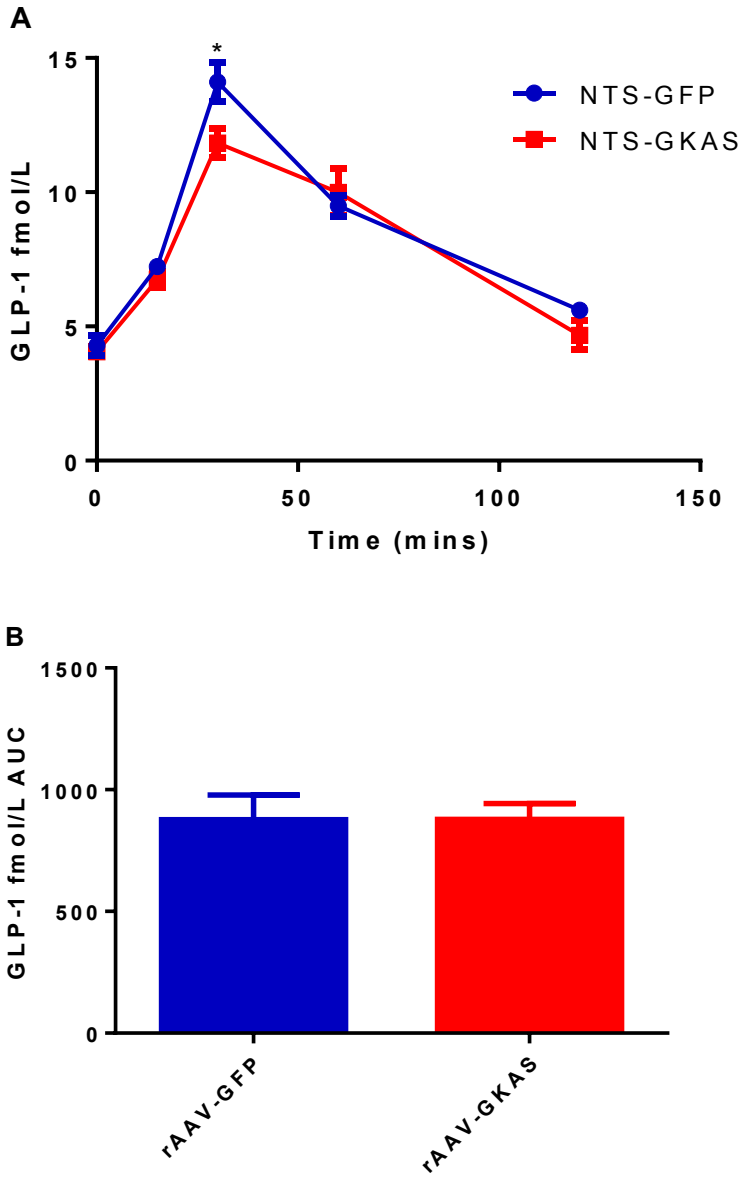


Figure 3.7: NTS GK knockdown did not significantly impair GLP-1 secretion during an oral GTT. Glucose tolerance test comparing the plasma GLP-1 concentration of male Wistar rats stereotactically injected with rAAV-GFP (n=10) or rAAV-GKAS (n=9) in the NTS. **(A)** GLP-1 concentration was measured using RIA and **(B)** the area under the curve was determined. Blood samples were collected via a tail vein cannula at t=0, 15, 30, 60 and 120 minutes post-ingestion of a 2.5g/kg oral glucose dose. Data is expressed as mean ± SEM and was analysed using an unpaired T-test at each time point: *$p<0.05$.

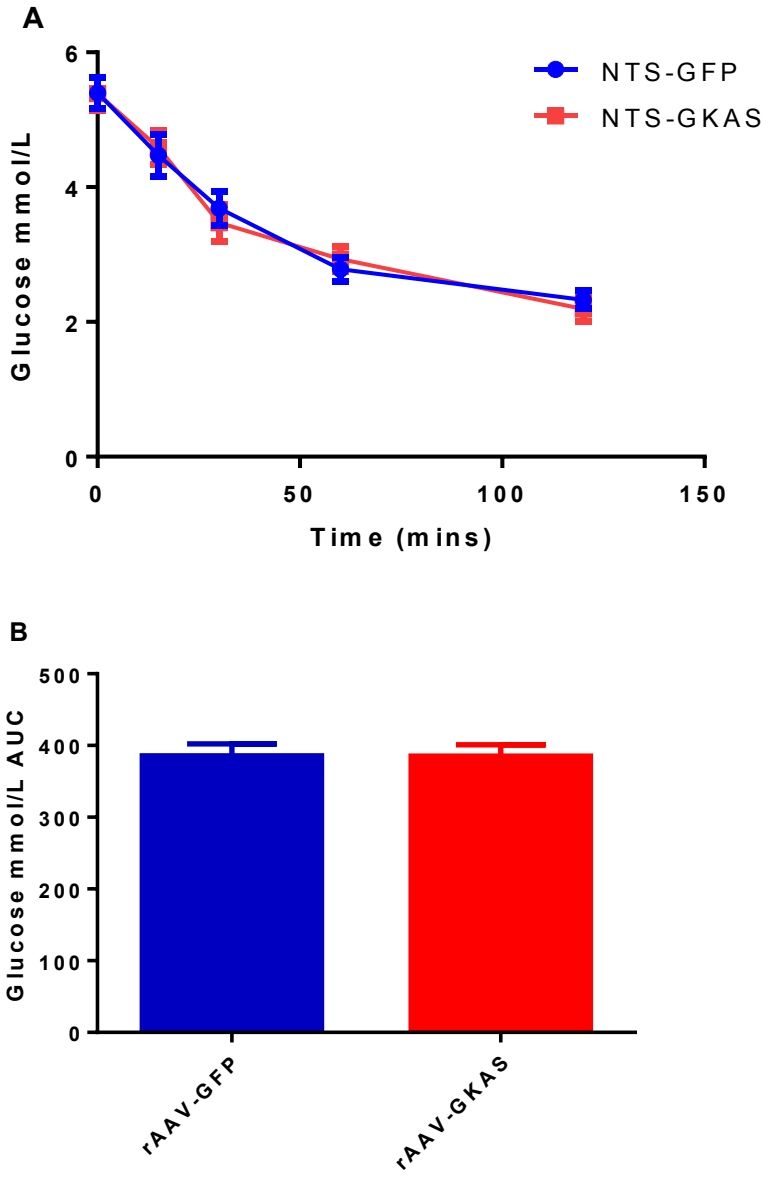


Figure 3.8: NTS GK knockdown did not affect the response to insulin-induced hypoglycaemia. Insulin tolerance test comparing plasma glucose concentration of male Wistar rats stereotactically injected with rAAV-GFP (n=10) or rAAV-GKAS (n=9) in the NTS. **(A)** Glucose concentration was measured using a glucose oxidase assay and **(B)** the area under the curve was determined. Blood samples were collected via a tail vein cannula at 0, 15, 30, 60 and 120 minutes following an IP insulin injection (2IU/kg). Data was analysed using an unpaired T-test at each time point.

3.3.3 Verification of GK knockdown in the NTS

Following the feeding study the rats were killed, the brain collected and *in situ* hybridization using a Woodchuck hepatitis virus Post-transcriptional Regulatory Element (WPRE) antisense labelling probe was performed to confirm trans-gene expression. This method revealed that rAAV-GKAS was accurately injected in the NTS and was localized to this region as WPRE was expressed within the mNTS tissue (Fig. 3.9). A GK activity assay was also performed to assess the degree of GK knockdown. Other hexokinases were inhibited to ensure that only GK activity was being measured. The assay showed that stereotactic rAAV-GKAS injection significantly reduced GK activity in the NTS by 18% (Fig. 3.10).

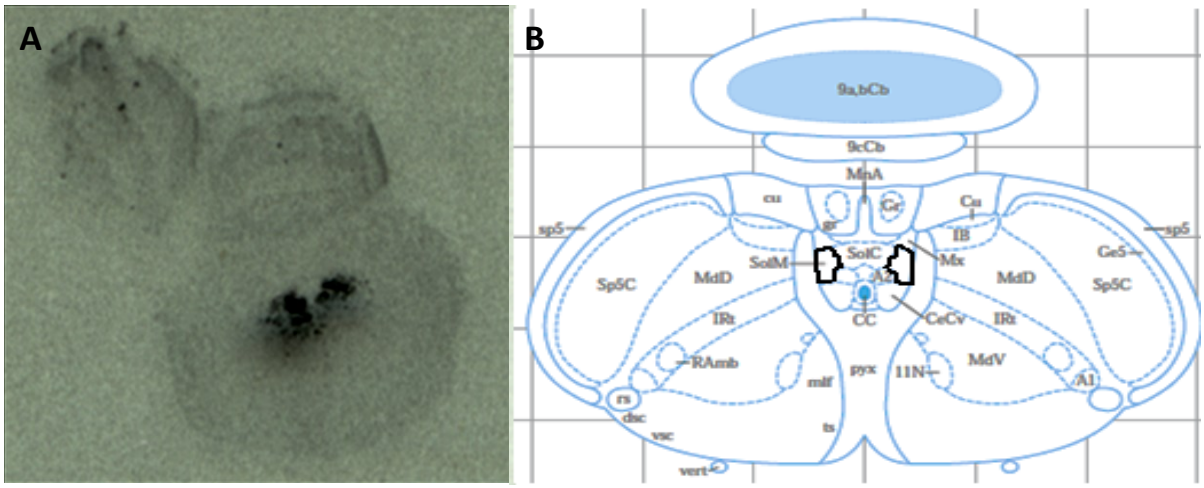


Figure 3.9: rAAV-GKAS injection was accurate and localized to the mNTS. (A) Representative image of rAAV-GKAS-injected brains labelled with WPRE antisense probe. Isolated brainstems were sliced 12µm thick, freeze-thaw mounted on glass slides and hybridized overnight with a WPRE antisense-expressing probe containing ^{35}S CTP. **(B)** Diagram of a coronal section of rat brainstem at coordinates -15.24mm from Bregma, interaural -6.24mm from the Rat Brain Atlas from Paxinos and Watson, with the injection area (mNTS) highlighted.

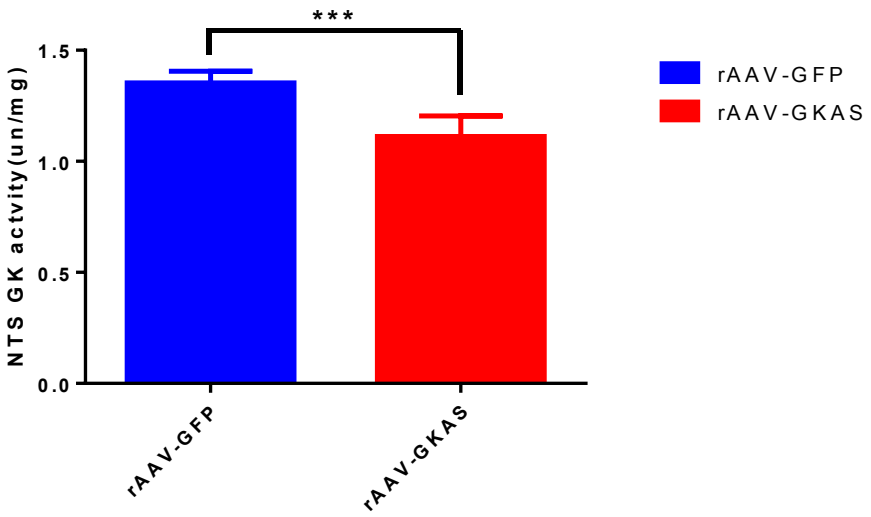


Figure 3.10: GK activity in the NTS was reduced by 18% in rAAV-GKAS rats. GK activity of rAAV-GFP (n=11) and rAAV-GKAS (n=10) rats was assessed in a GK activity assay. The NTS of each animal was collected using a micropunch biopsy. Data is expressed as mean ± SEM and was analysed using an unpaired T-test: ***p<0.001.

3.4 Discussion

3.4.1 Decreasing GK expression in the NTS does not influence feeding behaviour

To examine whether GK in the NTS has an effect on feeding behaviour, its expression was knocked down via stereotactic injection of recombinant adeno-associated virus (rAAV) containing antisense RNA for GK directly into the NTS. Appetite was then evaluated during a feeding study comprising standard chow diet with and without 10% w/v glucose solution being available at the same time.

Although a small increase in energy intake was observed in animals where NTS GK was knocked down, this difference was not significant between groups. Contrary to the hypothesis stated in section 3.2.1, NTS GK does not appear to play an important role in the regulation of appetite as the reduction in GK expression did not yield a significant difference in food intake, glucose consumption or the rate of body weight gain in comparison to control animals. Therefore although the NTS is critically involved in the regulation of satiety, GK is unlikely to play a part in this process.

The NTS limits energy intake as it is a key relay centre between the hypothalamus and the gut (Jovanovic and Yeo, 2010, Konner et al., 2009, Blevins et al., 2003, Blevins et al., 2009, Blevins et al., 2004, Sutton et al., 2004). Contreras *et al*. also hypothesized a complementary role between the NTS and the AP in the regulation of energy intake (Contreras et al., 1984).The observations described in the above paragraphs suggest that GK, despite its presence in the appetite-regulating centre, does not play a role in this NTS function. As of yet, no evidence has been presented supporting a role for NTS GK in the regulation of feeding behaviour. The glucose-sensor's function in the NTS remains to be explored.

3.4.2 NTS GK plays a role in the regulation of glucose homeostasis

Similarly to the feeding study, GK expression in the NTS was reduced by injecting rAAV-GKAS into the NTS. A GTT and ITT were performed to determine the effect of GK knockdown on glucose homeostasis. Blood samples were collected at various time points, after which plasma levels of glucose, insulin and GLP-1 were measured.

The oral GTT revealed that NTS GK knockdown appears to have compromised the rAAV-GKAS rats' ability to normalize their glycaemic levels following a glucose challenge, indicating that GK in this nucleus may be involved in the regulation of glucose homeostasis. Correspondingly to the higher glucose levels, insulin levels were significantly lower in rAAV-GKAS rats compared to control animals. This may suggest that glucose-stimulated insulin secretion (GSIS) was impaired in knockdowns, which would explain their elevated glycaemia during the GTT. NTS GK hence appears to regulate GSIS. Plasma GLP-1 levels were unaffected by the injection of rAAV-GKAS, implying that NTS GK has no influence on the secretion of this peptide.

The ITT showed no difference in glucose levels between the two groups, implying that the counter-regulatory response to hypoglycaemia was unaffected by the rAAV-GKAS injection. NTS GK hence does not appear to play a role in counteracting hypoglycaemia.

The data collected suggest that GK in the NTS is involved in restoring euglycaemia following an increase in plasma glucose levels by stimulating the release of insulin from pancreatic β-cells. I propose the following mechanism.

Following glucose ingestion during the oral GTT, plasma glucose levels increase dramatically. Glucose enters the NTS via the AP, a highly fenestrated circumventricular organ in the DVC that enables the

movement of large molecules such as glucose through the blood-brain barrier (BBB) (Stein and Loewy, 2010). Glucose then diffuses into the adjacent NTS and into the neurons via GLUT2 (Lamy et al., 2014), at which point GK senses the increase in circulating glucose levels. GK thus appears to be expressed in GE neurons, which are mostly present in the medial NTS. It appears to be involved in NTS neuronal firing as its inhibitor glucosamine prevented the depolarization of NTS GABAergic GE neurons during a patch-clamp recording (Boychuk et al., 2015). Tolbutamide also blocked the depolarizing response, suggesting that K_{ATP} channels are important in this process (Boychuk et al., 2015).

GK's effects on GSIS are likely to occur by the transmission of parasympathetic efferent signals from the medial NTS to the pancreas via the vagus nerve (Berthoud and Powley, 1990, Ahren, 2000). Indeed, the pancreas possesses vagal innervations and signalling from the NTS to the pancreas has been reported previously (Rinaman and Miselis, 1987). For instance, GABAergic GLUT2-expressing neurons project to pancreatic α-cells and increase glucagon secretion following detection of hypoglycaemia (Lamy et al., 2014). Parasympathetic vagal projections are thought to extend directly to β-cells, as stimulation of the vagus nerve increased insulin secretion (N'Guyen et al., 1994). This was observed in a hyperglycaemic environment, which mirrors the conditions of the GTT. The DMV is likely to serve as a relay centre in the NTS-pancreas pathway as it provides the pre-ganglionic motor fibers that project to the viscera (Travagli et al., 2006). It also innervates the intra-pancreatic ganglia and is believed to contribute to the modulation of pancreatic secretory functions, including glucose homeostasis (Berthoud and Powley, 1990, Berthoud and Powley, 1987, Berthoud, 2006, Ionescu et al., 1983, Love et al., 2007, Babic et al., 2012, Babic et al., 2013, Streefland et al., 1998). Microstimulation of the DMV causes the release of insulin from the pancreas (Laughton and Powley, 1987). Parasympathetic vagal activity may induce insulin secretion by releasing the neurotransmitter acetylcholine (ACh), which likely acts on post-synaptic nicotinic as well as muscarinic M2 and M3 receptors located on pancreatic β-cells (Sobocki et al., 2005, Ahren, 2000, Woods and Bernstein,

1980). Indeed, electrical vagal stimulation of isolated rat pancreas with vagal innervation produced an increase in insulin secretion. The response was partially suppressed by the infusion of the muscarinic antagonist atropine and by nicotinic blockade using hexamethonium (Mussa and Verberne, 2008, Mussa et al., 2011, Nishi et al., 1987, Ahren et al., 1986). Some evidence suggests, however, that efferent muscarinic activity may not play a role in inducing insulin secretion. For instance a study conducted in humans demonstrated that insulin secretion was in fact increased by peripheral atropine administration, although this was determined by measuring glucose and C-peptide levels rather than insulin directly (Plamboeck et al., 2015). Various other non-cholinergic neurotransmitters are believed to contribute to the parasympathetic control of islet secretory response, including vasoactive intestinal polypeptide (VIP), gastrin-releasing peptide (GRP) and pituitary adenylate cyclase activating polypeptide (PACAP) (Ahren et al., 1986, Havel et al., 1997, Knuhtsen et al., 1987, Fridolf et al., 1992, Holst et al., 1987). These substances are present in islet parasympathetic terminals and act to stimulate insulin release (Gregersen and Ahren, 1996, Straub and Sharp, 1996).

While the NTS is an important glucose-sensing nucleus, increases in glucose levels may also be detected by regions of the brain such as the hypothalamus. The ARC, VMN, DMN and PVN all possess glucose-sensing properties and express various components required in this process (Hussain et al., 2015, Alvarez et al., 2002, Roncero et al., 2004, De Backer et al., 2016). The response to a glucose challenge may thus be initiated by hypothalamic nuclei, in which case the NTS may function as an effector of the response. Numerous connections exist between the hypothalamus and NTS, many of which are involved in the neuronal regulation of appetite (Geerling et al., 2010, Blevins et al., 2004).

Further research is required to identify the mechanism at play, as the downstream pathway following GK activation is unknown. As NTS GK knockdown decreased glucose tolerance, GK appears

to be expressed in GE neurons. The mechanism of activation of these neurons may be similar to that of pancreatic β-cells, which also become depolarized following a glucose challenge. Glucose phosphorylation by GK may inhibit K_{ATP} channel activity by increasing the production of ATP through the electron transport chain. K_{ATP} channel inhibition would cause an accumulation of K^+ ions and a change in membrane potential. Depolarisation of NTS neurons could then ensue due to Ca^{2+} entry through Ca^{2+} channels. The signal may propagate towards the pancreas along the parasympathetic branch of the vagus nerve and may culminate in the release of a neurotransmitter such as ACh. The neurotransmitter may in turn trigger a signal to stimulate insulin secretion from pancreatic β-cells. The question of whether signal transmission from the NTS to pancreatic β-cells occurs via parasympathetic vagal projections or through another pathway needs to be explored.

3.4.3 Methods and measurements of altered GK activity

Recombinant AAV encoding GK antisense was utilized to decrease the expression of endogenous GK. The *in situ* hybridization image (section 3.3.4) confirmed trans-gene expression as they revealed that WPRE was expressed in the NTS of rAAV-GKAS animals. WPRE was included in the plasmid construct as it increases the expression of gene delivered via viral vectors, in this case the GK antisense sequence (Klein et al., 2006). It also acts as a marker indicating whether trans-gene expression was successful as its expression in the NTS confirms that the rAAV successfully induced gene transfer within neurons. It is therefore a strong indication that the GK antisense sequence, which was contained in the rAAV construct along with WPRE, was also expressed by the host tissue. The localisation of WPRE expression shown in the *in situ* hybridization image suggests that the AAV injected may have spread outside of the medial NTS, where GK is likely to be expressed, to other NTS regions such as the lateral NTS, ventricular NTS or dorsal NTS. The AAV remained in the NTS, however, demonstrating that it was accurately injected into the targeted area.

Although WPRE expression provides a valuable indication of trans-gene expression, it does not reveal the degree of GK knockdown. To test the efficacy of the plasmid to alter GK *in vivo*, GK activity in isolated NTS of rAAV-GKAS rats was determined and compared to that of rAAV-GFP animals. GK activity was calculated using a modified NADPH assay as described previously (Goward et al., 1986, Hussain et al., 2015). The assay revealed that stereotactic rAAV-GKAS injection into the NTS reduced GK activity by 18% compared to that of rAAV-GFP rats. This demonstrates that rAAV-GKAS can significantly alter GK activity *in vivo*. The level of knockdown observed in this study is inferior to that of previous studies. For instance, a rAAV-GKAS injection into the arcuate nucleus (ARC) resulted in a 50% reduction in GK expression (Hussain et al., 2015). The low level of trans-gene expression may have impacted the results collected. If the extent of knockdown of GK activity in the NTS had been near 50% as expected, the results may have been more pronounced than those observed. The level of glucose during a GTT may have been even higher in rAAV-GKAS rats compared to control animals and an effect on appetite could have been observed. One can hence hypothesize that NTS GK may play a more important role in the regulation of energy homeostasis than the results described here would indicate. Inducing a higher level of knockdown of GK expression will enable a more accurate assessment of the physiological role of NTS GK in the regulation of energy homeostasis.

3.4.4 Conclusions

Feeding studies revealed that GK in the NTS is not involved in the control of appetite. NTS GK is more likely to play a role in the regulation of glucose homeostasis. The data collected suggest that GK in the NTS is important in re-establishing euglycaemia following a glucose challenge by playing a role in

regulating GSIS from pancreatic β-cells. An influence of NTS GK on peripheral insulin secretion has not been shown previously and additional investigation is necessary to shed light on this effect.

Chapter 4 – The role of glucokinase in the paraventricular nucleus

4.1 Introduction

The hypothalamus is composed of several nuclei. The PVN is one such nucleus and is believed to be involved in the regulation of homeostasis. Located at the top of the third ventricle it is divided into two major sections, the magnocellular and parvocellular, which have distinct neuronal connections and functions. Axons from neurons of the magnocellular division mainly terminate in the posterior pituitary and play a role in oxytocin and vasopressin release (Hill, 2012). The autonomic neurons of the parvocellular division project to the NTS, the DMV and to the intermediolateral cell column of the spinal cord containing sympathetic preganglionic fiber cell bodies (Geerling et al., 2010). These connections establish a neuronal link via the vagus nerve between this section and numerous peripheral organs including the stomach, pancreas and intestines (Jansen et al., 1997, Rogers and Hermann, 1985, Li et al., 2014). The parvocellular PVN is therefore predominantly associated with the regulation of feeding and energy homeostasis.

4.1.1 The PVN and appetite

Interest in the PVN as a potential regulator of appetite arose when lesions were reported to cause weight gain and hyperphagia in rodents (Yoshida et al., 1989, Wang and Powley, 2007, Wang et al., 2007), and to date numerous studies have implicated this hypothalamic nucleus in the control of feeding behaviour.

A number of peptides involved in the control of feeding are expressed in the PVN, including cocaine and amphetamine regulated transcript (CART), thyrotropin-releasing hormone (TRH) and oxytocin (Wynick and Bacon, 2002, Blevins et al., 2004, Wang et al., 2000, Simmons and Swanson, 2009).

Numerous studies showed that the PVN plays an important role in integrating information regarding food intake to regulate energy homeostasis. For instance, microinjection of peptides directly into the PVN influenced feeding behaviour. Microinjection of galanin into the PVN increased food intake, particularly for carbohydrate or fat rich food (Crawley et al., 1990, Kyrkouli et al., 2006, Tempel et al., 1988, Karatayev et al., 2009). Similarly, injections of neuropeptide Y (NPY) directly into the PVN resulted in a marked increase in food intake compared to controls (Stanley et al., 1985) and orexin A injection into the PVN also stimulated food intake (Edwards et al., 1999). In addition, intracerebroventricular (ICV) injections of CART resulted in decreased food intake and a reduction in PVN neuronal activation, while intra-PVN (iPVN) CART injections decreased NPY-induced feeding (Stanley et al., 2001, Wang et al., 2000). Moreover, GLP-1 injections into the PVN also had an inhibitory effect on feeding behaviour (Katsurada et al., 2014). Genetic modulation of PVN peptide expression can also alter appetite. For example, genetic over-expression of NPY in the rat PVN led to an increased rate of body weight gain (Tiesjema et al., 2007). On the other hand, genetic over-expression of leptin within the PVN reduced energy intake (Bagnasco et al., 2003). Genetic over-expression of CART in the PVN of rats increased food intake and weight gain compared to control animals (Smith et al., 2008). Food intake in rodents was also modified by pharmacologically modulating the activity of certain PVN peptides. For instance, injection of galanin antagonists into the PVN decreased food intake (Corwin et al., 1993, Crawley et al., 1993). Interestingly, one study reported a decreased fat preference following iPVN injection of galanin antagonists (Odorizzi et al., 2002). Likewise, suppression of PVN NPY via injection of anti-NPY gamma-globulin significantly decreased food intake in rats (Shibasaki et al., 1993).

The PVN forms part of a well-established forebrain-hindbrain mechanism contributing to the initiation of satiety, which has been described in section 3.1.1. Following a meal leptin in the ARC stimulates the release of αMSH, which acts on MC4 receptors (MC4Rs) in the PVN. The activation of these receptors then stimulates oxytocin signalling from the PVN, which triggers the release of

satiety signals such as CCK8 (Blevins et al., 2004) and GLP-1 (Williams et al., 2006) in the NTS. The signal is then propagated to the gut via the vagus nerve. MC4R-expressing neurons in the PVN also project to the NTS directly (Blevins et al., 2009).

4.1.2 Glucose-sensing neurons in the PVN

In addition to its role in appetite regulation, the PVN is believed to act as a glucose-sensing centre. Its involvement in glucose-sensing is not well understood, however, as few studies have examined the glucose-sensing properties of this nucleus.

Electrophysiology and immunocytochemistry studies suggest the presence of glucose-sensing neurons in the PVN, particularly in the parvocellular region, as parvocellular PVN glucopenia hyperpolarized some neurons and depolarised others (Melnick et al., 2011). The PVN may hence contain both GE and GI neurons as neuronal firing rates were altered by varying ambient glucose concentrations.

K_{ATP} channels, which form part of the glucose-sensing mechanism of GE neurons, may be expressed in the PVN. Several studies have demonstrated their existence in this nucleus using various methods such as receptor autoradiographic binding and electrophysiology (Hoyda and Ferguson, 2010, Levin and Dunn-Meynell, 1997). For instance, patch-clamp recordings of PVN neurons demonstrated that pharmacological modulation of K_{ATP} channel activity altered the firing rate of PVN neurons (Li et al., 2010). Evidence against the expression of K_{ATP} channels in the PVN also exists; however, as another study reported that neither K_{ATP} channel inhibitors nor activators changed the firing rate of GE neurons in response to PVN glucopenia (Melnick et al., 2011).

GLUT2 is moderately expressed in the PVN. It may be involved in glucose-sensing by enabling the influx of glucose into neurons as GLUT2 has high affinity for glucose and only saturates at glucose concentrations above 30mM (Arluison et al., 2004, Navarro et al., 1996, Oosterveer and Schoonjans, 2014). Low levels of GLUT1 and GLUT3, which is generally considered to be the main glucose transporter in neurons, mRNA have also been found in PVN neurons (Koehler-Stec et al., 2000).

4.1.3 Glucokinase in the PVN

The PVN exhibits a moderate expression of GK mRNA compared to other hypothalamic regions where its expression is high, such as the ARC (Lynch et al., 2000, Nishio et al., 2006, Dunn-Meynell et al., 2002). GK regulatory protein (GKRP) was also detected in this nucleus (Alvarez et al., 2002). The highest density of GK-expressing neurons was located in the parvocellular division of the PVN (Lynch et al., 2000, Lenglos et al., 2014).

Some studies have suggested the expression of PVN GK varies according to nutrient availability. For instance, Lenglos *et al.* reported that PVN GK mRNA expression is higher in diet-induced obese (DIO) rats than in diet-restricted (DR) rats (Lenglos et al., 2014). Another claimed that chronic hypoglycaemia causes up-regulation of GK and CRH in the PVN (Briski et al., 2009). Little work has been done to characterise the role of GK in the PVN and its function in this nucleus is poorly understood.

GK may play a role in PVN glucose-sensing. Increases in ambient glucose concentrations stimulated oxytocin and vasopressin release during a hypothalamic explant study and the use of GK inhibitors suggested that this effect may occur via GK. It also increased cellular Ca^{2+} levels (Sladek et al., 2016, Song et al., 2014), indicating that glucokinase-expressing neurons in the SON are GE in type. The

glucokinase-induced release of oxytocin is consistent with the PVN's role in satiety, as PVN oxytocin neurons project to the NTS to induce CCK release (Blevins et al., 2003). GLUT2 and GK are co-localised in the SON, further implying a role for GK in PVN glucose-sensing (Navarro et al., 1996).

4.2 Hypothesis and Aims

4.2.1 Hypothesis

It is hypothesized that PVN GK plays an important role in energy homeostasis and that regulation of both appetite and glucose homeostasis will be impacted by genetic and pharmacological modulation of PVN GK expression. It is also hypothesized that K_{ATP} channels are involved in the downstream signalling pathway following GK activation.

4.2.2 Aims

The role of glucokinase in the PVN in the regulation of appetite and glucose homeostasis will be determined according to the following methodology.

1. GK expression will be knocked down via stereotactic injection of rAAV-GKAS. The accuracy of the injection will be confirmed using a GK activity assay.
2. GK-deficient and control rats' chow and glucose solution intake, as well as total energy intake and body weight gain, will be measured during a feeding study.
3. Glucose tolerance tests (both oral and intraperitoneal glucose delivery) and an insulin tolerance test, as well as oral gavage of L-arginine, will be performed following tail vein cannulation. Blood samples will be collected at various time points and plasma glucose, insulin, GLP-1 (7-36) and glucagon levels will be analysed.
4. The effects of GK knockdown on insulin and GLP-1 (7-36) secretion will be investigated. The level of glucose-stimulated insulin secretion from isolated islets of rAAV-GKAS rats will be compared to that of rAAV-GFP animals. Gene expression of proglucagon and PYY in the ileum of GK-deficient rats will then be compared to that of control animals.

5. The expression of GK will be up-regulated via stereotactic injection of rAAV-GKS and the accuracy of the injection will be confirmed using a GK activity assay. Step 3 will be repeated to further assess the role of PVN GK in glucose homeostasis.
6. A unilateral iPVN cannula will be stereotactically fixed in WT animals to enable intra-nuclear injections directly into the PVN. The location of the cannula will be verified using cresyl violet staining.
7. The effects of pharmacologically increasing the activity of PVN GK via iPVN injections of CpdA on glucose homeostasis will be examined during an oral GTT. The involvement of K_{ATP} channels in PVN GK's control of glucose homeostasis will be determined by pharmacologically activating and inhibiting these channels using iPVN injections of diazoxide and glibenclamide prior to an oral GTT. Glucose will also be delivered into the PVN prior to an oral GTT. Plasma glucose, insulin, GLP-1 (7-36) and glucagon levels will be analysed at the end of each test.

4.3 Results

4.3.1 The role of PVN GK in the regulation of appetite

A feeding study was conducted following the protocol described in 3.3.2 to determine whether PVN GK is involved in appetite regulation.

Knockdown of GK in the PVN did not induce a change in the rate of body weight gain when the animals were offered chow alone or when glucose solution was also presented (Fig. 4.1). Likewise, no difference in food intake was observed regardless of the availability of glucose (Fig. 4.2). No difference in the consumption of glucose solution was noted (Fig 4.3). There was therefore no change in total energy intake between the two groups (Fig. 4.4). The feeding study revealed that PVN GK does not appear to be involved in the control of feeding behaviour.

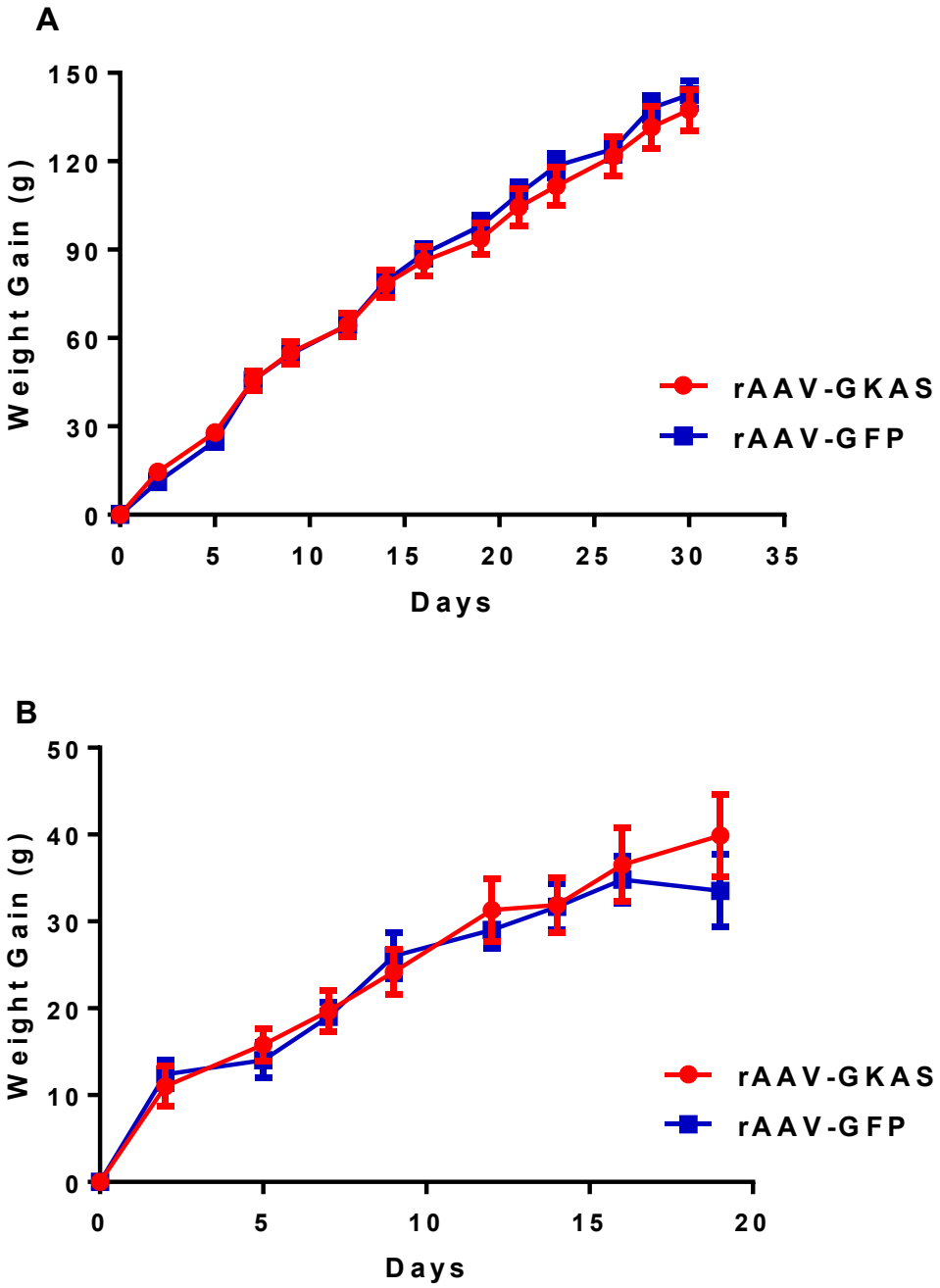


Figure 4.1: GK knockdown had no effect on the rate body weight gain compared to controls animals, both in the absence and presence of glucose solution. Feeding study comparing male Wistar rats injected with either rAAV-GKAS (n=7) or rAAV-GFP (n=9) into the PVN. The rate of body weight gain of the animals with *ad libitum* access to **(A)** food only or **(B)** both food and 10%w/v glucose solution was monitored. All values are expressed as mean ± SEM. Data were analysed using Generalized Estimating Equation.

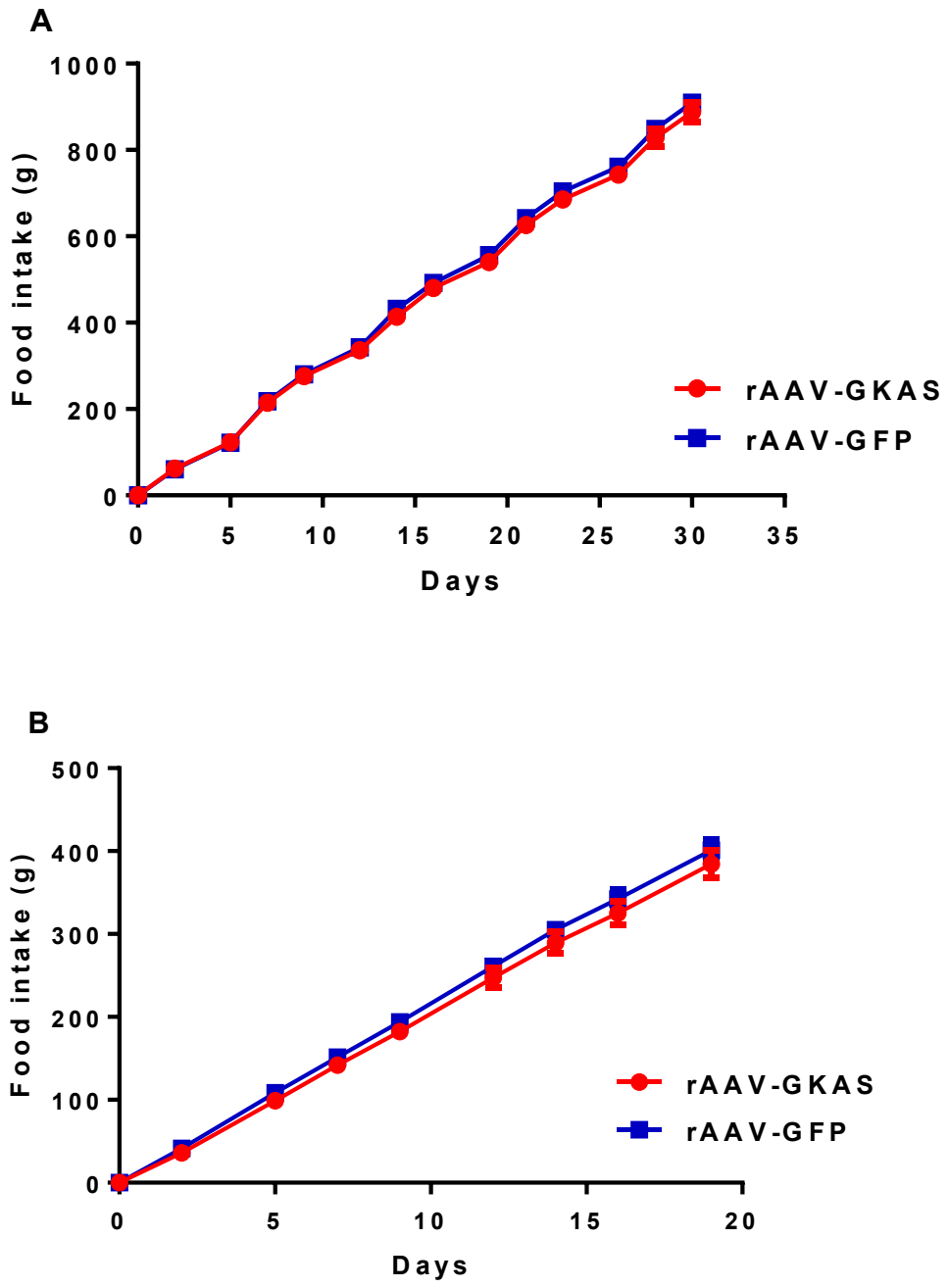


Figure 4.2: GK knockdown had no effect on food intake compared to controls animals, both in the absence and presence of glucose solution. Feeding study comparing male Wistar rats injected with either rAAV-GKAS (n=7) or rAAV-GFP (n=9) into the PVN. Chow intake of the animals with *ad libitum* access to **(A)** food only or **(B)** both food and 10%w/v glucose solution was monitored. All values are expressed as mean ± SEM. Data were analysed using Generalized Estimating Equation.

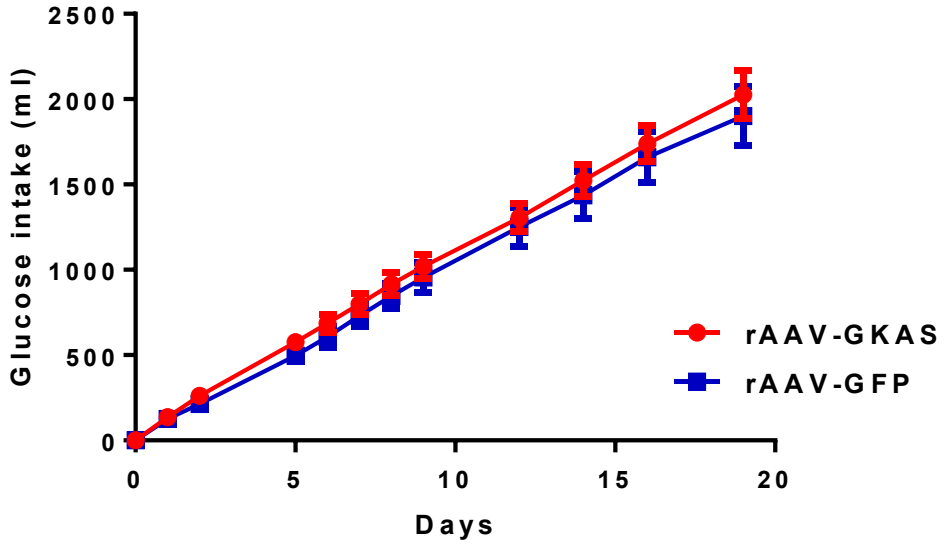


Figure 4.3: GK knockdown had no effect on glucose intake compared to controls animals. Feeding study comparing male Wistar rats injected with either rAAV-GKAS (n=7) or rAAV-GFP (n=9) into the PVN. Glucose intake of the animals with *ad libitum* access to both food and 10%w/v glucose solution was monitored. All values are expressed as mean ± SEM. Data were analysed using Generalized Estimating Equation.

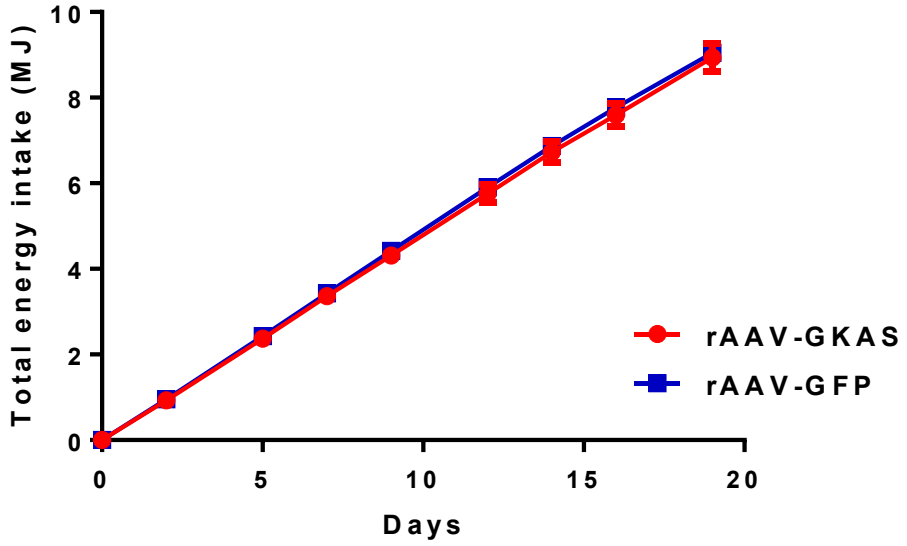


Figure 4.4: GK knockdown had no effect on total energy intake compared to controls animals, both in the absence and presence of glucose solution. Feeding study comparing male Wistar rats injected with either rAAV-GKAS (n=7) or rAAV-GFP (n=9) into the PVN. Total energy intake (glucose solution + food) of the animals with *ad libitum* access to both food and 10%w/v glucose solution was monitored. All values are expressed as mean ± SEM. Data were analysed using Generalized Estimating Equation.

4.3.2 The role of PVN GK in the regulation of glucose homeostasis

The role of PVN GK in glucose homeostasis was assessed in both rAAV-GKAS and rAAV-GKS rats as well as in control rAAV-GFP animals. An oral glucose tolerance test (GTT), intraperitoneal (i.p.) GTT and an insulin tolerance test (ITT) were conducted for each group. Blood samples were collected at various time points using a tail vein cannula, after which the plasma levels of glucose, insulin, GLP-1 (7-36) and glucagon were determined.

4.3.2.1 Oral glucose tolerance test

The animals were fasted overnight prior to the oral GTT and given an oral dose of glucose (2.5g/kg) at the start of the two hour test.

RAAV-GKAS rats had significantly higher plasma glucose levels than control animals at 30 minutes (GFP: 8.22±0.29mmol/L, n=9; GKAS: 9.06±0.33mmol/L, n=9; $p<0.05$) (Fig. 4.5A), suggesting a possible disruption in these animals' ability to normalize glycaemia following a glucose challenge. The overall glucose levels did not differ between the two groups over 120 minutes however, as is demonstrated in the AUC graph (Fig. 4.5B). Knockdown of PVN GK significantly reduced insulin release after 15 minutes compared to control animals (GFP: 3.01±0.26mmol/L, n=9; GKAS: 2.12±0.25mmol/L, n=9; $p<0.05$) (Fig. 4.6A). This may suggest that glucose-stimulated insulin secretion (GSIS) was impaired in rAAV-GKAS rats, which would explain their elevated glycaemia after 30 minutes. The initial insulin response seemed to be specifically affected rather than its overall secretion throughout the test, as AUC analysis revealed no difference in overall insulin release between the two groups (Fig. 4.6B). Secretion of active GLP-1 (7-36) seemed to be highly affected by PVN GK knockdown. Although AUC analysis did not reveal a significant difference in the overall plasma GLP-1 (7-36) concentration

during the oral GTT (Fig. 4.7B), the initial GLP-1 response to a glucose challenge observed in control animals at 30 minutes was abolished in rAAV-GKAS rats (GFP: 6.64±0.31mmol/L, n=8; GKAS: 5.47±0.13mmol/L, n=9; $p<0.01$) (Fig. 4.7A). This may explain the decrease in insulin secretion in GK-deficient animals as GLP-1 is an incretin and stimulates insulin secretion from pancreatic islets. Finally, no difference in plasma glucagon levels was found between the two groups (Fig. 4.8).

Rats overexpressing GK in the PVN had significantly lower plasma glucose levels than control rats after 15 (GFP: 8.66±0.34mmol/L, n=11; GKAS: 7.72±0.22mmol/L, n=12; $p<0.05$) and 30 (GFP: 8.93±0.25mmol/L, n=11; GKAS: 8.20±0.21mmol/L, n=12; $p<0.05$) minutes of an oral GTT (Fig. 4.9A). Similarly to rAAV-GKAS animals, however, the AUC indicates the overall glucose levels throughout the study did not differ between the treatment and wild-type animals (Fig. 4.9B). Whereas insulin secretion appeared to be impaired in rAAV-GKAS animals as described above, insulin secretion was enhanced in rAAV-GKS rats after 15 minutes compared to rAAV-GFP animals (GFP: 2.88±0.13mmol/L, n=11; GKAS: 3.73±0.27mmol/L, n=11; $p<0.01$), suggesting a role of PVN GK in GSIS (Fig. 4.10A). Only the initial insulin response appeared to have been affected by PVN GK up-regulation as overall insulin levels were not statistically different between the two groups (Fig. 4.10B). GLP-1 (7-36) levels were also significantly higher in rAAV-GKS than in rAAV-GFP rats at 30 minutes (GFP: 6.27±0.18mmol/L, n=11; GKAS: 6.88±0.21mmol/L, n=12; $p<0.05$) (Fig. 4.11). As suggested in the study in rAAV-GKAS animals, altering PVN GK expression appears to influence the initial GLP-1 (7-36) response to glucose.

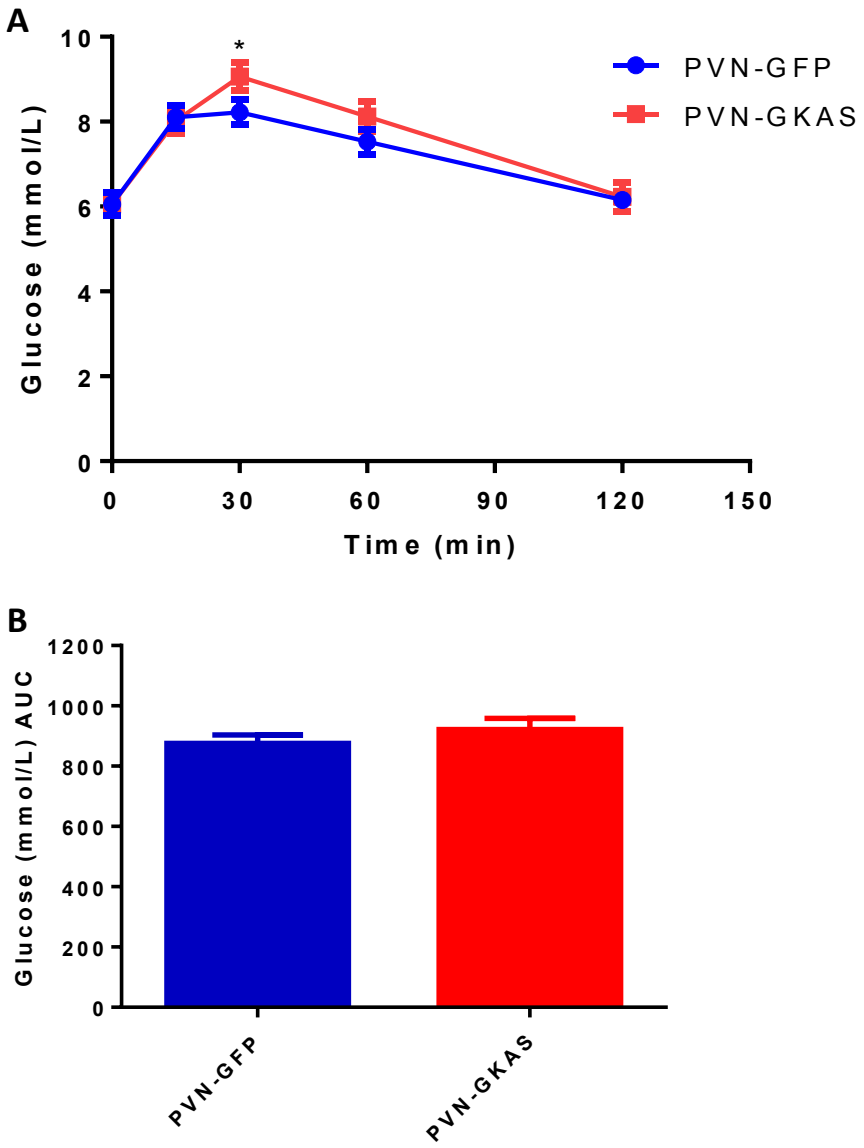


Figure 4.5: PVN GK knockdown impaired initial glucose clearance during an oral GTT. Oral glucose tolerance test comparing plasma glucose concentration of male Wistar rats stereotactically injected with rAAV-GFP (n=9) or rAAV-GKAS (n=9) in the PVN. **(A)** Glucose concentration was measured using a glucose oxidase assay and **(B)** the area under the curve was determined. Blood samples were collected via a tail vein cannula at t=0, 15, 30, 60 and 120 minutes post-ingestion of a 2.5g/kg oral glucose dose. Data is expressed as mean ± SEM and was analysed using an unpaired T-test at each time point using GraphPad Prism 6: *$p<0.05$.

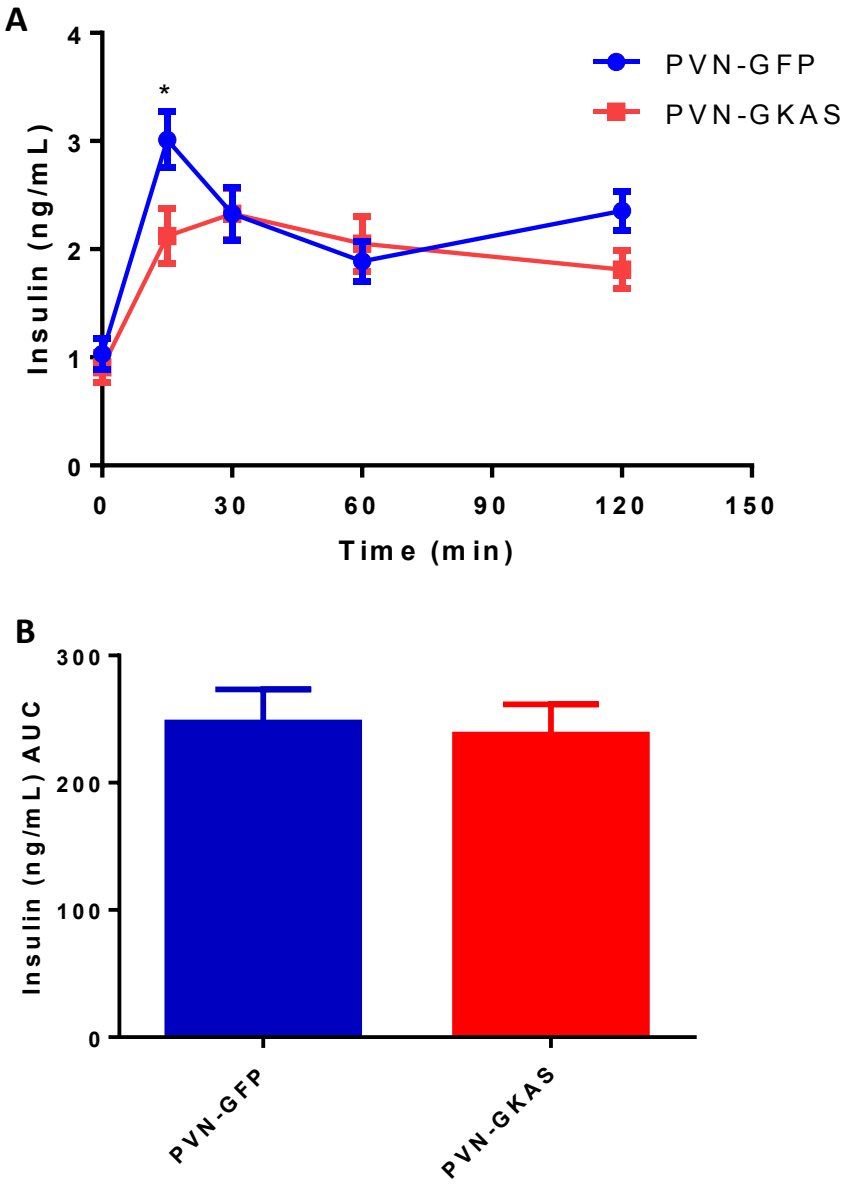


Figure 4.6: The initial insulin response was impaired by PVN GK knockdown during an oral GTT. Oral glucose tolerance test comparing the plasma insulin concentration of male Wistar rats stereotactically injected with rAAV-GFP (n=9) or rAAV-GKAS (n=9) in the PVN. **(A)** Insulin concentration was measured using ELISA and **(B)** the area under the curve was determined. Blood samples were collected via a tail vein cannula at t=0, 15, 30, 60 and 120 minutes post-ingestion of a 2.5g/kg oral glucose dose. Data is expressed as mean ± SEM and was analysed using an unpaired T-test at each time point using GraphPad Prism 6: *p<0.05.

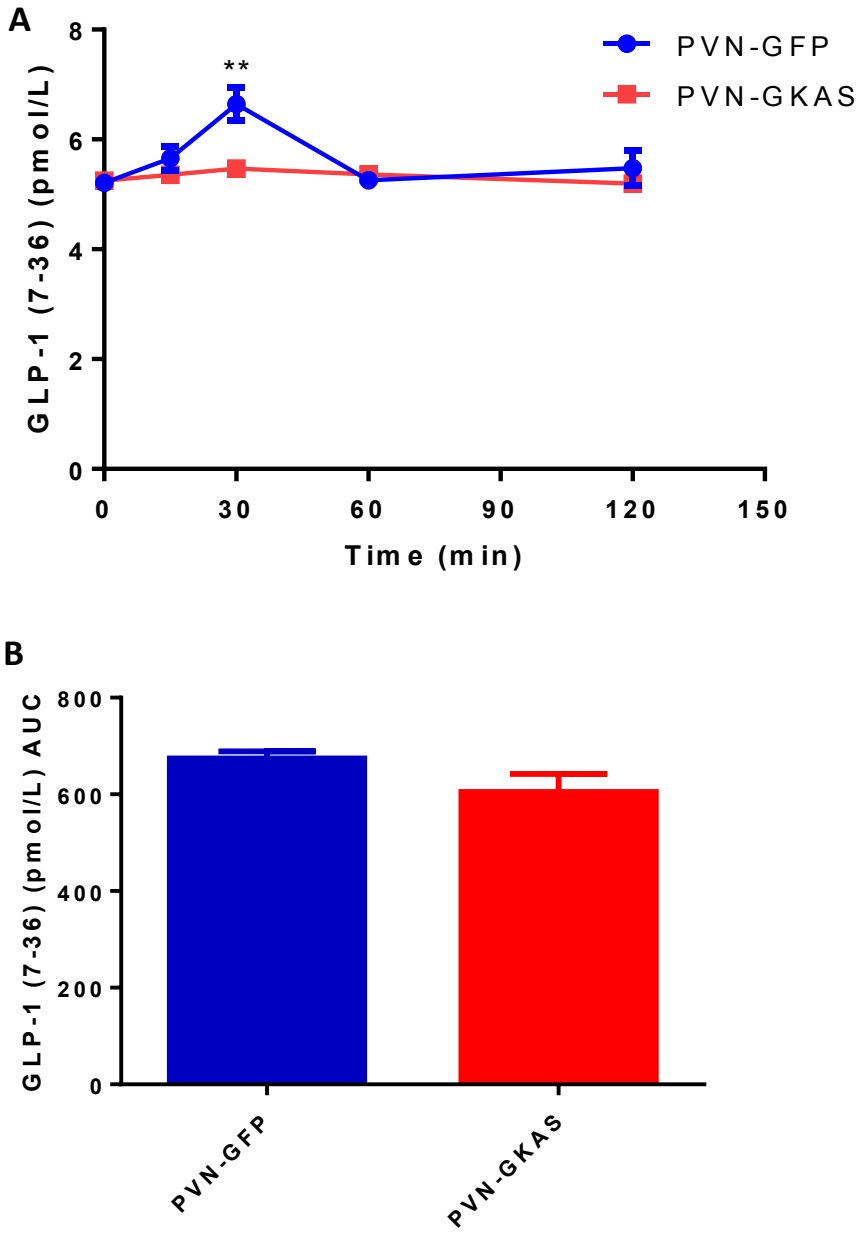


Figure 4.7: PVN GK knockdown disrupted the initial GLP-1 (7-36) response to glucose during an oral GTT. Oral glucose tolerance test comparing the plasma GLP-1 (7-36) concentration of male Wistar rats stereotactically injected with rAAV-GFP (n=8) or rAAV-GKAS (n=9) in the PVN. **(A)** GLP-1 (7-36) concentration was measured using ELISA and **(B)** the area under the curve was determined. Blood samples were collected via a tail vein cannula at t=0, 15, 30, 60 and 120 minutes post-ingestion of a 2.5g/kg oral glucose dose. Data is expressed as mean ± SEM and was analysed using an unpaired T-test at each time point using GraphPad Prism 6: **p<0.01.

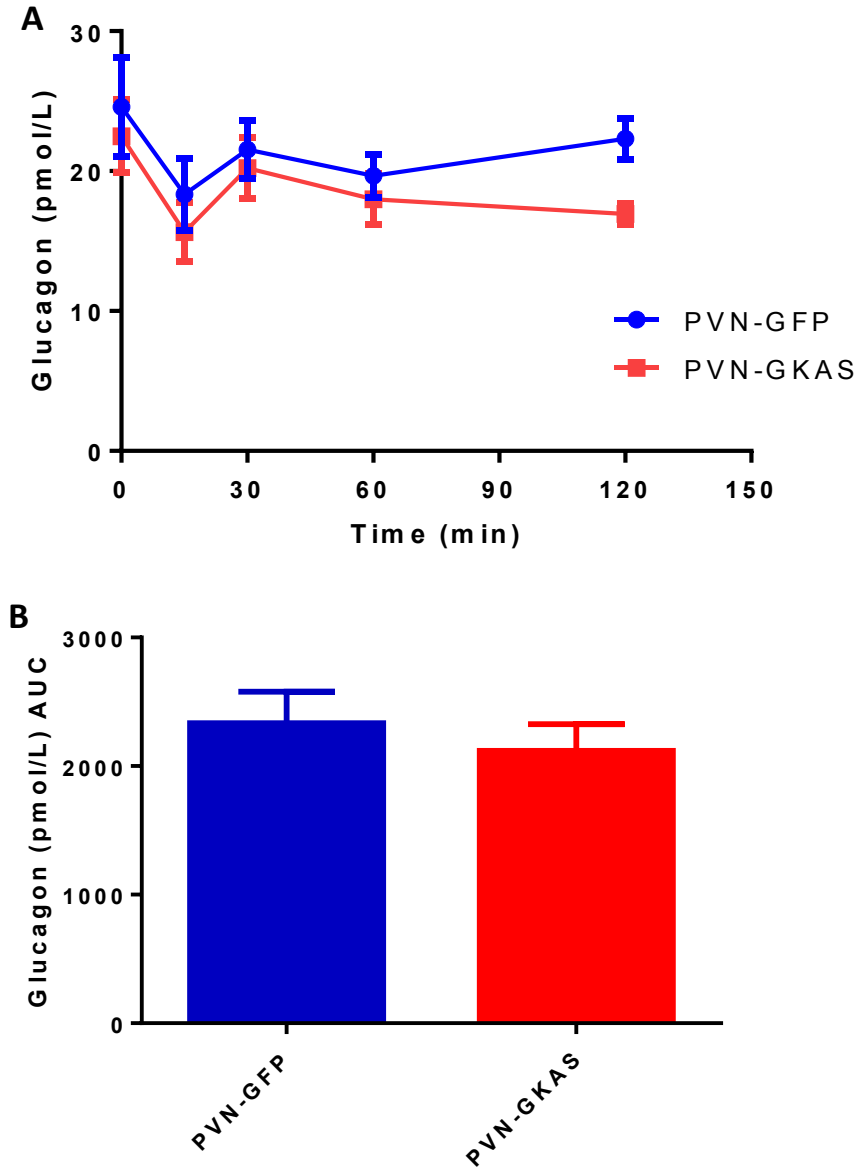


Figure 4.8: PVN GK knockdown did not significantly impair glucagon secretion during an oral GTT. Oral glucose tolerance test comparing the plasma glucagon concentration of male Wistar rats stereotactically injected with rAAV-GFP (n=9) or rAAV-GKAS (n=9) in the PVN. **(A)** GLP-1 (7-36) concentration was measured using ELISA and **(B)** the area under the curve was determined. Blood samples were collected via a tail vein cannula at t=0, 15, 30, 60 and 120 minutes post-ingestion of a 2.5g/kg oral glucose dose. Data is expressed as mean ± SEM and was analysed using an unpaired T-test at each time point using GraphPad Prism 6.

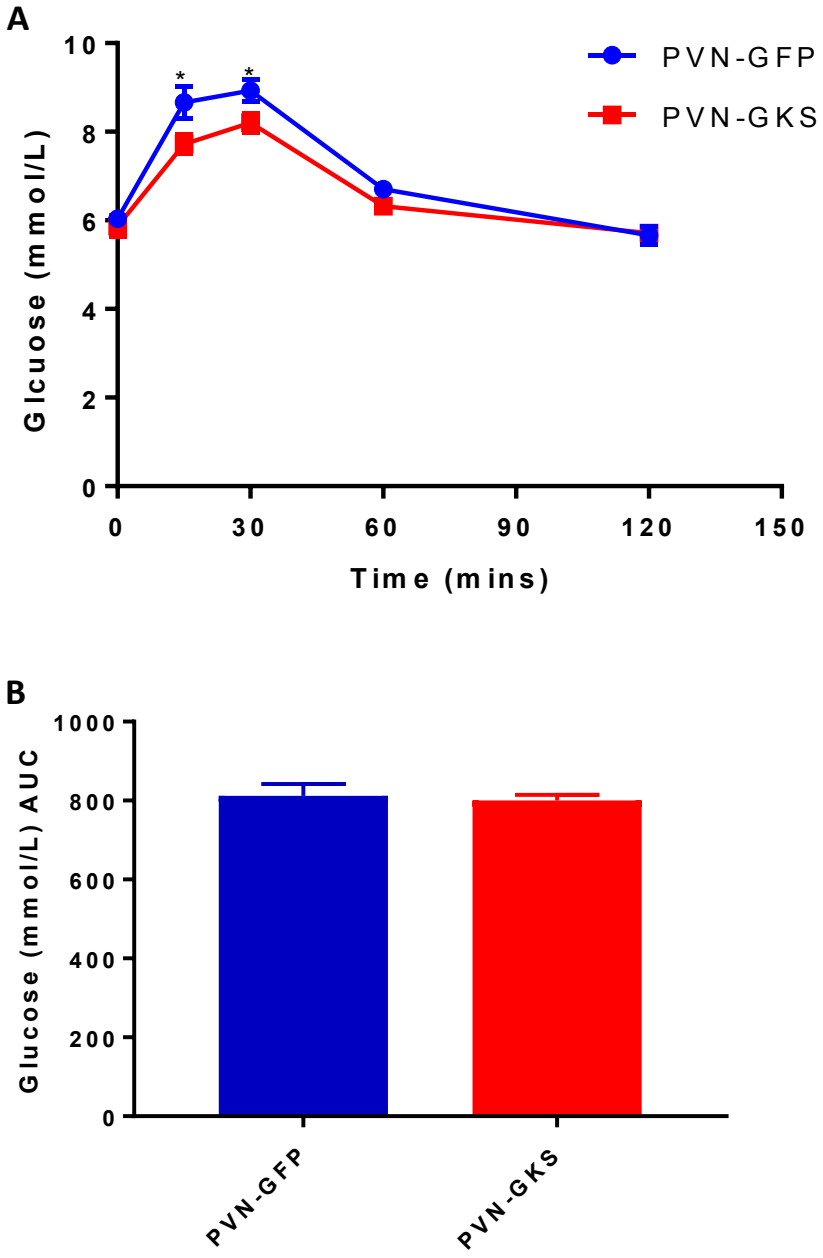


Figure 4.9: PVN GK up-regulation enhanced initial glucose clearance during an oral GTT. Oral glucose tolerance test comparing plasma glucose concentration of male Wistar rats stereotactically injected with rAAV-GFP (n=11) or rAAV-GKS (n=12) in the PVN. **(A)** Glucose concentration was measured using a glucose oxidase assay and **(B)** the area under the curve was determined. Blood samples were collected via a tail vein cannula at t=0, 15, 30, 60 and 120 minutes post-ingestion of a 2.5g/kg oral glucose dose. Data is expressed as mean ± SEM and was analysed using an unpaired T-test at each time point using GraphPad Prism 6: *p<0.05.

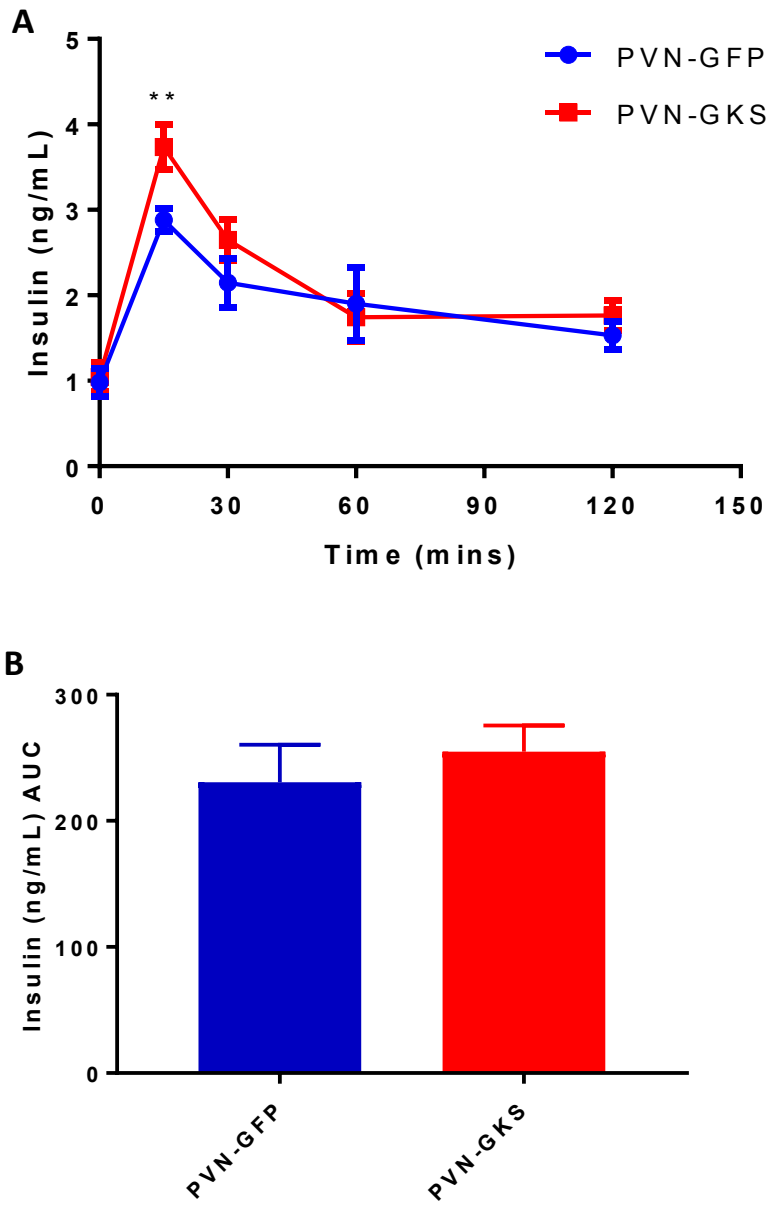


Figure 4.10: PVN GK up-regulation increased the initial insulin response to glucose during an oral GTT. Oral glucose tolerance test comparing the plasma insulin concentration of male Wistar rats stereotactically injected with rAAV-GFP (n=11) or rAAV-GKS (n=12) in the PVN. **(A)** Insulin concentration was measured using ELISA and **(B)** the area under the curve was determined. Blood samples were collected via a tail vein cannula at t=0, 15, 30, 60 and 120 minutes post-ingestion of a 2.5g/kg oral glucose dose. Data is expressed as mean ± SEM and was analysed using an unpaired T-test at each time point using GraphPad Prism 6: **p<0.01.

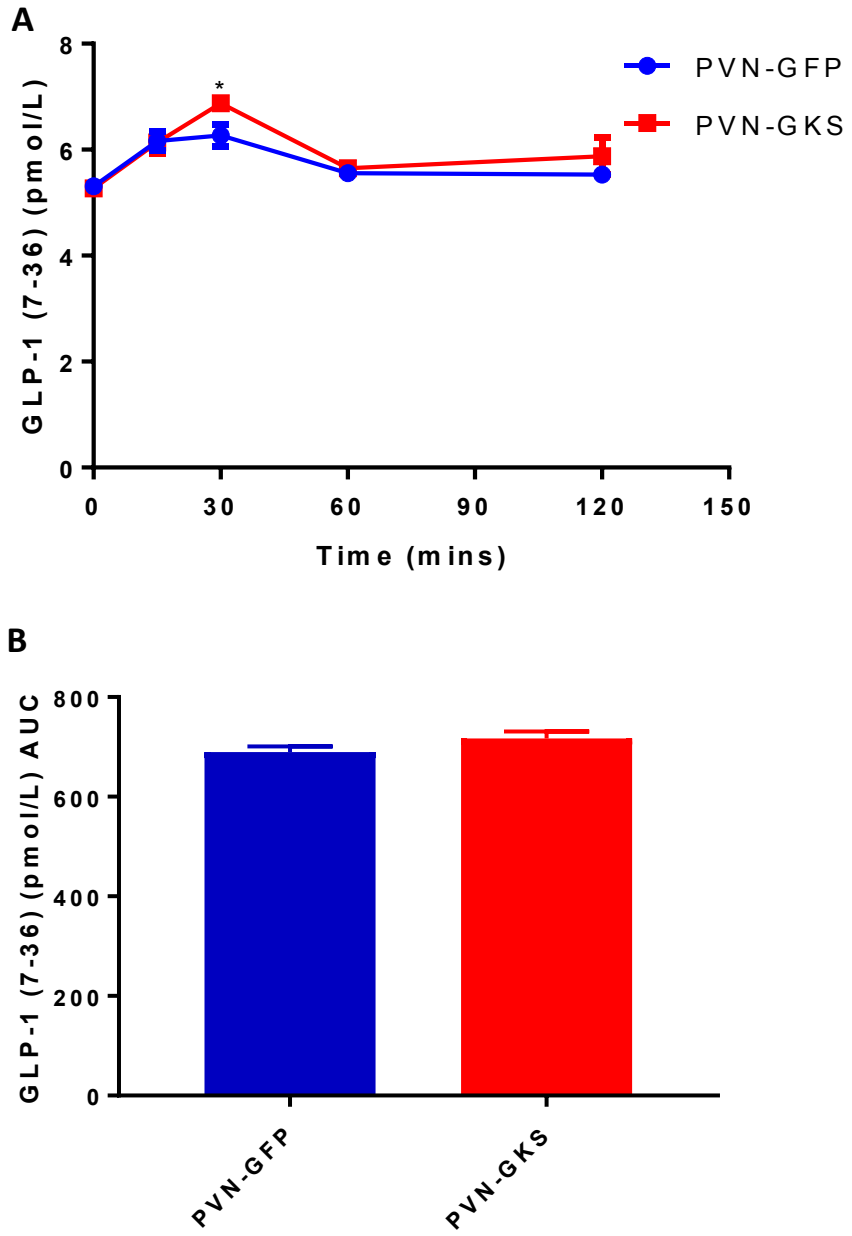


Figure 4.11: PVN GK up-regulation enhanced the initial GLP-1 (7-36) response during an oral GTT. Oral glucose tolerance test comparing the plasma GLP-1 (7-36) concentration of male Wistar rats stereotactically injected with rAAV-GFP (n=11) or rAAV-GKS (n=12) in the PVN. **(A)** GLP-1 (7-36) concentration was measured using ELISA and **(B)** the area under the curve was determined. Blood samples were collected via a tail vein cannula at t=0, 15, 30, 60 and 120 minutes post-ingestion of a 2.5g/kg oral glucose dose. Data is expressed as mean ± SEM and was analysed using an unpaired T-test at each time point using GraphPad Prism 6: *p<0.05.

4.3.2.2 Intraperitoneal glucose tolerance test

The protocol described 4.3.2.1 was followed, with the exception that the animals were administered glucose (1.2g/kg) intraperitoneally rather than orally. This test was performed in addition to the oral test to confirm the involvement of the incretin hormone GLP-1 (7-36) in PVN GK-regulated glucose homeostasis.

Similarly to what was found during the oral GTT, a significant increase in glucose concentration at 30 minutes was detected in rAAV-GKAS rats compared to control animals (GFP: 7.38±0.13mmol/L, n=9; GKAS: 8.15±0.14mmol/L, n=9; $p<0.001$) (Fig. 4.12A). This observation reinforces the possibility that PVN GK knockdown impairs glucose clearance. This only seems to apply to the initial clearance immediately following a glucose challenge; however, as the overall plasma glucose levels of GK-deficient rats over the 120 minute test were not statistically different to those of the rAAV-GFP group (Fig. 4.12B). The decrease in the initial insulin response to glucose caused by PVN GK knockdown in the oral GTT was also observed during the i.p. GTT. Insulin levels were significantly lower in rAAV-GKAS animals than control rats after 15 minutes (GFP: 4.20±0.40mmol/L, n=8; GKAS: 2.92±0.33mmol/L, n=8; $p<0.01$) (Fig. 4.13A). This strengthens the hypothesis that GSIS may be compromised in GK-deficient rats. However, plasma insulin concentration became higher in these animals after 30 minutes (GFP: 3.18±0.31mmol/L, n=8; GKAS: 3.96±0.31mmol/L, n=8; $p<0.05$) and there is no difference in overall insulin release during the test between the two groups, as is demonstrated on the AUC graph (Fig. 4.13B). Plasma GLP-1 (7-36) levels did not differ between the two groups at any time point. As glucose was injected into the fasted animals it did not pass through the digestive tract and thus bypassed the incretin effect. GLP-1 (7-36) levels thus remained constant throughout the study (Fig. 4.14). Finally, similarly to what was seen with the oral GTT, no difference in plasma glucagon levels was found between the two groups (Fig. 4.15). These data suggest that GK in the PVN does not contribute to the regulation of glucagon secretion from pancreatic α-cells.

Consistent with the observations in the rAAV-GKAS study, rAAV-GKS rats exhibited a decrease in plasma glucose levels compared to the control animals at 30 minutes (GFP: 8.55±0.17mmol/L, n=12; GKAS: 7.90±0.17mmol/L, n=12; $p<0.01$) (Fig. 16A). Again however, no significant difference in overall glucose levels was detected throughout the i.p.GTT (Fig. 4.16B), suggesting that the up-regulation of PVN GK may specifically enhance the initial glucose clearance following glucose consumption. Unlike previous observations during an i.p. GTT with rAAV-GKAS animals, the genetic alteration of PVN GK expression had no effect on insulin secretion. Up-regulating PVN GK expression did not increase insulin secretion as was observed with rAAV-GKS rats in the oral GTT (Fig. 4.17). As the glucose dose was administered directly into the bloodstream, the incretin effect was bypassed and GLP-1 release was unchanged throughout the study. As expected, there was no difference in plasma GLP-1 (7-36) concentrations between treatment groups (Fig. 4.18).

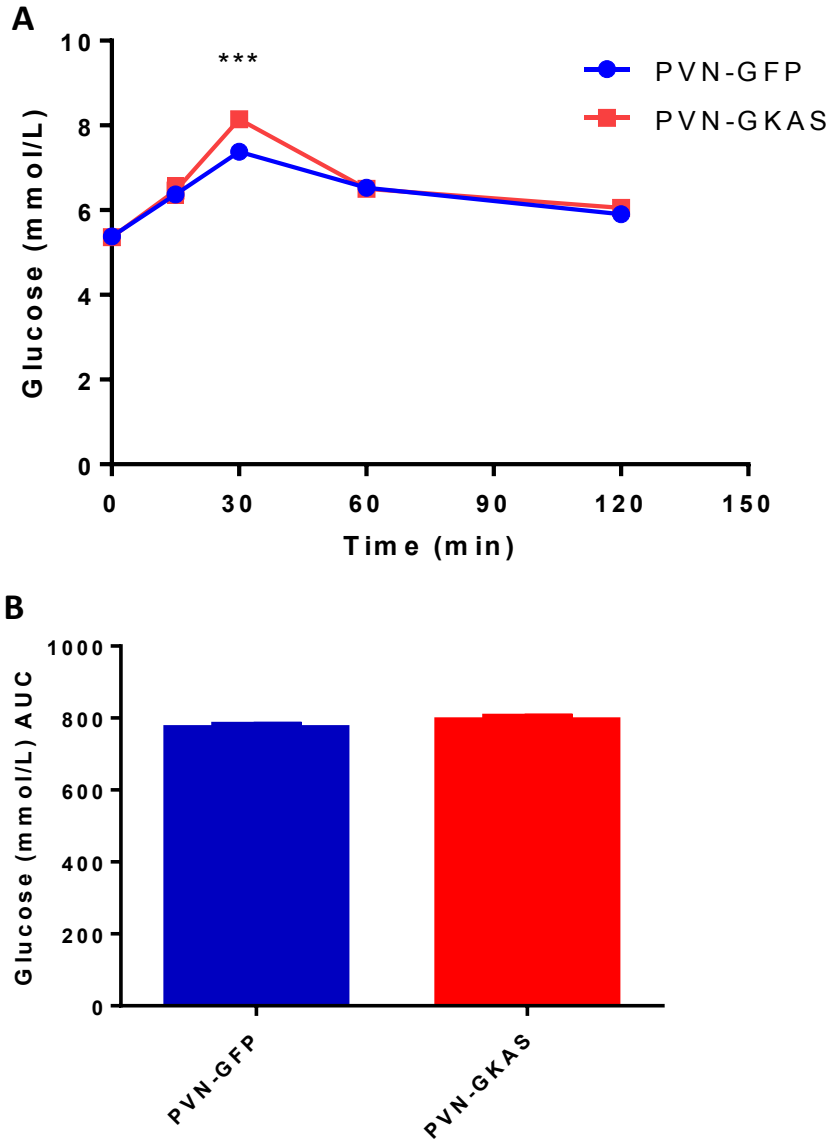


Figure 4.12: PVN GK knockdown impaired initial glucose clearance during an i.p. GTT. Intraperitoneal glucose tolerance test comparing plasma glucose concentration of male Wistar rats stereotactically injected with rAAV-GFP (n=9) or rAAV-GKAS (n=9) in the PVN. **(A)** Glucose concentration was measured using a glucose oxidase assay and **(B)** the area under the curve was determined. Blood samples were collected via a tail vein cannula at t=0, 15, 30, 60 and 120 minutes post-injection of a 1.2g/kg i.p. glucose dose. Data is expressed as mean ± SEM and was analysed using an unpaired T-test at each time point using GraphPad Prism 6: ***p<0.001.

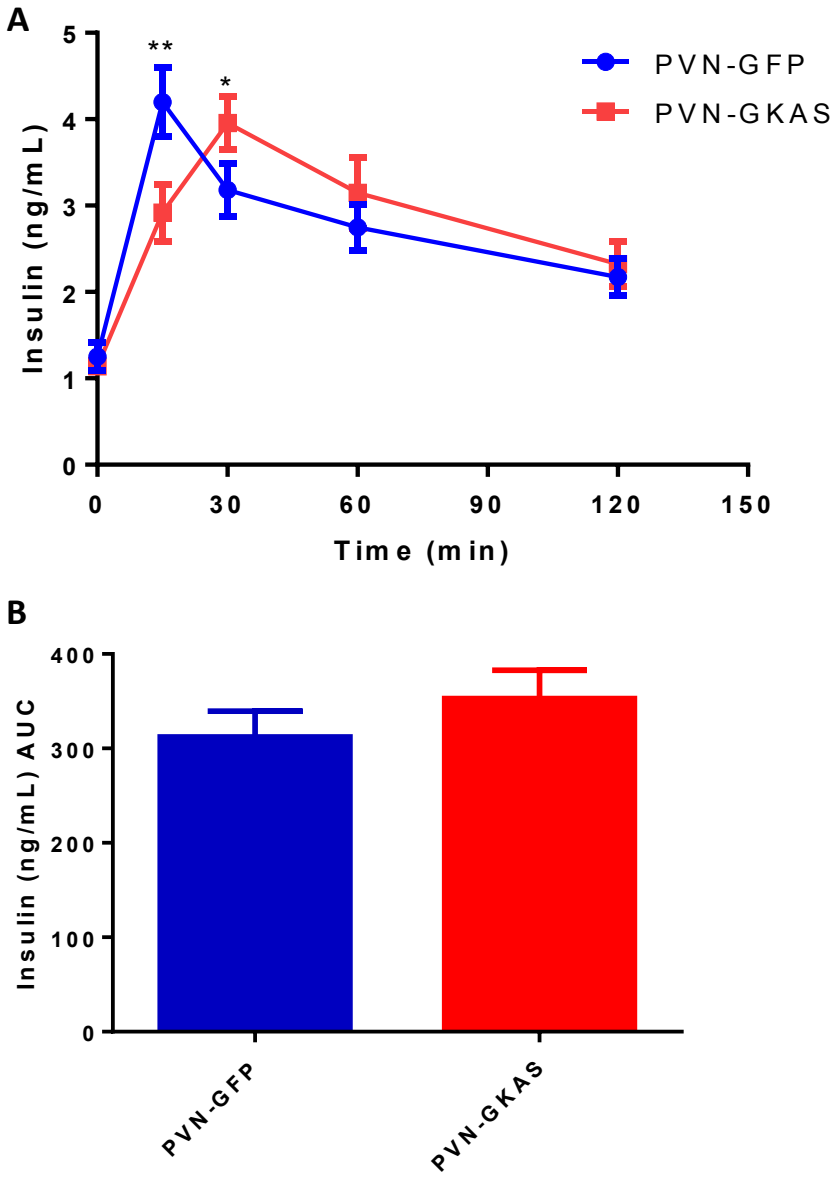


Figure 4.13: The initial insulin response to glucose was disrupted by PVN GK knockdown during an i.p. GTT. Intraperitoneal glucose tolerance test comparing the plasma insulin concentration of male Wistar rats stereotactically injected with rAAV-GFP (n=8) or rAAV-GKAS (n=8) in the PVN. **(A)** Insulin concentration was measured using ELISA and **(B)** the area under the curve was determined. Blood samples were collected via a tail vein cannula at t=0, 15, 30, 60 and 120 minutes post-injection of a 1.2g/kg i.p. glucose dose. Data is expressed as mean ± SEM and was analysed using an unpaired T-test at each time point using GraphPad Prism 6: **p<0.01, *p<0.05.

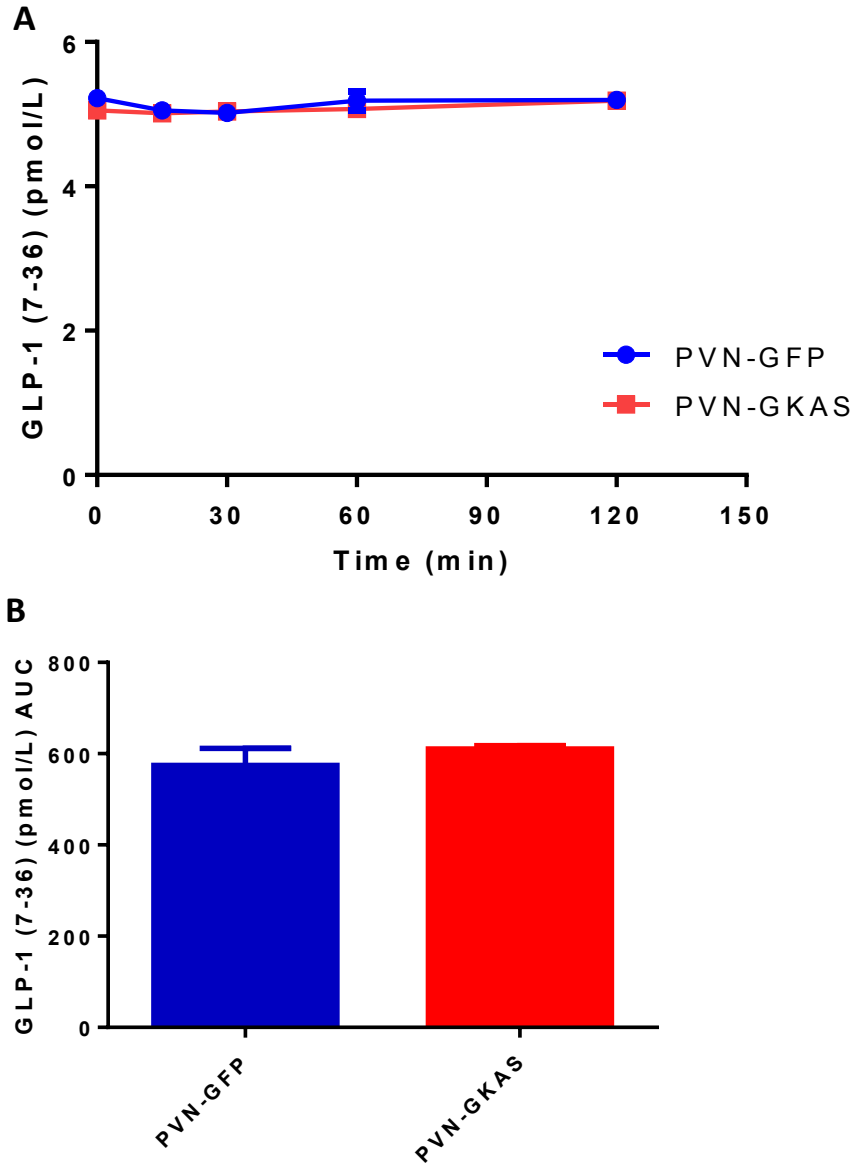


Figure 4.14: GLP-1 (7-36) secretion was unaffected by PVN GK knockdown during an i.p. GTT. Intraperitoneal glucose tolerance test comparing the plasma GLP-1 (7-36) concentration of male Wistar rats stereotactically injected with rAAV-GFP (n=9) or rAAV-GKAS (n=8) in the PVN. **(A)** GLP-1 (7-36) concentration was measured using ELISA and **(B)** the area under the curve was determined. Blood samples were collected via a tail vein cannula at t=0, 15, 30, 60 and 120 minutes post-injection of a 1.2g/kg i.p. glucose dose. Data is expressed as mean ± SEM and was analysed using an unpaired T-test at each time point using GraphPad Prism 6.

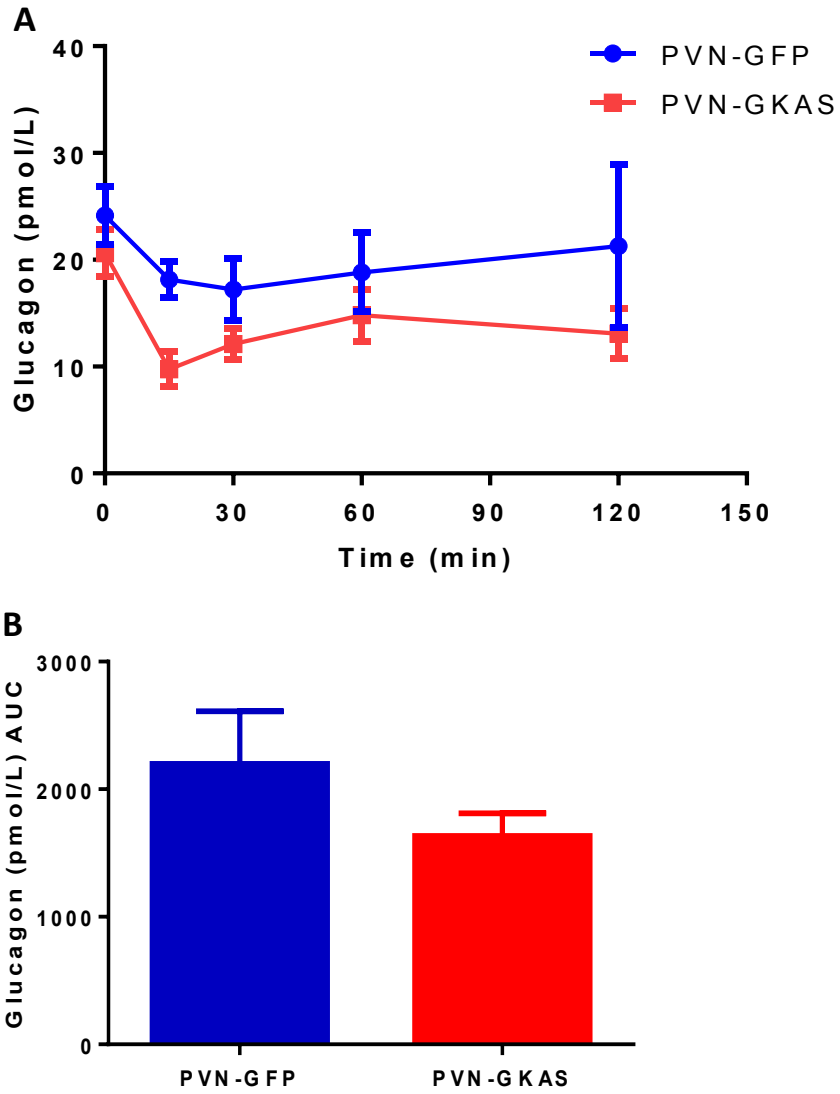


Figure 4.15: PVN GK knockdown did not affect glucagon secretion during an i.p. GTT. Intraperitoneal glucose tolerance test comparing the plasma glucagon concentration of male Wistar rats stereotactically injected with rAAV-GFP (n=9) or rAAV-GKAS (n=9) in the PVN. **(A)** GLP-1 (7-36) concentration was measured using ELISA and **(B)** the area under the curve was determined. Blood samples were collected via a tail vein cannula at t=0, 15, 30, 60 and 120 minutes post-injection of a 1.2g/kg i.p. glucose dose. Data is expressed as mean ± SEM and was analysed using an unpaired T-test at each time point using GraphPad Prism 6.

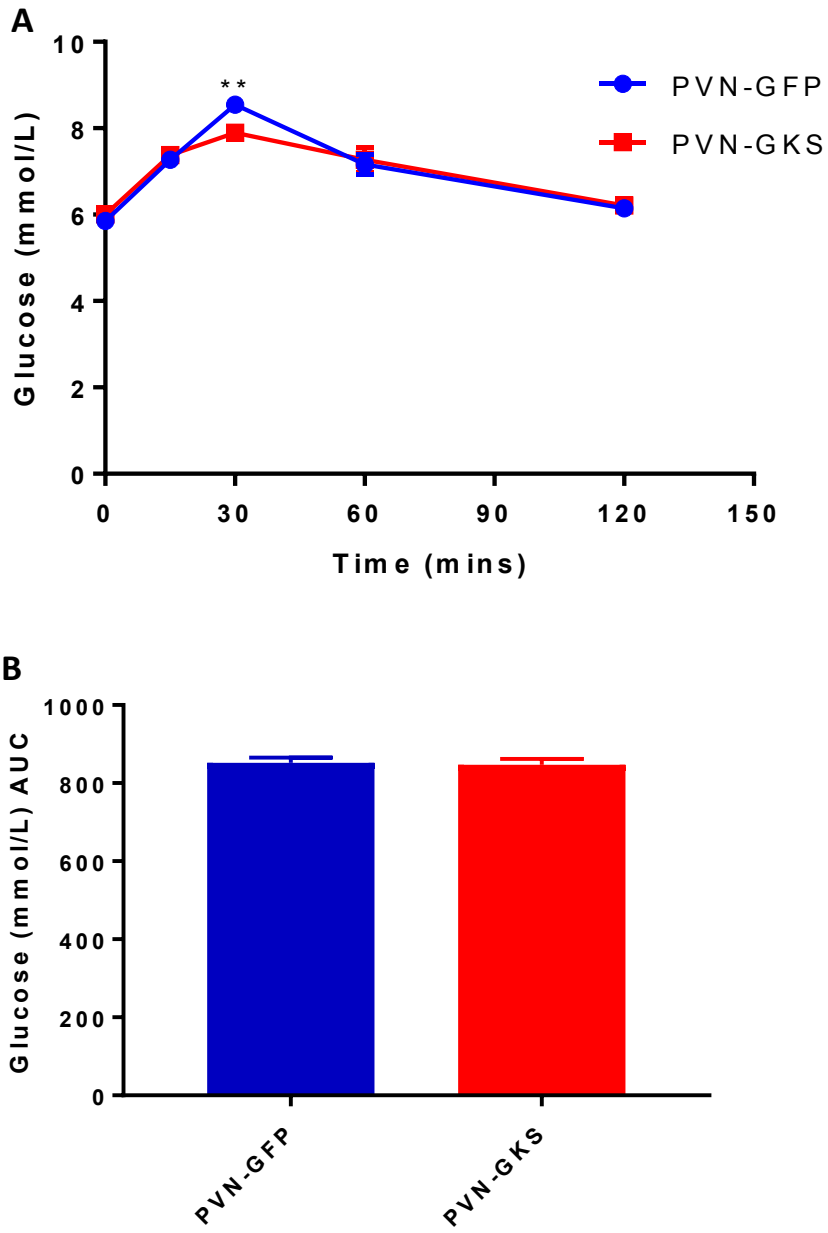


Figure 4.16: PVN GK up-regulation enhanced initial glucose clearance during an i.p. GTT. Intraperitoneal glucose tolerance test comparing plasma glucose concentration of male Wistar rats stereotactically injected with rAAV-GFP (n=12) or rAAV-GKS (n=12) in the PVN. **(A)** Glucose concentration was measured using a glucose oxidase assay and **(B)** the area under the curve was determined. Blood samples were collected via a tail vein cannula at t=0, 15, 30, 60 and 120 minutes post-injection of a 1.2g/kg i.p. glucose dose. Data is expressed as mean ± SEM and was analysed using an unpaired T-test at each time point using GraphPad Prism 6: **p<0.01.

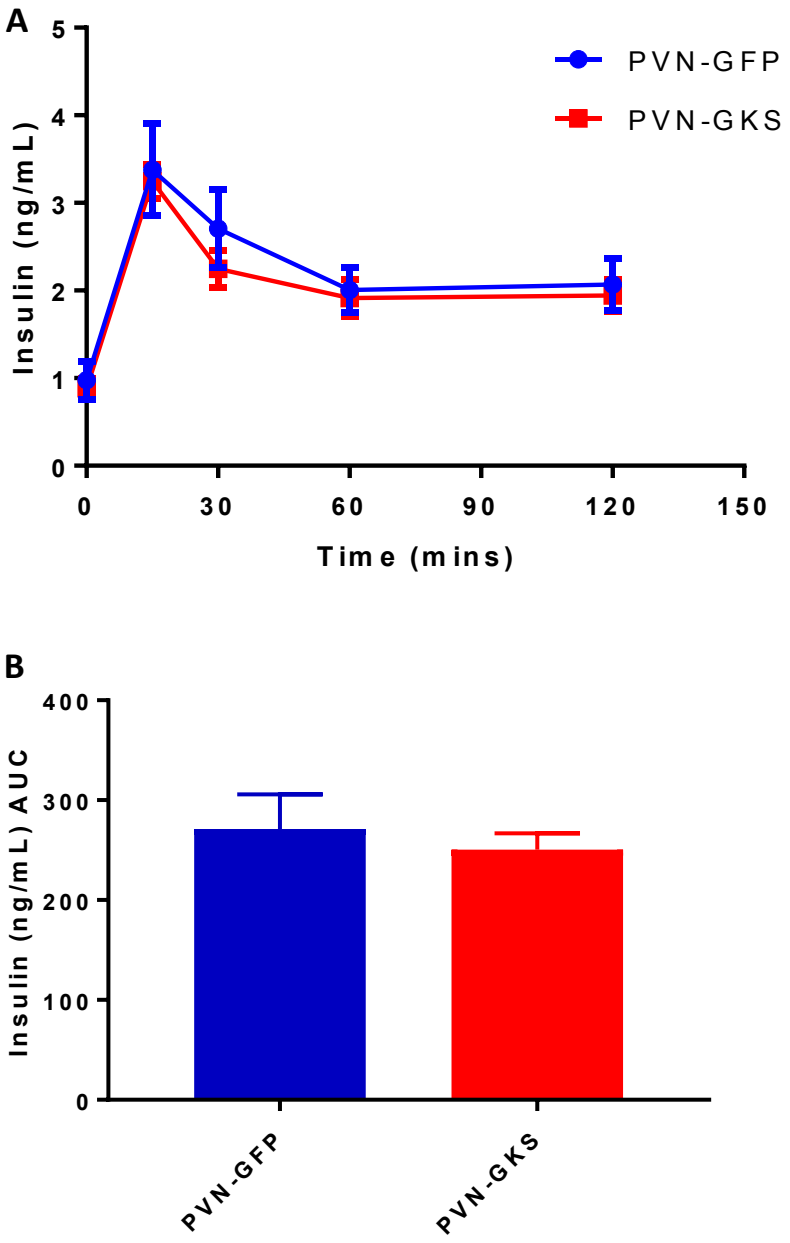


Figure 4.17: Up-regulation of PVN GK expression had no effect on insulin secretion during an i.p. GTT. Intraperitoneal glucose tolerance test comparing the plasma insulin concentration of male Wistar rats stereotactically injected with rAAV-GFP (n=12) or rAAV-GKS (n=12) in the PVN. **(A)** Insulin concentration was measured using ELISA and **(B)** the area under the curve was determined. Blood samples were collected via a tail vein cannula at t=0, 15, 30, 60 and 120 minutes post-injection of a 1.2g/kg i.p. glucose dose. Data is expressed as mean ± SEM and was analysed using an unpaired T-test at each time point using GraphPad Prism 6.

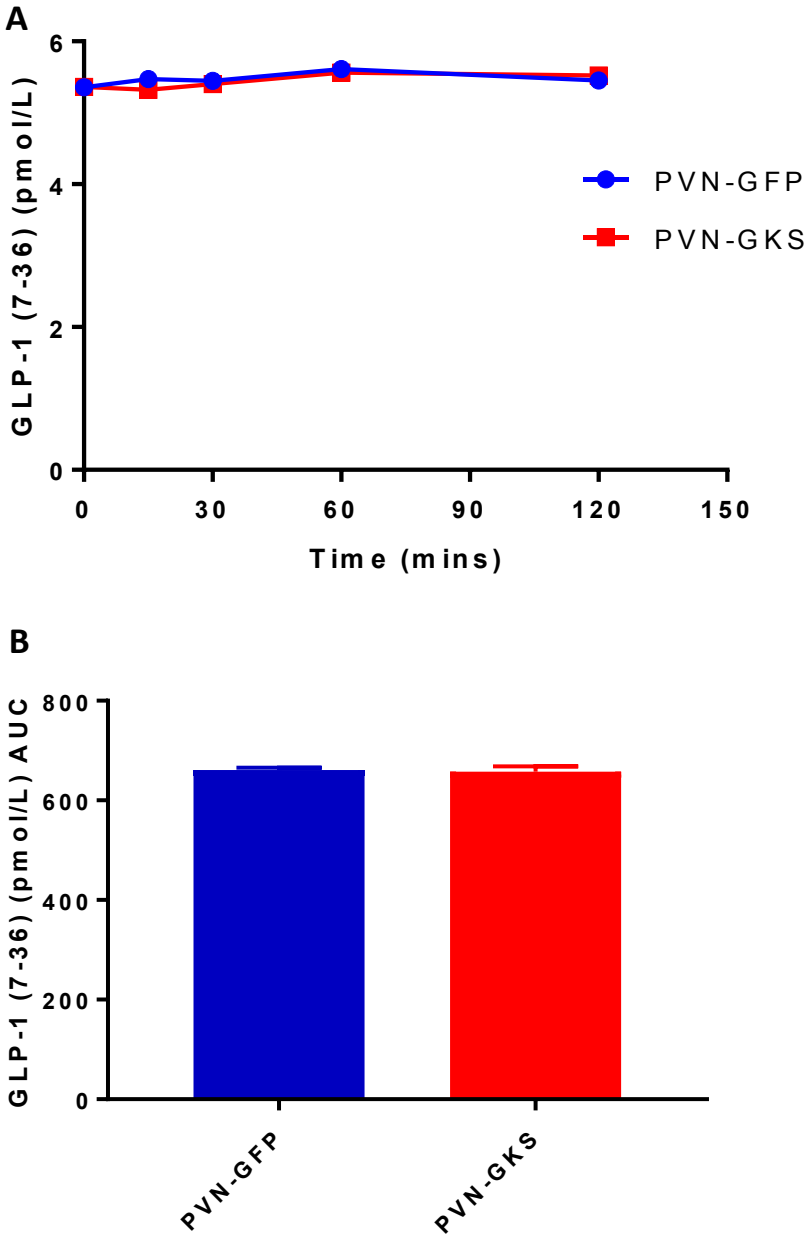


Figure 4.18: GLP-1 (7-36) secretion was unaffected by up-regulation of PVN GK during an i.p. GTT. Intraperitoneal glucose tolerance test comparing the plasma GLP-1 (7-36) concentration of male Wistar rats stereotactically injected with rAAV-GFP (n=12) or rAAV-GKS (n=12) in the PVN. **(A)** GLP-1 (7-36) concentration was measured using ELISA and **(B)** the area under the curve was determined. Blood samples were collected via a tail vein cannula at t=0, 15, 30, 60 and 120 minutes post-injection of a 1.2g/kg i.p. glucose dose. Data is expressed as mean ± SEM and was analysed using an unpaired T-test at each time point using GraphPad Prism 6.

4.3.2.3 Insulin tolerance test

To conduct the ITT, the same procedure as described in 4.3.2.1 was used, with the following exceptions. The animals were fasted 4 hours prior to the start of the study and were administered a 2IU/kg dose of insulin intraperitoneally.

No difference in plasma glucose levels was noted between rAAV-GKAS and rAAV-GFP animals at any time point during an ITT (Fig. 4.19). Likewise, there was no difference in glucose concentrations between rAAV-GFP and rAAV-GKS rats (Fig. 4.20).

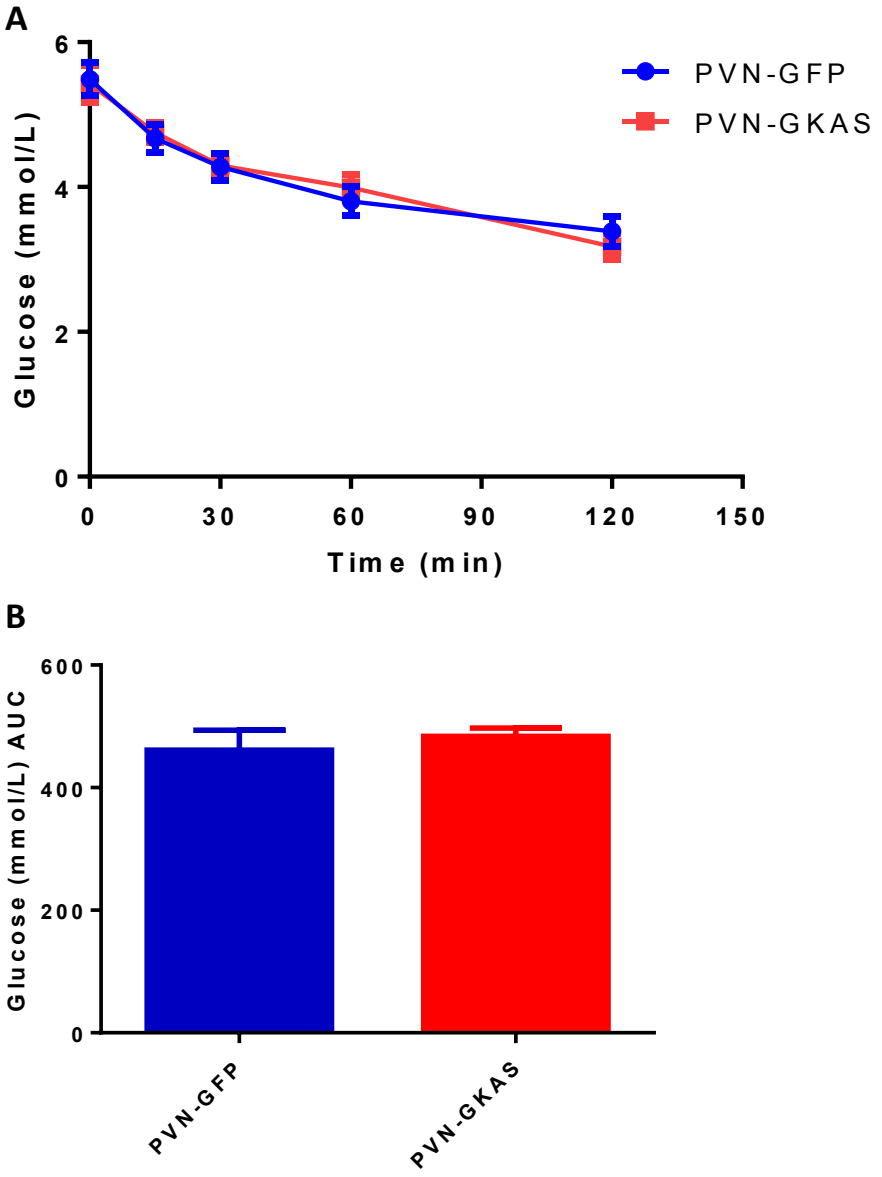


Figure 4.19: PVN GK knockdown did not affect the response to insulin-induced hypoglycaemia. Plasma glucose concentrations of male Wistar rats stereotactically injected with rAAV-GFP (n=9) or rAAV-GKAS (n=9) in the PVN were analysed and compared during an insulin tolerance test using a glucose oxidase assay. Blood samples were collected via a tail vein cannula at 0, 15, 30, 60 and 120 minutes following an i.p. insulin injection (2IU/kg). Data is expressed as mean ± SEM and was analysed using a T-test at each time point using GraphPad Prism 6.

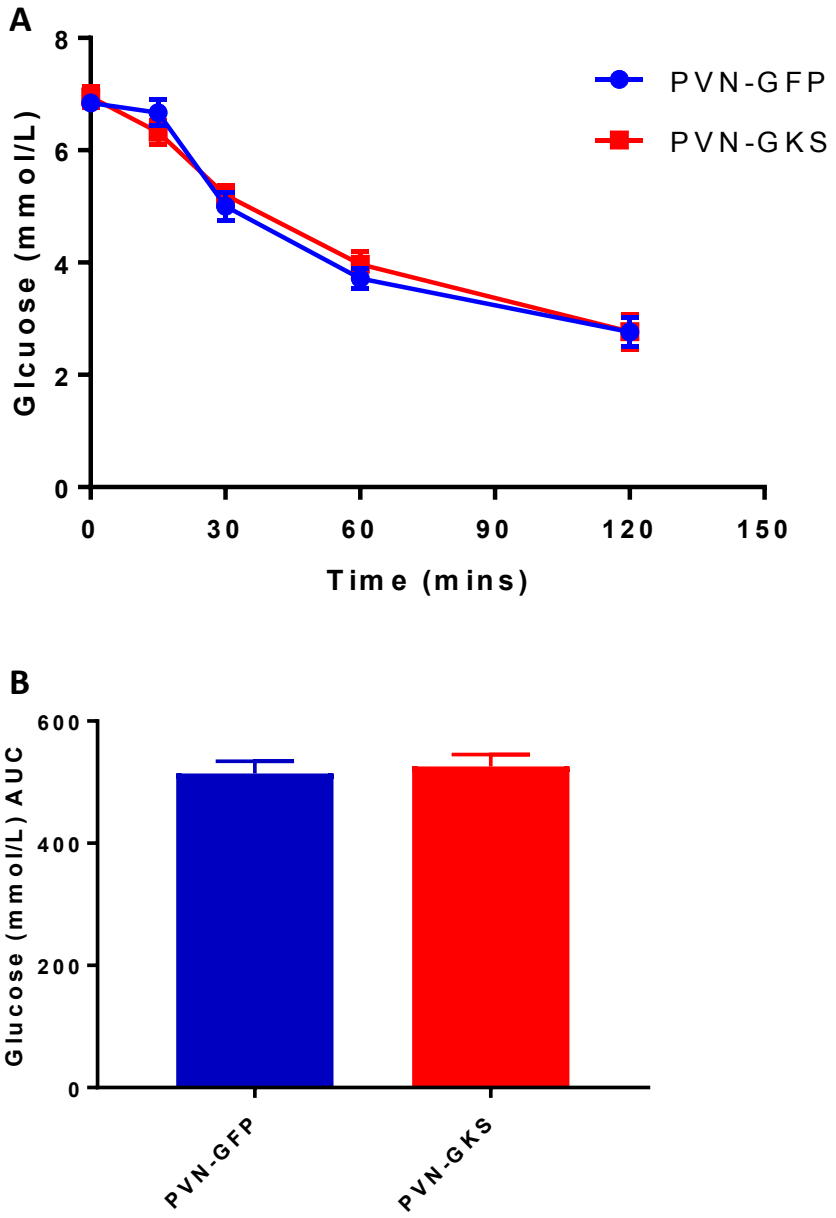


Figure 4.20: The response to insulin-induced hypoglycaemia was unaffected by the up-regulation of PVN GK expression. Plasma glucose concentrations of male Wistar rats stereotactically injected with rAAV-GFP (n=12) or rAAV-GKS (n=12) in the PVN were analysed and compared during an insulin tolerance test using a glucose oxidase assay. Blood samples were collected via a tail vein cannula at 0, 15, 30, 60 and 120 minutes following an i.p. insulin injection (2IU/kg). Data is expressed as mean ± SEM and was analysed using a T-test at each time point using GraphPad Prism 6.

4.3.2.4 Oral gavage of L-arginine

The procedure described in 4.3.2.1 was again followed during this study, except that the animals were given a dose of 16mmol/kg L-arginine via oral gavage. This test was used as a means to verify whether the impairment of the initial GLP-1 response observed during the oral GTT is specific to glucose or whether it applies to other nutrients as well.

Amino acid gavage had the same effect on plasma glucose, insulin, GLP-1 (7-36) and glucagon levels in rAAV-GKAS as in rAAV-GFP animals (Figs. 4.21-4.24). There were no differences in these parameters between the groups at any time point. For this reason, this experiment was not repeated in rAAV-GKS rats.

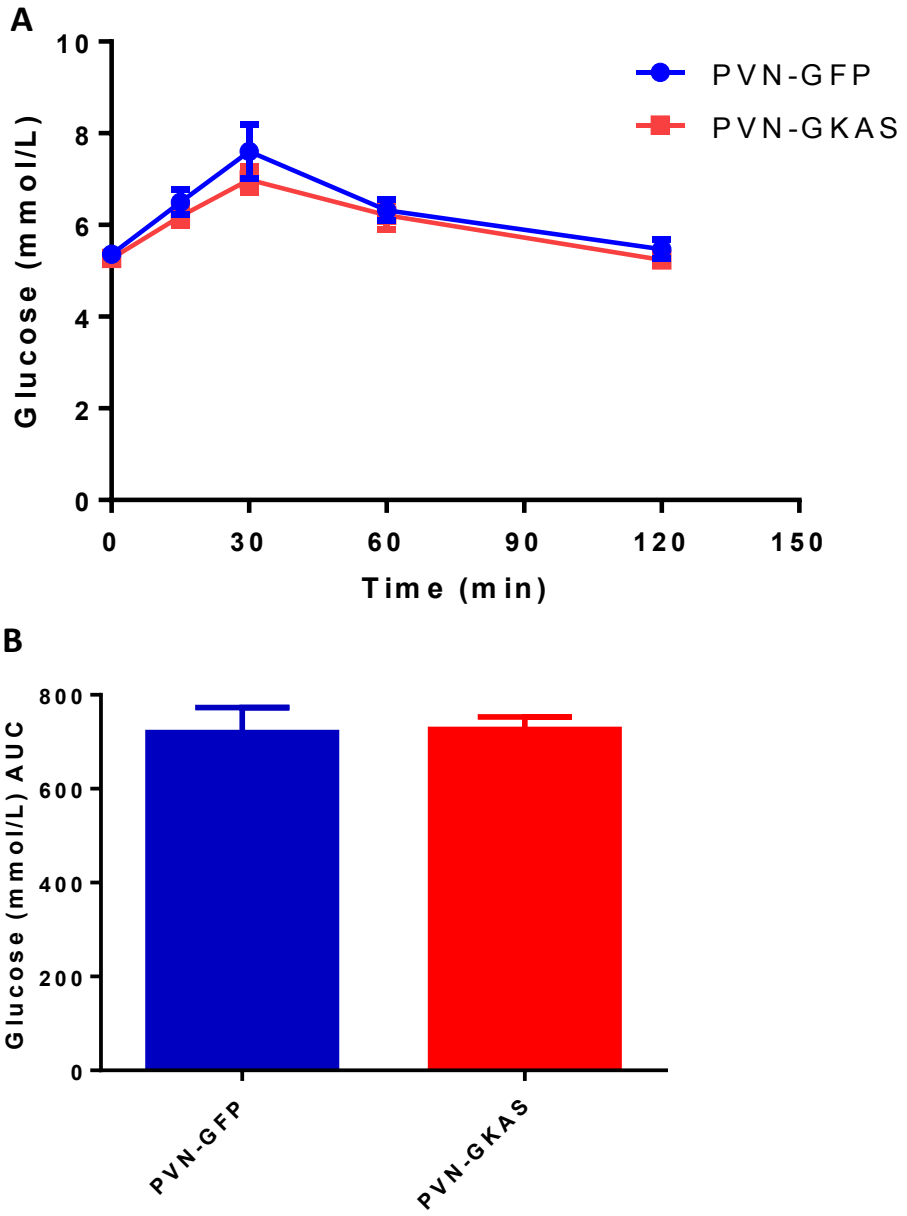


Figure 4.21: PVN GK knockdown did not affect plasma glucose levels following oral gavage of L-arginine. Glucose tolerance test following oral gavage of L-arginine (16mmol/kg) comparing plasma glucose concentration of male Wistar rats stereotactically injected with rAAV-GFP (n=9) or rAAV-GKAS (n=9) in the PVN. **(A)** Glucose concentration was measured using a glucose oxidase assay and **(B)** the area under the curve was determined. Blood samples were collected via a tail vein cannula at t=0, 15, 30, 60 and 120 minutes following oral gavage of L-arginine (16mmol/kg). Data is expressed as mean ± SEM and was analysed using an unpaired T-test at each time point using GraphPad Prism 6.

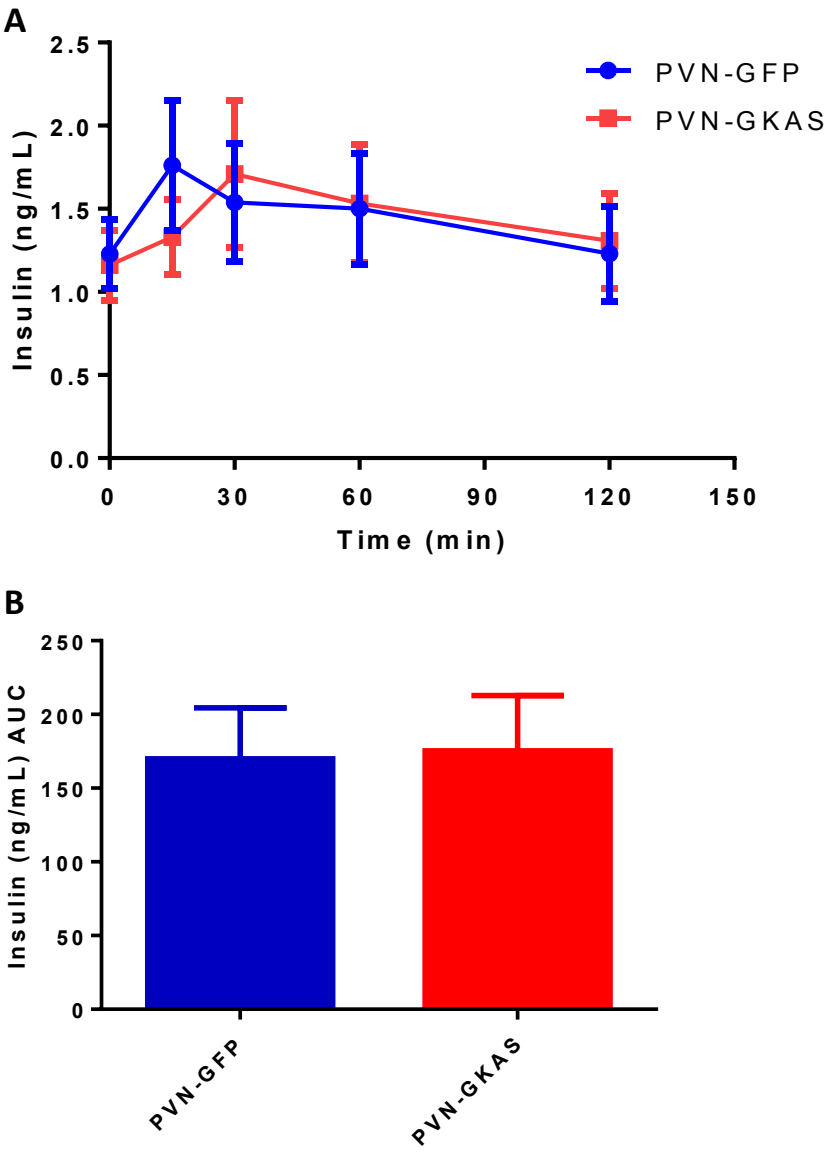


Figure 4.22: PVN GK knockdown did not affect plasma insulin levels following oral gavage of L-arginine. Glucose tolerance test following oral gavage of L-arginine (16mmol/kg) comparing the plasma insulin concentration of male Wistar rats stereotactically injected with rAAV-GFP (n=8) or rAAV-GKAS (n=8) in the PVN. **(A)** Insulin concentration was measured using ELISA and **(B)** the area under the curve was determined. Blood samples were collected via a tail vein cannula at t=0, 15, 30, 60 and 120 minutes following oral gavage of L-arginine (16mmol/kg). Data is expressed as mean ± SEM and was analysed using an unpaired T-test at each time point using GraphPad Prism 6.

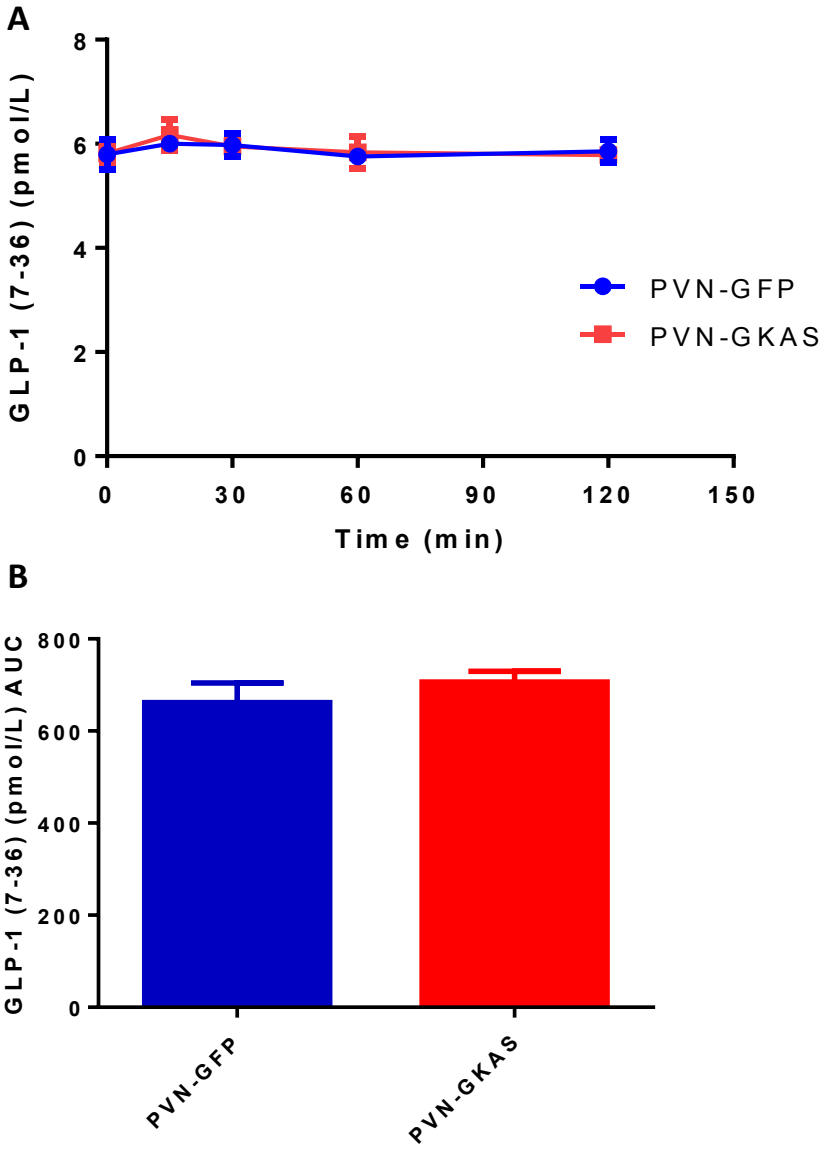


Figure 4.23: PVN GK knockdown did not affect active GLP-1 (7-36) secretion following oral gavage of L-arginine. Glucose tolerance test following oral gavage of L-arginine (16mmol/kg) comparing the plasma GLP-1 (7-36) concentration of male Wistar rats stereotactically injected with rAAV-GFP (n=9) or rAAV-GKAS (n=8) in the PVN. **(A)** GLP-1 (7-36) concentration was measured using ELISA and **(B)** the area under the curve was determined. Blood samples were collected via a tail vein cannula at t=0, 15, 30, 60 and 120 minutes following oral gavage of L-arginine (16mmol/kg). Data is expressed as mean ± SEM and was analysed using an unpaired T-test at each time point using GraphPad Prism 6.

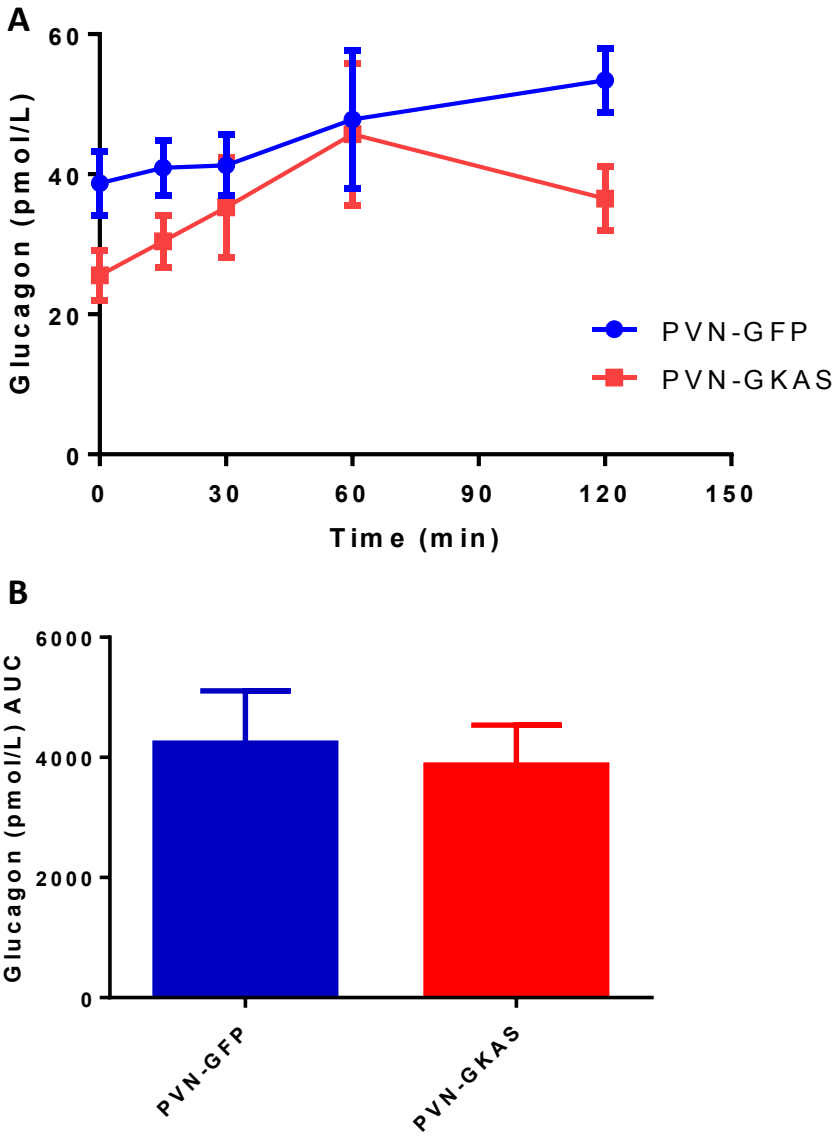


Figure 4.24: PVN GK knockdown did not affect glucagon secretion following oral gavage of L-arginine. Glucose tolerance test following oral gavage of L-arginine (16mmol/kg) comparing the plasma glucagon concentration of male Wistar rats stereotactically injected with rAAV-GFP (n=9) or rAAV-GKAS (n=9) in the PVN. **(A)** GLP-1 (7-36) concentration was measured using ELISA and **(B)** the area under the curve was determined. Blood samples were collected via a tail vein cannula at t=0, 15, 30, 60 and 120 minutes following oral gavage of L-arginine (16mmol/kg). Data is expressed as mean ± SEM and was analysed using an unpaired T-test at each time point using GraphPad Prism 6.

4.3.3 Effects of PVN GK knockdown on glucose-stimulated insulin secretion from isolated β-cells

In a pilot study conducted on a small separate cohort of animals given an iPVN injection of either rAAV-GKAS or rAAV-GFP, β-cell secretory function was analysed to assess whether PVN GK knockdown had an effect on the extent of insulin release in response to glucose. Insulin secretion was measured as a percentage of total islet insulin content. Although the power was too small to obtain a statistically significant result, GSIS from isolated islets of GK-deficient rats (n=2) appeared to be reduced compared to that of control animals (n=2) (Fig. 4.25).

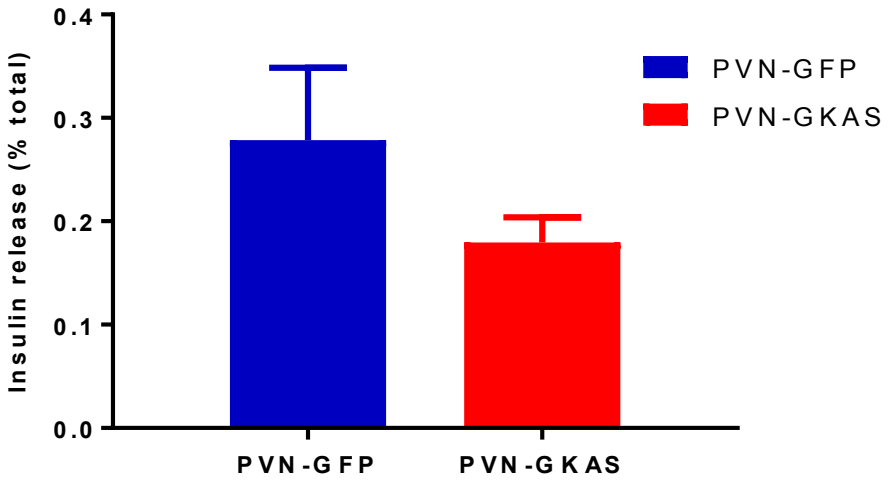


Figure 4.25: Effect of PVN GK knockdown on glucose-stimulated insulin secretion from isolated pancreatic β-cells. Pilot study comparing insulin secretion from isolated pancreatic β-cells of rAAV-GKAS animals (n=2) to that of rAAV-GFP animals (n=2) in response to exposure to 17mm glucose during a secretion assay. The islets were collected by injecting collagenase into the pancreatic duct of the genetically altered animals and isolated manually using a stereo dissecting microscope. Data is presented as a percentage of total β-cell insulin content and expressed as mean ± SEM. Statistical analysis was performed using an unpaired T-test on GraphPad Prism 6.

4.3.4 The role of PVN GK in ileal GLP-1 (7-36) and PYY gene expression

Knocking down GK in the PVN reduced the initial GLP-1 (7-36) response to glucose during a GTT and up-regulating it had the opposite effect. In order to evaluate the effect of PVN GK on GLP-1 (7-36) secretion, the expression of the proglucagon (GCG) gene in the ileum of genetically altered rats was determined using qPCR and compared to that of control animals. The genetic expression of PYY was also measured to further assess the effects of PVN GK on the secretory function of L-cells. No significant difference in gene expression of either the GCG or PYY gene was observed between the genetically altered groups and the control group (Fig. 4.26).

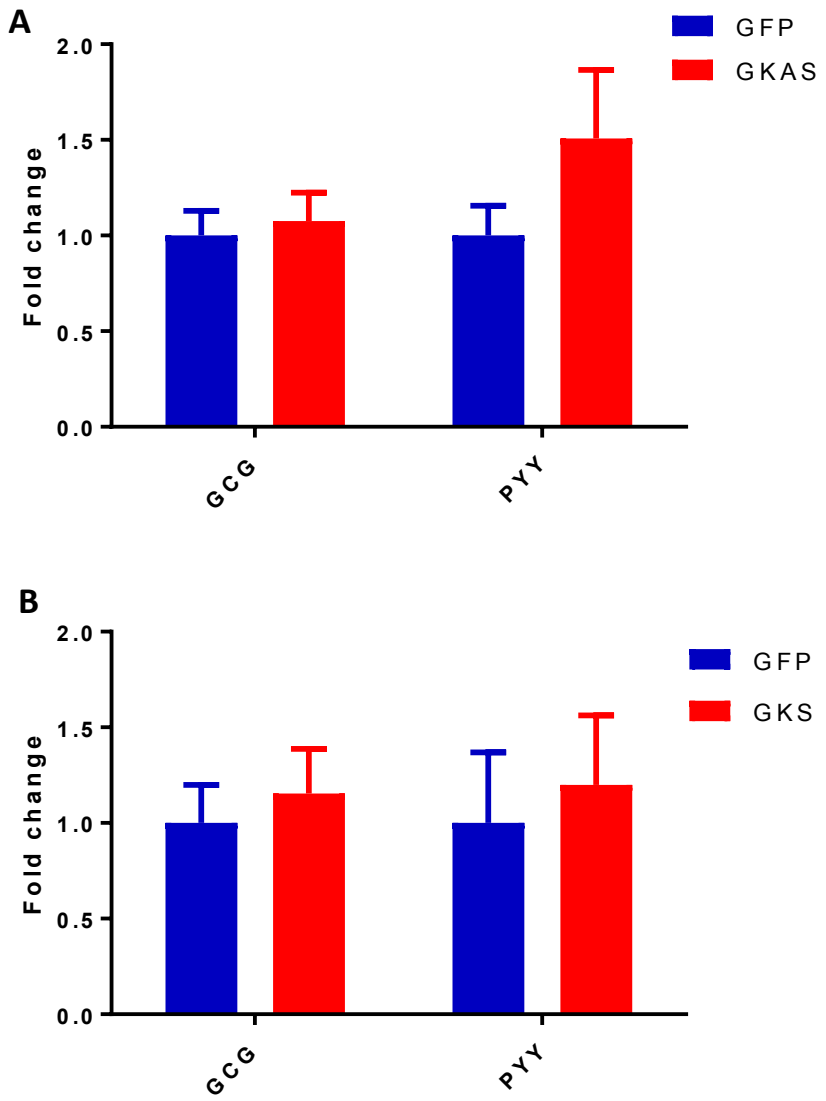


Figure 4.26: Levels of GCG and PYY mRNA in genetically altered and wild-type rat ileum. **(A)** GK knockdown in the PVN does not alter the level of genetic expression of proglucagon or PYY in the ileum. Ileal expression of the proglucagon and PYY gene in rats following iPVN injection of either rAAV-GFP (n=10) or rAAV-GKAS (n=10). **(B)** Up-regulation of GK activity in the PVN does not alter the level of genetic expression of proglucagon or PYY in the ileum. Ileal expression of the proglucagon and PYY gene in rats following iPVN injection of either rAAV-GFP (n=11) or rAAV-GKS (n=12). RNA was extracted from isolated ileum of rAAV-GFP, rAAV-GKAS and rAAV-GKS animals and converted to cDNA, following which the level of expression of the proglucagon and PYY genes was determined using qPCR. Data is expressed as mean ± SEM and was analysed using an unpaired T-test on GraphPad Prism 6.

4.3.5 Verifying changes in GK activity in the PVN of genetically altered animals

The brains of the rAAV-GFP, rAAV-GKAS and rAAV-GKS animals were dissected and the PVN removed by performing a micropunch biopsy. A GK activity assay was performed to evaluate the change in GK activity induced by rAAV-GKAS and rAAV-GKS. GK activity was also assessed in the neighbouring ARC and VMN to ensure that trans-gene expression only occurred in the targeted PVN. Other hexokinases were inhibited to ensure that only GK activity was being measured. The assay showed that stereotactic rAAV-GKAS injection into the PVN significantly lowered GK activity in the PVN. A 44% reduction in activity was observed in rAAV-GKAS animals compared to controls (rAAV-GFP: 4.45±0.41, n=10; rAAV-GKAS: 2.48±0.21, n=10; $p<0.01$). This decrease was localised to the PVN, as there was no difference in GK activity between groups in either the ARC or VMN (Fig. 4.27A). On the other hand, stereotactically injecting rAAV-GKS into the PVN significantly enhanced GK activity in this nucleus. GK activity was augmented by 40% in rAAV-GKS animals compared to controls (rAAV-GFP: 4.55±0.55, n=11; rAAV-GKS: 7.60±0.51, n=12; $p<0.001$) and this increase was localised to the PVN (Fig. 4.27B).

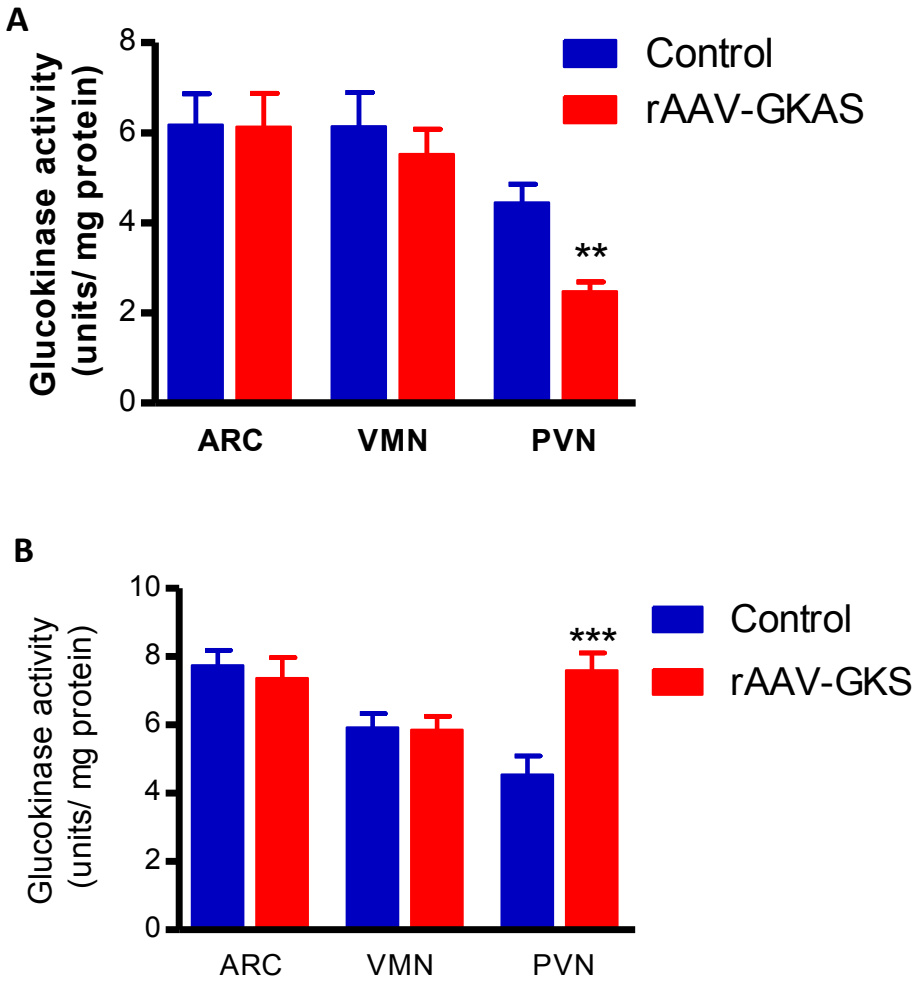


Figure 4.27: GK activity in the ARC, VMN and PVN of genetically altered and wild-type rats. (A) GK activity in the PVN was significantly reduced in rAAV-GKAS rats. GK activity of rAAV-GFP (n=10) and rAAV-GKAS (n=10) rats was assessed in a GK activity assay. **(B)** GK activity in the PVN was significantly enhanced in rAAV-GKS rats. GK activity of rAAV-GFP (n=11) and rAAV-GKS (n=12) rats was assessed in a GK activity assay. The PVN, ARC and VMN of each animal were collected using a micropunch biopsy. Data is expressed as mean ± SEM and was analysed using an unpaired T-test on GraphPad Prism 6: **p<0.01, ***p<0.001.

4.3.6 Pharmacological modulation of GK and K_{ATP} channel activity in the PVN

In order to investigate the mechanism behind the effects of PVN GK on glucose homeostasis, various pharmacological compounds were delivered directly into the PVN and the effects on plasma glucose,

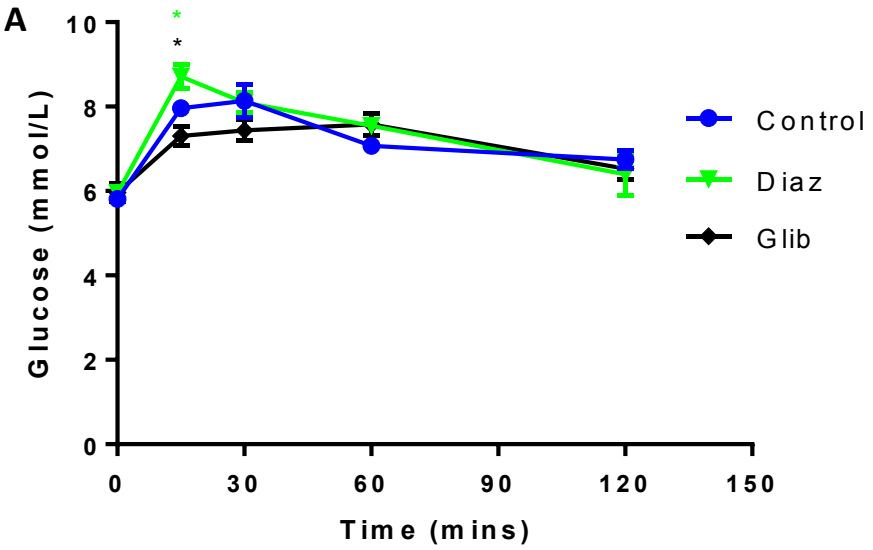
insulin and GLP-1 (7-36) levels were observed. The K_{ATP} channel blocker glibenclamide and K_{ATP} channel activator diazoxide were used to determine whether K_{ATP} channels form part of the mechanism downstream of PVN GK activation. The glucokinase activator compound A (CpdA) was also administered into the PVN in order to assess the effects of enhanced PVN GK activity on glucose homeostasis. It was hypothesized that glibenclamide and diazoxide would mimic the effects of over-expressing and knocking down GK, respectively, and that CpdA would yield similar results to glibenclamide and rAAV-GKS. Finally, D-Glucose was injected to test the ability of this nucleus' glucose-sensing machinery to respond to a local rise in glucose concentration.

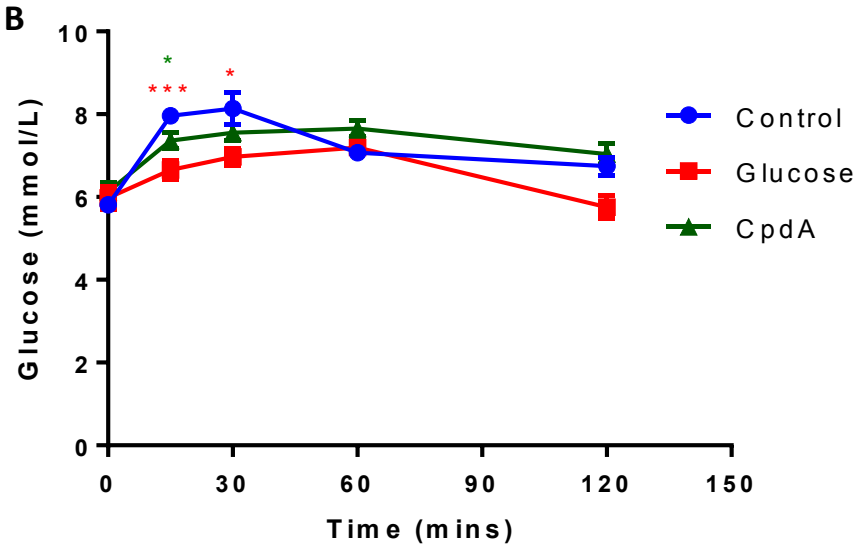
Diazoxide, which causes K_{ATP} channel opening, had effects comparable to rAAV-GKAS as expected. On the other hand, the K_{ATP} channel inhibitor glibenclamide had the opposite effect and yielded responses similar to those seen in rats over-expressing GK in the PVN. CpdA also generated similar results to those from rAAV-GKS rats.

4.3.6.1 Effects of iPVN injections on glucose clearance during an oral GTT

Diazoxide administration into the PVN caused a significant rise in plasma glucose levels after 15 minutes during an oral GTT compared to iPVN injection of vehicle (Control: 7.96±0.18, n=12; diazoxide: 8.71±0.29, n=12; $p<0.05$) (Fig. 4.28A). It thus had a comparable effect on glucose clearance than rAAV-GKAS delivery into the PVN. On the other hand, plasma glucose levels decreased after 15 minutes following iPVN injection of glibenclamide during the oral GTT in comparison to rats injected with vehicle (Control: 7.96±018., n=12; glibenclamide: 7.30±0.23, n=12; $p<0.05$) (Fig. 4.28A). CpdA and glibenclamide had a similar effect to one another (Control: 7.96±018., n=12; CpdA: 7.36±0.20, n=12; $p<0.05$) (Fig. 4.28B) and, as hypothesized, iPVN delivery of CpdA and glibenclamide produced a response comparable to that seen in rAAV-GKS animals. Each compound

only had an effect on the initial glucose clearance following a glucose challenge, as the overall plasma glucose level throughout the 120 minute study did not differ between treatment groups compared to control (Fig. 4.28B). Finally, plasma glucose levels were significantly reduced after 15 (Control: 7.96±0.18, n=12; glucose: 6.65±0.24, n=12; $p<0.001$) and 30 (Control: 7.96±0.18, n=12; glucose: 6.97±0.21, n=12; $p<0.05$) minutes by the administration of D-glucose into the PVN (Fig. 4.28B). They remained lower than those of vehicle-injected rats throughout the study, as demonstrated by AUC analysis (Fig. 4.28C).


A
Glucose (mmol/L)
Time (mins)
Control
Diaz
Glib


B
Glucose (mmol/L)
Time (mins)
Control
Glucose
CpdA

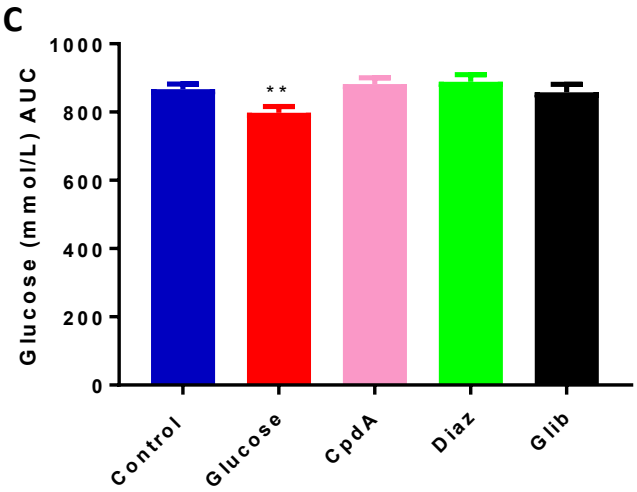
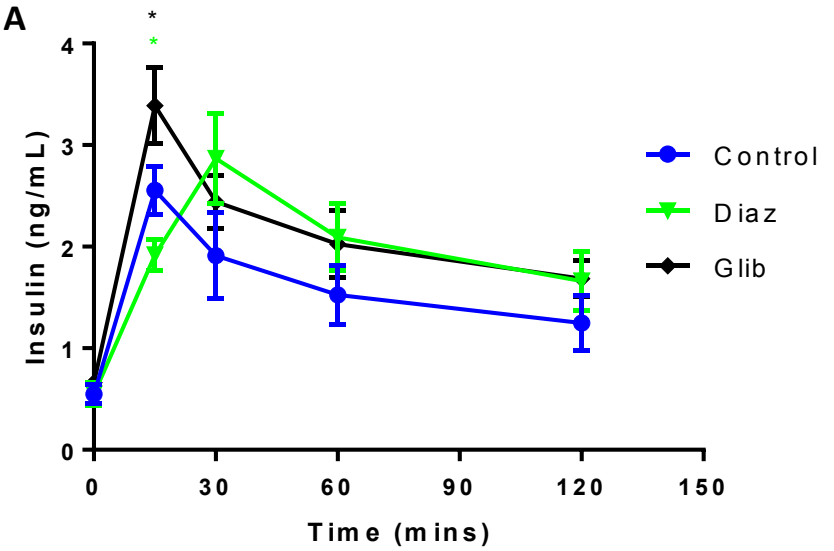

C
Glucose (mmol/L) AUC
Control
Glucose
CpdA
Diaz
Glib

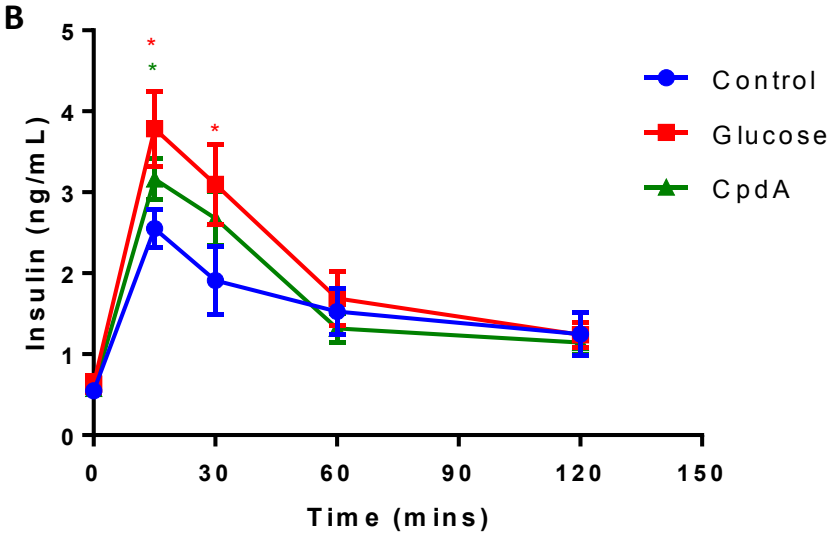
Figure 4.28: The effect of iPVN injections of various pharmacological agents on plasma glucose levels during an oral GTT. Oral glucose tolerance test comparing plasma glucose concentration following administration of **(A)** vehicle (n=12), glibenclamide (2nmol, n=12) or diazoxide (1nmol, n=12) or **(B)** CpdA (0.5nmol, n=12), D-glucose (1.5mg/ml, n=12) or vehicle (n=12) into the PVN. This was performed in a cross-over study on iPVN-cannulated male Wistar rats. 1µl was injected for each compound at a rate of 120µl/hour. Glucose concentration was measured using a glucose oxidase assay and **(C)** the area under the curve of each compound was determined. Blood samples were collected via a tail vein cannula at t=0, 15, 30, 60 and 120 minutes post-ingestion of a 2.5g/kg oral glucose dose. Data is expressed as mean ± SEM and was analysed using an unpaired T-test at each time point using GraphPad Prism 6: *p<0.05, **p<0.01, ***p<0.001 compared to control.

4.3.6.2 Effects of iPVN injections on insulin secretion during an oral GTT

Diazoxide had similar effects to rAAV-GKAS on insulin release during an oral GTT. Rats given an iPVN injection of diazoxide had significantly lower plasma insulin levels than control animals after 15 minutes (Control: 2.55±0.24, n=12; diazoxide: 1.92±0.16, n=12; p<0.05) (Fig. 4.29A). This may explain the higher plasma glucose concentration of diazoxide-injected rats in comparison to rats given vehicle. As expected, glibenclamide (Fig. 4.29A) and CpdA (Fig. 4.29B) again generated results comparable to those observed in rAAV-GKS animals as they both induced a significant rise in insulin levels compared to vehicle after 15 minutes (Control: 2.55±0.24, n=12; glibenclamide: 3.39±0.39, n=12; p<0.05; CpdA: 3.16±0.26, n=12; p<0.05). D-glucose administration into the PVN triggered an increase in insulin secretion at 15 (Control: 2.55±0.24, n=12; glucose: 3.79±0.46, n=12; p<0.05) and 30 (Control: 2.55±0.24, n=12; glucose: 3.10±0.50, n=12; p<0.05) minutes (Fig. 4.29B), which may have caused the decrease in circulating glucose levels in these animals. Similarly to what was observed when PVN GK expression was genetically altered, each compound administered only

affected the initial insulin response to a glucose challenge. Overall, however, the plasma levels of insulin of each group were not significantly different (Fig. 4.29C).


A
Insulin (ng/mL)
Time (mins)
Control
Diaz
Glib


B
Insulin (ng/mL)
Time (mins)
Control
Glucose
CpdA

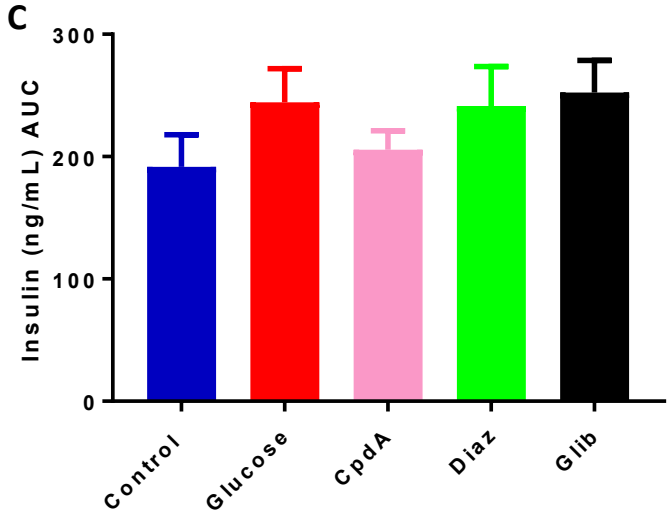
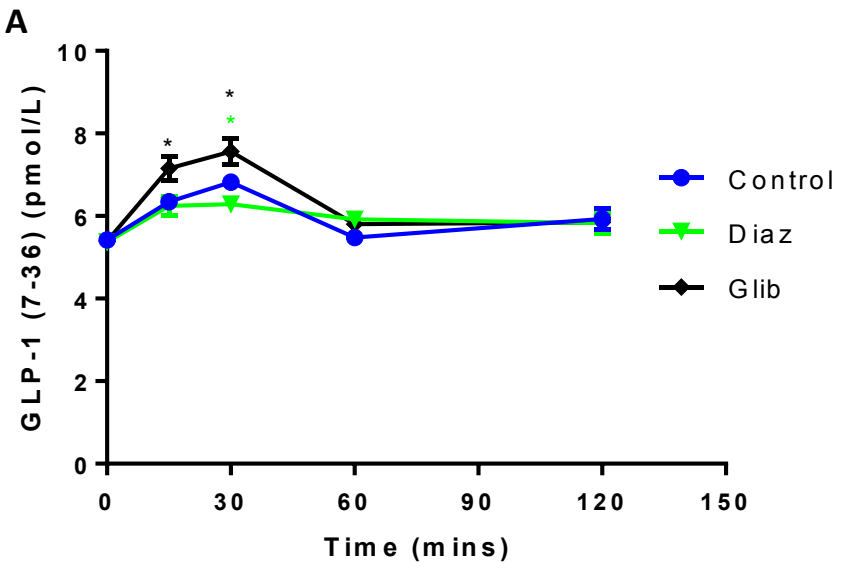
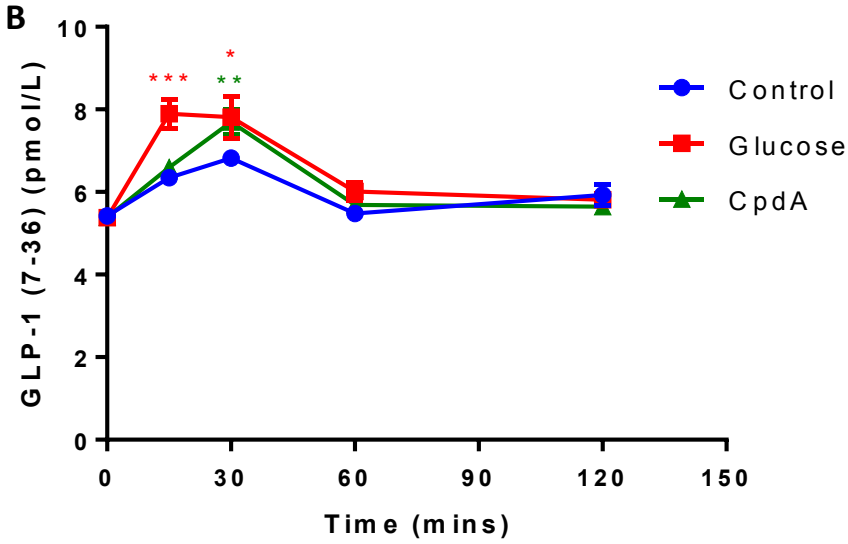

C
Insulin (ng/mL) AUC
Control
Glucose
CpdA
Diaz
Glib

Figure 4.29: The effect of iPVN injections of various pharmacological agents on insulin secretion during an oral GTT. Oral glucose tolerance test comparing plasma insulin levels following administration of **(A)** vehicle (n=12), glibenclamide (2nmol, n=12) or diazoxide (1nmol, n=12) or **(B)** CpdA (0.5nmol, n=12), D-glucose (1.5mg/ml, n=12) or vehicle (n=12) into the PVN. This was performed in a cross-over study on iPVN-cannulated male Wistar rats. 1µl was injected for each compound at a rate of 120µl/hour. Insulin concentration was measured using ELISA and **(C)** the area under the curve of each compound was determined. Blood samples were collected via a tail vein cannula at t=0, 15, 30, 60 and 120 minutes post-ingestion of a 2.5g/kg oral glucose dose. Data is expressed as mean ± SEM and was analysed using an unpaired T-test at each time point using GraphPad Prism 6: *p<0.05 compared to control.

4.3.6.3 Effects of iPVN injections on GLP-1 (7-36) secretion during an oral GTT

Similarly to rAAV-GKAS, diazoxide induced a significant decrease in GLP-1 (7-36) secretion after 30 minutes of an oral GTT (Control: 6.81±0.15, n=12; diazoxide: 6.29±0.16, n=12; p<0.05) (Fig. 4.30A). Glibenclamide (Fig. 4.30A) and CpdA (Fig. 4.30B) had the opposite effect and generated a response comparable to that of rAAV-GKS rats. Glibenclamide promoted GLP-1 (7-36) release as animals injected with this compound had significantly higher plasma GLP-1 (7-36) levels than vehicle-injected rats after both 15 (Control: 6.35±0.19, n=12; glibenclamide: 7.16±0.30, n=12; p<0.05) and 30 (Control: 6.81±0.15, n=12; glibenclamide: 7.56±0.33, n=12; p<0.05) minutes (Fig. 4.30A). GLP-1 (7-36) levels remained higher in rats given glibenclamide than vehicle throughout the oral GTT (Fig. 4.30C). Administration of CpdA into the PVN also stimulated GLP-1 (7-36) secretion after 30 minutes (Control: 6.81±0.15, n=12; CpdA: 7.69±0.31, n=12; p<0.01) (Fig. 4.30B). Delivery of D-glucose into the PVN stimulated GLP-1 (7-36) release after both 15 (Control: 6.35±0.19, n=12; D-glucose: 7.89±0.35, n=12; p<0.001) and 30 (Control: 6.81±0.15, n=12; D-glucose: 7.81±0.51, n=12; p<0.05) minutes (Fig. 4.30B). AUC analysis revealed that the Rats administered iPVN D-glucose also had higher plasma GLP-1 (7-36) levels than controls rats throughout the 120 minute study (Fig. 4.30C).


A
GLP-1 (7-36) (pmol/L)
Time (mins)
Control
Diaz
Glib


B
GLP-1 (7-36) (pmol/L)
Time (mins)
Control
Glucose
CpdA

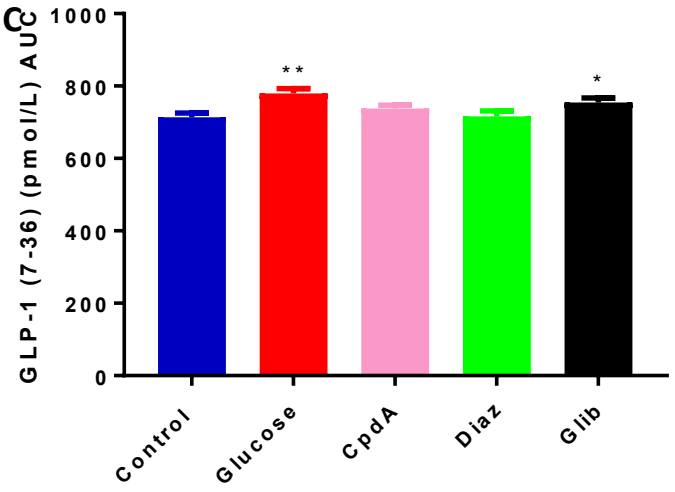

C
GLP-1 (7-36) (pmol/L) AUC
Control
Glucose
CpdA
Diaz
Glib

Figure 4.30: The effect of iPVN injections of various pharmacological agents on GLP-1 (7-36) secretion during an oral GTT. Oral glucose tolerance test comparing plasma GLP-1 (7-36) levels following administration of **(A)** vehicle (n=12), glibenclamide (2nmol, n=12) or diazoxide (1nmol, n=12) or **(B)** CpdA (0.5nmol, n=12), D-glucose (1.5mg/ml, n=12) or vehicle (n=12) into the PVN. This was performed in a cross-over study on iPVN-cannulated male Wistar rats. 1µl was injected for each compound at a rate of 120µl/hour. GLP-1 (7-36) concentration was measured using ELISA and **(C)** the area under the curve of each compound was determined. Blood samples were collected via a tail vein cannula at t=0, 15, 30, 60 and 120 minutes post-ingestion of a 2.5g/kg oral glucose dose. Data is expressed as mean ± SEM and was analysed using an unpaired T-test at each time point using GraphPad Prism 6: *p<0.05, **p<0.01, ***p<0.001 compared to control.

4.3.6.5 Confirmation of cannula placement using cresyl violet staining

Following the study the rats were sacrificed, 1µl Indian ink was injected into the PVN through the cannula implant and the brains of each animal were collected. They were sliced into sections 40µm thick which were mounted on poly-D-lysine coated slides. Cresyl violet staining was performed to reveal the site of injection and determine the accuracy of the cannula implant. This method revealed that the cannulae were accurately implanted into the targeted area as ink was detected in the PVN (Fig. 4.31A).

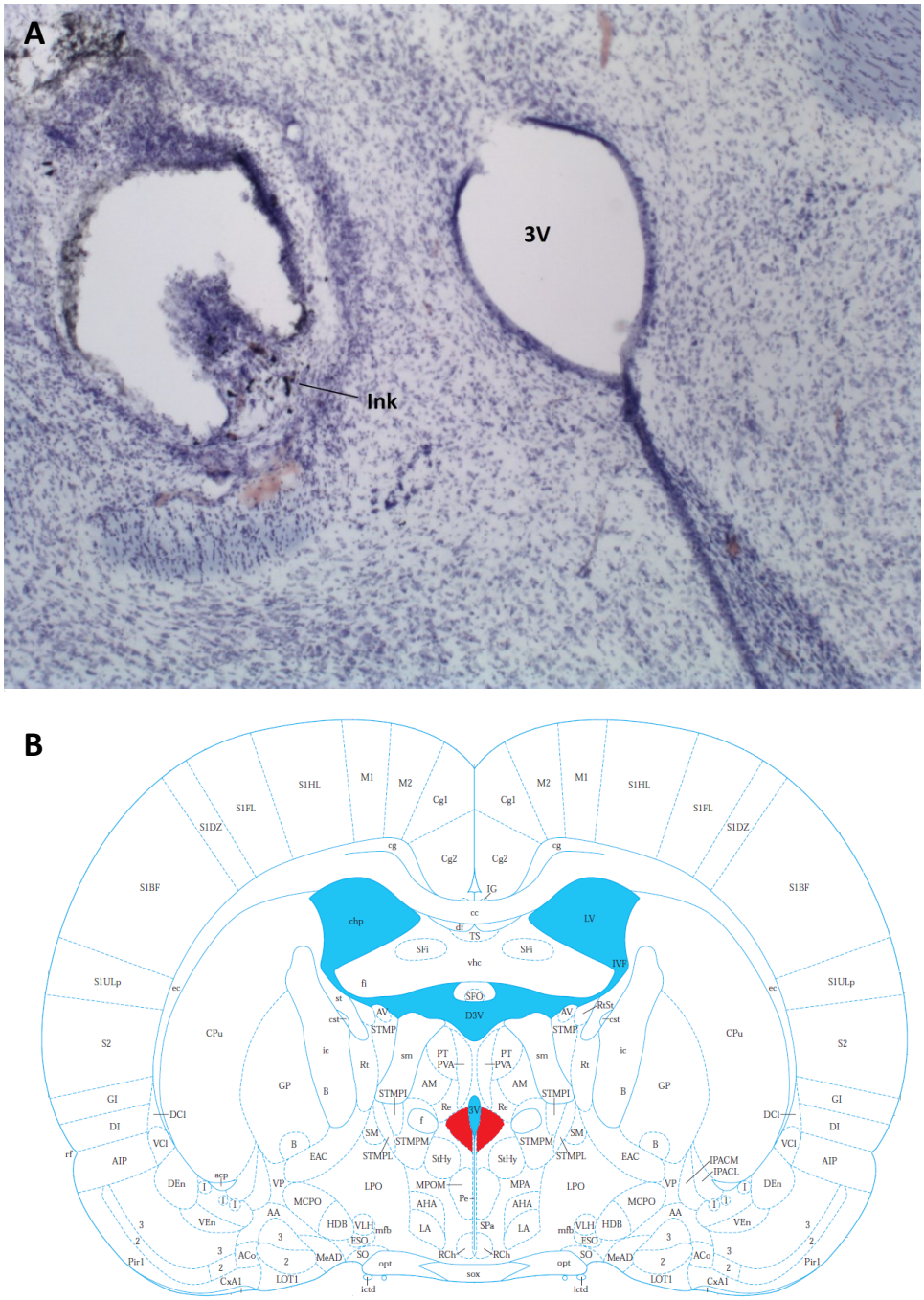


Figure 4.31: Confirmation of cannula placement in rats cannulated into the PVN. (A) Cresyl violet stained 40µm coronal brain section at 100x magnification showing ink in within the PVN in a representative animal. **(B)** Diagram of a coronal section of rat brain at coordinates -1.08mm from Bregma, interaural 7.92mm from the Rat Brain Atlas from Paxinos and Watson, with the injection area (PVN) highlighted. 3V: third ventricle.

4.4 Discussion

4.4.1 Knockdown of GK activity in the PVN does not influence feeding behaviour

Similarly to the work described in Chapter 3, the expression of GK in the PVN was knocked down via stereotactic injection of recombinant adeno-associated virus (rAAV) containing antisense RNA for GK in order to examine whether GK in the PVN plays a role in the regulation of appetite. Food intake was then measured during a feeding study comprising standard chow diet with and without 10% w/v glucose solution being available at the same time.

No difference in food intake, glucose consumption or the rate of body weight gain was observed in rAAV-GKAS rats compared to control animals. In contradiction to the hypothesis and despite the PVN playing a key role in the regulation of satiety, PVN GK does not appear to be involved in regulating feeding behaviour.

The PVN expresses numerous anorexigenic peptides, including cocaine and amphetamine regulated transcript (CART) and oxytocin (Wynick and Bacon, 2002, Blevins et al., 2004, Wang et al., 2000, Simmons and Swanson, 2009), and forms part of a well-established forebrain-hindbrain mechanism contributing to the initiation of satiety (Blevins et al., 2004, Blevins et al., 2009, Williams et al., 2006). As discussed in section 4.1, numerous studies have shown that the PVN plays an important role in integrating information regarding food intake to regulate energy homeostasis. For instance, iPVN injection of various peptides altered the feeding behaviour of rodents (Crawley et al., 1990, Kyrkouli et al., 2006, Tempel et al., 1988, Karatayev et al., 2009, Stanley et al., 1985, Edwards et al., 1999, Katsurada et al., 2014). This effect was also achieved by genetically altering the expression of these peptides (Tiesjema et al., 2007, Shibasaki et al., 1993, Bagnasco et al., 2003).

GK in the PVN was hypothesized to play a role in the regulation of feeding behaviour due to the PVN's important involvement in the control of appetite. However the data from a feeding study with GK-deficient rats presented here suggests that GK, despite its presence in the appetite-regulating centre, does not play a role in this PVN function. This is supported by the findings of Hussain *et al.*, who suggested that PVN GK activity is not affected by hunger as fasting did not alter GK mRNA levels in the PVN (Hussain et al., 2015). As of yet, no evidence has been presented supporting a role for PVN GK in the regulation of food intake.

4.4.2 PVN GK plays a role in the regulation of glucose homeostasis

4.4.2.1 Evidence from the genetic knockdown and enhancement of GK expression

To examine the potential role of PVN GK in glucose homeostasis, its expression was again knocked down via stereotactic injection of rAAV-GKAS directly into the PVN. It was also up-regulated by injecting rAAV-GKS. An oral and intraperitoneal (i.p.) GTT as well as an ITT were performed to determine the effects of GK knockdown and up-regulation on glucose homeostasis. Blood samples were collected at various time points, after which plasma levels of glucose, insulin, GLP-1 (7-36) and glucagon were measured.

GK activity in the PVN of rAAV-GKAS, rAAV-GKS and rAAV-GFP animals was measured *in vitro* in order to evaluate the extent of GK knockdown caused by the rAAV. Its level of activity was also assessed in the neighbouring ARC and VMN to determine whether the rAAV had spread to other nuclei. GK activity was calculated using a modified NADPH assay as described previously (Goward et al., 1986, Hussain et al., 2015). It was found that stereotactic administration of rAAV encoding GKAS produced a 44% knockdown in the PVN of rAAV-GKAS animals compared to

those injected with rAAV-GFP, thus demonstrating that rAAV-GKAS can significantly alter GK activity *in vivo*. No change in GK activity was detected in either the ARC or VMN, indicating that the effects of the rAAV were localised to the PVN. This degree of knockdown was expected as use of rAAV-GKAS in rats had previously yielded reductions in GK activity of around 50% (Hussain et al., 2015). Stereotactic injection of rAAV-GKS into the PVN increased GK activity by 40% in rAAV-GKS animals compared to controls. No difference in GK activity was detected between rAAV-GKS and rAAV-GFP animals in either the ARC or VMN.

The plasma glucose levels of rAAV-GKAS rats were significantly higher than those of rAAV-GFP animals during both an oral and i.p. GTT after 30 minutes, suggesting that knocking down GK activity in the PVN substantially disrupted the rats' ability to restore euglycaemia immediately after a glucose challenge. Up-regulating PVN GK expression had the opposite effect and decreased the plasma glucose levels of rAAV-GKS rats compared to control animals after 30 minutes during both tolerance tests. PVN GK hence appears to play a role in the regulation of glucose homeostasis.

A significant difference in plasma insulin concentrations was observed between the two groups, indicating that PVN GK may play a role in insulin release from β-cells. In both the oral and i.p. GTTs, insulin levels were initially lower in rAAV-GKAS animals but then became higher than those of rAAV-GFP rats after 30 minutes. The initial insulin response to the glucose challenge seemed to be lost. Instead a delayed response was observed, suggesting that GK in the PVN may be involved in the regulation of GSIS. On the other hand up-regulating the expression of GK in the PVN increased insulin secretion in rAAV-GKS rats after 15 minutes, thus reinforcing PVN GK as a potential contributor of GSIS. This is supported by a study reporting a decrease in insulin secretion following ICV delivery of the GK inhibitors glucosamine and mannoheptulose into the third ventricle during an intravenous (IV) GTT (Osundiji et al., 2012). Moreover, Tokunaga *et al.* demonstrated that PVN lesions caused a rise in plasma glucose and insulin levels in rats (Tokunaga et al., 1986). The extent of

insulin release during the initial response to a glucose challenge appears to be proportional to the level of GK expression in the PVN. However during an i.p. GTT, increasing PVN GK expression in rAAV-GKS animals did not have an effect on insulin secretion whereas PVN GK knockdown significantly impaired it. Though this casts doubt on the nature of its involvement in insulin release, the majority of the evidence generated in both rAAV-GKAS and rAAV-GKS studies points towards an important role of PVN GK in the regulation of GSIS.

A glucose-stimulated insulin secretion assay on isolated islets of rAAV-GKAS rats suggested a disruption in the secretory function of β-cells. The result obtained is consistent with the previously observed decrease in plasma insulin concentration in rAAV-GKAS animals during oral and i.p. GTTs. It suggests that the reduction of insulin release in response to a glucose challenge following PVN GK knockdown is due, at least in part, to decreased pancreatic β-cell secretory function. The islets were handpicked using a stereo dissecting microscope. Although time consuming, this method restricts the risk of damage to the islets during the isolation process (Ravier, 2010).

Glucose-stimulated GLP-1 (7-36) release was reduced in rAAV-GKAS rats compared to rAAV-GFP animals during an oral GTT. Conversely, its release was augmented when GK was over-expressed in the PVN. PVN GK hence appears to aid GLP-1 (7-36) release from intestinal L-cells. This finding may help explain the loss of the insulin response in rAAV-GKAS animals as GLP-1 (7-36), an incretin, increases GSIS (Creutzfeldt and Ebert, 1985, Gefel et al., 1990). GLP-1 (7-36) is also believed augment supplies of insulin for secretion by promoting insulin biosynthesis (Papastamataki et al., 2014). This constitutes part of the initial insulin response to a glucose challenge. The delay in the initial insulin response observed in rAAV-GKAS animals during an oral GTT may thus have been due to the considerable drop in GLP-1 (7-36) release exhibited in these animals following oral ingestion of glucose. Insulin secretion during the oral GTT cannot only be due to GLP-1 action on β-cells; however, as the initial insulin response was still impaired when the incretin effect was bypassed

during the i.p. GTT. PVN GK thus appears to also act directly on pancreatic β-cells to induce insulin release. The qPCR analysis of ileum tissue suggests that alteration of PVN GK expression did not induce a permanent change in GLP-1 (7-36) expression at a genetic level as the GCG and PYY mRNA levels of both rAAV-GKAS and rAAV-GFP rats unchanged compared to those of control animals. This implies that the effect of reduced PVN GK activity on GLP-1 (7-36) release during the GTT was due to a dysfunction in the PVN-L-cell circuit following a glucose challenge.

An oral gavage of the amino acid L-arginine was performed on rats previously injected with rAAV-GFP, rAAV-GKS or rAAV-GKAS in the PVN. This test was done in order to assess whether the impairment of the initial GLP-1 response observed during the oral GTT was specific to glucose or whether it also applies to other nutrients. In other words, the aim of this study was to determine whether PVN GK knockdown disrupted the GLP-1 response to amino acids in the same way that it impaired the response to glucose. The amino acid L-arginine was chosen for this study as the literature demonstrates oral consumption of this amino acid causes gut hormone release, including GLP-1. Thus if oral gavage of L-arginine leads to a change in GLP-1 secretion in rAAV-GKAS animals compared to controls rAAV-GFP rats, it would suggest that PVN GK regulates GLP-1 secretion in response to amino acid intake as well as to glucose intake. This would suggest that PVN GK is not solely involved in the regulation of glucose homeostasis, but also of amino acid homeostasis. The dose of L-arginine administered was determined from literature as well as from previous studies (Alamshah et al., 2016). Plasma GLP-1 (7-36) levels in response to the oral gavage of L-arginine were not statistically different between the two groups. This indicates that the GLP-1 system in response to amino acid intake appears to be intact in rAAV-GKAS animals, suggesting that the PVN GK-driven suppression of the initial GLP-1 response observed during the oral GTT may be specific to glucose. Thus, PVN GK's influence on the regulation of glucose homeostasis appears to rely partly on releasing GLP-1. The similar response to L-arginine in rAAV-GFP and rAAV-GKAS rats presents

evidence that PVN GK is not involved in the regulation of amino acid homeostasis and suggests that it may be exclusive to that of glucose.

The ITT revealed no difference in glucose levels between the treatment and control groups, suggesting that neither the rAAV-GKAS nor rAAV-GKS injection impaired the counter-regulatory response to insulin-induced hypoglycaemia. GK in the PVN hence does not appear to play a role in counteracting hypoglycaemia. This is corroborated by the findings of Hussain *et al.*, who reported that the mRNA levels of GK in the PVN are unchanged by periods of hypoglycaemia (Hussain et al., 2015).

4.4.2.2 Investigating the mechanism behind PVN GK's effects on glucose homeostasis

In order to investigate the mechanism behind GK's influence on glucose homeostasis, various pharmacological agents were injected directly into the PVN through an implanted cannula. The K_{ATP} channel activator diazoxide and inhibitor glibenclamide were used to assess the involvement of K_{ATP} channels in the pathway leading to changes in insulin and GLP-1 (7-36) secretion. It was hypothesized that they would mimic the effects of GK knockdown and up-regulation, respectively. The GK activator Compound A (CpdA) was also administered in order to further investigate the physiological role of GK in the regulation of glucose homeostasis. The concentration of each drug was chosen based on previous studies (Hussain et al., 2015). Ink injections into the PVN through the cannula were used to evaluate the accuracy of the cannula implant. Cresyl violet staining of ink-injected brains revealed that the cannulation was accurate and that injections into this cannula were delivered accurately into the PVN.

CpdA induced a comparable effect on glucose homeostasis to that seen in rAAV-GKS rats, confirming that the responses seen in the genetically altered animals during the GTTs were due to an increase in GK activity. The data generated by iPVN CpdA administration bolster the evidence implicating PVN GK as an important regulator of insulin and GLP-1 (7-36) release.

Administration of D-glucose directly into the PVN promoted insulin and GLP-1 (7-36) secretion and decreased plasma glucose levels during an oral GTT compared to animals injected with vehicle. It appears the local rise in glucose concentration was sensed by the PVN, which initiated a feedback response to restore euglycaemia, thus leading to a reduction in circulating glucose concentration. The PVN neurons involved in this response thus appear to be GE in nature as the local increase in glucose levels stimulated neuronal firing.

K_{ATP} channels play a crucial role in initiating GE neuron depolarisation (De Backer et al., 2016). Glibenclamide and diazoxide produced effects on glucose homeostasis similar to those seen after increasing and decreasing, respectively, the genetic expression of PVN GK. The ability of these pharmacological agents to mimic the responses obtained in rAAV-GKS and rAAV-GKAS animals suggests that K_{ATP} channels are a key component of the signalling cascade leading to changes in glucose clearance as well as insulin and GLP-1 (7-36) secretion following PVN GK activation. In addition as CpdA, glibenclamide and diazoxide were injected into the same site and all produced an effect, GK and K_{ATP} channels are likely to be co-localized in PVN glucose-sensing neurons.

GK-induced inhibition of K_{ATP} channels causes neuronal depolarisation via Ca^{2+} influx through Ca^{2+} channels in certain glucose-sensing neurons (Hussain et al., 2015). The depolarisation of GK-expressing PVN neurons leading to changes insulin and GLP-1 (7-36) levels may hence also occur via the inhibition of these channels.

GK's effects on glucose homeostasis are likely to occur by the transmission of parasympathetic efferent signals from the PVN to the β-cells and L-cells via the vagus nerve. It may regulate these cells' secretory function via a mechanism similar to that utilised by GK in the NTS and described in Chapter 3, section 3.4.2 (Berthoud et al., 1991, Ahren et al., 1986). The DMV is likely to act as a relay centre transmitting PVN signals to the periphery. The PVN provides a moderately dense input to the DMV (Geerling et al., 2010). This site is the origin for the parasympathetic outflow that targets the stomach and pancreas (Hopkins et al., 1996). The DMV provides the pre-ganglionic motor fibers that project to the viscera (Travagli et al., 2006), innervates the intra-pancreatic ganglia and is thought to play a role in the regulation of pancreatic secretory functions (Berthoud and Powley, 1990, Berthoud and Powley, 1987, Berthoud, 2006, Ionescu et al., 1983, Love et al., 2007, Babic et al., 2012, Babic et al., 2013). In addition, microstimulation of the DMV induces insulin secretion from β-cells (Laughton and Powley, 1987). Parasympathetic vagal activity may induce insulin secretion. It may do so by releasing acetylcholine (ACh), which activates post-synaptic nicotinic receptors as well as muscarinic M2 and M3 receptors located on pancreatic β-cells (Sobocki et al., 2005, Ahren, 2000, Woods and Bernstein, 1980). Other neurotransmitters present in islet parasympathetic terminals may also be at play, such as vasoactive intestinal polypeptide (VIP), gastrin releasing peptide (GRP) and pituitary adenylate cyclase activating polypeptide (PACAP) (Ahren et al., 1986, Havel et al., 1997, Knuhtsen et al., 1987, Fridolf et al., 1992, Holst et al., 1987, Gregersen and Ahren, 1996, Straub and Sharp, 1996).

The work presented in this thesis suggests that PVN GK plays an important role in GLP-1 (7-36) release. This is likely to be mediated by a similar mechanism than that regulating insulin release involving the DMV and the vagus nerve. As stated earlier, a dense network of PVN neurons project to the DMV (Geerling et al., 2010). Many neurons of the DMV project to the small and large intestine via the celiac branch of the vagus nerve. Parasympathetic preganglionic neurons that innervate the GI tract are topographically organized in the DMV. The lateral part of the DMV projects to the colon and ileum, where GLP-1 (-36) is synthesized (Hayakawa et al., 2013). A study reported that

stimulation of the distal end of the celiac branch of the sub-diaphragmatic vagus nerve significantly increased gut glucagon-like peptide immunoreactivity (Rocca and Brubaker, 1999).

The decrease in GLP-1 release observed during an oral GTT may be partly responsible for the delayed initial insulin response following a glucose challenge. As an incretin, GLP-1 has a stimulatory effect on insulin secretion (Creutzfeldt and Ebert, 1985, Gefel et al., 1990, Papastamataki et al., 2014). In response to glucose ingestion, GLP-1 is released from L-cells. GLP-1 stimulates GSIS directly by acting on GLP-1 receptors (GLP-1Rs) on pancreatic β-cells (Holst and Deacon, 2005, Drucker, 2006, Larsen and Holst, 2005), but may also do so indirectly by activating a neuronal pathway linking the intestines to the pancreas. GLP-1 released from L-cells may interact with GLP-1Rs present in the nodose ganglion, sending impulses to the NTS and onwards to the hypothalamus, more specifically to the ARC and PVN (Nakagawa et al., 2004). The signal is thought to be carried from the DVC to the hypothalamus via GLP-1 production in the NTS, which may then act on post-synaptic GLP-1Rs in the ARC and PVN. GLP-1 synthesized in the periphery may also aid in relaying the signal after crossing the BBB into the DVC and hypothalamus via the AP and median eminence, respectively (Kastin et al., 2002). Indeed, microinjection of the GLP-1 analogue Exendin-4 into the DVC increased insulin secretion from the pancreas in anaesthetised rats (Babic et al., 2012). The hypothalamus then sends an efferent signal back to the DVC, which transfers it the pancreas through the vagus nerve to stimulate the release of insulin (Holst and Deacon, 2005). The effects of GLP-1 can be blocked by vagotomy, suggesting that the vagus nerve plays a key role in mediating the effects of GLP-1 (Abbott et al., 2005).

4.4.3 Conclusions

In conclusion, PVN GK appears to play an important role in the regulation of energy homeostasis. While it does not seem to influence feeding behaviour, evidence suggests that it plays a role in the regulation of glucose homeostasis. It may help to re-establish euglycaemia following a glucose challenge by inducing the release of insulin. PVN GK appears to do so in two ways: by directly signalling pancreatic islets to stimulate secretion from β-cells and by promoting GLP-1 (7-36) release from intestinal L-cells, which in turn also causes further insulin secretion. K_{ATP} channels appear to form part of the mechanism at play and the signal may be transmitted to the pancreas and intestines via the DMV and the vagus nerve.

Chapter Five – General Discussion

5.1 Introduction

Obesity is a growing epidemic in Western society and the need for effective treatments has never been more pressing. Although the drive to feed is known to be largely controlled by neuronal processes, the exact circuitry responsible for the regulation of energy homeostasis is unclear (Scarlett and Schwartz, 2015, Sam et al., 2012, Leibowitz and Wortley, 2004). The brainstem and hypothalamus both play a key role in this process (Scarlett and Schwartz, 2015, Young, 2012).

Glucokinase (GK), a key enzyme in the processes of glycolysis and glycogenesis, is expressed in numerous areas of the brainstem and hypothalamus (Lynch et al., 2000, Maekawa et al., 2000, Dunn-Meynell et al., 2002). Although the purpose of GK in the ARC and VMN in the regulation of energy homeostasis has been a major focus of metabolic research, the function of GK in other nuclei remains virtually unexplored. While the NTS and PVN are established appetite-regulating centres of the brain, little is known about the role of GK in these brain regions. This thesis investigates the physiological role of GK in the NTS and PVN in the regulation of energy homeostasis.

The work presented in this thesis investigated the physiological role of NTS and PVN GK in the regulation of energy homeostasis. It focused on two elements, GK's potential role in the regulation of appetite and of glucose homeostasis. The function of GK was examined by reducing its expression in the NTS and PVN by stereotactically injecting rAAV-GKAS into these brain nuclei. GK activity was reduced in both regions by 18% and 44%, respectively.

5.2 The role of NTS and PVN GK in the regulation of energy homeostasis

The results obtained from feeding studies suggested that neither GK in the NTS nor in the PVN is involved in the regulation of appetite as the knockdown of GK had no effect on the rate of body weight gain, food intake, glucose intake or total energy intake. This finding was unexpected as both of these brain regions are highly involved in the control of appetite and GK was hypothesized to play a role in this process, perhaps by sensing increases in glucose levels during a meal and promoting satiety to terminate feeding. As the role of NTS and PVN GK in appetite regulation has not been extensively investigated, little comparisons can be made between the results obtained and the literature.

A series of GTTs and ITTs revealed that GK in both the NTS and PVN plays a role in the regulation of glucose homeostasis. Knockdown of GK in these regions caused a reduction in plasma insulin levels in response to glucose during a GTT. A considerable decrease in GLP-1 (7-36) release was also observed in animals with reduced GK activity in the PVN. Genetically up-regulating GK activity in the PVN had the opposite effect and increased insulin and GLP-1 (7-36) secretion while reducing plasma glucose concentrations during both an oral and i.p. GTT. On the other hand, no significant differences in glycaemia were detected between control animals and either rAAV-GKAS or rAAV-GKS following injection of insulin during an ITT. These results suggest that both NTS and PVN GK play an important role in GSIS. Upon sensing an increase in glucose levels, they appear to contribute to the initial insulin response by stimulating insulin secretion following a glucose challenge. They also seem to influence GLP-1 (7-36) secretion from L-cells, which itself promotes insulin release and is released post-prandially (Papastamataki et al., 2014, Verdich et al., 2001). This theory is in line with the original hypothesis that GK's function includes limiting energy intake and reducing circulating glucose levels.

Administration of various pharmacological compounds directly into the PVN provided an indication of a possible mechanism responsible for PVN GK's effects on peripheral glucose homeostasis.

Glucose-sensing neurons of the PVN appear to be stimulated by increases in extracellular glucose levels as iPVN delivery of D-glucose stimulated insulin and GLP-1 (7-36) release, suggesting that GK expressed in GE neurons is important in regulating glucose homeostasis. In addition, inhibiting and activating K_{ATP} channels generated a similar response during an oral GTT than increasing and decreasing GK's genetic expression in the PVN, respectively. This implies that following a glucose challenge, K_{ATP} channel inhibition may be important in inducing neuronal depolarisation. The literature suggests that the signal from the PVN may be transmitted through the vagus nerve via the DMV (Geerling et al., 2010, Hopkins et al., 1996, Travagli et al., 2006, Hayakawa et al., 2013, Rocca and Brubaker, 1999, Berthoud and Powley, 1990, Ahren, 2000), however direct evidence of a link between PVN GK and β- and L-cells is lacking.

GK's effects on GSIS are thought to occur by the transmission of central parasympathetic efferent signals to the pancreas via the vagus nerve (Berthoud and Powley, 1990, Ahren, 2000). The pancreas possesses vagal innervations emanating from both the NTS and PVN (Hopkins et al., 1996, Geerling et al., 2010, Rinaman and Miselis, 1987). Parasympathetic vagal projections extend directly to β-cells (N'Guyen et al., 1994). The DMV is likely to serve as a relay centre in the NTS-pancreas pathway as it provides the pre-ganglionic motor fibers that project to the viscera (Travagli et al., 2006). It also innervates the intra-pancreatic ganglia and is believed to contribute to the modulation of pancreatic secretory functions, including glucose homeostasis (Berthoud and Powley, 1990, Berthoud and Powley, 1987, Berthoud, 2006, Ionescu et al., 1983, Love et al., 2007, Babic et al., 2012, Babic et al., 2013, Streefland et al., 1998). Parasympathetic vagal activity may induce insulin secretion by releasing the neurotransmitter acetylcholine (ACh), which likely acts on post-synaptic nicotinic as well as muscarinic M2 and M3 receptors located on pancreatic β-cells (Sobocki et al., 2005, Ahren, 2000, Woods and Bernstein, 1980, Mussa and Verberne, 2008, Mussa et al., 2011, Nishi et al., 1987, Ahren et al., 1986). Various other non-cholinergic neurotransmitters are believed to contribute to the parasympathetic control of islet secretory response, including vasoactive intestinal polypeptide

(VIP), gastrin-releasing peptide (GRP) and pituitary adenylate cyclase activating polypeptide (PACAP) (Ahren et al., 1986, Havel et al., 1997, Knuhtsen et al., 1987, Fridolf et al., 1992, Holst et al., 1987). These substances are present in islet parasympathetic terminals and act to stimulate insulin release (Gregersen and Ahren, 1996, Straub and Sharp, 1996).

The results reported in this thesis suggest that PVN GK plays an important role in GLP-1 (7-36) release, possibly by a similar mechanism to that regulating insulin release involving the DMV and the vagus nerve. A dense network of PVN neurons project to the DMV (Geerling et al., 2010) and DMV neurons project to the small and large intestine via the celiac branch of the vagus nerve. As an incretin, GLP-1 has a stimulatory effect on insulin secretion (Creutzfeldt and Ebert, 1985, Gefel et al., 1990, Papastamataki et al., 2014). GLP-1 is released from L-cells in response to glucose ingestion and binds to GLP-1 receptors (GLP-1Rs) on pancreatic β-cells (Holst and Deacon, 2005, Drucker, 2006, Larsen and Holst, 2005). It may also stimulate GSIS via activation of a neuronal pathway by acting on GLP-1Rs present in the nodose ganglion, sending impulses to the NTS and onwards to the ARC and PVN (Nakagawa et al., 2004). The signal may be propagated from the DVC to the hypothalamus via GLP-1 production in the NTS. The DVC and hypothalamus then send an efferent signal back to the DVC, which transfers it to the pancreas through the vagus nerve to stimulate the release of insulin (Holst and Deacon, 2005).

NTS and PVN GK appear to have similar roles in the regulation of glucose homeostasis as they both seem to detect increases in plasma glucose levels and to stimulate the initial insulin response. GK in these nuclei may induce this response via a common mechanism. The effects of GK in either nucleus alone seem sufficient to induce a response; however the possibility of a combined and perhaps cumulative effect of NTS and PVN GK on insulin secretion exists. The presence of multiple inter-connected glucose-sensing centres would enable alterations in glucose levels to be detected rapidly while ensuring the appropriate degree of response is generated. However, no such mechanism has been discovered as of yet.

5.3 The use of rAAV to alter the genetic expression of neuronal GK

The physiological role of GK in the NTS and PVN was investigated by both reducing and up-regulating its activity in these nuclei. This was achieved through the use of rAAV encoding GKAS and GKS, respectively, which was stereotactically injected directly into the targeted nucleus. While numerous types of viral vectors exist, AAV was selected as it is practically non-immunogenic, inserts stably into the host genome and its effects on gene expression *in vivo* are long-lasting (Ponnazhagan et al., 1997, Klein et al., 1999, Leone et al., 2012). In addition, AAV2 is known to be effective for gene delivery to neurons and therefore represented a suitable vector to alter GK expression in the brain (Howard et al., 2008, Lentz et al., 2012).

Glucokinase activity was determined using a modified NADPH assay as described previously (Goward et al., 1986, Hussain et al., 2015). Other assays measuring GK activity are less GK-specific due to hexokinases' higher affinity and lower Km for glucose (Printz et al., 1993). These methods measure NADP+ in two separate experiments at a high and low concentration of glucose (20mM and 0.5mM, respectively); where GK activity should be lower than hexokinase activity at low glucose concentrations. A comparison between the two experiments is necessary to eliminate the effects of other hexokinases, but total elimination cannot be confirmed (Osundiji et al., 2012).

The ability of the rAAV construct encoding GKAS to modulate GK expression was first tested in liver hepatocellular carcinoma (HEPG2) cells. This is a liver cell line expressing GK. The cells were transfected with GKAS plasmid and GK activity in cell lysates was measured 48 hours later. A 38% knockdown in GK activity was generated following transfection with GKAS plasmid compared with

control plasmid. In addition, a 56% knockdown of NPY expression was observed in RIN56 NPY-containing cells transfected with rAAV-GKAS (Gardiner et al., 2005).

Alternative approaches exist to reduce GK activity *in vivo*. Global knockouts have been used in the past to identify the function of a protein; however this model would not be appropriate as it would not shed light on the role of GK in specific tissues. In addition, mice with homozygous or heterozygous deletion for the GK gene are diabetic due to the combined effects of decreased GK in the liver, pancreas and CNS (Grupe et al., 1995, Baker et al., 2014). These models may hence not provide a representative indication of the physiological role of GK. Another possible method is to use the 'Cre-lox' approach in transgenic mice. This technique enables the localisation of genetic modification to the targeted area. The gene of interest is flanked by Lox-P sequences, which are 'floxed' by Cre recombinase following stereotactic injection of rAAV containing the enzyme into the site of interest. In order to compare with previous studies of GK knockdown in rats and because these techniques are predominantly performed in mice, however, the use of rAAV was preferred to the alternative approaches as it enables the decrease of GK activity in rats.

5.4 Clinical implications

The glucose-lowering effects of iPVN CpdA and glibenclamide administration have potential clinical implications in the treatment of *diabetes mellitus*.

Injecting the glucokinase activator CpdA directly into the PVN significantly decreased glucose levels in hyperglycaemic rats by boosting insulin and GLP-1 (7-36) secretion, suggesting that enhancing GK activity specifically in the PVN may have therapeutic effects by helping to restore euglycaemia. However, specifically targeting GK in the PVN may be challenging in humans as delivery of the GK

activator directly into the PVN on a regular basis is not feasible. Designing a drug selective for GK in this nucleus may also be problematic as the GK isoform located in the PVN is not structurally different to that in the rest of the CNS and pancreas (Roncero et al., 2000).

Inhibiting K_{ATP} channel activity in the PVN also significantly dampened hyperglycaemia in rats during both an oral and i.p. GTT and had the same effect as CpdA on insulin and GLP-1 (7-36) release, suggesting that targeting this channel may also represent a potential therapeutic option. However the same obstacles exist with this strategy as with the targeting of PVN GK.

Nevertheless, the results presented in this thesis provide a couple of possible drug targets for the amelioration of glucose tolerance in diabetic patients. Further investigation is required in order to determine the viability of PVN GK and K_{ATP} channels as potential drug targets in the treatment of hyperglycaemia.

5.5 Limitations of findings

The studies discussed in this thesis have certain limitations which may affect the validity of the results. A major part of the studies involved altering GK expression through the use of rAAV stereotactically injected into the brain region of interest. A disadvantage of stereotactic injection of vectors is that this technique relies greatly on the accuracy of the injection. It thus requires training and experience to avoid variable results. Moreover, maximal gene expression is often not reached until approximately three to four weeks. Nevertheless, viral gene transfer remains a powerful tool for examining the neuronal mechanisms regulating energy homeostasis *in vivo* (Ponnazhagan et al., 1997, Klein et al., 1999, Leone et al., 2012).

The degree of change in GK activity was measured using a GK activity assay. In order to analyse GK activity, the brain region of interest was isolated by performing a micropunch biopsy. Due to the small size of the nucleus in question, this technique requires precision and a strong knowledge of the brain anatomy. A mistake in this process, such as isolating a portion of a neighbouring nucleus along with the area of interest, would undermine the validity of the NTS and PVN GK activity assays presented in this thesis.

An indwelling cannula was implanted into the PVN in order to enable direct administration of pharmacological agents into this nucleus. Direct cannulation is a valuable tool in the research of neuronal control of energy homeostasis; however injections cannot be administered repeatedly as this induces inflammation of the cannulated brain area. A minimal recovery period is required to avoid damage to the targeted region. Therefore although direct cannulation represents a valuable tool for acute studies, it is not suitable for chronic studies. In addition, although the accuracy of the cannula implant was histochemically verified in ink-injected brains, the drugs injected may not have only affected the targeted neurons but may have spread to non-GK expressing neurons of the PVN as well. This may have led to unwanted effects.

The role of NTS and PVN GK in the regulation of glucose homeostasis was determined by conducting a series of GTTs and ITTs on genetically altered rats and collecting blood samples at various time points. Blood was collected using a cannula implanted in the tail vein. This technique was chosen rather than tail bleeds in an effort to minimise the stress inflicted on the animals during each study. However, a certain amount of stress is likely to have been caused to each animal due to repeated handling and blood sampling, particularly following an i.p. or iPVN injection. This may have impacted the results by, for instance, increasing the animals' basal plasma glucose levels.

Plasma levels of glucose, insulin, GLP-1 (7-36) and glucagon were analysed using a glucose assay and ELISA. These assays are generally conducted in triplicate to avoid variability in the results however due to the limited volume of blood that can be collected at each time point, not enough plasma was available for triplicate analysis. Each assay was therefore performed in singlet, which may reduce the reliability of the data. Despite this, the variability of the data was generally negligible, with the SEM often being within 10% of the mean at each time point.

5.6 Future studies

The results presented in this thesis suggest a key role of NTS and PVN GK in the regulation of glucose homeostasis, however further investigation is required to shed light on GK's role in these nuclei.

Additional work is required to determine the exact mechanism behind the effects of PVN GK on glucose homeostasis. K_{ATP} channels were found to play an important role in inducing insulin and GLP-1 (7-36) secretion in the periphery. These channels also form part of the downstream GK signalling cascade in the ARC and were shown to induce Ca^{2+} influx via Ca^{2+} channels (Hussain et al., 2015). Various pharmacological compounds inhibiting different Ca^{2+} channels will be directly administered into the PVN via an implanted cannula to determine whether Ca^{2+} channels are involved in the regulation of glucose homeostasis by PVN GK. A secretion assay performed in isolated pancreatic islets of rAAV-GKAS and rAAV-GFP animals hinted that PVN GK may directly influence β-cell secretory function, but the low *n* power seemed to prevent the result from reaching statistical significance. This study must be repeated with islets from a greater number of animals in order to strengthen the data obtained previously. This will help establish whether GK in the PVN contributes to the regulation of insulin release from β-cells. Both of these studies will also be performed in the

NTS in order to determine whether NTS GK is also involved in glucose homeostasis via this mechanism.

The results presented in this thesis suggest a similar role for NTS and PVN GK in the regulation of glucose homeostasis, more specifically in promoting insulin secretion following a rise in plasma glucose levels. Additionally, GK in these nuclei appears to induce this effect via a common mechanism. Although the effects of GK in either nucleus seem sufficient to induce a response, this suggests that GK in the NTS and PVN may have a combined and perhaps cumulative effect on glucose homeostasis, as discussed earlier. This possibility will be explored in future studies. It will be investigated by knocking down GK in both the NTS and PVN of rats. The glucose tolerance of these 'double knockdown' rats will be assessed in a series of GTTs, both oral and i.p. as performed previously, and their ability to restore euglycaemia following IIH will be determined during an ITT. Their plasma glucose, insulin and GLP-1 (7-36) levels during the GTTs and ITT will be compared to those of rats where GK was knocked down in a single nucleus (either the NTS or PVN) as well as to those of control animals injected with rAAV-GFP in both the NTS and PVN. A difference in plasma glucose, insulin or GLP-1 (7-36) concentrations between the double and single knockdown groups would suggest that GK in the NTS and PVN have a combined glucose-sensing role and may have a cumulative effect on β-cell secretory function during times of hyperglycaemia.

The physiological role of GK in other areas of the brain needs to be examined to assess whether it also plays a role in energy homeostasis. GK is expressed in other hypothalamic nuclei such as the ARC, VMN, lateral hypothalamic area (LHA) and dorsomedial nucleus (DMN). It has also been detected in the AP and DMV of the brainstem and in the medial amygdalar nucleus (MAN) (De Backer et al., 2016, Li et al., 2003, Lynch et al., 2000, Navarro et al., 1996, Dunn-Meynell et al., 2002, Roncero et al., 2009, Nishio et al., 2006, Polakof et al., 2009). Many types of neurons expressing GK exhibit glucose-sensing properties (Adachi et al., 1995, Blouet and Schwartz, 2012, Dunn-Meynell et

al., 2002, Halmos et al., 2015, Lynch et al., 2000, Li et al., 2014, Roncero et al., 2004, Roncero et al., 2000, Maekawa et al., 2000). GK in the ARC is believed to contribute to the regulation of appetite, particularly for glucose-rich foods. Increasing GK activity in the ARC was recently shown to augment chow and glucose intake in rats, while down-regulating it had the opposite effect (Hussain et al., 2015). In addition GK levels rise during fasting, suggesting it is involved in the regulation of energy homeostasis (Kang et al., 2008, Sanz et al., 2007, Hussain et al., 2015). Some studies do not support a role for ARC GK in appetite regulation, however. For instance, knockdown of GK activity in the VMH did not alter feeding behaviour while ICV injection of the GK inhibitor glucosamine increased food intake (Dunn-Meynell et al., 2009, Zhou et al., 2011). GK in the LHA has been implicated in the neuronal glucose-sensing machinery as its activity increased during insulin-induced hypoglycaemia (IIH) (Cherian and Briski, 2010). Although little research has been done to shed light on its function, a study suggested that GK in the LHA may play a role in initiating glucoprivic feeding as ICV injections of the GK inhibitor glucosamine in rats promoted c-fos expression in LHA orexin neurons and stimulated food intake (Zhou et al., 2011). GK in the VMH and MAN is believed to mediate the counter-regulatory response (CRR) to hypoglycaemia. VMH GK has been described as an important regulator of the CRR. Its exact role is unclear, however. For instance, an ICV microinjection of the GK inhibitor alloxan into the third ventricle of rats impaired their CRR to hypoglycaemia induced by 2-deoxy-D-glucose (2-DG), while microinjection of the GK activator Compound A was also reported to diminish the CRR (Sanders et al., 2004, Levin et al., 2008). GK in the MAN may also contribute to the initiation of the CRR. Although little work has been done to characterise its function in this nucleus, a study reported that lesions in the MAN suppressed the CRR whereas 2-DG infusion amplified it. In addition, MAN glucoprivation during mild systemic hypoglycaemia amplified the CRR, suggesting that this nucleus is able to sense decreases in local in glucose levels and trigger a response (Zhou et al., 2010).

5.7 Conclusions

GK in both the NTS and PVN appears to aid in the regulation of energy homeostasis by playing a role in the control of glucose homeostasis. Its function in both nuclei seems to be to detect increases in circulating glucose levels and restore euglycaemia by stimulating insulin secretion from β-cells and GLP-1 (7-36) release from L-cells. In the PVN, the signal to the periphery may be initiated by neuronal depolarisation triggered by the inhibition of K_{ATP} channels following glucose phosphorylation by GK. The work described in this thesis presents novel evidence for an important homeostatic pathway initiated by the glucose-sensor GK located in both the brainstem and hypothalamus.

Chapter Six - References

ABBOTT, C. R., MONTEIRO, M., SMALL, C. J., SAJEDI, A., SMITH, K. L., PARKINSON, J. R., GHATEI, M. A. & BLOOM, S. R. 2005. The inhibitory effects of peripheral administration of peptide YY(3-36) and glucagon-like peptide-1 on food intake are attenuated by ablation of the vagal-brainstem-hypothalamic pathway. *Brain Res,* 17**,** 127-31.

ABRAHAM, M. A., FILIPPI, B. M., KANG, G. M., KIM, M. S. & LAM, T. K. 2014. Insulin action in the hypothalamus and dorsal vagal complex. *Exp Physiol*.

ADACHI, A. & KOBASHI, M. 1985. Chemosensitive neurons within the area postrema of the rat. *Neurosci Lett,* 55**,** 137-40.

ADACHI, A., KOBASHI, M. & FUNAHASHI, M. 1995. Glucose-responsive neurons in the brainstem. *Obes Res,* 3 Suppl 5**,** 735s-740s.

AHREN, B. 2000. Autonomic regulation of islet hormone secretion--implications for health and disease. *Diabetologia,* 43**,** 393-410.

AHREN, B., TABORSKY, G. J., JR. & PORTE, D., JR. 1986. Neuropeptidergic versus cholinergic and adrenergic regulation of islet hormone secretion. *Diabetologia,* 29**,** 827-36.

AKACHE, B., GRIMM, D., PANDEY, K., YANT, S. R., XU, H. & KAY, M. A. 2006. The 37/67-kilodalton laminin receptor is a receptor for adeno-associated virus serotypes 8, 2, 3, and 9. *J Virol,* 80**,** 9831-6.

AKACHE, B., GRIMM, D., SHEN, X., FUESS, S., YANT, S. R., GLAZER, D. S., PARK, J. & KAY, M. A. 2007. A two-hybrid screen identifies cathepsins B and L as uncoating factors for adeno-associated virus 2 and 8. *Mol Ther,* 15**,** 330-9.

ALVAREZ, E., RONCERO, I., CHOWEN, J. A., THORENS, B. & BLAZQUEZ, E. 1996. Expression of the glucagon-like peptide-1 receptor gene in rat brain. *J Neurochem,* 66**,** 920-7.

ALVAREZ, E., RONCERO, I., CHOWEN, J. A., VAZQUEZ, P. & BLAZQUEZ, E. 2002. Evidence that glucokinase regulatory protein is expressed and interacts with glucokinase in rat brain. *J Neurochem,* 80**,** 45-53.

AMIEL, S. A. 1995. Organ fuel selection: brain. *Proc Nutr Soc,* 54**,** 151-5.

ANAND, B. K. & BROBECK, J. R. 1951. Localization of a "feeding center" in the hypothalamus of the rat. *Proc Soc Exp Biol Med,* 77**,** 323-4.

ANAND, B. K., CHHINA, G. S., SHARMA, K. N., DUA, S. & SINGH, B. 1964. ACTIVITY OF SINGLE NEURONS IN THE HYPOTHALAMIC FEEDING CENTERS: EFFECT OF GLUCOSE. *Am J Physiol,* 207**,** 1146-54.

APONTE, Y., ATASOY, D. & STERNSON, S. M. 2011. AGRP neurons are sufficient to orchestrate feeding behavior rapidly and without training. *Nat Neurosci,* 14**,** 351-5.

ARKHAMMAR, P., NILSSON, T., RORSMAN, P. & BERGGREN, P. O. 1987. Inhibition of ATP-regulated K+ channels precedes depolarization-induced increase in cytoplasmic free Ca2+ concentration in pancreatic beta-cells. *J Biol Chem,* 262**,** 5448-54.

ARLETTI, R., BENELLI, A. & BERTOLINI, A. 1990. Oxytocin inhibits food and fluid intake in rats. *Physiol Behav,* 48**,** 825-30.

ARLUISON, M., QUIGNON, M., NGUYEN, P., THORENS, B., LELOUP, C. & PENICAUD, L. 2004. Distribution and anatomical localization of the glucose transporter 2 (GLUT2) in the adult rat brain--an immunohistochemical study. *J Chem Neuroanat,* 28**,** 117-36.

ASHFORD, M. L., BODEN, P. R. & TREHERNE, J. M. 1990. Glucose-induced excitation of hypothalamic neurones is mediated by ATP-sensitive K+ channels. *Pflugers Arch,* 415**,** 479-83.

ASOKAN, A., HAMRA, J. B., GOVINDASAMY, L., AGBANDJE-MCKENNA, M. & SAMULSKI, R. J. 2006. Adeno-associated virus type 2 contains an integrin alpha5beta1 binding domain essential for viral cell entry. *J Virol,* 80**,** 8961-9.

ATCHISON, R. W., CASTO, B. C. & HAMMON, W. M. 1965. ADENOVIRUS-ASSOCIATED DEFECTIVE VIRUS PARTICLES. *Science,* 149**,** 754-6.

BABIC, T., BHAGAT, R., WAN, S., BROWNING, K. N., SNYDER, M., FORTNA, S. R. & TRAVAGLI, R. A. 2013. Role of the vagus in the reduced pancreatic exocrine function in copper-deficient rats. *Am J Physiol Gastrointest Liver Physiol,* 304**,** 28.

BABIC, T., BROWNING, K. N., KAWAGUCHI, Y., TANG, X. & TRAVAGLI, R. A. 2012. Pancreatic insulin and exocrine secretion are under the modulatory control of distinct subpopulations of vagal motoneurones in the rat. *J Physiol,* 590**,** 3611-22.

BADY, I., MARTY, N., DALLAPORTA, M., EMERY, M., GYGER, J., TARUSSIO, D., FORETZ, M. & THORENS, B. 2006. Evidence from glut2-null mice that glucose is a critical physiological regulator of feeding. *Diabetes,* 55**,** 988-95.

BAGNASCO, M., DUBE, M. G., KATZ, A., KALRA, P. S. & KALRA, S. P. 2003. Leptin expression in hypothalamic PVN reverses dietary obesity and hyperinsulinemia but stimulates ghrelin. *Obes Res,* 11**,** 1463-70.

BAKER, D. J., ATKINSON, A. M., WILKINSON, G. P., COOPE, G. J., CHARLES, A. D. & LEIGHTON, B. 2014. Characterization of the heterozygous glucokinase knockout mouse as a translational disease model for glucose control in type 2 diabetes. *Br J Pharmacol,* 171**,** 1629-41.

BALFOUR, R. H., HANSEN, A. M. & TRAPP, S. 2006. Neuronal responses to transient hypoglycaemia in the dorsal vagal complex of the rat brainstem. *J Physiol,* 570**,** 469-84.

BANO, G. 2013. Glucose homeostasis, obesity and diabetes. *Best Pract Res Clin Obstet Gynaecol,* 27**,** 715-26.

BARABOI, E. D., SMITH, P., FERGUSON, A. V. & RICHARD, D. 2010. Lesions of area postrema and subfornical organ alter exendin-4-induced brain activation without preventing the hypophagic effect of the GLP-1 receptor agonist. *Am J Physiol Regul Integr Comp Physiol,* 298**,** R1098-110.

BARBARIC, I., MILLER, G. & DEAR, T. N. 2007. Appearances can be deceiving: phenotypes of knockout mice. *Brief Funct Genomic Proteomic,* 6**,** 91-103.

BELLINGER, L. L. & BERNARDIS, L. L. 2002. The dorsomedial hypothalamic nucleus and its role in ingestive behavior and body weight regulation: lessons learned from lesioning studies. *Physiol Behav,* 76**,** 431-42.

BERTHOUD, H. R. 2006. Homeostatic and non-homeostatic pathways involved in the control of food intake and energy balance. *Obesity,* 14**,** 197S-200S.

BERTHOUD, H. R., CARLSON, N. R. & POWLEY, T. L. 1991. Topography of efferent vagal innervation of the rat gastrointestinal tract. *Am J Physiol,* 260**,** R200-7.

BERTHOUD, H. R. & POWLEY, T. L. 1987. Characteristics of gastric and pancreatic responses to vagal stimulation with varied frequencies: evidence for different fiber calibers? *J Auton Nerv Syst,* 19**,** 77-84.

BERTHOUD, H. R. & POWLEY, T. L. 1990. Identification of vagal preganglionics that mediate cephalic phase insulin response. *Am J Physiol,* 258**,** R523-30.

BEWICK, G. A., GARDINER, J. V., DHILLO, W. S., KENT, A. S., WHITE, N. E., WEBSTER, Z., GHATEI, M. A. & BLOOM, S. R. 2005. Post-embryonic ablation of AgRP neurons in mice leads to a lean, hypophagic phenotype. *Faseb j,* 19**,** 1680-2.

BI, S., LADENHEIM, E. E., SCHWARTZ, G. J. & MORAN, T. H. 2001. A role for NPY overexpression in the dorsomedial hypothalamus in hyperphagia and obesity of OLETF rats. *Am J Physiol Regul Integr Comp Physiol,* 281**,** R254-60.

BIGGERS, D. W., MYERS, S. R., NEAL, D., STINSON, R., COOPER, N. B., JASPAN, J. B., WILLIAMS, P. E., CHERRINGTON, A. D. & FRIZZELL, R. T. 1989. Role of brain in counterregulation of insulin-induced hypoglycemia in dogs. *Diabetes,* 38**,** 7-16.

BLAKE, C. B. & SMITH, B. N. 2012. Insulin reduces excitation in gastric-related neurons of the dorsal motor nucleus of the vagus. *Am J Physiol Regul Integr Comp Physiol,* 303**,** R807-14.

BLEVINS, J. E., EAKIN, T. J., MURPHY, J. A., SCHWARTZ, M. W. & BASKIN, D. G. 2003. Oxytocin innervation of caudal brainstem nuclei activated by cholecystokinin. *Brain Res,* 993**,** 30-41.

BLEVINS, J. E., MORTON, G. J., WILLIAMS, D. L., CALDWELL, D. W., BASTIAN, L. S., WISSE, B. E., SCHWARTZ, M. W. & BASKIN, D. G. 2009. Forebrain melanocortin signaling enhances the hindbrain satiety response to CCK-8. *Am J Physiol Regul Integr Comp Physiol,* 296**,** R476-84.

BLEVINS, J. E., SCHWARTZ, M. W. & BASKIN, D. G. 2004. Evidence that paraventricular nucleus oxytocin neurons link hypothalamic leptin action to caudal brain stem nuclei controlling meal size. *Am J Physiol Regul Integr Comp Physiol,* 287**,** R87-96.

BLOMER, U., NALDINI, L., KAFRI, T., TRONO, D., VERMA, I. M. & GAGE, F. H. 1997. Highly efficient and sustained gene transfer in adult neurons with a lentivirus vector. *J Virol,* 71**,** 6641-9.

BLOUET, C., JO, Y. H., LI, X. & SCHWARTZ, G. J. 2009. Mediobasal hypothalamic leucine sensing regulates food intake through activation of a hypothalamus-brainstem circuit. *J Neurosci,* 29**,** 8302-11.

BLOUET, C. & SCHWARTZ, G. J. 2012. Brainstem nutrient sensing in the nucleus of the solitary tract inhibits feeding. *Cell Metab,* 16**,** 579-87.

BORG, W. P., SHERWIN, R. S., DURING, M. J., BORG, M. A. & SHULMAN, G. I. 1995. Local ventromedial hypothalamus glucopenia triggers counterregulatory hormone release. *Diabetes,* 44**,** 180-4.

BORISON, H. L. & WANG, S. C. 1953. Physiology and pharmacology of vomiting. *Pharmacol Rev,* 5**,** 193-230.

BORNET, F. R., JARDY-GENNETIER, A. E., JACQUET, N. & STOWELL, J. 2007. Glycaemic response to foods: impact on satiety and long-term weight regulation. *Appetite,* 49**,** 535-53.

BOYCHUK, C. R., GYARMATI, P., XU, H. & SMITH, B. N. 2015. Glucose sensing by GABAergic neurons in the mouse nucleus tractus solitarii. *J Neurophysiol,* 114**,** 999-1007.

BRISKI, K. P., KALE, A. Y. & VAVAIYA, K. V. 2009. Impact of recurring intermediate insulin-induced hypoglycemia on hypothalamic paraventricular corticotropin-releasing hormone, oxytocin, vasopressin and glucokinase gene profiles: role of type II glucocorticoid receptors. *Exp Brain Res,* 195**,** 499-507.

BRISKI, K. P. & SYLVESTER, P. W. 2001. Hypothalamic orexin-A-immunpositive neurons express Fos in response to central glucopenia. *Neuroreport,* 12**,** 531-4.

BROBERGER, C., DE LECEA, L., SUTCLIFFE, J. G. & HOKFELT, T. 1998. Hypocretin/orexin- and melanin-concentrating hormone-expressing cells form distinct populations in the rodent lateral hypothalamus: relationship to the neuropeptide Y and agouti gene-related protein systems. *J Comp Neurol,* 402**,** 460-74.

BROWN, D. F. & FLOODY, O. R. 1987. Gold thioglucose-induced brain lesions in hamsters. *Physiol Behav,* 39**,** 315-20.

BUHMANN, H., LE ROUX, C. W. & BUETER, M. 2014. The gut-brain axis in obesity. *Best Pract Res Clin Gastroenterol,* 28**,** 559-71.

BUKRINSKY, M. I., HAGGERTY, S., DEMPSEY, M. P., SHAROVA, N., ADZHUBEL, A., SPITZ, L., LEWIS, P., GOLDFARB, D., EMERMAN, M. & STEVENSON, M. 1993. A nuclear localization signal within HIV-1 matrix protein that governs infection of non-dividing cells. *Nature,* 365**,** 666-9.

BURCELIN, R. & THORENS, B. 2001. Evidence that extrapancreatic GLUT2-dependent glucose sensors control glucagon secretion. *Diabetes,* 50**,** 1282-9.

BURDAKOV, D., LUCKMAN, S. M. & VERKHRATSKY, A. 2005. Glucose-sensing neurons of the hypothalamus. *Philos Trans R Soc Lond B Biol Sci,* 360**,** 2227-35.

BURGGRAF, K. K., WILLING, A. E. & KOOPMANS, H. S. 1997. The effects of glucose or lipid infused intravenously or intragastrically on voluntary food intake in the rat. *Physiol Behav,* 61**,** 787-93.

CAI, X. J., EVANS, M. L., LISTER, C. A., LESLIE, R. A., ARCH, J. R., WILSON, S. & WILLIAMS, G. 2001. Hypoglycemia activates orexin neurons and selectively increases hypothalamic orexin-B levels: responses inhibited by feeding and possibly mediated by the nucleus of the solitary tract. *Diabetes,* 50**,** 105-12.

CANABAL, D. D., POTIAN, J. G., DURAN, R. G., MCARDLE, J. J. & ROUTH, V. H. 2007. Hyperglycemia impairs glucose and insulin regulation of nitric oxide production in glucose-inhibited neurons in the ventromedial hypothalamus. *Am J Physiol Regul Integr Comp Physiol,* 293**,** R592-600.

CARLSON, A. J. 1916. The control of hunger in health and disease. *The University of Chicago Press,* III.

CHAPMAN, I. M., GOBLE, E. A., WITTERT, G. A., MORLEY, J. E. & HOROWITZ, M. 1998. Effect of intravenous glucose and euglycemic insulin infusions on short-term appetite and food intake. *Am J Physiol,* 274**,** R596-603.

CHERIAN, A. K. & BRISKI, K. P. 2010. Effects of adrenalectomy on neuronal substrate fuel transporter and energy transducer gene expression in hypothalamic and hindbrain metabolic monitoring sites. *Neuroendocrinology,* 91**,** 56-63.

CONE, R. D., COWLEY, M. A., BUTLER, A. A., FAN, W., MARKS, D. L. & LOW, M. J. 2001. The arcuate nucleus as a conduit for diverse signals relevant to energy homeostasis. *Int J Obes Relat Metab Disord,* 25 Suppl 5**,** S63-7.

CONSIGLIO, A., QUATTRINI, A., MARTINO, S., BENSADOUN, J. C., DOLCETTA, D., TROJANI, A., BENAGLIA, G., MARCHESINI, S., CESTARI, V., OLIVERIO, A., BORDIGNON, C. & NALDINI, L. 2001. In vivo gene therapy of metachromatic leukodystrophy by lentiviral vectors: correction of neuropathology and protection against learning impairments in affected mice. *Nat Med,* 7**,** 310-6.

CONTRERAS, R. J., KOSTEN, T. & BIRD, E. 1984. Area postrema: part of the autonomic circuitry of caloric homeostasis. *Fed Proc,* 43**,** 2966-8.

CORWIN, R. L., ROBINSON, J. K. & CRAWLEY, J. N. 1993. Galanin antagonists block galanin-induced feeding in the hypothalamus and amygdala of the rat. *Eur J Neurosci,* 5**,** 1528-33.

COX, J. E. & POWLEY, T. L. 1981. Prior vagotomy blocks VMH obesity in pair-fed rats. *Am J Physiol,* 240**,** E573-83.

COX, K. H., DELEON, D. V., ANGERER, L. M. & ANGERER, R. C. 1984. Detection of mrnas in sea urchin embryos by in situ hybridization using asymmetric RNA probes. *Dev Biol,* 101**,** 485-502.

CRAIG, A. D. 1996. An ascending general homeostatic afferent pathway originating in lamina I. *Prog Brain Res,* 107**,** 225-42.

CRAWLEY, J. N., AUSTIN, M. C., FISKE, S. M., MARTIN, B., CONSOLO, S., BERTHOLD, M., LANGEL, U., FISONE, G. & BARTFAI, T. 1990. Activity of centrally administered galanin fragments on stimulation of feeding behavior and on galanin receptor binding in the rat hypothalamus. *J Neurosci,* 10**,** 3695-700.

CRAWLEY, J. N., ROBINSON, J. K., LANGEL, U. & BARTFAI, T. 1993. Galanin receptor antagonists M40 and C7 block galanin-induced feeding. *Brain Res,* 600**,** 268-72.

CREUTZFELDT, W. & EBERT, R. 1985. New developments in the incretin concept. *Diabetologia,* 28**,** 565-73.

D'SOUZA A, M., ASADI, A., JOHNSON, J. D., COVEY, S. D. & KIEFFER, T. J. 2014. Leptin deficiency in rats results in hyperinsulinemia and impaired glucose homeostasis. *Endocrinology,* 155**,** 1268-79.

DA SILVA, A. A., SPRADLEY, F. T., GRANGER, J. P., HALL, J. E. & DO CARMO, J. M. 2015. Brain-mediated antidiabetic, anorexic, and cardiovascular actions of leptin require melanocortin-4 receptor signaling. *J Neurophysiol,* 113**,** 2786-91.

DALLAPORTA, M., PERRIN, J. & ORSINI, J. C. 2000. Involvement of adenosine triphosphate-sensitive K+ channels in glucose-sensing in the rat solitary tract nucleus. *Neurosci Lett,* 278**,** 77-80.

DAVIS, J. D., WIRTSHAFTER, D., ASIN, K. E. & BRIEF, D. 1981. Sustained intracerebroventricular infusion of brain fuels reduces body weight and food intake in rats. *Science,* 212**,** 81-3.

DAYA, S. & BERNS, K. I. 2008. Gene therapy using adeno-associated virus vectors. *Clin Microbiol Rev,* 21**,** 583-93.

DE BACKER, I., HUSSAIN, S. S., BLOOM, S. R. & GARDINER, J. V. 2016. Insights into the role of neuronal glucokinase. *Am J Physiol Endocrinol Metab,* 311**,** E42-55.

DE LECEA, L., KILDUFF, T. S., PEYRON, C., GAO, X., FOYE, P. E., DANIELSON, P. E., FUKUHARA, C., BATTENBERG, E. L., GAUTVIK, V. T., BARTLETT, F. S., 2ND, FRANKEL, W. N., VAN DEN POL, A. N., BLOOM, F. E., GAUTVIK, K. M. & SUTCLIFFE, J. G. 1998. The hypocretins: hypothalamus-specific peptides with neuroexcitatory activity. *Proc Natl Acad Sci U S A,* 95**,** 322-7.

DE VRIES, M. G., ARSENEAU, L. M., LAWSON, M. E. & BEVERLY, J. L. 2003. Extracellular glucose in rat ventromedial hypothalamus during acute and recurrent hypoglycemia. *Diabetes,* 52**,** 2767-73.

DELAERE, F., AKAOKA, H., DE VADDER, F., DUCHAMPT, A. & MITHIEUX, G. 2013. Portal glucose influences the sensory, cortical and reward systems in rats. *Eur J Neurosci,* 38**,** 3476-86.

DHILLO, W. S., SMALL, C. J., STANLEY, S. A., JETHWA, P. H., SEAL, L. J., MURPHY, K. G., GHATEI, M. A. & BLOOM, S. R. 2002. Hypothalamic interactions between neuropeptide Y, agouti-related protein, cocaine- and amphetamine-regulated transcript and alpha-melanocyte-stimulating hormone in vitro in male rats. *J Neuroendocrinol,* 14**,** 725-30.

DOMINGOS, A. I., SORDILLO, A., DIETRICH, M. O., LIU, Z. W., TELLEZ, L. A., VAYNSHTEYN, J., FERREIRA, J. G., EKSTRAND, M. I., HORVATH, T. L., DE ARAUJO, I. E. & FRIEDMAN, J. M. 2013. Hypothalamic melanin concentrating hormone neurons communicate the nutrient value of sugar. *Elife,* 2**,** e01462.

DRUCKER, D. J. 2006. Enhancing the action of incretin hormones: a new whey forward? *Endocrinology,* 147**,** 3171-2.

DUAN, D., LI, Q., KAO, A. W., YUE, Y., PESSIN, J. E. & ENGELHARDT, J. F. 1999. Dynamin is required for recombinant adeno-associated virus type 2 infection. *J Virol,* 73**,** 10371-6.

DUNN-MEYNELL, A. A., ROUTH, V. H., KANG, L., GASPERS, L. & LEVIN, B. E. 2002. Glucokinase is the likely mediator of glucosensing in both glucose-excited and glucose-inhibited central neurons. *Diabetes,* 51**,** 2056-65.

DUNN-MEYNELL, A. A., SANDERS, N. M., COMPTON, D., BECKER, T. C., EIKI, J., ZHANG, B. B. & LEVIN, B. E. 2009. Relationship among brain and blood glucose levels and spontaneous and glucoprivic feeding. *J Neurosci,* 29**,** 7015-22.

EDWARDS, C. M., ABUSNANA, S., SUNTER, D., MURPHY, K. G., GHATEI, M. A. & BLOOM, S. R. 1999. The effect of the orexins on food intake: comparison with neuropeptide Y, melanin-concentrating hormone and galanin. *J Endocrinol,* 160**,** R7-12.

EFEYAN, A., COMB, W. C. & SABATINI, D. M. 2015. Nutrient-sensing mechanisms and pathways. *Nature,* 517**,** 302-10.

EMOND, M., SCHWARTZ, G. J. & MORAN, T. H. 2001. Meal-related stimuli differentially induce c-Fos activation in the nucleus of the solitary tract. *Am J Physiol Regul Integr Comp Physiol,* 280**,** R1315-21.

ERICKSON, J. C., CLEGG, K. E. & PALMITER, R. D. 1996. Sensitivity to leptin and susceptibility to seizures of mice lacking neuropeptide Y. *Nature,* 381**,** 415-21.

EVANS, M. L., MCCRIMMON, R. J., FLANAGAN, D. E., KESHAVARZ, T., FAN, X., MCNAY, E. C., JACOB, R. J. & SHERWIN, R. S. 2004. Hypothalamic ATP-sensitive K + channels play a key role in sensing hypoglycemia and triggering counterregulatory epinephrine and glucagon responses. *Diabetes,* 53**,** 2542-51.

EZQUER, F., NUNEZ, M. T. & ISRAEL, Y. 2005. Antisense gene delivered by an adenoassociated viral vector inhibits iron uptake in human intestinal cells: potential application in hemochromatosis. *Biochem Pharmacol,* 69**,** 1559-66.

FANELLI, C. G., DE FEO, P., PORCELLATI, F., PERRIELLO, G., TORLONE, E., SANTEUSANIO, F., BRUNETTI, P. & BOLLI, G. B. 1992. Adrenergic mechanisms contribute to the late phase of hypoglycemic glucose counterregulation in humans by stimulating lipolysis. *J Clin Invest,* 89**,** 2005-13.

FILIPPI, B. M., BASSIRI, A., ABRAHAM, M. A., DUCA, F. A., YUE, J. T. & LAM, T. K. 2014. Insulin signals through the dorsal vagal complex to regulate energy balance. *Diabetes,* 63**,** 892-9.

FIORAMONTI, X., LORSIGNOL, A., TAUPIGNON, A. & PENICAUD, L. 2004. A new ATP-sensitive K+ channel-independent mechanism is involved in glucose-excited neurons of mouse arcuate nucleus. *Diabetes,* 53**,** 2767-75.

FRIDOLF, T., SUNDLER, F. & AHREN, B. 1992. Pituitary adenylate cyclase-activating polypeptide (PACAP): occurrence in rodent pancreas and effects on insulin and glucagon secretion in the mouse. *Cell Tissue Res,* 269**,** 275-9.

FRIEDMAN, J. M. 2003. A war on obesity, not the obese. *Science,* 299**,** 856-8.
FUNAHASHI, M. & ADACHI, A. 1993. Glucose-responsive neurons exist within the area postrema of the rat: in vitro study on the isolated slice preparation. *Brain Res Bull,* 32**,** 531-5.
GARDINER, J. V., KONG, W. M., WARD, H., MURPHY, K. G., DHILLO, W. S. & BLOOM, S. R. 2005. AAV mediated expression of anti-sense neuropeptide Y cRNA in the arcuate nucleus of rats results in decreased weight gain and food intake. *Biochem Biophys Res Commun,* 327**,** 1088-93.
GARDLIK, R., PALFFY, R., HODOSY, J., LUKACS, J., TURNA, J. & CELEC, P. 2005. Vectors and delivery systems in gene therapy. *Med Sci Monit,* 11**,** 24.
GEERLING, J. C., SHIN, J. W., CHIMENTI, P. C. & LOEWY, A. D. 2010. Paraventricular hypothalamic nucleus: axonal projections to the brainstem. *J Comp Neurol,* 518**,** 1460-99.
GEFEL, D., HENDRICK, G. K., MOJSOV, S., HABENER, J. & WEIR, G. C. 1990. Glucagon-like peptide-I analogs: effects on insulin secretion and adenosine 3',5'-monophosphate formation. *Endocrinology,* 126**,** 2164-8.
GERICH, J. E., LANGLOIS, M., NOACCO, C., KARAM, J. H. & FORSHAM, P. H. 1973. Lack of glucagon response to hypoglycemia in diabetes: evidence for an intrinsic pancreatic alpha cell defect. *Science,* 182**,** 171-3.
GOWARD, C. R., HARTWELL, R., ATKINSON, T. & SCAWEN, M. D. 1986. The purification and characterization of glucokinase from the thermophile Bacillus stearothermophilus. *Biochem J,* 237**,** 415-20.
GREGERSEN, S. & AHREN, B. 1996. Studies on the mechanisms by which gastrin releasing peptide potentiates glucose-induced insulin secretion from mouse islets. *Pancreas,* 12**,** 48-57.
GRIBBLE, F. M., TUCKER, S. J. & ASHCROFT, F. M. 1997. The essential role of the Walker A motifs of SUR1 in K-ATP channel activation by Mg-ADP and diazoxide. *Embo j,* 16**,** 1145-52.
GRILL, H. J. & HAYES, M. R. 2009. The nucleus tractus solitarius: a portal for visceral afferent signal processing, energy status assessment and integration of their combined effects on food intake. *Int J Obes (Lond),* 33 Suppl 1**,** S11-5.
GRIMM, D., KERN, A., PAWLITA, M., FERRARI, F., SAMULSKI, R. & KLEINSCHMIDT, J. 1999. Titration of AAV-2 particles via a novel capsid ELISA: packaging of genomes can limit production of recombinant AAV-2. *Gene Ther,* 6**,** 1322-30.
GROPP, E., SHANABROUGH, M., BOROK, E., XU, A. W., JANOSCHEK, R., BUCH, T., PLUM, L., BALTHASAR, N., HAMPEL, B., WAISMAN, A., BARSH, G. S., HORVATH, T. L. & BRUNING, J. C. 2005. Agouti-related peptide-expressing neurons are mandatory for feeding. *Nat Neurosci,* 8**,** 1289-91.
GRUPE, A., HULTGREN, B., RYAN, A., MA, Y. H., BAUER, M. & STEWART, T. A. 1995. Transgenic knockouts reveal a critical requirement for pancreatic beta cell glucokinase in maintaining glucose homeostasis. *Cell,* 83**,** 69-78.
GUAN, X. 2014. The CNS glucagon-like peptide-2 receptor in the control of energy balance and glucose homeostasis. *Am J Physiol Regul Integr Comp Physiol,* 307**,** 2.
GUAN, X. M., YU, H., TRUMBAUER, M., FRAZIER, E., VAN DER PLOEG, L. H. & CHEN, H. 1998. Induction of neuropeptide Y expression in dorsomedial hypothalamus of diet-induced obese mice. *Neuroreport,* 9**,** 3415-9.
GUILLOD-MAXIMIN, E., LORSIGNOL, A., ALQUIER, T. & PENICAUD, L. 2004. Acute intracarotid glucose injection towards the brain induces specific c-fos activation in hypothalamic nuclei: involvement of astrocytes in cerebral glucose-sensing in rats. *J Neuroendocrinol,* 16**,** 464-71.
HALMOS, K. C., GYARMATI, P., XU, H., MAIMAITI, S., JANCSO, G., BENEDEK, G. & SMITH, B. N. 2015. Molecular and functional changes in glucokinase expression in the brainstem dorsal vagal complex in a murine model of type 1 diabetes. *Neuroscience,* 306**,** 115-122.
HAVEL, P. J., DUNNING, B. E., VERCHERE, C. B., BASKIN, D. G., O'DORISIO, T. & TABORSKY, G. J., JR. 1997. Evidence that vasoactive intestinal polypeptide is a parasympathetic neurotransmitter in the endocrine pancreas in dogs. *Regul Pept,* 71**,** 163-70.

HAYAKAWA, T., KUWAHARA-OTANI, S., MAEDA, S., TANAKA, K. & SEKI, M. 2013. Collateral projections of the dorsal motor nucleus of the vagus nerve to the stomach and the intestines in the rat. *Okajimas Folia Anat Jpn,* 90**,** 7-15.

HAYES, M. R., SKIBICKA, K. P., LEICHNER, T. M., GUARNIERI, D. J., DILEONE, R. J., BENCE, K. K. & GRILL, H. J. 2010. Endogenous leptin signaling in the caudal nucleus tractus solitarius and area postrema is required for energy balance regulation. *Cell Metab,* 11**,** 77-83.

HETHERINGTON, R. 1983. Nutrition Classics. The Anatomical Record, Volume 78, 1940: Hypothalamic lesions and adiposity in the rat. *Nutr Rev,* 41**,** 124-7.

HILL, J. W. 2012. PVN pathways controlling energy homeostasis. *Indian J Endocrinol Metab,* 16**,** S627-36.

HOESS, R. H. & ABREMSKI, K. 1985. Mechanism of strand cleavage and exchange in the Cre-lox site-specific recombination system. *J Mol Biol,* 181**,** 351-62.

HOLST, J. J. & DEACON, C. F. 2005. Glucagon-like peptide-1 mediates the therapeutic actions of DPP-IV inhibitors. *Diabetologia,* 48**,** 612-5.

HOLST, J. J., FAHRENKRUG, J., KNUHTSEN, S., JENSEN, S. L., NIELSEN, O. V., LUNDBERG, J. M. & HOKFELT, T. 1987. VIP and PHI in the pig pancreas: coexistence, corelease, and cooperative effects. *Am J Physiol,* 252**,** G182-9.

HOPKINS, R. J., GIRARDI, L. S. & TURNEY, E. A. 1996. Relationship between Helicobacter pylori eradication and reduced duodenal and gastric ulcer recurrence: a review. *Gastroenterology,* 110**,** 1244-52.

HOWARD, D. B., POWERS, K., WANG, Y. & HARVEY, B. K. 2008. Tropism and toxicity of adeno-associated viral vector serotypes 1, 2, 5, 6, 7, 8, and 9 in rat neurons and glia in vitro. *Virology,* 372**,** 24-34.

HOYDA, T. D. & FERGUSON, A. V. 2010. Adiponectin modulates excitability of rat paraventricular nucleus neurons by differential modulation of potassium currents. *Endocrinology,* 151**,** 3154-62.

HURTADO-CARNEIRO, V., RONCERO, I., BLAZQUEZ, E., ALVAREZ, E. & SANZ, C. 2013. PAS kinase as a nutrient sensor in neuroblastoma and hypothalamic cells required for the normal expression and activity of other cellular nutrient and energy sensors. *Mol Neurobiol,* 48**,** 904-20.

HURTADO-CARNEIRO, V., RONCERO, I., EGGER, S. S., WENGER, R. H., BLAZQUEZ, E., SANZ, C. & ALVAREZ, E. 2014. PAS kinase is a nutrient and energy sensor in hypothalamic areas required for the normal function of AMPK and mTOR/S6K1. *Mol Neurobiol,* 50**,** 314-26.

HUSSAIN, S., RICHARDSON, E., MA, Y., HOLTON, C., DE BACKER, I., BUCKLEY, N., DHILLO, W., BEWICK, G., ZHANG, S., CARLING, D., BLOOM, S. & GARDINER, J. 2015. Glucokinase activity in the arcuate nucleus regulates glucose intake. *J Clin Invest,* 125**,** 337-49.

HUSSAIN, S. S. & BLOOM, S. R. 2011. The pharmacological treatment and management of obesity. *Postgrad Med,* 123**,** 34-44.

IBRAHIM, N., BOSCH, M. A., SMART, J. L., QIU, J., RUBINSTEIN, M., RONNEKLEIV, O. K., LOW, M. J. & KELLY, M. J. 2003. Hypothalamic proopiomelanocortin neurons are glucose responsive and express K(ATP) channels. *Endocrinology,* 144**,** 1331-40.

IMAI, Y., PATEL, H. R., HAWKINS, E. J., DOLIBA, N. M., MATSCHINSKY, F. M. & AHIMA, R. S. 2007. Insulin secretion is increased in pancreatic islets of neuropeptide Y-deficient mice. *Endocrinology,* 148**,** 5716-23.

INAGAKI, N., GONOI, T., CLEMENT, J. P., WANG, C. Z., AGUILAR-BRYAN, L., BRYAN, J. & SEINO, S. 1996. A family of sulfonylurea receptors determines the pharmacological properties of ATP-sensitive K+ channels. *Neuron,* 16**,** 1011-7.

IONESCU, E., ROHNER-JEANRENAUD, F., BERTHOUD, H. R. & JEANRENAUD, B. 1983. Increases in plasma insulin levels in response to electrical stimulation of the dorsal motor nucleus of the vagus nerve. *Endocrinology,* 112**,** 904-10.

IYNEDJIAN, P. B. 2009. Molecular physiology of mammalian glucokinase. *Cell Mol Life Sci,* 66**,** 27-42.

IYNEDJIAN, P. B., PILOT, P. R., NOUSPIKEL, T., MILBURN, J. L., QUAADE, C., HUGHES, S., UCLA, C. & NEWGARD, C. B. 1989. Differential expression and regulation of the glucokinase gene in liver and islets of Langerhans. *Proc Natl Acad Sci U S A,* 86**,** 7838-42.

JAMES, W. P. 2008. The fundamental drivers of the obesity epidemic. *Obes Rev,* 9 Suppl 1**,** 6-13.

JANSEN, A. S., HOFFMAN, J. L. & LOEWY, A. D. 1997. CNS sites involved in sympathetic and parasympathetic control of the pancreas: a viral tracing study. *Brain Res,* 766**,** 29-38.

JETTON, T. L., LIANG, Y., PETTEPHER, C. C., ZIMMERMAN, E. C., COX, F. G., HORVATH, K., MATSCHINSKY, F. M. & MAGNUSON, M. A. 1994. Analysis of upstream glucokinase promoter activity in transgenic mice and identification of glucokinase in rare neuroendocrine cells in the brain and gut. *J Biol Chem,* 269**,** 3641-54.

JOVANOVIC, Z. & YEO, G. S. 2010. Central leptin signalling: beyond the arcuate nucleus. *Auton Neurosci,* 156**,** 8-14.

KAGEYAMA, H., TAKENOYA, F., HIRAKO, S., WADA, N., KINTAKA, Y., INOUE, S., OTA, E., OGAWA, T. & SHIODA, S. 2012. Neuronal circuits involving neuropeptide Y in hypothalamic arcuate nucleus-mediated feeding regulation. *Neuropeptides,* 46**,** 285-9.

KANG, L., DUNN-MEYNELL, A. A., ROUTH, V. H., GASPERS, L. D., NAGATA, Y., NISHIMURA, T., EIKI, J., ZHANG, B. B. & LEVIN, B. E. 2006. Glucokinase is a critical regulator of ventromedial hypothalamic neuronal glucosensing. *Diabetes,* 55**,** 412-20.

KANG, L., ROUTH, V. H., KUZHIKANDATHIL, E. V., GASPERS, L. D. & LEVIN, B. E. 2004. Physiological and molecular characteristics of rat hypothalamic ventromedial nucleus glucosensing neurons. *Diabetes,* 53**,** 549-59.

KANG, L., SANDERS, N. M., DUNN-MEYNELL, A. A., GASPERS, L. D., ROUTH, V. H., THOMAS, A. P. & LEVIN, B. E. 2008. Prior hypoglycemia enhances glucose responsiveness in some ventromedial hypothalamic glucosensing neurons. *Am J Physiol Regul Integr Comp Physiol,* 294**,** R784-92.

KANTOR, B., BAILEY, R. M., WIMBERLY, K., KALBURGI, S. N. & GRAY, S. J. 2014. Methods for gene transfer to the central nervous system. *Adv Genet,* 87**,** 125-97.

KARATAYEV, O., BAYLAN, J. & LEIBOWITZ, S. F. 2009. Increased intake of ethanol and dietary fat in galanin overexpressing mice. *Alcohol,* 43**,** 571-80.

KARSCHIN, C., ECKE, C., ASHCROFT, F. M. & KARSCHIN, A. 1997. Overlapping distribution of K(ATP) channel-forming Kir6.2 subunit and the sulfonylurea receptor SUR1 in rodent brain. *FEBS Lett,* 401**,** 59-64.

KASHIWAKURA, Y., TAMAYOSE, K., IWABUCHI, K., HIRAI, Y., SHIMADA, T., MATSUMOTO, K., NAKAMURA, T., WATANABE, M., OSHIMI, K. & DAIDA, H. 2005. Hepatocyte growth factor receptor is a coreceptor for adeno-associated virus type 2 infection. *J Virol,* 79**,** 609-14.

KASTIN, A. J., AKERSTROM, V. & PAN, W. 2002. Interactions of glucagon-like peptide-1 (GLP-1) with the blood-brain barrier. *J Mol Neurosci,* 18**,** 7-14.

KATSURADA, K., MAEJIMA, Y., NAKATA, M., KODAIRA, M., SUYAMA, S., IWASAKI, Y., KARIO, K. & YADA, T. 2014. Endogenous GLP-1 acts on paraventricular nucleus to suppress feeding: projection from nucleus tractus solitarius and activation of corticotropin-releasing hormone, nesfatin-1 and oxytocin neurons. *Biochem Biophys Res Commun,* 451**,** 276-81.

KATZEN, H. M. & SCHIMKE, R. T. 1965. Multiple forms of hexokinase in the rat: tissue distribution, age dependency, and properties. *Proc Natl Acad Sci U S A,* 54**,** 1218-25.

KHOO, N. K., MO, L., ZHARIKOV, S., KAMGA-PRIDE, C., QUESNELLE, K., GOLIN-BISELLO, F., LI, L., WANG, Y. & SHIVA, S. 2014. Nitrite augments glucose uptake in adipocytes through the protein kinase A-dependent stimulation of mitochondrial fusion. *Free Radic Biol Med,* 70**,** 45-53.

KIM, E. R., WU, Z., SUN, H., XU, Y., MANGIERI, L. R. & TONG, Q. 2015. Hypothalamic Non-AgRP, Non-POMC GABAergic Neurons Are Required for Postweaning Feeding and NPY Hyperphagia. *J Neurosci,* 35**,** 10440-50.

KLEIN, R., RUTTKOWSKI, B., KNAPP, E., SALMONS, B., GUNZBURG, W. H. & HOHENADL, C. 2006. WPRE-mediated enhancement of gene expression is promoter and cell line specific. *Gene,* 372**,** 153-61.

KLEIN, R. L., MUIR, D., KING, M. A., PEEL, A. L., ZOLOTUKHIN, S., MOLLER, J. C., KRUTTGEN, A., HEYMACH, J. V., JR., MUZYCZKA, N. & MEYER, E. M. 1999. Long-term actions of vector-derived nerve growth factor or brain-derived neurotrophic factor on choline acetyltransferase and Trk receptor levels in the adult rat basal forebrain. *Neuroscience,* 90**,** 815-21.

KNUHTSEN, S., HOLST, J. J., SCHWARTZ, T. W., JENSEN, S. L. & NIELSEN, O. V. 1987. The effect of gastrin-releasing peptide on the endocrine pancreas. *Regul Pept,* 17**,** 269-76.

KOEHLER-STEC, E. M., LI, K., MAHER, F., VANNUCCI, S. J., SMITH, C. B. & SIMPSON, I. A. 2000. Cerebral glucose utilization and glucose transporter expression: response to water deprivation and restoration. *J Cereb Blood Flow Metab,* 20**,** 192-200.

KONNER, A. C., KLOCKENER, T. & BRUNING, J. C. 2009. Control of energy homeostasis by insulin and leptin: targeting the arcuate nucleus and beyond. *Physiol Behav,* 97**,** 632-8.

KREYMANN, B., WILLIAMS, G., GHATEI, M. A. & BLOOM, S. R. 1987. Glucagon-like peptide-1 7-36: a physiological incretin in man. *Lancet,* 2**,** 1300-4.

KRISKY, D. M., MARCONI, P. C., OLIGINO, T. J., ROUSE, R. J., FINK, D. J., COHEN, J. B., WATKINS, S. C. & GLORIOSO, J. C. 1998. Development of herpes simplex virus replication-defective multigene vectors for combination gene therapy applications. *Gene Ther,* 5**,** 1517-30.

KURATA, K., FUJIMOTO, K., SAKATA, T., ETOU, H. & FUKAGAWA, K. 1986. D-glucose suppression of eating after intra-third ventricle infusion in rat. *Physiol Behav,* 37**,** 615-20.

KURITA, H., XU, K. Y., MAEJIMA, Y., NAKATA, M., DEZAKI, K., SANTOSO, P., YANG, Y., ARAI, T., GANTULGA, D., MUROYA, S., LEFOR, A. K., KAKEI, M., WATANABE, E. & YADA, T. 2015. Arcuate Na+,K+-ATPase senses systemic energy states and regulates feeding behavior through glucose-inhibited neurons. *Am J Physiol Endocrinol Metab,* 309**,** E320-33.

KYRKOULI, S. E., STRUBBE, J. H. & SCHEURINK, A. J. 2006. Galanin in the PVN increases nutrient intake and changes peripheral hormone levels in the rat. *Physiol Behav,* 89**,** 103-9.

LAM, A. P. & DEAN, D. A. 2010. Progress and prospects: nuclear import of nonviral vectors. *Gene Ther,* 17**,** 439-47.

LAM, C. K., CHARI, M. & LAM, T. K. 2009. CNS regulation of glucose homeostasis. *Physiology (Bethesda),* 24**,** 159-70.

LAM, C. K., CHARI, M., RUTTER, G. A. & LAM, T. K. 2011. Hypothalamic nutrient sensing activates a forebrain-hindbrain neuronal circuit to regulate glucose production in vivo. *Diabetes,* 60**,** 107-13.

LAMY, C. M., SANNO, H., LABOUEBE, G., PICARD, A., MAGNAN, C., CHATTON, J. Y. & THORENS, B. 2014. Hypoglycemia-activated GLUT2 neurons of the nucleus tractus solitarius stimulate vagal activity and glucagon secretion. *Cell Metab,* 19**,** 527-38.

LANGLET, F., MULLIER, A., BOURET, S. G., PREVOT, V. & DEHOUCK, B. 2013. Tanycyte-like cells form a blood-cerebrospinal fluid barrier in the circumventricular organs of the mouse brain. *J Comp Neurol,* 521**,** 3389-405.

LARSEN, P. J. & HOLST, J. J. 2005. Glucagon-related peptide 1 (GLP-1): hormone and neurotransmitter. *Regul Pept,* 128**,** 97-107.

LARSEN, P. J., SEIER, V., FINK-JENSEN, A., HOLST, J. J., WARBERG, J. & VRANG, N. 2003. Cocaine- and amphetamine-regulated transcript is present in hypothalamic neuroendocrine neurones and is released to the hypothalamic-pituitary portal circuit. *J Neuroendocrinol,* 15**,** 219-26.

LARSEN, P. J., VRANG, N., PETERSEN, P. C. & KRISTENSEN, P. 2000. Chronic intracerebroventricular administration of recombinant CART(42-89) peptide inhibits and causes weight loss in lean and obese Zucker (fa/fa) rats. *Obes Res,* 8**,** 590-6.

LAUGHTON, W. B. & POWLEY, T. L. 1987. Localization of efferent function in the dorsal motor nucleus of the vagus. *Am J Physiol,* 252**,** R13-25.

LEIBOWITZ, S. F. & WORTLEY, K. E. 2004. Hypothalamic control of energy balance: different peptides, different functions. *Peptides,* 25**,** 473-504.
LEINO, R. L., GERHART, D. Z., VAN BUEREN, A. M., MCCALL, A. L. & DREWES, L. R. 1997. Ultrastructural localization of GLUT 1 and GLUT 3 glucose transporters in rat brain. *J Neurosci Res,* 49**,** 617-26.
LELOUP, C., OROSCO, M., SERRADAS, P., NICOLAIDIS, S. & PENICAUD, L. 1998. Specific inhibition of GLUT2 in arcuate nucleus by antisense oligonucleotides suppresses nervous control of insulin secretion. *Brain Res Mol Brain Res,* 57**,** 275-80.
LENGLOS, C., MITRA, A., GUEVREMONT, G. & TIMOFEEVA, E. 2014. Regulation of expression of relaxin-3 and its receptor RXFP3 in the brain of diet-induced obese rats. *Neuropeptides,* 48**,** 119-32.
LENTZ, T. B., GRAY, S. J. & SAMULSKI, R. J. 2012. Viral vectors for gene delivery to the central nervous system. *Neurobiol Dis,* 48**,** 179-88.
LEONE, P., SHERA, D., MCPHEE, S. W., FRANCIS, J. S., KOLODNY, E. H., BILANIUK, L. T., WANG, D. J., ASSADI, M., GOLDFARB, O., GOLDMAN, H. W., FREESE, A., YOUNG, D., DURING, M. J., SAMULSKI, R. J. & JANSON, C. G. 2012. Long-term follow-up after gene therapy for canavan disease. *Sci Transl Med,* 4**,** 165ra163.
LEROITH, D. 2002. Beta-cell dysfunction and insulin resistance in type 2 diabetes: role of metabolic and genetic abnormalities. *Am J Med,* 113 Suppl 6A**,** 3s-11s.
LEVIN, B. E. 2006. Metabolic sensing neurons and the control of energy homeostasis. *Physiol Behav,* 89**,** 486-9.
LEVIN, B. E., BECKER, T. C., EIKI, J., ZHANG, B. B. & DUNN-MEYNELL, A. A. 2008. Ventromedial hypothalamic glucokinase is an important mediator of the counterregulatory response to insulin-induced hypoglycemia. *Diabetes,* 57**,** 1371-9.
LEVIN, B. E. & DUNN-MEYNELL, A. A. 1997. In vivo and in vitro regulation of [3H]glyburide binding to brain sulfonylurea receptors in obesity-prone and resistant rats by glucose. *Brain Res,* 776**,** 146-53.
LEVIN, B. E., ROUTH, V. H., KANG, L., SANDERS, N. M. & DUNN-MEYNELL, A. A. 2004. Neuronal glucosensing: what do we know after 50 years? *Diabetes,* 53**,** 2521-8.
LI, B., XI, X., ROANE, D. S., RYAN, D. H. & MARTIN, R. J. 2003. Distribution of glucokinase, glucose transporter GLUT2, sulfonylurea receptor-1, glucagon-like peptide-1 receptor and neuropeptide Y messenger RNAs in rat brain by quantitative real time RT-PCR. *Brain Res Mol Brain Res,* 113**,** 139-42.
LI, D. P., CHEN, S. R. & PAN, H. L. 2010. Adenosine inhibits paraventricular pre-sympathetic neurons through ATP-dependent potassium channels. *J Neurochem,* 113**,** 530-42.
LI, T. T., ZHANG, J. F., FEI, S. J., ZHU, S. P., ZHU, J. Z., QIAO, X. & LIU, Z. B. 2014. Glutamate microinjection into the hypothalamic paraventricular nucleus attenuates ulcerative colitis in rats. *Acta Pharmacol Sin,* 35**,** 185-94.
LOEWY, A. D. & HAXHIU, M. A. 1993. CNS cell groups projecting to pancreatic parasympathetic preganglionic neurons. *Brain Res,* 620**,** 323-30.
LOVE, J. A., YI, E. & SMITH, T. G. 2007. Autonomic pathways regulating pancreatic exocrine secretion. *Auton Neurosci,* 133**,** 19-34.
LUQUET, S., PEREZ, F. A., HNASKO, T. S. & PALMITER, R. D. 2005. NPY/AgRP neurons are essential for feeding in adult mice but can be ablated in neonates. *Science,* 310**,** 683-5.
LYNCH, R. M., TOMPKINS, L. S., BROOKS, H. L., DUNN-MEYNELL, A. A. & LEVIN, B. E. 2000. Localization of glucokinase gene expression in the rat brain. *Diabetes,* 49**,** 693-700.
MAEKAWA, F., TOYODA, Y., TORII, N., MIWA, I., THOMPSON, R. C., FOSTER, D. L., TSUKAHARA, S., TSUKAMURA, H. & MAEDA, K. 2000. Localization of glucokinase-like immunoreactivity in the rat lower brain stem: for possible location of brain glucose-sensing mechanisms. *Endocrinology,* 141**,** 375-84.

MAGNUSON, M. A. & SHELTON, K. D. 1989. An alternate promoter in the glucokinase gene is active in the pancreatic beta cell. *J Biol Chem,* 264**,** 15936-42.
MARANON, R., LIMA, R., SPRADLEY, F. T., DO CARMO, J. M., ZHANG, H., SMITH, A. D., BUI, E., THOMAS, R. L., MOULANA, M., HALL, J. E., GRANGER, J. P. & RECKELHOFF, J. F. 2015. Roles for the sympathetic nervous system, renal nerves, and CNS melanocortin-4 receptor in the elevated blood pressure in hyperandrogenemic female rats. *Am J Physiol Regul Integr Comp Physiol,* 308**,** R708-13.
MASSA, M. L., GAGLIARDINO, J. J. & FRANCINI, F. 2011. Liver glucokinase: An overview on the regulatory mechanisms of its activity. *IUBMB Life,* 63**,** 1-6.
MATSCHINSKY, F. M., MAGNUSON, M. A., ZELENT, D., JETTON, T. L., DOLIBA, N., HAN, Y., TAUB, R. & GRIMSBY, J. 2006. The network of glucokinase-expressing cells in glucose homeostasis and the potential of glucokinase activators for diabetes therapy. *Diabetes,* 55**,** 1-12.
MAYER, J. 1953. Glucostatic mechanism of regulation of food intake. *N Engl J Med,* 249**,** 13-6.
MAYER, J. 1955. Regulation of energy intake and the body weight: the glucostatic theory and the lipostatic hypothesis. *Ann N Y Acad Sci,* 63**,** 15-43.
MAYER, S. E., MAYFIELD, A. C. & HAAS, J. A. 1966. Heart muscle hexokinase: subcellular distribution and inhibition by glucose 6-phosphate. *Mol Pharmacol,* 2**,** 393-405.
MCCRIMMON, R. 2008. The mechanisms that underlie glucose sensing during hypoglycaemia in diabetes. *Diabet Med,* 25**,** 513-22.
MCCRIMMON, R. J., EVANS, M. L., FAN, X., MCNAY, E. C., CHAN, O., DING, Y., ZHU, W., GRAM, D. X. & SHERWIN, R. S. 2005. Activation of ATP-sensitive K+ channels in the ventromedial hypothalamus amplifies counterregulatory hormone responses to hypoglycemia in normal and recurrently hypoglycemic rats. *Diabetes,* 54**,** 3169-74.
MCCRIMMON, R. J., FAN, X., CHENG, H., MCNAY, E., CHAN, O., SHAW, M., DING, Y., ZHU, W. & SHERWIN, R. S. 2006. Activation of AMP-activated protein kinase within the ventromedial hypothalamus amplifies counterregulatory hormone responses in rats with defective counterregulation. *Diabetes,* 55**,** 1755-60.
MCCRIMMON, R. J. & SHERWIN, R. S. 2010. Hypoglycemia in type 1 diabetes. *Diabetes,* 59**,** 2333-9.
MELNICK, I. V., PRICE, C. J. & COLMERS, W. F. 2011. Glucosensing in parvocellular neurons of the rat hypothalamic paraventricular nucleus. *Eur J Neurosci,* 34**,** 272-82.
MERCER, R. E., CHEE, M. J. & COLMERS, W. F. 2011. The role of NPY in hypothalamic mediated food intake. *Front Neuroendocrinol,* 32**,** 398-415.
MICHAEL, M. D., KULKARNI, R. N., POSTIC, C., PREVIS, S. F., SHULMAN, G. I., MAGNUSON, M. A. & KAHN, C. R. 2000. Loss of insulin signaling in hepatocytes leads to severe insulin resistance and progressive hepatic dysfunction. *Mol Cell,* 6**,** 87-97.
MIKI, T., LISS, B., MINAMI, K., SHIUCHI, T., SARAYA, A., KASHIMA, Y., HORIUCHI, M., ASHCROFT, F., MINOKOSHI, Y., ROEPER, J. & SEINO, S. 2001. ATP-sensitive K+ channels in the hypothalamus are essential for the maintenance of glucose homeostasis. *Nat Neurosci,* 4**,** 507-12.
MINOR, R. K., CHANG, J. W. & DE CABO, R. 2009. Hungry for life: How the arcuate nucleus and neuropeptide Y may play a critical role in mediating the benefits of calorie restriction. *Mol Cell Endocrinol,* 299**,** 79-88.
MISELIS, R. R. & EPSTEIN, A. N. 1975. Feeding induced by intracerebroventricular 2-deoxy-D-glucose in the rat. *Am J Physiol,* 229**,** 1438-47.
MIWA, I., MITA, Y., MURATA, T., OKUDA, J., SUGIURA, M., HAMADA, Y. & CHIBA, T. 1994. Utility of 3-O-methyl-N-acetyl-D-glucosamine, an N-acetylglucosamine kinase inhibitor, for accurate assay of glucokinase in pancreatic islets and liver. *Enzyme Protein,* 48**,** 135-42.
MONROE, A. T., REDDY, S. C. & PEDDADA, A. V. 2014. Dorsal vagal complex of the brainstem: conformal avoidance to reduce nausea. *Pract Radiat Oncol,* 4**,** 267-71.
MONTERO, S., CUELLAR, R., LEMUS, M., AVALOS, R., RAMIREZ, G. & DE ALVAREZ-BUYLLA, E. R. 2012. Brain-derived neurotrophic factor in the nucleus tractus solitarii modulates glucose homeostasis after carotid chemoreceptor stimulation in rats. *Adv Exp Med Biol,* 758**,** 233-9.

MORIGUCHI, T., SAKURAI, T., NAMBU, T., YANAGISAWA, M. & GOTO, K. 1999. Neurons containing orexin in the lateral hypothalamic area of the adult rat brain are activated by insulin-induced acute hypoglycemia. *Neurosci Lett,* 264**,** 101-4.

MORITA, S. & MIYATA, S. 2013. Accessibility of low-molecular-mass molecules to the median eminence and arcuate hypothalamic nucleus of adult mouse. *Cell Biochem Funct,* 31**,** 668-77.

MORRISH, N. J., WANG, S. L., STEVENS, L. K., FULLER, J. H. & KEEN, H. 2001. Mortality and causes of death in the WHO Multinational Study of Vascular Disease in Diabetes. *Diabetologia,* 44 Suppl 2**,** S14-21.

MORRISON, S. F. 2016. Central control of body temperature. *F1000Res,* 5.

MOUNTJOY, P. D. & RUTTER, G. A. 2007. Glucose sensing by hypothalamic neurones and pancreatic islet cells: AMPle evidence for common mechanisms? *Exp Physiol,* 92**,** 311-9.

MUECKLER, M. & THORENS, B. 2013. The SLC2 (GLUT) family of membrane transporters. *Mol Aspects Med,* 34**,** 121-38.

MUROYA, S., YADA, T., SHIODA, S. & TAKIGAWA, M. 1999. Glucose-sensitive neurons in the rat arcuate nucleus contain neuropeptide Y. *Neurosci Lett,* 264**,** 113-6.

MURPHY, B. A., FAKIRA, K. A., SONG, Z., BEUVE, A. & ROUTH, V. H. 2009. AMP-activated protein kinase and nitric oxide regulate the glucose sensitivity of ventromedial hypothalamic glucose-inhibited neurons. *Am J Physiol Cell Physiol,* 297**,** C750-8.

MURUVE, D. A. 2004. The innate immune response to adenovirus vectors. *Hum Gene Ther,* 15**,** 1157-66.

MUSSA, B. M., SARTOR, D. M., RANTZAU, C. & VERBERNE, A. J. 2011. Effects of nitric oxide synthase blockade on dorsal vagal stimulation-induced pancreatic insulin secretion. *Brain Res,* 7**,** 62-70.

MUSSA, B. M. & VERBERNE, A. J. 2008. Activation of the dorsal vagal nucleus increases pancreatic exocrine secretion in the rat. *Neurosci Lett,* 433**,** 71-6.

N'GUYEN, J. M., MAGNAN, C., LAURY, M. C., THIBAULT, C., LEVETEAU, J., GILBERT, M., PENICAUD, L. & KTORZA, A. 1994. Involvement of the autonomic nervous system in the in vivo memory to glucose of pancreatic beta cell in rats. *J Clin Invest,* 94**,** 1456-62.

NAKAGAWA, A., SATAKE, H., NAKABAYASHI, H., NISHIZAWA, M., FURUYA, K., NAKANO, S., KIGOSHI, T., NAKAYAMA, K. & UCHIDA, K. 2004. Receptor gene expression of glucagon-like peptide-1, but not glucose-dependent insulinotropic polypeptide, in rat nodose ganglion cells. *Auton Neurosci,* 110**,** 36-43.

NAKAGAWA, T., OGAWA, Y., EBIHARA, K., YAMANAKA, M., TSUCHIDA, A., TAIJI, M., NOGUCHI, H. & NAKAO, K. 2003. Anti-obesity and anti-diabetic effects of brain-derived neurotrophic factor in rodent models of leptin resistance. *Int J Obes Relat Metab Disord,* 27**,** 557-65.

NAVARRO, M., RODRIQUEZ DE FONSECA, F., ALVAREZ, E., CHOWEN, J. A., ZUECO, J. A., GOMEZ, R., ENG, J. & BLAZQUEZ, E. 1996. Colocalization of glucagon-like peptide-1 (GLP-1) receptors, glucose transporter GLUT-2, and glucokinase mRNAs in rat hypothalamic cells: evidence for a role of GLP-1 receptor agonists as an inhibitory signal for food and water intake. *J Neurochem,* 67**,** 1982-91.

NISHI, S., SEINO, Y., ISHIDA, H., SENO, M., TAMINATO, T., SAKURAI, H. & IMURA, H. 1987. Vagal regulation of insulin, glucagon, and somatostatin secretion in vitro in the rat. *J Clin Invest,* 79**,** 1191-6.

NISHIO, T., TOYODA, Y., HIRAMATSU, M., CHIBA, T. & MIWA, I. 2006. Decline in glucokinase activity in the arcuate nucleus of streptozotocin-induced diabetic rats. *Biol Pharm Bull,* 29**,** 216-9.

NOGUCHI, R., KUBOTA, H., YUGI, K., TOYOSHIMA, Y., KOMORI, Y., SOGA, T. & KURODA, S. 2013. The selective control of glycolysis, gluconeogenesis and glycogenesis by temporal insulin patterns. *Mol Syst Biol,* 9**,** 664.

NOWAK, A. & BOJANOWSKA, E. 2008. Effects of peripheral or central GLP-1 receptor blockade on leptin-induced suppression of appetite. *J Physiol Pharmacol,* 59**,** 501-10.

O'MALLEY, D., REIMANN, F., SIMPSON, A. K. & GRIBBLE, F. M. 2006. Sodium-coupled glucose cotransporters contribute to hypothalamic glucose sensing. *Diabetes,* 55**,** 3381-6.

ODORIZZI, M., FERNETTE, B., ANGEL, E., BURLET, C., TANKOSIC, P. & BURLET, A. 2002. Galanin receptor antagonists decrease fat preference in Brattleboro rat. *Neuropharmacology,* 42**,** 134-41.

OGUNNOWO-BADA, E. O., HEELEY, N., BROCHARD, L. & EVANS, M. L. 2014. Brain glucose sensing, glucokinase and neural control of metabolism and islet function. *Diabetes Obes Metab,* 16 Suppl 1**,** 26-32.

OH, S. W., HARRIS, J. A., NG, L., WINSLOW, B., CAIN, N., MIHALAS, S., WANG, Q., LAU, C., KUAN, L., HENRY, A. M., MORTRUD, M. T., OUELLETTE, B., NGUYEN, T. N., SORENSEN, S. A., SLAUGHTERBECK, C. R., WAKEMAN, W., LI, Y., FENG, D., HO, A., NICHOLAS, E., HIROKAWA, K. E., BOHN, P., JOINES, K. M., PENG, H., HAWRYLYCZ, M. J., PHILLIPS, J. W., HOHMANN, J. G., WOHNOUTKA, P., GERFEN, C. R., KOCH, C., BERNARD, A., DANG, C., JONES, A. R. & ZENG, H. 2014. A mesoscale connectome of the mouse brain. *Nature,* 508**,** 207-14.

OOSTERVEER, M. H. & SCHOONJANS, K. 2014. Hepatic glucose sensing and integrative pathways in the liver. *Cell Mol Life Sci,* 71**,** 1453-67.

ORBAN, P. C., CHUI, D. & MARTH, J. D. 1992. Tissue- and site-specific DNA recombination in transgenic mice. *Proc Natl Acad Sci U S A,* 89**,** 6861-5.

OSBAK, K. K., COLCLOUGH, K., SAINT-MARTIN, C., BEER, N. L., BELLANNE-CHANTELOT, C., ELLARD, S. & GLOYN, A. L. 2009. Update on mutations in glucokinase (GCK), which cause maturity-onset diabetes of the young, permanent neonatal diabetes, and hyperinsulinemic hypoglycemia. *Hum Mutat,* 30**,** 1512-26.

OSUNDIJI, M. A., LAM, D. D., SHAW, J., YUEH, C. Y., MARKKULA, S. P., HURST, P., COLLIVA, C., RODA, A., HEISLER, L. K. & EVANS, M. L. 2012. Brain glucose sensors play a significant role in the regulation of pancreatic glucose-stimulated insulin secretion. *Diabetes,* 61**,** 321-8.

OSUNDIJI, M. A., ZHOU, L., SHAW, J., MOORE, S. P., YUEH, C. Y., SHERWIN, R., HEISLER, L. K. & EVANS, M. L. 2010. Brain glucosamine boosts protective glucoprivic feeding. *Endocrinology,* 151**,** 1499-508.

PAGE, K. A., SEO, D., BELFORT-DEAGUIAR, R., LACADIE, C., DZUIRA, J., NAIK, S., AMARNATH, S., CONSTABLE, R. T., SHERWIN, R. S. & SINHA, R. 2011. Circulating glucose levels modulate neural control of desire for high-calorie foods in humans. *J Clin Invest,* 121**,** 4161-9.

PANKSEPP, J. & ROSSI, J., 3RD 1981. D-glucose infusions into the basal ventromedial hypothalamus and feeding. *Behav Brain Res,* 3**,** 381-92.

PAPASTAMATAKI, M., PAPASSOTIRIOU, I., BARTZELIOTOU, A., VAZEOU, A., ROMA, E., CHROUSOS, G. P. & KANAKA-GANTENBEIN, C. 2014. Incretins, amylin and other gut-brain axis hormones in children with coeliac disease. *Eur J Clin Invest,* 44**,** 74-82.

PARK, Y. B., CHOI, Y. J., PARK, S. Y., KIM, J. Y., KIM, S. H., SONG, D. K., WON, K. C. & KIM, Y. W. 2011. ATP-Sensitive Potassium Channel-Deficient Mice Show Hyperphagia but Are Resistant to Obesity. *Diabetes Metab J,* 35**,** 219-25.

PARTON, L. E., YE, C. P., COPPARI, R., ENRIORI, P. J., CHOI, B., ZHANG, C. Y., XU, C., VIANNA, C. R., BALTHASAR, N., LEE, C. E., ELMQUIST, J. K., COWLEY, M. A. & LOWELL, B. B. 2007. Glucose sensing by POMC neurons regulates glucose homeostasis and is impaired in obesity. *Nature,* 449**,** 228-32.

PERUZZO, B., PASTOR, F. E., BLAZQUEZ, J. L., SCHOBITZ, K., PELAEZ, B., AMAT, P. & RODRIGUEZ, E. M. 2000. A second look at the barriers of the medial basal hypothalamus. *Exp Brain Res,* 132**,** 10-26.

PLAMBOECK, A., VEEDFALD, S., DEACON, C. F., HARTMANN, B., VILSBOLL, T., KNOP, F. K. & HOLST, J. J. 2015. The role of efferent cholinergic transmission for the insulinotropic and glucagonostatic effects of GLP-1. *Am J Physiol Regul Integr Comp Physiol,* 309**,** R544-51.

POCAI, A., OBICI, S., SCHWARTZ, G. J. & ROSSETTI, L. 2005. A brain-liver circuit regulates glucose homeostasis. *Cell Metab,* 1**,** 53-61.

POLAKOF, S., RODRIGUEZ-ALONSO, M. & SOENGAS, J. L. 2009. Immunohistochemical localization of glucokinase in rainbow trout brain. *Comp Biochem Physiol A Mol Integr Physiol,* 153**,** 352-8.
PONNAZHAGAN, S., MUKHERJEE, P., YODER, M. C., WANG, X. S., ZHOU, S. Z., KAPLAN, J., WADSWORTH, S. & SRIVASTAVA, A. 1997. Adeno-associated virus 2-mediated gene transfer in vivo: organ-tropism and expression of transduced sequences in mice. *Gene,* 190**,** 203-10.
POWLEY, T. L. & PRECHTL, J. C. 1986. Gold thioglucose selectively damages dorsal vagal nuclei. *Brain Res,* 367**,** 192-200.
PRINTZ, R. L., MAGNUSON, M. A. & GRANNER, D. K. 1993. Mammalian glucokinase. *Annu Rev Nutr,* 13**,** 463-96.
QIAN, S., CHEN, H., WEINGARTH, D., TRUMBAUER, M. E., NOVI, D. E., GUAN, X., YU, H., SHEN, Z., FENG, Y., FRAZIER, E., CHEN, A., CAMACHO, R. E., SHEARMAN, L. P., GOPAL-TRUTER, S., MACNEIL, D. J., VAN DER PLOEG, L. H. & MARSH, D. J. 2002. Neither agouti-related protein nor neuropeptide Y is critically required for the regulation of energy homeostasis in mice. *Mol Cell Biol,* 22**,** 5027-35.
QIAO, W., YANG, L., LI, X. Y., CAO, N., WANG, W. Z., CHAI, C. & LU, Y. 2011. The cardiovascular inhibition functions of hydrogen sulfide within the nucleus tractus solitarii are mediated by the activation of KATP channels and glutamate receptors mechanisms. *Pharmazie,* 66**,** 287-92.
QING, K., MAH, C., HANSEN, J., ZHOU, S., DWARKI, V. & SRIVASTAVA, A. 1999. Human fibroblast growth factor receptor 1 is a co-receptor for infection by adeno-associated virus 2. *Nat Med,* 5**,** 71-7.
RAVIER, M. A., RUTTER, G.A. 2010. Isolation and Culture of Mouse Pancreatic Islets for Ex Vivo Imaging Studies with Trappable or Recombinant Fluorescent Probes. *Methods in Molecular Biology***,** 171-184.
REMEDI, M. S., KOSTER, J. C., PATTON, B. L. & NICHOLS, C. G. 2005. ATP-sensitive K+ channel signaling in glucokinase-deficient diabetes. *Diabetes,* 54**,** 2925-31.
RIEDIGER, T., SCHMID, H. A., LUTZ, T. A. & SIMON, E. 2002. Amylin and glucose co-activate area postrema neurons of the rat. *Neurosci Lett,* 328**,** 121-4.
RINAMAN, L. 2010. Ascending projections from the caudal visceral nucleus of the solitary tract to brain regions involved in food intake and energy expenditure. *Brain Res,* 1350**,** 18-34.
RINAMAN, L. & MISELIS, R. R. 1987. The organization of vagal innervation of rat pancreas using cholera toxin-horseradish peroxidase conjugate. *J Auton Nerv Syst,* 21**,** 109-25.
RITTER, S., DINH, T. T. & ZHANG, Y. 2000. Localization of hindbrain glucoreceptive sites controlling food intake and blood glucose. *Brain Res,* 856**,** 37-47.
RITTER, S. & STONE, S. L. 1987. Area postrema lesions block feeding induced by systemic injections of monosodium glutamate. *Physiol Behav,* 41**,** 21-4.
RITTER, S. & TAYLOR, J. S. 1990. Vagal sensory neurons are required for lipoprivic but not glucoprivic feeding in rats. *Am J Physiol,* 258**,** R1395-401.
ROBERTS, D. J. & MIYAMOTO, S. 2015. Hexokinase II integrates energy metabolism and cellular protection: Akting on mitochondria and TORCing to autophagy. *Cell Death Differ,* 22**,** 248-57.
ROCCA, A. S. & BRUBAKER, P. L. 1999. Role of the vagus nerve in mediating proximal nutrient-induced glucagon-like peptide-1 secretion. *Endocrinology,* 140**,** 1687-94.
ROE, T., REYNOLDS, T. C., YU, G. & BROWN, P. O. 1993. Integration of murine leukemia virus DNA depends on mitosis. *Embo j,* 12**,** 2099-108.
ROGERS, R. C. & HERMANN, G. E. 1985. Gastric-vagal solitary neurons excited by paraventricular nucleus microstimulation. *J Auton Nerv Syst,* 14**,** 351-62.
ROJAS, J. M. & SCHWARTZ, M. W. 2014. Control of hepatic glucose metabolism by islet and brain. *Diabetes Obes Metab,* 16 Suppl 1**,** 33-40.
RONCERO, I., ALVAREZ, E., CHOWEN, J. A., SANZ, C., RABANO, A., VAZQUEZ, P. & BLAZQUEZ, E. 2004. Expression of glucose transporter isoform GLUT-2 and glucokinase genes in human brain. *J Neurochem,* 88**,** 1203-10.

RONCERO, I., ALVAREZ, E., VAZQUEZ, P. & BLAZQUEZ, E. 2000. Functional glucokinase isoforms are expressed in rat brain. *J Neurochem,* 74**,** 1848-57.
RONCERO, I., SANZ, C., ALVAREZ, E., VAZQUEZ, P., BARRIO, P. A. & BLAZQUEZ, E. 2009. Glucokinase and glucokinase regulatory proteins are functionally coexpressed before birth in the rat brain. *J Neuroendocrinol,* 21**,** 973-81.
ROUTH, V. H. 2002. Glucose-sensing neurons: are they physiologically relevant? *Physiol Behav,* 76**,** 403-13.
SAINSBURY, A. & ZHANG, L. 2010. Role of the arcuate nucleus of the hypothalamus in regulation of body weight during energy deficit. *Mol Cell Endocrinol,* 316**,** 109-19.
SAKURAZAWA, N., MANO-OTAGIRI, A., NEMOTO, T. & SHIBASAKI, T. 2013. Effects of intracerebroventricular ghrelin on food intake and Fos expression in the arcuate nucleus of the hypothalamus in female rats vary with estrous cycle phase. *Neurosci Lett,* 541**,** 204-8.
SALGADO, M., TARIFENO-SALDIVIA, E., ORDENES, P., MILLAN, C., YANEZ, M. J., LLANOS, P., VILLAGRA, M., ELIZONDO-VEGA, R., MARTINEZ, F., NUALART, F., URIBE, E. & DE LOS ANGELES GARCIA-ROBLES, M. 2014. Dynamic localization of glucokinase and its regulatory protein in hypothalamic tanycytes. *PLoS One,* 9**,** e94035.
SAM, A. H., TROKE, R. C., TAN, T. M. & BEWICK, G. A. 2012. The role of the gut/brain axis in modulating food intake. *Neuropharmacology,* 63**,** 46-56.
SAMBROOK J., F. E. F., MANIATIS T. 1989. *Molecular Cloning. A Laboratory Manual,* Cold Spring Harbor, NY, Cold Spring Harbor Laboratory Press.
SANDERS, N. M., DUNN-MEYNELL, A. A. & LEVIN, B. E. 2004. Third ventricular alloxan reversibly impairs glucose counterregulatory responses. *Diabetes,* 53**,** 1230-6.
SANLIOGLU, S., BENSON, P. K., YANG, J., ATKINSON, E. M., REYNOLDS, T. & ENGELHARDT, J. F. 2000. Endocytosis and nuclear trafficking of adeno-associated virus type 2 are controlled by rac1 and phosphatidylinositol-3 kinase activation. *J Virol,* 74**,** 9184-96.
SANZ, C., RONCERO, I., VAZQUEZ, P., NAVAS, M. A. & BLAZQUEZ, E. 2007. Effects of glucose and insulin on glucokinase activity in rat hypothalamus. *J Endocrinol,* 193**,** 259-67.
SAWCHENKO, P. E. & SWANSON, L. W. 1985. Localization, colocalization, and plasticity of corticotropin-releasing factor immunoreactivity in rat brain. *Fed Proc,* 44**,** 221-7.
SCARLETT, J. M. & SCHWARTZ, M. W. 2015. Gut-brain mechanisms controlling glucose homeostasis. *F1000Prime Rep,* 7**,** 12.
SCHNEEBERGER, M., GOMIS, R. & CLARET, M. 2014. Hypothalamic and brainstem neuronal circuits controlling homeostatic energy balance. *J Endocrinol,* 220**,** T25-46.
SCHRODER, E. A., BURGESS, D. E., MANNING, C. L., ZHAO, Y., MOSS, A. J., PATWARDHAN, A., ELAYI, C. S., ESSER, K. A. & DELISLE, B. P. 2014. Light phase-restricted feeding slows basal heart rate to exaggerate the type-3 long QT syndrome phenotype in mice. *Am J Physiol Heart Circ Physiol,* 307**,** H1777-85.
SCHUIT, F. C., HUYPENS, P., HEIMBERG, H. & PIPELEERS, D. G. 2001. Glucose sensing in pancreatic beta-cells: a model for the study of other glucose-regulated cells in gut, pancreas, and hypothalamus. *Diabetes,* 50**,** 1-11.
SCOTT, M. M., WILLIAMS, K. W., ROSSI, J., LEE, C. E. & ELMQUIST, J. K. 2011. Leptin receptor expression in hindbrain Glp-1 neurons regulates food intake and energy balance in mice. *J Clin Invest,* 121**,** 2413-21.
SEINO, S. & MIKI, T. 2003. Physiological and pathophysiological roles of ATP-sensitive K+ channels. *Prog Biophys Mol Biol,* 81**,** 133-76.
SHAPIRO, R. E. & MISELIS, R. R. 1985. The central neural connections of the area postrema of the rat. *J Comp Neurol,* 234**,** 344-64.
SHEPPARD, D. N. & ROBINSON, K. A. 1997. Mechanism of glibenclamide inhibition of cystic fibrosis transmembrane conductance regulator Cl- channels expressed in a murine cell line. *J Physiol,* 503 (Pt 2)**,** 333-46.

SHIBASAKI, T., ODA, T., IMAKI, T., LING, N. & DEMURA, H. 1993. Injection of anti-neuropeptide Y gamma-globulin into the hypothalamic paraventricular nucleus decreases food intake in rats. *Brain Res,* 601**,** 313-6.

SILVER, I. A. & ERECINSKA, M. 1998. Glucose-induced intracellular ion changes in sugar-sensitive hypothalamic neurons. *J Neurophysiol,* 79**,** 1733-45.

SIMMONS, D. M. & SWANSON, L. W. 2009. Comparison of the spatial distribution of seven types of neuroendocrine neurons in the rat paraventricular nucleus: toward a global 3D model. *J Comp Neurol,* 516**,** 423-41.

SIMPSON, I. A., VANNUCCI, S. J., DEJOSEPH, M. R. & HAWKINS, R. A. 2001. Glucose transporter asymmetries in the bovine blood-brain barrier. *J Biol Chem,* 276**,** 12725-9.

SLADEK, C. D., STEVENS, W., SONG, Z., JOHNSON, G. C. & MACLEAN, P. S. 2016. The "metabolic sensor" function of rat supraoptic oxytocin and vasopressin neurons is attenuated during lactation but not in diet-induced obesity. *Am J Physiol Regul Integr Comp Physiol,* 310**,** R337-45.

SLUSSER, P. G. & RITTER, R. C. 1980. Increased feeding and hyperglycemia elicited by intracerebroventricular 5-thioglucose. *Brain Res,* 202**,** 474-8.

SMITH, K. L., GARDINER, J. V., WARD, H. L., KONG, W. M., MURPHY, K. G., MARTIN, N. M., GHATEI, M. A. & BLOOM, S. R. 2008. Overexpression of CART in the PVN increases food intake and weight gain in rats. *Obesity (Silver Spring),* 16**,** 2239-44.

SOBOCKI, J., KROLCZYK, G., HERMAN, R. M., MATYJA, A. & THOR, P. J. 2005. Influence of vagal nerve stimulation on food intake and body weight--results of experimental studies. *J Physiol Pharmacol,* 6**,** 27-33.

SONG, Z., LEVIN, B. E., MCARDLE, J. J., BAKHOS, N. & ROUTH, V. H. 2001. Convergence of pre- and postsynaptic influences on glucosensing neurons in the ventromedial hypothalamic nucleus. *Diabetes,* 50**,** 2673-81.

SONG, Z., LEVIN, B. E., STEVENS, W. & SLADEK, C. D. 2014. Supraoptic oxytocin and vasopressin neurons function as glucose and metabolic sensors. *Am J Physiol Regul Integr Comp Physiol,* 306**,** R447-56.

SONG, Z. & ROUTH, V. H. 2005. Differential effects of glucose and lactate on glucosensing neurons in the ventromedial hypothalamic nucleus. *Diabetes,* 54**,** 15-22.

SONNTAG, F., SCHMIDT, K. & KLEINSCHMIDT, J. A. 2010. A viral assembly factor promotes AAV2 capsid formation in the nucleolus. *Proc Natl Acad Sci U S A,* 107**,** 10220-5.

SPANSWICK, D., SMITH, M. A., MIRSHAMSI, S., ROUTH, V. H. & ASHFORD, M. L. 2000. Insulin activates ATP-sensitive K+ channels in hypothalamic neurons of lean, but not obese rats. *Nat Neurosci,* 3**,** 757-8.

STANLEY, B. G., ANDERSON, K. C., GRAYSON, M. H. & LEIBOWITZ, S. F. 1989. Repeated hypothalamic stimulation with neuropeptide Y increases daily carbohydrate and fat intake and body weight gain in female rats. *Physiol Behav,* 46**,** 173-7.

STANLEY, B. G., DANIEL, D. R., CHIN, A. S. & LEIBOWITZ, S. F. 1985. Paraventricular nucleus injections of peptide YY and neuropeptide Y preferentially enhance carbohydrate ingestion. *Peptides,* 6**,** 1205-11.

STANLEY, B. G., KYRKOULI, S. E., LAMPERT, S. & LEIBOWITZ, S. F. 1986. Neuropeptide Y chronically injected into the hypothalamus: a powerful neurochemical inducer of hyperphagia and obesity. *Peptides,* 7**,** 1189-92.

STANLEY, S., DOMINGOS, A. I., KELLY, L., GARFIELD, A., DAMANPOUR, S., HEISLER, L. & FRIEDMAN, J. 2013. Profiling of Glucose-Sensing Neurons Reveals that GHRH Neurons Are Activated by Hypoglycemia. *Cell Metab,* 18**,** 596-607.

STANLEY, S. A., SMALL, C. J., MURPHY, K. G., RAYES, E., ABBOTT, C. R., SEAL, L. J., MORGAN, D. G., SUNTER, D., DAKIN, C. L., KIM, M. S., HUNTER, R., KUHAR, M., GHATEI, M. A. & BLOOM, S. R. 2001. Actions of cocaine- and amphetamine-regulated transcript (CART) peptide on

regulation of appetite and hypothalamo-pituitary axes in vitro and in vivo in male rats. *Brain Res,* 893**,** 186-94.
STEIN, M. K. & LOEWY, A. D. 2010. Area postrema projects to FoxP2 neurons of the pre-locus coeruleus and parabrachial nuclei: brainstem sites implicated in sodium appetite regulation. *Brain Res,* 1359**,** 116-27.
STEVENS, G. A., SINGH, G. M., LU, Y., DANAEI, G., LIN, J. K., FINUCANE, M. M., BAHALIM, A. N., MCINTIRE, R. K., GUTIERREZ, H. R., COWAN, M., PACIOREK, C. J., FARZADFAR, F., RILEY, L. & EZZATI, M. 2012. National, regional, and global trends in adult overweight and obesity prevalences. *Popul Health Metr,* 10**,** 22.
STEWART, S. L., BLACK, R. M., WOLEVER, T. M. S. & ANDERSON, G. H. 1997. The relationship between the glycaemic response to breakfast cereals and subjective appetite and food intake. *Nutrition Research,* 17**,** 1249-1260.
STRAUB, S. G. & SHARP, G. W. 1996. Mechanisms of action of VIP and PACAP in the stimulation of insulin release. *Ann N Y Acad Sci,* 805**,** 607-12.
STREEFLAND, C., MAES, F. W. & BOHUS, B. 1998. Autonomic brainstem projections to the pancreas: a retrograde transneuronal viral tracing study in the rat. *J Auton Nerv Syst,* 74**,** 71-81.
SUMMERFORD, C., BARTLETT, J. S. & SAMULSKI, R. J. 1999. AlphaVbeta5 integrin: a co-receptor for adeno-associated virus type 2 infection. *Nat Med,* 5**,** 78-82.
SUMMERFORD, C. & SAMULSKI, R. J. 1998. Membrane-associated heparan sulfate proteoglycan is a receptor for adeno-associated virus type 2 virions. *J Virol,* 72**,** 1438-45.
SUTTON, G. M., DUOS, B., PATTERSON, L. M. & BERTHOUD, H. R. 2005. Melanocortinergic modulation of cholecystokinin-induced suppression of feeding through extracellular signal-regulated kinase signaling in rat solitary nucleus. *Endocrinology,* 146**,** 3739-47.
SUTTON, G. M., PATTERSON, L. M. & BERTHOUD, H. R. 2004. Extracellular signal-regulated kinase 1/2 signaling pathway in solitary nucleus mediates cholecystokinin-induced suppression of food intake in rats. *J Neurosci,* 24**,** 10240-7.
SZEPIETOWSKA, B., ZHU, W. & SHERWIN, R. S. 2013. beta2-Adrenergic receptor agonist administration promotes counter-regulatory responses and recovery from hypoglycaemia in rats. *Diabetologia,* 56**,** 2517-23.
TEMPEL, D. L., LEIBOWITZ, K. J. & LEIBOWITZ, S. F. 1988. Effects of PVN galanin on macronutrient selection. *Peptides,* 9**,** 309-14.
THOMAS, P. M., COTE, G. J., HALLMAN, D. M. & MATHEW, P. M. 1995. Homozygosity mapping, to chromosome 11p, of the gene for familial persistent hyperinsulinemic hypoglycemia of infancy. *Am J Hum Genet,* 56**,** 416-21.
THORENS, B. 2011. Brain glucose sensing and neural regulation of insulin and glucagon secretion. *Diabetes Obes Metab,* 13 Suppl 1**,** 82-8.
THORENS, B. 2012. Sensing of glucose in the brain. *Handb Exp Pharmacol***,** 277-94.
THORENS, B. 2014. GLUT2, glucose sensing and glucose homeostasis. *Diabetologia*.
THORENS, B., SARKAR, H. K., KABACK, H. R. & LODISH, H. F. 1988. Cloning and functional expression in bacteria of a novel glucose transporter present in liver, intestine, kidney, and beta-pancreatic islet cells. *Cell,* 55**,** 281-90.
TIESJEMA, B., LA FLEUR, S. E., LUIJENDIJK, M. C., BRANS, M. A., LIN, E. J., DURING, M. J. & ADAN, R. A. 2007. Viral mediated neuropeptide Y expression in the rat paraventricular nucleus results in obesity. *Obesity (Silver Spring),* 15**,** 2424-35.
TOKUNAGA, K., FUKUSHIMA, M., KEMNITZ, J. W. & BRAY, G. A. 1986. Effect of vagotomy on serum insulin in rats with paraventricular or ventromedial hypothalamic lesions. *Endocrinology,* 119**,** 1708-11.
TONG, Q., YE, C. P., JONES, J. E., ELMQUIST, J. K. & LOWELL, B. B. 2008. Synaptic release of GABA by AgRP neurons is required for normal regulation of energy balance. *Nat Neurosci,* 11**,** 998-1000.

TRAVAGLI, R. A., HERMANN, G. E., BROWNING, K. N. & ROGERS, R. C. 2006. Brainstem circuits regulating gastric function. *Annu Rev Physiol,* 68**,** 279-305.

TSAI, H. J. & WILSON, J. E. 1996. Functional organization of mammalian hexokinases: both N- and C-terminal halves of the rat type II isozyme possess catalytic sites. *Arch Biochem Biophys,* 329**,** 17-23.

TSUCHIDA, A., NONOMURA, T., ONO-KISHINO, M., NAKAGAWA, T., TAIJI, M. & NOGUCHI, H. 2001. Acute effects of brain-derived neurotrophic factor on energy expenditure in obese diabetic mice. *Int J Obes Relat Metab Disord,* 25**,** 1286-93.

TSUJII, S. & BRAY, G. A. 1990. Effects of glucose, 2-deoxyglucose, phlorizin, and insulin on food intake of lean and fatty rats. *Am J Physiol,* 258**,** E476-81.

TUCKER, S. J., GRIBBLE, F. M., PROKS, P., TRAPP, S., RYDER, T. J., HAUG, T., REIMANN, F. & ASHCROFT, F. M. 1998. Molecular determinants of KATP channel inhibition by ATP. *Embo j,* 17**,** 3290-6.

ULDRY, M., IBBERSON, M., HOSOKAWA, M. & THORENS, B. 2002. GLUT2 is a high affinity glucosamine transporter. *FEBS Lett,* 524**,** 199-203.

VAN DEN TOP, M., LYONS, D. J., LEE, K., CODERRE, E., RENAUD, L. P. & SPANSWICK, D. 2007. Pharmacological and molecular characterization of ATP-sensitive K(+) conductances in CART and NPY/AgRP expressing neurons of the hypothalamic arcuate nucleus. *Neuroscience,* 144**,** 815-24.

VERBERNE, A. J., SABETGHADAM, A. & KORIM, W. S. 2014. Neural pathways that control the glucose counterregulatory response. *Front Neurosci,* 8**,** 38.

VERDICH, C., TOUBRO, S., BUEMANN, B., LYSGARD MADSEN, J., JUUL HOLST, J. & ASTRUP, A. 2001. The role of postprandial releases of insulin and incretin hormones in meal-induced satiety--effect of obesity and weight reduction. *Int J Obes Relat Metab Disord,* 25**,** 1206-14.

WANG, C., BILLINGTON, C. J., LEVINE, A. S. & KOTZ, C. M. 2000. Effect of CART in the hypothalamic paraventricular nucleus on feeding and uncoupling protein gene expression. *Neuroreport,* 11**,** 3251-5.

WANG, F. B. & POWLEY, T. L. 2007. Vagal innervation of intestines: afferent pathways mapped with new en bloc horseradish peroxidase adaptation. *Cell Tissue Res,* 329**,** 221-30.

WANG, H., SHARMA, N., ARIAS, E. B. & CARTEE, G. D. 2016. Insulin Signaling and Glucose Uptake in the Soleus Muscle of 30-Month-Old Rats After Calorie Restriction With or Without Acute Exercise. *J Gerontol A Biol Sci Med Sci,* 71**,** 323-32.

WANG, J., LING, S., USAMI, T., MURATA, T., NARITA, K. & HIGUCHI, T. 2007. Effects of ghrelin, corticotrophin-releasing hormone, and melanotan-II on food intake in rats with paraventricular nucleus lesions. *Exp Clin Endocrinol Diabetes,* 115**,** 669-73.

WANG, Q., LIU, C., UCHIDA, A., CHUANG, J. C., WALKER, A., LIU, T., OSBORNE-LAWRENCE, S., MASON, B. L., MOSHER, C., BERGLUND, E. D., ELMQUIST, J. K. & ZIGMAN, J. M. 2014. Arcuate AgRP neurons mediate orexigenic and glucoregulatory actions of ghrelin. *Mol Metab,* 3**,** 64-72.

WANG, R., LIU, X., HENTGES, S. T., DUNN-MEYNELL, A. A., LEVIN, B. E., WANG, W. & ROUTH, V. H. 2004. The regulation of glucose-excited neurons in the hypothalamic arcuate nucleus by glucose and feeding-relevant peptides. *Diabetes,* 53**,** 1959-65.

WILCOX, J. N. 1993. Fundamental principles of in situ hybridization. *J Histochem Cytochem,* 41**,** 1725-33.

WILLIAMS, D. L., BASKIN, D. G. & SCHWARTZ, M. W. 2006. Leptin regulation of the anorexic response to glucagon-like peptide-1 receptor stimulation. *Diabetes,* 55**,** 3387-93.

WILSON, J. E. 1995. Hexokinases. *Rev Physiol Biochem Pharmacol,* 126**,** 65-198.

WILSON, J. E. 2003. Isozymes of mammalian hexokinase: structure, subcellular localization and metabolic function. *J Exp Biol,* 206**,** 2049-57.

WOOD, S. & LOUDON, A. 2014. Clocks for all seasons: unwinding the roles and mechanisms of circadian and interval timers in the hypothalamus and pituitary. *J Endocrinol,* 222**,** R39-59.

WOOD, W. G., WACHTER, C. & SCRIBA, P. C. 1981. Experiences using chloramine-T and 1, 3, 4, 6-tetrachloro-3 alpha, 6 alpha-diphenylglycoluril (Iodogen) for radioiodination of materials for radioimmunoassay. *J Clin Chem Clin Biochem,* 19**,** 1051-6.

WOODS, S. C. & BERNSTEIN, I. L. 1980. Cephalic insulin response as a test for completeness of vagotomy to the pancreas. *Physiol Behav,* 24**,** 485-8.

WOODS, S. C., STEIN, L. J., MCKAY, L. D. & PORTE, D., JR. 1984. Suppression of food intake by intravenous nutrients and insulin in the baboon. *Am J Physiol,* 247**,** R393-401.

WORLD HEALTH ORGANIZATION 2015a. Fact Sheet 311 - Obesity and Overweight. Geneva: World Health Organization.

WORLD HEALTH ORGANIZATION 2015b. Fact Sheet 312 - Diabetes.

WYNICK, D. & BACON, A. 2002. Targeted disruption of galanin: new insights from knock-out studies. *Neuropeptides,* 36**,** 132-44.

WYNNE, K., STANLEY, S., MCGOWAN, B. & BLOOM, S. 2005. Appetite control. *J Endocrinol,* 184**,** 291-318.

XIE, Q., BU, W., BHATIA, S., HARE, J., SOMASUNDARAM, T., AZZI, A. & CHAPMAN, M. S. 2002. The atomic structure of adeno-associated virus (AAV-2), a vector for human gene therapy. *Proc Natl Acad Sci U S A,* 99**,** 10405-10.

XU, B., GOULDING, E. H., ZANG, K., CEPOI, D., CONE, R. D., JONES, K. R., TECOTT, L. H. & REICHARDT, L. F. 2003. Brain-derived neurotrophic factor regulates energy balance downstream of melanocortin-4 receptor. *Nat Neurosci,* 6**,** 736-42.

YANG, X. J., KOW, L. M., PFAFF, D. W. & MOBBS, C. V. 2004. Metabolic pathways that mediate inhibition of hypothalamic neurons by glucose. *Diabetes,* 53**,** 67-73.

YANG, X. J., MASTAITIS, J., MIZUNO, T. & MOBBS, C. V. 2007. Glucokinase regulates reproductive function, glucocorticoid secretion, food intake, and hypothalamic gene expression. *Endocrinology,* 148**,** 1928-32.

YOSHIDA, T., YOSHIOKA, K., NISHIOKA, H. & KONDO, M. 1989. Lesions of the hypothalamic paraventricular nucleus and norepinephrine turnover in rats. *Endocrinol Jpn,* 36**,** 187-94.

YOUNG, A. A. 2012. Brainstem sensing of meal-related signals in energy homeostasis. *Neuropharmacology,* 63**,** 31-45.

ZHAN, C., ZHOU, J., FENG, Q., ZHANG, J. E., LIN, S., BAO, J., WU, P. & LUO, M. 2013. Acute and long-term suppression of feeding behavior by POMC neurons in the brainstem and hypothalamus, respectively. *J Neurosci,* 33**,** 3624-32.

ZHANG, G., GURTU, V. & KAIN, S. R. 1996. An enhanced green fluorescent protein allows sensitive detection of gene transfer in mammalian cells. *Biochem Biophys Res Commun,* 227**,** 707-11.

ZHAO, S., KANOSKI, S. E., YAN, J., GRILL, H. J. & HAYES, M. R. 2012. Hindbrain leptin and glucagon-like-peptide-1 receptor signaling interact to suppress food intake in an additive manner. *Int J Obes,* 36**,** 1522-1528.

ZHENG, F., KIM, Y. J., CHAO, P. T. & BI, S. 2013. Overexpression of neuropeptide Y in the dorsomedial hypothalamus causes hyperphagia and obesity in rats. *Obesity (Silver Spring),* 21**,** 1086-92.

ZHOU, L., PODOLSKY, N., SANG, Z., DING, Y., FAN, X., TONG, Q., LEVIN, B. E. & MCCRIMMON, R. J. 2010. The medial amygdalar nucleus: a novel glucose-sensing region that modulates the counterregulatory response to hypoglycemia. *Diabetes,* 59**,** 2646-52.

ZHOU, L., YUEH, C. Y., LAM, D. D., SHAW, J., OSUNDIJI, M., GARFIELD, A. S., EVANS, M. & HEISLER, L. K. 2011. Glucokinase inhibitor glucosamine stimulates feeding and activates hypothalamic neuropeptide Y and orexin neurons. *Behav Brain Res,* 222**,** 274-8.

Chapter Seven - Appendix

7.1 Solutions

ABC Buffer

Solutions A, B and C were combined in the following proportions: 100:250:150 and stored at -20°C.

Solution A

1ml of 125mM $MgCl_2$ and 1.25M Tris-HCl (pH 8.0) were added to 18µl mercaptoethanol, 5µl 100mM dATP, 5µl 100 mM dTTP and 5µl dGTP.

Solution B

2M Hepes (pH6.6) was titrated with 4M NaOH.

Solution C

Random oligonucleotides (112µg/ml)

0.25% (v/v) acetic anhydride in 0.1M TEA

1ml of acetic anhydride was added to 400ml of 0.1M TEA (pH 8)

Acidified ethanol

To make 500ml, 375ml of absolute ethanol were added to 117.5ml GDW and 7.5ml of 1M HCl solution containing 0.1% Triton X.

Amasino wash buffer

250ml of 1M sodium phosphate buffer (pH 7.2), 2ml of 500mM EDTA and 100ml of 20% SDS were mixed with 650ml GDW.

5M Ammonium acetate

385g of ammonium acetate (CH_3COONH_4) were dissolved in 600ml autoclaved GDW then made up to 1L.

Ampicillin (100mg/ml)

1g ampicillin was dissolved in 10ml GDW, sterilised by passage through a 0.2µm filter and distributed in 1ml aliquots.

Assay buffer (RIA buffer)

48g of sodium phosphate dibasic hydrate ($Na_2HPO_4.2H_2O$), 4.13g potassium phosphate (KH_2PO_4), 18.61g $C_{10}H_{14}H_2O_8Na_2.2H_2O$ and 2.5g NaN_3 were dissolved in 5L boiled and cooled GDW. The pH was adjusted to 7.4.

2.5mM Aurintricarboxylic acid (ATA)

0.1183g ATA was dissolved in 100ml GDW.

Baker's yeast tRNA (10mg/ml)

Baker's yeast tRNA was made up with GDW, aliquoted and stored at -20°C.

2M calcium chloride ($CaCl_2$)

111g $CaCl_2$ were dissolved in 500ml GDW

Caesium chloride-saturated propan-2-ol

100g $CsCl_2$ were mixed with 100ml GDW and 100ml propan-2-ol and left to settle.

Compound A (CpdA)

Compound A (CpdA) was dissolved in 100% DMSO. It was then aliquoted and stored at -80°C. Prior to use, aliquots were dissolved in 1% DMSO to a working concentration of 0.5 nmol.

1% Cresyl violet solution

1mg of cresyl Violet was added to 99ml GDW and passed through a Whatman GF/C filter.

Diazoxide

Diazoxide was aliquoted and dissolved in 0.05M NaOH and 1% DMSO in GDW to a working concentration of 1 nmol.

100x Denhart's solution

10g ficoll, 10g polyvinylpyrrolidone (PVP) and 10g BSA (Pentax fraction V) were dissolved and made up to 500ml with GDW.

Denaturing solution (DNA)

43.5g NaCl were dissolved in 430ml GDW. 25ml of 10M NaOH were added and the mixture was made up to 500ml with GDW.

1M Dithiothreitol (DTT)

154g Dithiothreitol ($C_4H_{10}O_2S_2$) were dissolved in 1L GDW, aliquoted and stored at -20°C.

0.5M Ethylenediaminetetra-acetic acid (EDTA) (pH 8.0)

181.6g of ethylenediaminetetra-acetic acid ($C_{10}H_{14}H_2O_8Na.2H_2O$) were dissolved in 800ml GDW and adjusted to pH 8.0 with NaOH. It was then made up to 1L with GDW.

Extraction buffer for GK activity assay

0.508g $MgCl_2$, 0.913g Na^+EDTA, 5.591g KCl and 0.35ml 2-mercaptoethanol were added to 400ml GDW.

The pH was adjusted to 7.3 using KOH then made up to 500ml with autoclaved GDW.

4% Formaldehyde in 0.01M PBS

8ml 40% formaldehyde solution were added to 400ml 0.01M PBS.

Formamide (de-ionised)

2.7g duolite MB were added to 100ml formamide and stirred until the duolite turned brown (~1 hour). The duolite was removed by passing through Whatman GF/C filters. The mixture was aliquoted and stored at -20°C.

Glucose Tris EDTA (GTE)

Final concentrations of 50mM glucose, 25mM Tris and 10mM EDTA

Glibenclamide

Glibenclamide was aliquoted and dissolved with 0.05M NaOH and 1% DMSO in GDW to a working concentration of 2 nmol.

Gly-Gly buffer

6.6g Gly-Gly were dissolved in 400ml GDW. The pH was adjusted to 8.0 using KOH, after which the buffer was made up to 500ml with GDW.

1x Hepes buffered saline (HBS) (pH 7.05)

0.8g NaCl, 37.5mg KCl, 10.5mg, Na2HPO4, 0.11g dextrose and 0.5g Hepes were dissolved in a total volume of 90ml GDW. The pH was adjusted to 7.05 with 0.5M NaOH and GDW was added to a final volume of 100ml. The buffer was sterilised by passing through a 0.2µm filter and stored in 5ml aliquots at -20°C.

Hybridisation buffer for northern blot analysis and for dot-blot analysis

0.5g dried milk powder and 0.5ml 500mM EDTA were added to 48ml GDW and left to dissolve at 37°C. The mixture was allowed to cool, after which 25ml of 1M sodium phosphate buffer, 25ml 20% SDS and 1ml 2.5M ATA were added.

Hybridisation buffer for *in situ* hybridisation

Dextran sulphate solution was prepared by adding 1.5ml GDW to 1g dextran sulphate. The solution was incubated in a water bath at 60°C for two hours. Bubbling was avoided whenever possible. In a total volume of 4ml, the following reagents were added: 1.25ml formamide, 300µl 5M NaCl, 200µl tRNA (10mg/ml), 50µl of 100x Denhart's, 50µl 1M Tris (pH 8.0), 40µl 1M dithiothreitol (DTT), 10µl 0.5M EDTA (pH 8.0), 1.1ml GDW and 1ml (50%) dextran sulphate.

Krebs Ringer Bicarbonate buffer

120 mM NaCl, 4.8 mM potassium chloride (KCl), 2.5 mM $CaCl_2$, 1.2 mM magnesium chloride ($MgCl_2$), and 24 mM sodium bicarbonate ($NaHCO_3$) were dissolved in 600ml GDW. The buffer was gassed with O_2/CO_2 for 15 minutes.

The pH was adjusted to 7.2.

The following were then added: 1 mg/ml BSA, 5 mM HEPES, and 10 mM glucose. The pH was adjusted to 7.30–7.35 with 1M NaOH.

The buffer was supplemented with penicillin at 100 IU/ml and streptomycin 100µg/ml.

400ml of the KRB were filter sterilized into a sterile glass bottle with a 0.2µM filter.

3µg of DNase I were added to the remaining KRB (~200 ml), which was filtered into another sterile glass bottle (KRB + DNase I).

Krebs-Ringer Bicarbonate Hepes (KRBH) solution

<u>Prepare stock of Mixed Hepes-bicarbonate (4X):</u>

To 1L of GDW, 9.53g Hepes, 0.672g sodium bicarbonate ($NaHCO_3$) and 2.338g of NaCl were added.

Prepare stock of mixed salts (5X):

To 1L of GDW, 37.98g NaCl, 1.326g KCl, 0.345g NaH_2PO_4, 0.616g $MgSO_4$ and 1.12g $CaCl_2$ were added.

Prepare Krebs-Ringer Bicarbonate Hepes (KRBH) solution:

50mL Hepes-bicarbonate (4X) and 40mL Mixed salts (5X) were added to 80ml GDW. The pH was adjusted to 7.4 using NaOH and the mixture was supplemented with 0.1%BSA (0.2 g). It was then gassed with 95% O_2 and 5% CO_2 for 10 minutes.

LB culture medium (pH 7.5)

10g NaCl, 10g tryptone and 5g yeast extract were dissolved in 800ml GDW. The pH was adjusted to 7.5 with 10M NaOH. The medium was then sterilised by autoclaving and made up to 1L.

LB (amp) agar plates

7g agar were added to 500ml LB and melted by autoclaving. 1ml of 100mg/mL ampicillin was then added, after which the agar was set in plates at 4°C.

Loading Buffer for DNA/RNA

3.125ml of 80% glycerol, 50µl of 0.5M $C_{10}H_{14}H_2O_8Na2.H_2O$ were mixed in 6.075ml autoclaved GDW, following which 10mg orange G were added.

2M Magnesium chloride ($MgCl_2$)

406.6g magnesium chloride hexahydrate ($MgCl_2.6H_2O$) were dissolved in 1L GDW.

Neutralising solution (pH 7.5)

43.5g NaCl and 60.2g of Tris (hydroxymethyl) aminomethane hydrochloride ($NH_2C(CH_2OH)_3$) were dissolved in 430 ml GDW and the pH was adjusted 7.5 with approximately 35ml HCl.

Phosphate buffered saline (PBS):

0.1M PBS (10x)

80g NaCl, 2g KCl, 14.4g disodium phosphate (Na_2HPO_4) and 2.4g potassium dihydrogen phosphate (KH_2PO_4) were dissolved in 800ml GDW.

0.01M PBS (1x)

100ml 0.1M PBS were added to 900ml GDW.

5M Potassium acetate (KAc)

Dissolve 294.4g potassium acetate (CH_3COOK) in 500ml GDW. 115ml of ice cold acetic acid were then added, following which the buffer was made up to 1L with GDW.

3M Potassium hydroxide

198g KOH were dissolved in 1L GDW.

Proteinase K (20mg/ml)

20mg were dissolved in 1ml GDW, distributed into 100µl aliquots and stored at -20°C.

RNase A (10mg/ml)

100mg RNase A was dissolved in 10ml GDW and the mixture was boiled for up to fifteen minutes to denature DNAses. It was allowed to cool, distributed into 800µl aliquots and stored at -20°C.

20x Saline sodium citrate (SSC) buffer (pH 7.0)

1.735g NaCl and 882g $Na_3C_6H_5O_7.2H_2O$ were dissolved in 8L GDW. The pH was adjusted to 7.0 and made up to 10L.

Sephadex G50

8g of fine grade Sephadex G50 beads (diameter: 20-80µm), 2ml 100x TE and 0.1ml 20% SDS were added to 200ml GDW and autoclaved to expand the beads.

2M Sodium acetate (pH 5.2)

164.1g sodium acetate (CH_3COONa) were dissolved in 800ml GDW. The pH was adjusted to 5.2 with ice cold acetic acid and the solution was made up to 1L with GDW.

3M Sodium chloride

175.3g NaCl were dissolved in 1L GDW.

5M Sodium chloride

292.2g NaCl were dissolved in 1L GDW.

20% (w/v) Sodium dodecyl sulphate (SDS)

200g Sodium dodecyl sulphate were added to 800ml GDW and the mixture was heated to 60°C while stirring. It was allowed to cool and made up to 1L with GDW.

0.2M Sodium hydroxide/1%SDS

3ml 10M NaOH were added to 140ml GDW. The solution was mixed and 7.5ml 20% SDS was added add.

10M Sodium hydroxide

400g NaOH were dissolved in 500ml GDW. The buffer was made up to 1Lwith GDW.

1M Sodium phosphate buffer (pH 6.8)

26g of monosodium phosphate (NaH_2PO_4) and 44.6g disodium phosphate (Na_2HPO_4) were dissolved in 1L GDW.

20x Sodium chloride, sodium hydrogen phosphate, EDTA (SSPE) buffer (pH 7.7)

1.753g NaCl, 14.2g disodium phosphate (Na_2HPO_4) and 7.4g EDTA $C_{10}H_{14}H_2O_8Na2.2H_2O$ were dissolved in 700ml GDW. The pH was adjusted to 7.7 with 10M NaOH and made up to 1L with GDW.

40% sucrose solution

200g sucrose was dissolved in 300ml GDW.

0.1M Triethanolamine (TEA) buffer (pH 8.0)

18.6g Triethanolamine ($C_6H_{15}NO_3$.HCl) were dissolved in 800ml GDW. NaOH was added to raise the pH to 8.0 and the buffer was made up to 1L with GDW.

50x Tris-acetate-EDTA (TAE) buffer

242g Tris (hydroxymethyl) aminomethane hydrochloride ($NH_2C(CH_2OH)_3$) were dissolved in 843ml GDW, after which 57ml ice cold acetic acid and 100ml 0.5M EDTA ($C_{10}H_{14}H_2O_8Na2.2H_2O$) were added.

100x Tris-EDTA (TE) buffer (pH 7.5)

121.1g Tris (hydroxymethyl) aminomethane hydrochloride ($NH_2C(CH_2OH)_3$) and 3.7g EDTA ($C_{10}H_{14}H_2O_8Na2.2H_2O$) were dissolved in 800ml GDW. The pH was adjusted to 7.5 with hydrochloric acid and the buffer was made up to 1L with GDW.

Tris-EDTA-Sodium chloride (TES) buffer

25ml 1M of Tris-HCl (pH 8.0), 5ml of 5M NaCl and 5ml Tris (hydroxymethyl) aminomethane hydrochloride ($NH_2C(CH_2OH)_3$) were mixed and made up to 500ml with GDW.

Versene

16g NaCl, 0.4g KCl, 2.88g disodium phosphate ($Na_2HPO_4.2H_2O$), 1.2g Tris (hydroxymethyl) aminomethane hydrochloride ($NH_2C(CH_2OH)_3$) and 0.4g monopotassium sulphate (KH_2PO_4) were dissolved in 1L GDW. 3ml phenol red was added and the solution was made up to 2L with GDW. It was sterilised by autoclaving.

7.2 Coronal sections of the rat brain

7.2.1 Coronal section of the brainstem showing the *nucleus tractus solitarius*

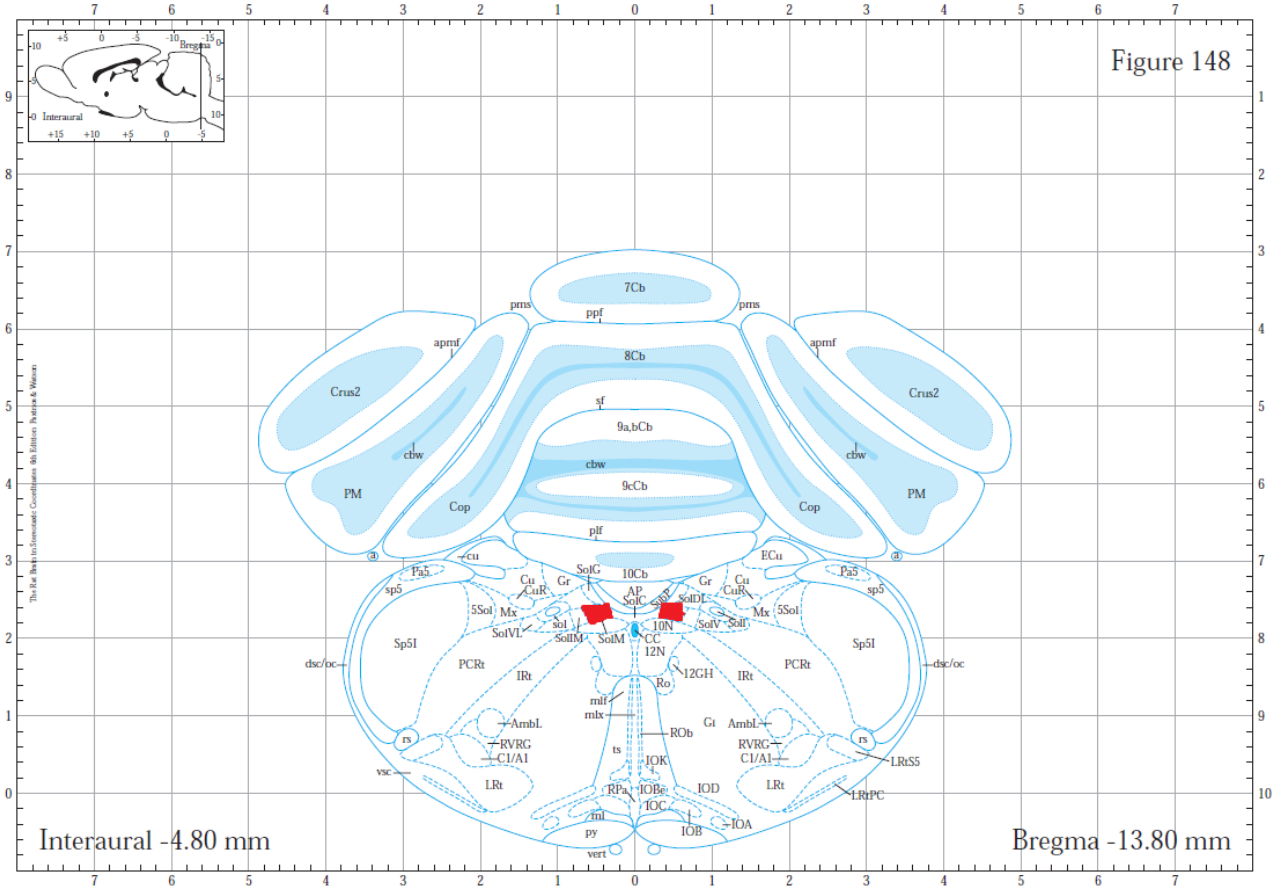


Figure 7.1: Schematic of a coronal section of the rat brainstem. Schematic showing 13.80mm posterior to bregma corresponding to the coordinates used to target the NTS in this work. The medial NTS is highlighted in red. Reproduced from "The Rat Brain in Stereotaxic Co-ordinates" (Paxinos and Watson 2007).

7.2.2 Coronal section of the hypothalamus showing the paraventricular nucleus

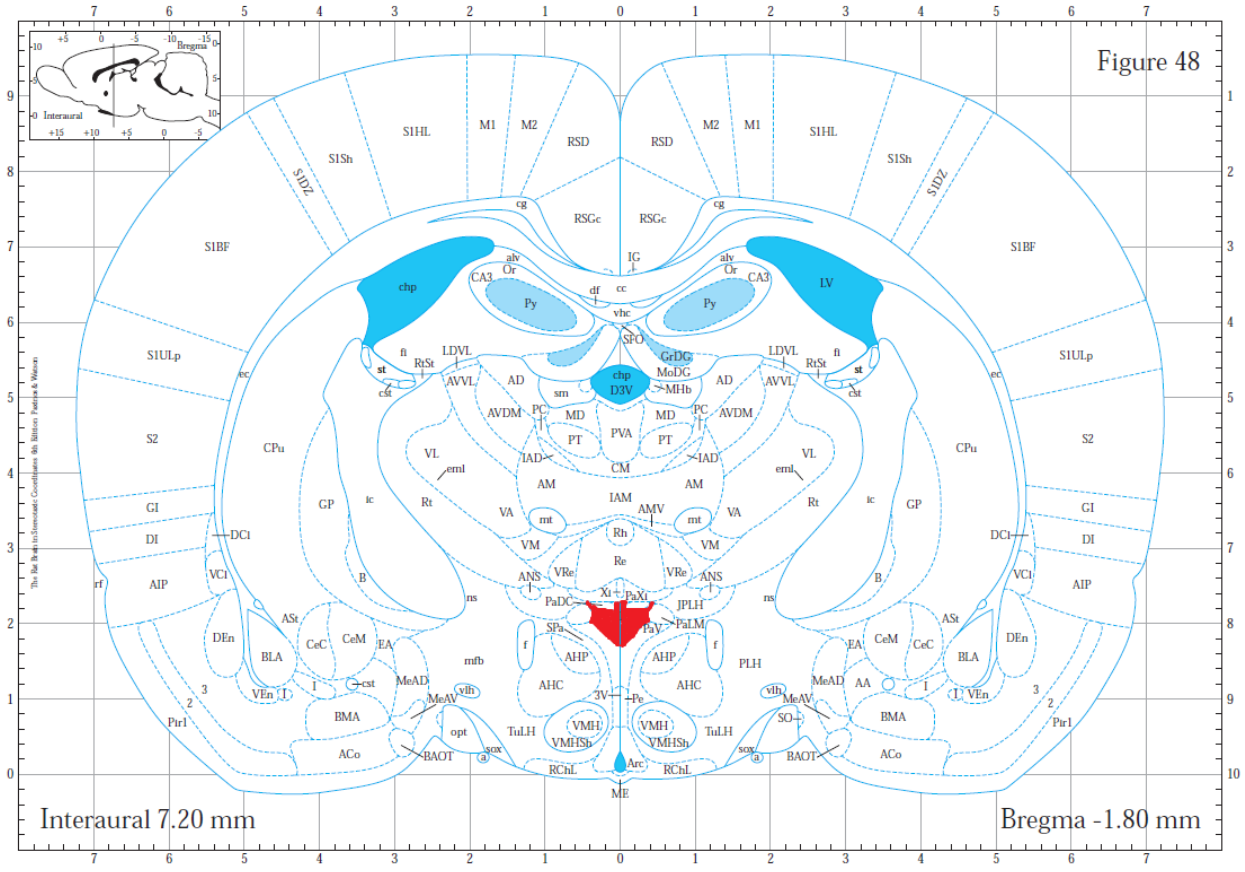


Figure 7.2: Schematic of a coronal section of the rat brain. Schematic showing 1.80mm posterior to bregma corresponding to the coordinates used to target the PVN in this work. The PVN is highlighted in red. Reproduced from “The Rat Brain in Stereotaxic Co-ordinates” (Paxinos and Watson 2007).

7.3 Nutritional information for RM1 standard chow diet

NUTRIENTS		Total	Supp (9)
Proximate Analysis			
Moisture (1)	%	10.00	
Crude Oil	%	2.71	
Crude Protein	%	14.37	
Crude Fibre	%	4.65	
Ash	%	6.00	
Nitrogen Free Extract	%	61.65	
Digestibility Co-Efficients (7)			
Digestible Crude Oil	%	2.46	
Digestible Crude Protein	%	12.91	
Carbohydrates, Fibre and Non Starch Polysaccharides (NSP)			
Total Dietary Fibre	%	17.04	
Pectin	%	1.52	
Hemicellulose	%	10.16	
Cellulose	%	4.32	
Lignin	%	1.68	
Starch	%	44.91	
Sugar	%	4.05	
Energy (5)			
Gross Energy	MJ/kg	14.72	
Digestible Energy (15)	MJ/kg	11.89	
Metabolisable Energy (15)	MJ/kg	10.75	
Atwater Fuel Energy (AFE) (8)	MJ/kg	13.73	
AFE from Oil	%	7.43	
AFE from Protein	%	17.50	
AFE from Carbohydrate	%	75.08	
Fatty Acids			
Saturated Fatty Acids			
C12:0 Lauric	%	0.02	
C14:0 Myristic	%	0.14	
C16:0 Palmitic	%	0.31	
C18:0 Stearic	%	0.04	
Monounsaturated Fatty Acids			
C14:1 Myristoleic	%	0.02	
C16:1 Palmitoleic	%	0.09	
C18:1 Oleic	%	0.77	
Polyunsaturated Fatty Acids			
C18:2(ω6) Linoleic	%	0.69	
C18:3(ω3) Linolenic	%	0.06	
C20:4(ω6) Arachidonic	%	0.13	
C22:5(ω3) Clupanodonic	%		
Amino Acids			
Arginine	%	0.91	
Lysine (6)	%	0.66	0.07
Methionine	%	0.22	0.04
Cystine	%	0.24	
Tryptophan	%	0.18	
Histidine	%	0.35	
Threonine	%	0.49	
Isoleucine	%	0.54	
Leucine	%	0.98	
Phenylalanine	%	0.66	
Valine	%	0.69	
Tyrosine	%	0.49	
Taurine	%		
Glycine	%	1.11	
Aspartic Acid	%	0.67	

NUTRIENTS		Total	Supp (9)
Glutamic Acid	%	3.17	
Proline	%	1.19	
Serine	%	0.55	
Hydroxyproline	%		
Hydroxylysine	%		
Alanine	%	0.16	
Macro Minerals			
Calcium	%	0.73	0.63
Total Phosphorus	%	0.52	0.05
Phytate Phosphorus	%	0.24	
Available Phosphorus	%	0.28	0.05
Sodium	%	0.25	0.19
Chloride	%	0.38	0.32
Potassium	%	0.67	
Magnesium	%	0.23	
Micro Minerals			
Iron	mg/kg	159.23	82.95
Copper	mg/kg	11.49	1.98
Manganese	mg/kg	72.40	19.58
Zinc	mg/kg	35.73	
Cobalt	µg/kg	633.94	550.63
Iodine	µg/kg	1202.49	1085.36
Selenium	µg/kg	298.87	100.73
Fluorine	mg/kg	10.48	
Vitamins			
β-Carotene (2)	mg/kg	0.16	
Retinol (2)	µg/kg	14996.23	14400.82
Vitamin A (2)	iu/kg	49987.07	48002.69
Cholecalciferol (3)	µg/kg	88.05	85.00
Vitamin D (3)	iu/kg	3522.02	3400.00
α-Tocopherol (4)	mg/kg	189.43	166.09
Vitamin E (4)	iu/kg	208.37	182.70
Vitamin B_1 (Thiamine)	mg/kg	54.26	46.11
Vitamin B_2 (Riboflavin)	mg/kg	61.17	57.83
Vitamin B_6 (Pyridoxine)	mg/kg	55.56	50.03
Vitamin B_{12} (Cyanocobalamine)	µg/kg	69.63	66.01
Vitamin C (Ascorbic Acid)	mg/kg	2.68	
Vitamin K (Menadione)	mg/kg	84.75	81.36
Folic Acid (Vitamin B_9)	mg/kg	19.06	17.64
Nicotinic Acid (Vitamin PP) (6)	mg/kg	183.08	120.50
Pantothenic Acid (Vitamin B_{5x})	mg/kg	56.20	40.74
Choline (Vitamin B_{Y1})	mg/kg	1079.89	367.51
Inositol	mg/kg	2366.38	27.21
Biotin (Vitamin H) (6)	µg/kg	753.39	461.81

Notes

1. All values are calculated using a moisture basis of 10%.
   Typical moisture levels will range between 9.5 - 11.5%.
2. a. Vitamin A includes Retinol and the Retinol equivalents of β-carotene
   b. Retinol includes the Retinol equivalents of β-Carotene.
   c. 0.48 µg Retinol = 1 µg β-carotene = 1.6 iu Vitamin A activity
   d. 1 µg Retinol = 3.33* iu Vitamin A activity
   e. 1 iu Vitamin A = 0.3 µg Retinol = 0.6 µg β-carotene
   f. The standard analysis for Vitamin A does not detect β-carotene
3. 1µg Cholecalciferol (D_3) = 40.0 iu Vitamin D
4. 1 mg all-*rac*-α-tocopherol = 1.1 iu Vitamin E activity
   1 mg all-*rac*-α-tocopherol acetate = 1.0 iu Vitamin E activity
5. 1 MJ = 239.23 Kcalories = 239.23 Calories = 239,230 calories
6. These nutrients coming from natural raw materials such as cereals may have low availabilities due to the interactions with other compounds.
7. Based on in-vitro digestibility analysis.
8. AF Energy = Atwater Fuel Energy = (((CO%/100)*9000)+((CP%/100)*4000)+((NFE%/100)*4000))/239.23
9. Supplemented nutrients from manufactured and mined sources.
15. Calculated.

Figure 7.3: Nutritional information for RM1 standard chow diet.

7.4 DNA sequencing of plasmid for *in situ* hybridization

BLAST analysis of the GK-pTR-CGW sequence revealed that the plasmid contained a 69bp sequence with 100% homology to the rat pancreatic GK sequence (GenBank: M25807.1).

ACCGCGGTGGCGGCCGCTCTAGAACTAGTGGATCCGGTACTCGAGCTACCGGTATTCAGA

TCTGGTACCTGGGCTGGTGGCTGCGCAGATGCTGGATGACAGAGCCAGGATGGAGGCCAC

CAAGAAGGAAAAGGTCGAGCAGATCCTGGCAGAGTTCCAGCTGCAGGAATTCGATATCAA

GCTTATCGATACCGTCGACCTCGAGGGGGGGCCCGGTACCCAGCTTTTGTTCCCTTTAGT

GAGGGTTAATTGCGCGCTTGGCGTAATCATGGTCATAGCTGTTTCCTGTGTGAAATTGTT

ATCCGCTCACAATTCCACACAACATACGAGCCGGAAGCATAAAGTGTAAAGCCTGGGGTG

CCTAATGAGTGAGCTAACTCACATTAATTGCGTTGCGCTCACTGCCCGCTTTCCAGTCGG

GAAACCTGTCGTGCCAGCTGCATTAATGAATCGGCCAACGCGCGGGGAGAGGCGGTTTGC

GTATTGGGCGCTCTTCCGCTTCCTCGCTCACTGACTCGCTGCGCTCGGTCGTTCGGCTGC

GGCGAGCGG

Figure 7.4: Sequence of GK-pTR-CGW-plasmid. The sequence containing GK insert is underlined.

7.5 List of suppliers

Abbott Laboratories Ltd, Chicago, IL, USA

Applied Biosystems Ltd, Foster City, CA, USA

Bayer, Leverkusen, Germany

Biotek Instruments Ltd, Winooski, VT, USA

BOC, Guildford, UK

Boehringer Ingelheim, Ingelheim, Germany

Braun Medical Ltd., Sheffield, UK

Bright Instruments, Luton, UK

Calbiochem, San Diego, CA, USA

Clintech, Guildford, UK

CP Pharmaceuticals, Wrexham, UK

Crystal Chem Inc, Downers Grove, IL, USA

Dako, Santa Clara, CA, USA

Eli Lilly & Co. Ltd, Basingstoke, UK

Enzo Life Science, Farmingdale, NY, USA

Eppendorf, Hamburg, Germany

Foredom, Bethel, CT, USA

GE Healthcare, Chicago, IL, USA

GraphPad Software; San Diego, USA

Hettich Zentrifugen, Tuttlingen, Germany

Jet X-Ray, London, UK

Kemdent, Swindon, UK

Kodak, Rochester, NY, USA

Kopf Instruments, Tujunga, CA, USA

LabX, Midland, Canada

Millipore, Watford, UK

Millpledge Veterinary, Nottinghamshire, UK

Montrose Fasteners, High Wycombe, UK

New England Biolabs, Ipswich, MA, USA

Nikon, Tokyo, Japan

Plastics One, Roanoke, VA, USA

Promega, Fitchburg, WI, USA

Randox, Crumlin, UK

Santa Cruz Biotechnology, Santa Cruz, CA, USA

Sarstedt, Numbrecht, Germany

Schering-Plough Ltd., Kenilworth, NJ, USA

Seton Scholl Healthcare Ltd., London, UK

Sigma-Aldrich, St Louis, USA

StarLab, Milton Keynes, UK

Stata, Stata Corp LP, USA

Thermo Fisher Scientific, Waltham, MA, USA

Tyco Healthcare Ltd, Hampshire, UK

Vector Labs, Burlingame, CA, USA

Vet Tech Solutions Ltd, Congleton, UK

VWR, Radnor, PA, USA

Wockhardt, Wrexham, UK

World Precision Instruments, Sarasota, FL, USA